NASA Contractor Report 191462

Practical Input Optimization for Aircraft Parameter Estimation Experiments

Eugene A. Morelli

The George Washington University
Joint Institute for Advancement of Flight Sciences
Hampton, Virginia

Cooperative Agreement NCC1-29
May 1993

National Aeronautics and
Space Administration

Langley Research Center
Hampton, Virginia 23681-0001

ABSTRACT

Mathematical models of aircraft dynamics typically contain quantities called parameters, which depend, in general, on the flight condition and the aircraft geometry. It is important to be able to estimate these parameters accurately from flight testing the aircraft. The parameter estimates from flight data are used to corroborate wind tunnel parameter estimates, validate and improve *a priori* aerodynamic calculations, update aircraft dynamic models for flight control system refinement, and predict aircraft responses for realistic flight simulation and ground-based pilot training.

Today, many fighter aircraft are designed with inherent longitudinal static instability in order to enhance maneuverability and performance. These aircraft must employ stability augmentation systems which, because of safety considerations, cannot be turned off. In addition, multiple control surfaces are required for enhanced performance in expanded flight envelopes, such as high angle of attack flight.

The object of this research is to develop an algorithm for the design of practical, optimal flight test inputs for aircraft parameter estimation experiments. This algorithm must be capable of designing multiple input experiments for estimation of open loop model parameters from (necessarily) closed loop flight test data.

A general, single pass technique was developed which allows global optimization of the flight test input design for parameter estimation using the principles of dynamic programming. Provision was made for practical constraints on the input form, including amplitude constraints, control system dynamics, and selected input frequency range exclusions. In addition, the input design was accomplished while imposing output amplitude constraints required by model validity and considerations of safety during the flight test. The algorithm has multiple input design capability, with optional inclusion of a constraint that only one control move at a time, so that a human pilot can implement the inputs. The dissertation includes a new formulation of the optimal input design problem, a description of a new approach to the solution, and a summary of the characteristics of the algorithm, followed by three example applications of the new technique

which demonstrate the quality and expanded capabilities of the input designs produced by the new technique. In all cases, the new input design approach showed significant improvement over previous input design methods in terms of achievable parameter accuracies.

The work described in this document was done in partial fulfillment of the requirements for the Doctor of Science degree in Aerospace Engineering at The George Washington University Joint Institute for the Advancement of Flight Sciences (JIAFS), NASA Langley Research Center, Hampton, Virginia.

ACKNOWLEDGEMENTS

First, I would like to thank my advisor, Dr. Vladislav Klein, for his help, encouragement, and friendship, and for showing me by example what it means to be an effective academic advisor and a careful researcher. The outstanding research and academic opportunities afforded me by the George Washington University/NASA Langley JIAFS program are acknowledged and deeply appreciated. I thank my wife, Susan, for her unfailing support and optimism. I also thank my family for being interested, and for financial help. Finally, and most of all, I thank my parents, Dr. Marion A. Morelli and Ruth H. Morelli, for their boundless generosity, support, and enthusiasm for all my endeavors.

TABLE OF CONTENTS

LIST OF FIGURES

LIST OF TABLES

LIST OF SYMBOLS

AMPLAG(t)	control system dynamics function
b	wing span, m
c	wing chord, m or ft
det	determinant
d_{jk}	element of the dispersion matrix, j^{th} row, k^{th} column
d_{kk}	k^{th} diagonal element of the dispersion matrix
D	dispersion matrix
$\mathbf{D_i}$	sequential dispersion matrix
$\mathbf{D_1}$	initial sequential dispersion matrix
e	base of natural logarithms
E	input energy, rad^2-sec or deg^2-sec
E{ }	expectation operator
f	state dynamic vector function
F	state dynamic matrix
g	acceleration due to gravity, m/sec^2 or ft/sec^2
G	control matrix
h	output vector function
H	output matrix
i, j, k	indices
IOPTU	integer array containing integer input sequences
IREPU	integer array containing control parameters
I	identity matrix
$\mathbf{I_p}$	p-dimensional identity matrix
I_x	moment of inertia about the x-axis in body axes, kg-m^2 or slug-ft^2
I_y	moment of inertia about the y-axis in body axes, kg-m^2 or slug-ft^2
I_z	moment of inertia about the z-axis in body axes, kg-m^2 or slug-ft^2
j*(i)	output space index of the optimal value function at stage i
j_H	index for the upper side of the initial output space box
j_L	index for the lower side of the initial output space box
J	cost function
l_0	index for the zero control vector
L	log likelihood function
L	moment about the x-axis in body axes, N-m

L(j)	index for the last control at the j^{th} output space box, stage i
m	aircraft mass, kg or slugs ; number of control vector elements
min	minimum of
M	moment about the y-axis in body axes, N-m or ft-lbf
M	information matrix
n	number of state vector elements
$n_{L(j)}$	number of repetitions of $\mathbf{w}_{L(j)}$ at the j^{th} output space box
n_{fc}	number of stages for t_{fc}
n_{mp}	number of stages for t_{mp}
n_{sw}	number of stages for t_{sw}
n_{y_k}	number of output space boxes for the k^{th} constrained output
n_{max}	maximum number of time stages
$n_y(i)$	number of reachable output space boxes at stage i
N	moment about the z-axis in body axes, N-m
N	total number of sample times
$p(...\|...)$	conditional probability
p	roll rate, rad/sec ; number of parameter vector elements
q	pitch rate, deg/sec ; number of output vector elements
$\bar{q}$	dynamic pressure, Pa or lbf/ft^2
r	yaw rate, rad/sec
R	measurement noise covariance matrix
S	wing area, m^2 or ft^2
$\mathbf{S}_i$	i^{th} discrete sensitivity matrix
t	time, sec
t_{fc}	minimum time for final zero control vector
t_{mp}	minimum pulse width time
t_{sw}	control sequencing time
T	test time, sec
Tr	trace
T_{stage}	time for one stage
u(t)	m-dimensional input or control vector at time t
$\mathbf{u}_{old}$	saved control amplitude vector from array UASTR
$u^*(t)$	optimal scalar input
$u_j(t)$	j^{th} component of control vector **u**
U	admissible control set

U_b	admissible control set for "bang-bang" controls
U_j	admissible control set for the j^{th} control vector component
$U_{L(j)}$	admissible control set, last control vector, j^{th} output space box
U_1	admissible control set moving only control vector component 1
U_2	admissible control set moving only control vector component 2
UASTR	array containing saved control amplitudes
V	airspeed, m/sec or ft/sec
$\mathbf{w_1}$, $\mathbf{w_2}$, etc.	distinct m-dimensional square wave control vectors
$\mathbf{x}(t)$	n-dimensional state vector at time t
$\mathbf{y}(t)$	q-dimensional output vector at time t
$\mathbf{y}(i)$	q-dimensional output vector at time $t=i\Delta t$
$y_k(t)$	k^{th} component of output vector y(t)
$\mathbf{y_m}(i)$	q-dimensional measurement vector at time $t=i\Delta t$
y_1 , y_2	constrained output vector components
YLIM	array of boundary values for the constrained outputs
Y	force along the y direction in body axes
Y	one set of N measurement vectors, $\mathbf{y_m}(i)$
Z	force along the z direction in body axes

α	angle of attack, rad or deg
β	sideslip angle, rad
δ_a	aileron deflection, rad
δ_e	elevator deflection, deg
δ_h	symmetric stabilator deflection, deg
$\delta_{i\,j}$	Kronecker delta
$\delta\mu_j$	j^{th} input amplitude constraint decrement (positive constant)
δ_r	rudder deflection, rad
Δt	sampling interval, sec
ε_k	output space discretization for the k^{th} constrained output
ϕ	roll angle, rad
η_c	longitudinal stick deflection, in
η_k	k^{th} output amplitude constraint (positive constant)
ϑ	input sequence to stage i
ϑ_j	input sequence to stage i and output space box j

ϑ^*_j	input sequence to stage i and output space box j with lowest Ψ_i
λ_{max}	maximum eigenvalue
μ_j	j^{th} input amplitude constraint (positive constant), rad or deg
μ_α	control system angle of attack parameter, sec^{-1}
μ_{δ_h}	control system symmetric stabilator parameter, sec^{-1}
μ_{η_e}	control system longitudinal stick parameter, $(in\text{-}sec)^{-1}$
μ_q	control system pitch rate parameter, dimensionless
μ_V	control system velocity parameter, ft^{-1}
σ_k	Cramer-Rao bound for the k^{th} parameter
σ_{k_i}	sequential Cramer-Rao bound for the k^{th} parameter
θ	p-dimensional parameter vector
$\hat{\theta}$	p-dimensional parameter vector estimate
θ_k	k^{th} component of the parameter vector
$\upsilon(i)$	q-dimensional Gaussian noise vector at time $t=i\Delta t$
$\Psi_i(\vartheta)$	value function for input sequence ϑ at stage i
Ψ_i^*	optimal value function at stage i
ζ_k	Cramer-Rao bound goal for the k^{th} parameter

$\forall$	for all, for every
$\lvert \bullet \rvert$	absolute value ; determinant
$\supset$	contains the set
$\in$	belongs to, is an element of
$\mathbf{0}$	zero vector

Superscripts

$^{-1}$	matrix inverse
^{T}	transpose
$\hat{}$	estimate
$\dot{}$	time derivative

Dimensional Stability and Control Derivatives:

Longitudinal

$$M_\alpha = \frac{\bar{q}Sc}{I_y} C_{m_\alpha} \qquad X_\alpha = \frac{\bar{q}S}{mV} C_{x_\alpha} \qquad Z_\alpha = \frac{\bar{q}S}{mV} C_{z_\alpha}$$

$$M_q = \frac{\bar{q}Sc^2}{2VI_y} C_{m_q} \qquad X_V = \frac{\bar{q}S}{mV^2} C_{x_V} \qquad Z_q = \frac{\bar{q}S}{2mV^2} C_{z_q}$$

$$M_{\delta_e} = \frac{\bar{q}Sc}{I_y} C_{m_{\delta_e}} \qquad Z_{\delta_e} = \frac{\bar{q}S}{mV} C_{z_{\delta_e}}$$

$$M_{\delta_h} = \frac{\bar{q}Sc}{I_y} C_{m_{\delta_h}} \qquad X_{\delta_h} = \frac{\bar{q}S}{mV} C_{x_{\delta_h}} \qquad Z_{\delta_h} = \frac{\bar{q}S}{mV} C_{z_{\delta_h}}$$

Where $C_{\gamma_\omega} = \frac{\partial C_\gamma}{\partial \omega}$ for $\gamma = m, x, \text{or } z$ and $\omega = \alpha, \delta_e, \text{or } \delta_h$

and $C_{\gamma_\omega} = \frac{\partial C_\gamma}{\partial \omega \frac{c}{2V}}$ for $\gamma = m$ and $\omega = q$

Lateral

$$L_\beta = \frac{\bar{q}Sb}{I_x} C_{l_\beta} \qquad N_\beta = \frac{\bar{q}Sb}{I_z} C_{n_\beta} \qquad Y_\beta = \frac{\bar{q}S}{mV} C_{y_\beta}$$

$$L_p = \frac{\bar{q}Sb^2}{2VI_x} C_{l_p} \qquad N_p = \frac{\bar{q}Sb^2}{2VI_z} C_{n_p}$$

$$L_r = \frac{\bar{q}Sb^2}{2VI_x} C_{l_r} \qquad N_r = \frac{\bar{q}Sb^2}{2VI_z} C_{n_r}$$

$$L_{\delta a} = \frac{\bar{q}Sb}{I_x} C_{l_{\delta a}} \qquad N_{\delta a} = \frac{\bar{q}Sb}{I_z} C_{n_{\delta a}}$$

$$L_{\delta r} = \frac{\bar{q}Sb}{I_x} C_{l_{\delta r}} \qquad N_{\delta r} = \frac{\bar{q}Sb}{I_z} C_{n_{\delta r}} \qquad Y_{\delta r} = \frac{\bar{q}S}{mV} C_{y_{\delta r}}$$

Where $C_{\gamma_\omega} = \frac{\partial C_\gamma}{\partial \omega}$ for $\gamma = l, n, \text{or } y$ and $\omega = \beta, \delta_a, \text{or } \delta_r$

and $C_{\gamma_\omega} = \frac{\partial C_\gamma}{\partial \omega \frac{b}{2V}}$ for $\gamma = l \text{ or } n$ and $\omega = p \text{ or } r$

Chapter I - Introduction

Aircraft flight tests designed specifically for parameter estimation are generally motivated by one or more of the following objectives:

1. The desire to correlate aircraft aerodynamic characteristics obtained from wind tunnel experiments and aerodynamic calculations with flight test data.

2. Refinement of the aircraft model for control system analysis and design.

3. Accurate prediction of the aircraft response using the mathematical model, including flight simulation and flight envelope expansion.

4. Aircraft acceptance testing.

The design of an experiment to achieve any of the above objectives involves specification of the instrumentation and signal conditioning, the flight test operational procedure, the inputs for the flight test maneuver, the model structure, and the parameter estimation algorithm. In this dissertation, the maneuver design, or, specifically, the design of flight test input signals, will be studied independently of the other aspects which impact the success of the flight test . Other considerations in the flight test design can be accounted for in the detail of the input design problem formulation. The fundamental principles and procedures regarding the design of the input remain unaltered.

In order to obtain the most accurate estimates of aircraft model parameters, the information content in the aircraft response during the flight test must be maximized. In general, an aircraft model contains multiple response variables and multiple aircraft model parameters. The information contained in the aircraft response is embodied in a matrix called the information matrix, whose elements are combinations of partial derivatives of the aircraft response variables with respect to the model parameters. These partial derivatives are called sensitivities, and are obtained by solving the so-called sensitivity equations that result from differentiating the state and output equations for the aircraft model with respect to each of the parameters

in the model. Information matrix elements also depend on the measurement sampling rate, and the measurement noise characteristics, which are indirectly specified when selecting the instrumentation system.

In this work, the model structure is assumed known, and aircraft model parameters are assumed to be estimated from the flight test data using an asymptotically unbiased and efficient parameter estimation technique known as maximum likelihood estimation [1]. It is not necessary that the parameter estimation algorithm be specifically maximum likelihood. Any other asymptotically unbiased and efficient estimator could be used instead. The accuracies of the estimated model parameters are given by parameter standard errors, which are computed as part of the parameter estimation algorithm. The standard error is the value of one standard deviation associated with the estimate of a model parameter. It can be shown that the theoretical best (lowest) values for the parameter standard errors depend only on the information content of the experiment, as embodied in the elements of the information matrix. These theoretical lower bounds on the parameter standard errors are referred to as Cramer-Rao bounds. The Cramer-Rao bounds are independent of the parameter estimation algorithm used to extract parameter estimates and standard errors from the data records, provided that the parameter estimation algorithm is asymptotically unbiased and efficient. Thus, the merit of an input design for aircraft parameter estimation can be determined by examining the Cramer-Rao bounds, since the latter depend only on the information matrix resulting from the response of the aircraft to the application of the input. Comparisons using the Cramer-Rao bounds separate the merits of the input design from the merits of the parameter estimation algorithm used to extract the model parameter estimates from the data. In other words, input designs are compared based only on the information content in the experiment, the latter being calculable before any parameter estimation is done, and thus independently of the particular algorithm used to estimate the values of the parameters.

The performance, and thus the optimality, of an input design depends on the values of the Cramer-Rao bounds associated with that input. Implicit in the computation of the Cramer-Rao bounds is the *a priori* dynamic system and measurement model. When designing inputs for aircraft parameter estimation flight tests, there must be a complete model (including parameter values) of the physical system to use during the process of the input design.

That is, a model complete with parameter values is necessary in order to design an experiment which will produce estimates of the parameters in the model. This has been called the "circularity" problem [2]. For aircraft, the problem is mitigated by use of parameter estimates obtained from either aerodynamic calculations or wind tunnel experiments. The calculation of the Cramer-Rao bounds also implicitly includes the time length of the flight test data run, along with any imposed constraints on either the input form or output response variables.

In the past, research works which addressed the input design problem for airplane parameter estimation used a linear time-invariant dynamic model, where the state variables were perturbations about some trim condition [2] [3] [4] [5] [6] [7] [8]. The most prevalent approach to optimizing the input for aircraft parameter estimation experiments was first done by Mehra [5]. The problem was formulated as a fixed time optimal control problem, with minimization of a time integral of a scalar function of the information matrix as the criterion of optimality. Some difficulty has arisen as a result of the desire to find the best input with respect to a scalar measure of optimality. A scalar norm of the information matrix must be used to encompass the multiple sensitivities contained in the information matrix. Denoting the information matrix by M, previous works have maximized $Tr[M]$, or $\det[M]$, or minimized $Tr[M^{-1}]$, $\det[M^{-1}]$, or $\lambda_{max}[M^{-1}]$ where λ_{max} is the maximum eigenvalue of M^{-1}, among others. There has been some debate as to which matrix norm should be used to obtain the "best" set of parameter standard errors. Reference [6] gives a discussion and review of the different matrix norms used by various researchers. Regardless of the scalar optimality criterion used for the input optimization, comparisons regarding the performance of the designed inputs must always be made by examining the Cramer-Rao bounds, since these are the theoretical lowest parameter standard errors achievable with a given input. The validity of using the Cramer-Rao bounds to assess relative efficacy of input designs for airplane parameter estimation experiments has been verified experimentally [2] [7]. The Cramer-Rao bounds are of principal significance in designing inputs for parameter estimation experiments.

In practice, there are often subsets of the entire parameter set which are of greater importance, and hence need to be estimated with greater accuracy than the remainder of the parameter set. The subsets depend strongly on the

end purpose of the parameter estimates. This situation considerably complicates the problem of choosing a suitable matrix norm of **M** for the optimal input design. In past work, a constant weighting matrix has been introduced in association with the information matrix, **M**, in order to account for varying importance of subsets of the entire parameter set [6].

Researchers who used any of the various matrix norms of **M** to design inputs for aircraft parameter estimation also used a fixed test time [2] [3] [4] [5] [6] [7] [8]. The value of the fixed test time was usually chosen by a heuristic argument based on previous experience. Chen [9] was the first to realize that the true situation in practice is that specific goals for the Cramer-Rao bounds could be specified *a priori*, and that the appropriate goal of the flight test was not to optimize some norm of **M** over a fixed time, but to reduce the (limited and expensive) flight test time required to achieve desired goals for the Cramer-Rao bounds. This approach eliminates the need for any weighting matrices, since the objective has been changed to a direct requirement that Cramer-Rao bounds be less than or equal to specified target values. Parameters with more stringent accuracy requirements are simply assigned lower target values for their respective Cramer-Rao bounds. This procedure implicitly implements parameter weighting. *A priori* Cramer-Rao bound goals are a function of the purpose for which the parameter estimate values are intended, and can be specified by the end user of the parameter estimates. Unfortunately, the Chen approach required extensive iteration and considerable judgment on the part of the analyst for its use. Rather than use an optimization procedure, Chen simply tried a number of candidate input designs, which were generated as members of an orthogonal function set called Walsh functions. Thus, the Chen solution lacked optimality properties, in that no conditions which correspond to an optimal solution (such as a zero gradient of the cost with respect to the input vector) were satisfied.

In many previous works, the input design for aircraft parameter estimation was done with the input subject to an energy constraint consisting of a time integral of the square of the input amplitude. Values used for the energy constraint were presumably based on experience with similar flight test situations. In cases where the optimal input problem has been formulated as an optimal control problem using a scalar norm of the information matrix integrated over a fixed time as the optimality criterion, an

energy constraint on the input was preferred due mostly to the computation simplicity which results from such a constraint. The justification of this constraint form has been that the designed input amplitudes are kept at a reasonable level, since the test time has been fixed, and the resulting output amplitudes are also (indirectly) limited. Another type of input energy constraint was used in the work of Reid [3], who required that the input amplitude be full positive or full negative amplitude at any time during a fixed test time. As shown in Chapter II, this amounts to a constraint on the input energy.

The relatively small number of references for this dissertation reflects the fact that much of the research done on optimal input design addresses energy constrained, single input, single output problems, often in the frequency domain, and often with few (one or two) model parameters. These works were not considered relevant to the general multiple input, multiple output, multiple parameter, relatively short time, optimal input design problem for aircraft parameter estimation, and were therefore omitted from the reference list. To the author's knowledge, the reference list given here represents the significant work in optimal input design for aircraft parameter estimation experiments.

The main purpose of this dissertation is to describe and demonstrate a new approach to the optimal input design problem for aircraft parameter estimation experiments. Motivation for the development of the new technique arose from several important considerations in the modern flight test environment which were either addressed poorly or not at all in previous works. These considerations are briefly outlined below.

Multiple input design - Flight testing of modern aircraft for parameter estimation often requires a multiple input design. Here, "input" can mean either control surface deflections directly, or pilot station inputs, depending on the flight test equipment. Modern aircraft have numerous control surfaces in order to achieve expanded flight envelopes and capabilities, and to improve failure robustness. The work described here provides multiple input design capability in a straightforward way.

Practical output constraints - Two important considerations require that inputs for parameter estimation flight experiments be designed so that output

variable amplitudes remain within specified limits. First, the safety of the pilot and the aircraft requires that output variable amplitudes be constrained, so as to avoid unusual aircraft attitudes from which the pilot cannot recover, or excessive accelerations or rotation rates which may damage the aircraft. Second, since the aircraft model is typically valid only over certain ranges of amplitudes of certain output variables, an experiment which takes the aircraft outside the flight regime where the mathematical model is assumed to be valid degrades the quality of the data for parameter estimation purposes. Previous works relied on the input energy constraint to keep output variable amplitudes reasonable. This approach becomes particularly difficult to use for multiple inputs or closed loop models, along with being unrepresentative of the true practical flight test situation. The present approach includes output amplitude constraints directly as part of the optimal input design problem formulation.

Closed loop models - Many modern aircraft are designed to be open loop unstable in order to enhance performance. This requires the use of full time stability augmentation systems (SAS) which employ automatic closed loop control. These systems cannot be turned off for any length of time because of safety considerations. For this case, it is necessary to include a model of the control system when analyzing the aircraft response, in order to be able to separate the effects of the automatic control system from the open loop aerodynamics of the airframe. The aircraft open loop parameters are of principal interest, since these are required to realize the objectives stated at the beginning of this chapter. The technique described here can accommodate the model structure necessary to design inputs for estimating open loop model parameters under the condition that only closed loop response data are available. The system response must, however, be limited to a region of linear control effectiveness and linear open loop dynamics. When nonlinearities are involved, the appropriate model structure is a function of the particular input used to excite the system [6]. But, the model structure is needed in the first place in order to design the input for parameter estimation purposes. Thus, input design for nonlinear systems involves a complex circularity. The problem of input design for nonlinear models is recognized as important and worthy of attention; however, this problem is also considered outside the scope of the present investigation, and is not

addressed. It was assumed that the capability for imposing arbitrary output amplitude constraints could be used in any flight condition to restrict the system behavior to a regime which could be adequately described by a linear model structure.

Practical control implementation - Regardless of whether a human pilot or a computer implements the designed inputs, it must be assured that the inputs can be realized. This means that control system dynamics should be included in the input design analysis insofar as possible. When a human pilot must implement the input design, allowance must be made for the limited accuracy and repeatability of input forms generated by humans, particularly for the case of multiple inputs. Additional practical limitations pertain to the input amplitude and the input frequency spectrum. It is preferable to include these practical constraints on the input form as an integral part of the analysis and input design procedure. The present approach does this.

Minimum flight test time - Resources are always limited; therefore, the flight test experiment should be designed to minimize the flight test time required to answer the questions which engendered the idea of an experiment. Minimizing the flight test time in the context of the present work is equivalent to designing so that the *a priori* Cramer-Rao bound goals can be achieved in the minimum flight test time. This factor is significant due to the limited availability of flight test aircraft, and the great expense associated with flight testing modern aircraft. In addition, for the case of flight testing at high angle of attack, the time available for flight maneuvers at a given flight condition is limited by altitude loss during the flight test. The approach described here uses the principles of dynamic programming and Bellman's principle of optimality [10] [11] to produce an input which is globally time optimal, subject to the constraints of the problem formulation.

Maximum parameter accuracy for a fixed flight test time - In practical flight test situations, it is often necessary to design an input for a fixed flight test time, chosen *a priori*. The principles of dynamic programming can be applied to this situation as well, rendering a global optimal solution for a chosen cost function which incorporates the minimization of the Cramer-Rao bounds, again subject to the constraints of the problem formulation.

This work is an exposition of a new approach to the optimal input design problem for aircraft parameter estimation experiments, as well as a demonstration of the capabilities of the new technique for producing practical, optimal input designs. The remainder of the dissertation will describe the problem formulation and solution methodology, followed by a summary of the solution algorithm characteristics and three example applications of the new technique. The first example is the solution of a problem studied by other researchers, and demonstrates improved input designs using the new approach. The second example is the solution of a problem not treated elsewhere, which highlights the multiple input capability, output amplitude constraint capability, and the practical input form constraint features included in the new technique. Finally, the third example demonstrates the optimal input design technique as applied to a closed loop model of the F-18 fighter aircraft longitudinal dynamics. A six degree of freedom nonlinear simulation which uses tabular wind tunnel data for the vehicle aerodynamics was used as the test aircraft. A summary and conclusions section completes the dissertation.

Chapter II - Problem Formulation

The goal of the work described here is to design optimal flight test inputs for a parameter estimation experiment. Optimality is a property whose meaning depends on the problem formulation. In general, the problem is specified by the dynamic system and measurement model, the criterion of optimality, the admissible control set, and the applicable constraints. In what follows, each of these aspects of the problem formulation will be discussed regarding its relationship to the physical situation of flight test for parameter estimation.

The dynamic system and output models are linear, with an n-dimensional state vector, $\mathbf{x}$, and system dynamic, control and observation matrices $\mathbf{F}$, $\mathbf{G}$, and $\mathbf{H}$, respectively, which, in general, depend on a p-dimensional parameter vector, $\boldsymbol{\theta}$. The state vector has zero initial conditions. The latter condition indicates the assumption of a perturbation model derived relative to some specified condition. This approach provides known initial conditions, which may be taken as zero with no loss of generality. An input vector, $\mathbf{u}$, of dimension m is assumed. The linear output model has an output vector $\mathbf{y}$ of dimension q, which depends on $\mathbf{x}$ and $\boldsymbol{\theta}$. Amplitude constraints are imposed on all inputs and on selected outputs, and are denoted by μ_j and η_k, respectively. The measurements y_m are made at N sampling times, separated by constant sampling intervals of length Δt, with additive white Gaussian measurement noise, υ. The statistical properties of the measurement noise are assumed known (e.g., from ground calibration of the instrumentation system). The preceding is expressed mathematically as:

$$\dot{\mathbf{x}}(t) = \mathbf{F}(\boldsymbol{\theta})\,\mathbf{x}(t) + \mathbf{G}(\boldsymbol{\theta})\,\mathbf{u}(t) \quad , \quad \mathbf{x}(0) = \mathbf{0} \tag{2-1}$$

$$\mathbf{y}(t) = \mathbf{H}(\boldsymbol{\theta})\,\mathbf{x}(t) \tag{2-2}$$

$$\mathbf{y_m}(i) = \mathbf{y}(i) + \upsilon(i) \qquad i = 1, 2, 3, \ldots, N \tag{2-3}$$

The measurement noise $\upsilon(i)$ is assumed Gaussian with

$$E\{\upsilon(i)\} = 0 \quad , \quad E\left\{\upsilon(i)\,\upsilon^T(j)\right\} = R\cdot\delta_{ij} \tag{2-4}$$

where $E\{\cdot\}$ is the expectation operator, and δ_{ij} is the Kronecker delta.

The following constraints are imposed on input and output amplitudes:

$$\left|u_j(t)\right| \le \mu_j \qquad \forall\, t, \quad j = 1, 2, \ldots, m \tag{2-5}$$

$$\left|y_k(t)\right| \le \eta_k \qquad \forall\, t, \quad k \in (1, 2, \ldots, q) \tag{2-6}$$

Equations (2-1) through (2-6) give the general form of the dynamic system and measurement model used in this work. A linear dynamic and aerodynamic model with multiple inputs is assumed, with amplitude constraints imposed on all inputs and selected outputs.

The issue of the robustness of the input design to inaccuracies in the *a priori* values for the model parameters is not addressed in this work. This problem is important and complex, but cannot be adequately treated here.

For the simple case of a single input, single output model with one model parameter, the best input for a parameter estimation experiment is the input which maximizes the sensitivity of the output quantity to changes in the parameter over the test time, T. This can be expressed as

$$u^*(t) = \max_{u(t)\,\in\,U}\left[\sum_{i=1}^{N}\left(\frac{\partial y(i)}{\partial\theta}\right)^2\right] = \min_{u(t)\,\in\,U}\left[\sum_{i=1}^{N}\left(\frac{\partial y(i)}{\partial\theta}\right)^2\right]^{-1} \tag{2-7}$$

where $u^*(t)$ is the scalar optimal control, U is the set of admissible controls, and the summation over N time points approximates a time integral, with

$$T = N\,\Delta t \tag{2-8}$$

where Δt represents the sample time.

The optimization of an input with respect to the scalar criterion in equation (2-7) is straightforward. In most practical situations of interest, however, there are multiple outputs and multiple model parameters. In this case, the sensitivity of the outputs to changes in the model parameters is embodied in a matrix called the information matrix. As discussed in Chapter I, in this case it is not clear what scalar optimization criterion should be used for the optimal input design. The (p x p) information matrix, **M**, is given by the following expression, derived in Appendix A:

$$\mathbf{M} = \left[\sum_{i=1}^{N} \left(\frac{\partial \mathbf{y}(i)}{\partial \boldsymbol{\theta}} \right)^{T} \mathbf{R}^{-1} \left(\frac{\partial \mathbf{y}(i)}{\partial \boldsymbol{\theta}} \right) \right] \tag{2-9}$$

The (q x p) matrix of sensitivities in the above expression is sometimes referred to as the discrete sensitivity matrix, $\mathbf{S}_i$:

$$\mathbf{S}_i = \frac{\partial \mathbf{y}(i)}{\partial \boldsymbol{\theta}} \tag{2-10}$$

The partial derivatives which appear in the expression for the information matrix are found using the so-called output sensitivity equations, which are obtained by differentiating (2-2) with respect to the components of the parameter vector, $\boldsymbol{\theta}$, denoted by θ_k,

$$\frac{\partial \mathbf{y}}{\partial \theta_k} = \mathbf{H} \frac{\partial \mathbf{x}}{\partial \theta_k} + \frac{\partial \mathbf{H}}{\partial \theta_k} \mathbf{x} \qquad k=1,2,\ldots,p \tag{2-11}$$

The partial derivatives of the state vector, **x**, with respect to θ_k, known as the state sensitivities, are found by differentiating (2-1) and switching the order of the differentiation on the left side of the equation (the latter procedure is valid as long as **x** is analytic, which is assumed) to obtain

$$\frac{d}{dt}\left[\frac{\partial \mathbf{x}}{\partial \theta_k} \right] = \mathbf{F} \frac{\partial \mathbf{x}}{\partial \theta_k} + \frac{\partial \mathbf{F}}{\partial \theta_k} \mathbf{x} + \frac{\partial \mathbf{G}}{\partial \theta_k} \mathbf{u} \qquad k=1,2,\ldots,p \tag{2-12}$$

The (n·p) state sensitivity equations (2-12) must be solved, along with the (n) system dynamic equations (2-1), with the results used in the (q·p) output sensitivity equations (2-11), in order to assemble the information matrix from equation (2-9). All initial conditions for equations (2-12) are zero, since the initial state is assumed to be known. Thus,

$$\frac{\partial \mathbf{x}(0)}{\partial \theta_k} = \mathbf{0} \quad , \quad k = 1,2,\ldots,p \tag{2-13}$$

The information matrix depends on the input indirectly through the output and state sensitivity equations, (2-11) and (2-12), because the state sensitivity dynamics depend on the input **u** directly, and both the output sensitivities and the state sensitivity dynamics depend on **x**, which is a function of **u** by the dynamic equations (2-1).

In Appendix A, it is shown that the inverse of the information matrix is the theoretical lower limit for model parameter covariances computed using any asymptotically unbiased and efficient parameter estimation algorithm with the flight test data used to assemble the information matrix. This theoretical lower limit is often called the dispersion matrix, **D**, and is given by

$$\mathbf{D} = \mathbf{M}^{-1} \tag{2-14}$$

Using (2-9), equation (2-14) may also be written as

$$\mathbf{D} = \left[\sum_{i=1}^{N} \left(\frac{\partial \mathbf{y}(i)}{\partial \boldsymbol{\theta}} \right)^{T} \mathbf{R}^{-1} \left(\frac{\partial \mathbf{y}(i)}{\partial \boldsymbol{\theta}} \right) \right]^{-1} \tag{2-15}$$

or, using (2-10),

$$\mathbf{D} = \left[\sum_{i=1}^{N} \mathbf{S}_i^{T} \mathbf{R}^{-1} \mathbf{S}_i \right]^{-1} \tag{2-16}$$

M and **D** are symmetric, positive definite matrices, since **R** must be symmetric and positive definite, and there can be no zero rows or columns in $\mathbf{S_i}$, as long as the model structure includes all the parameters.

M depends on the input time history; therefore, it follows from (2-14) that the theoretical lower bounds on the parameter covariances are also functions of the input time history. The diagonal elements of the dispersion matrix, **D**, are the theoretical minimum values of the individual parameter variances. The Cramer-Rao lower bounds for the parameter standard errors are given by the square root of the diagonal elements of the dispersion matrix. These values are denoted by σ_k ,

$$\sigma_k = \sqrt{d_{kk}} \quad , \quad k=1,2,...,p \tag{2-17}$$

where d_{jk} are the matrix elements of the dispersion matrix, **D**, i.e.,

$$\mathbf{D} = \left[d_{jk} \right] \quad , \quad j = 1,2,...,p \quad , \quad k = 1,2,...,p \tag{2-18}$$

The k^{th} diagonal element of the dispersion matrix corresponds to the k^{th} parameter in equations (2-11) and (2-12). The σ_k values in equation (2-17) may be thought of as the minimum possible value of one standard deviation (the standard error) for the estimate of the k^{th} parameter.

The present work borrows from Chen's [9] view of the optimal input design problem, in that the flight test time is minimized for attaining Cramer-Rao bound goals which are specified *a priori*. From equations (2-15) and (2-17), the achievable Cramer-Rao bounds from the dispersion matrix are a function of the total test time, T, since $T = N\Delta t$ by equation (2-8). As a result of this, an inferior input design will require a longer test time,T, to achieve specified Cramer-Rao bound goals.

There are actually two optimal input design cases solved in this work, both of which are useful for practical input designs in realistic flight test situations. The two cases are the minimum time optimal input design and the fixed time optimal input design.

In the first case, *the optimal input is that which achieves specified goals for the Cramer-Rao bounds in minimum time, subject to the constraints of*

the problem formulation. This is a minimum time problem, so that the cost, J, is given by

$$J = T \quad \text{when } \sigma_k \le \zeta_k \quad \forall\ k=1,2,\ldots,p \qquad (2\text{-}19)$$

where ζ_k are the goal values for the Cramer-Rao bounds specified *a priori,* and T is now a variable flight test time to be minimized. Minimizing J in equation (2-19) is equivalent to finding the input time history with minimum N in equation (2-15) when the condition $(d_{kk})^{1/2} \le \zeta_k \ \forall\ k=1,2,\ldots,p$ is satisfied.

In the second case, the flight test time, T, is fixed, and *the optimal input is that which achieves minimum Cramer-Rao bounds over a fixed time, T, subject to the constraints of the problem formulation.* This is a fixed time problem, with the cost function

$$J = \sum_{k=1}^{p} \left(\sigma_k \right)^2 \qquad (2\text{-}20)$$

where σ_k are the Cramer-Rao bounds from equation (2-17), and N is fixed in equation (2-15).

In chapter III, the method of solution is outlined for both the minimum time problem, with cost given by equation (2-19), and the fixed time problem, with cost given by equation (2-20). The topic of constraints is addressed next.

In past work, optimal input design for aircraft parameter estimation was carried out with the input subject to an energy constraint of the form:

$$\int_0^T \mathbf{u}(t)^T \mathbf{u}(t)\, dt = E \qquad (2\text{-}21)$$

where E is some fixed value of the allowable input energy. The interval of integration, [0,T], was fixed also, and corresponds to the flight test time. Values used for the energy constraint, E, and the flight test time, T, were typically chosen by heuristic arguments based on experience with similar flight test situations.

In practice, there is no direct constraint on the amount of input energy which can be applied during the flight test, since neither the pilot nor any control system have inherent energy limitations. The practical flight test situation dictates that the constraints be directly on the amplitudes of both the input and the output variables, as given by equations (2-5) and (2-6), respectively. Input amplitude constraints are necessary because any aircraft has limitations on control surface movements due to mechanical stops, flight control software limiters, or linear control effectiveness limitations. In addition, the safety of the aircraft and pilot during the flight test, as well as the validity of the aircraft model, require that selected output variable amplitudes stay below threshold values throughout the flight test. The constraint form (2-21) attempts to achieve all of these practical amplitude constraints in an indirect and imprecise way, in order to reap the benefit of computational simplicity for a fixed time optimal control solution using variational calculus. Use of the constraint (2-21) compromises the effectiveness of the input by not allowing full advantage to be realized within whatever amplitude constraints are imposed on the input and output variables by the circumstances of the flight test. Previous studies have imposed the constraint (2-21), and then, after the design was completed, checked the input and output amplitudes through simulation to make sure that the practical amplitude constraints were not violated during the flight test [2] [3] [4] [5] [7] [8] [9] [12]. The present work solves the optimal input design problem with amplitude constraints imposed directly on the input and output variables as part of the problem formulation. Further background material and rationale for this decision follows.

Define a "bang-bang" input as an input whose amplitude can only be full positive or full negative at any time, which means that the admissible control set, U_b, has only two elements for a scalar input, namely full positive amplitude and full negative amplitude,

$$U_b = \{ +\mu, -\mu \} \tag{2-22}$$

$$u(t) \in U_b \quad , \quad t \in [0,T] \tag{2-23}$$

where $+\mu$ and $-\mu$ are the upper and lower input amplitude constraints, respectively.

For any "bang-bang" input form over a fixed time interval, the energy constraint (2-21) is equivalent to an amplitude constraint. For example, the "bang-bang" input signals shown in figures 1(a) and 1(d) have the same total test time, and different energy, as computed from equation (2-21). It is thus necessary that these signals also have different amplitudes, as can be seen from figures 1(a) and 1(d). In fact, for these fixed time "bang-bang" input forms, energy and amplitude constraints are related by

$$E = \mu^2 T \tag{2-24}$$

For input forms other than the "bang-bang" type, this equivalence of amplitude and energy constraints is not valid; however, in some approximate sense, it may be claimed that the constraint in equation (2-21) amounts to an amplitude constraint on the input when the test time is fixed. The amplitude constraint via an energy constraint is imprecise to the extent that the input form being considered differs from the "bang-bang" type of input form.

In past work, various input designs were compared to one another by designing inputs with the same energy, computed from equation (2-22), and then comparing the resulting diagonal elements of the dispersion matrix resulting from each designed input. As seen from figures 1(a), 1(b), and 1(c), "bang-bang" input forms with the same energy have different amplitudes when the total test time is different. A review of equations (2-9) through (2-18) reveals that the Cramer-Rao bounds from the diagonal of the dispersion matrix are nonlinear functions of the input time history. The preceding statement is true even in the case of linear dynamic and output models, by virtue of equation (2-15). It follows in general that the diagonal elements of the dispersion matrix are nonlinear functions of the input amplitude. Thus, the overall performance of the input design is a nonlinear function of the input amplitude. This fact is highlighted when considering the different responses of a dynamic system to a high amplitude, short duration input such as figure 1(b), as opposed to a low amplitude, long duration input like figure 1(c), which have the same energy, computed from equation (2-21). It is clear that amplitude and test time may be adjusted over wide ranges without changing the input energy, while at the same time

drastically changing the system responses on which the merit of an input design is based. The diagonal elements of the dispersion matrix (σ_k from equation (2-17)) are the "bottom line", so to speak, when comparing various input designs for parameter estimation experiments. The above considerations raise questions regarding the validity of any previous comparisons done among input forms where only the input energy was kept constant. This type of comparison has been done routinely in the literature [2] [4] [6] [7] [9] [12].

Several interrelated attributes characterize an input design. This renders the task of equitable comparison among various input designs problematic. The above discussion concerning figure 1 pointed up the relationship between input amplitude, input energy, and total test time. In light of that discussion, the actual energy constraint on the input form is a composite result of the practical constraints on the input amplitude, the control system dynamics, and the flight test time. Thus, if one assumes the viewpoint that the flight test time should be minimized, there is no way to specify *a priori* what the value of this input energy constraint should be. Even with the test time and input amplitude fixed, control system dynamics can have a significant impact on the value of the input energy, so that it is still difficult to specify the value of the input energy constraint E in equation (2-21), *a priori.*

In general, the input form of figure 1(b) is often more effective in the sense of achieving specific Cramer-Rao bound goals in minimum time, compared to the input form in figure 1(c). This is the result of a more nearly impulsive input to the dynamic system in figure 1(b), even though the input energy is identical to that in figure 1(c). Thus there exists an interplay between allowable amplitude and required test time for given Cramer-Rao bound goals -- higher amplitudes result in shorter test times and lower amplitudes result in longer test times. For fixed time problems, higher input amplitude constraints are associated with potentially lower Cramer-Rao bounds for the same flight test time.

There are further interrelations. Assume now that a fixed output amplitude constraint is imposed, and consider the frequency of the input design in figure 1(a). In order to satisfy the fixed output amplitude constraint, the allowable input amplitude is related to the frequency of the input signal. For example, a low frequency input will require a relatively low amplitude so

that the resulting system output response will remain inside the fixed output amplitude constraint. Higher input frequencies would allow larger input amplitudes. But the dynamic system output response magnitudes depend on input frequency regardless of any constraints on the output amplitudes, since different input frequencies excite different dynamic response modes. This again impacts the allowable input amplitude as a function of the frequency of the input signal. But these effects on input amplitude also impact the required test time for minimum time solutions, or the achievable parameter accuracy for fixed time solutions, as mentioned above. The interrelations among input characteristics are seen to be complex, even for the simple "bang-bang" input forms of figure 1. The complexity arises from the fact that the dynamic system and output equations are involved, along with the matrix inversion of equation (2-15). Input forms other than "bang-bang" (e.g., sinusoidal) are subject to the same arguments in general; however, the issues are more difficult to discern.

In addition to the foregoing, there are practical considerations encountered when attempting to implement an input design in a real flight test environment. One such consideration is that the allowable frequencies contained in the input time history will be limited at the high end, due to limited instrument dynamic response, reduced dynamic system response to high frequency input, and the high frequency limitations of the pilot and control system. Another frequently overlooked issue might be called implementation distortion. This refers to the practical fact that a designed input may be distorted when actually implemented, owing to the limited capabilities of the pilot, or to control system dynamics, such as lag and hysteresis. As might be expected, some input designs are less susceptible than others to these practical difficulties. Accounting for these difficulties during the problem formulation can improve the input design. The optimal input design procedure described in the next chapter successfully addresses these and other constraint issues.

Previous studies of optimal input design for aircraft parameter estimation treated the topic of output constraints superficially. In some cases, the energy constraint on the input given in equation (2-21) was claimed as an indirect constraint on the output amplitudes. It has been argued that this type of indirect constraint on the output is appropriate, due to the gradual degradation of the descriptive capability of linear models with increasing

excursions from the trim condition [2]. However, this gradual degradation cannot be relied on for arbitrary flight conditions. Even if a gradual degradation could be guaranteed, such an approach cannot precisely limit output amplitudes, and thus compromises the effectiveness of the input by possibly not taking full advantage of the system response potential, subject to the practical limits on the output amplitudes. Typically in past studies, a design was completed, and the aircraft response was checked after the fact through simulation to assure that the output amplitudes did not exceed the threshold values. The direct method of including output amplitude constraints in the problem formulation has been alluded to in the literature, but not yet demonstrated, apparently because of the added computational complexity which would be introduced.

For a real flight test situation, it might be argued that the *a priori* model structure and parameter estimates may be an inaccurate description of the physical system to the extent that any claim to a precise control of the real output amplitudes is not valid. Still, a precise control on the output amplitudes for the *a priori* model provides a tool for conservative design of the input in terms of maximum output variable excursions, and thus gives the experiment designer the most control possible over the output variable amplitudes, given the *a priori* model. With precise control over output amplitude excursions, any lack of confidence in an *a priori* model can be compensated for to a controllable and quantifiable extent by using conservative output amplitude constraints during the optimal input design.

Since the input design for aircraft parameter estimation experiments must be done using *a priori* models and parameter values, it is in fact very likely that the *a priori* information does not precisely describe the physical situation (if this were not the case, motivation for the experiment would be lost). As a result, a flight test input design which is conservative as far as the output amplitudes produced, yet still effective relative to information content in the flight test data, is desirable. The task of keeping the aircraft response variables within limits is at odds with the objective of exciting aircraft motion as much as possible in order to obtain accurate parameter estimates. Including the output amplitude constraints directly in the input design problem formulation makes it possible to satisfy the output constraints while maximizing the information content in the data. This capability for conservative input design can help avoid *ad hoc* flight test procedure changes

during flight test operations, and also cut down on flight time requirements by assuring that data from flight test maneuvers can be analyzed using the same model structure used to design the input. For the case of multiple input design with higher order models, the direct inclusion of output constraints into the input design problem formulation is critical for the proper solution of the problem. The importance of output amplitude constraints to the proper design of the optimal input for parameter estimation experiments requires that these constraints be included as part of the problem formulation (equation (2-6)).

In the present work, the admissible control set was comprised of square wave inputs. Square wave inputs are defined as controls whose amplitudes at any time are either full positive, full negative, or zero, so that the admissible control set, U_j, for the j^{th} component of the m-dimensional **u** vector is given by

$$U_j = \{ +\mu_j, 0, -\mu_j \} \tag{2-25}$$

where μ_j is the j^{th} input amplitude constraint, and the j^{th} component of the **u**(t) vector, $u_j(t)$, must take one of the values of U_j at any time,

$$u_j(t) \in U_j \quad , \quad j = 1,2,...,m \quad , \quad t \in [0,T] \tag{2-26}$$

With each of the m components of the control vector able to assume any of three distinct values, it follows that the admissible control set, U, for the m-dimensional control vector, **u**, contains 3^m distinct members,

$$U = \{ \mathbf{w}_1, \mathbf{w}_2, \ldots, \mathbf{w}_{3^m} \} \tag{2-27}$$

where $\mathbf{w}_1$, $\mathbf{w}_2$, etc., are distinct m-dimensional control vectors. The control vector, **u**, must be equal to one of the members of the admissible control set for square wave inputs at any time,

$$\mathbf{u}(t) \in U \quad , \quad t \in [0,T] \tag{2-28}$$

The control vector u(t) represents perturbations about the input required for the nominal or trim condition at the start of the flight test. Thus the (generally nonzero) input associated with the nominal or trim condition is treated as zero deflection for the parameter estimation input. Limiting the possibilities for the input form is useful in the selection of the optimal input because it is easier to select the best input from the lot when the lot becomes smaller. The importance of this restriction on the input form will be made clearer in chapter III when the problem solution is described in detail.

There are several reasons for the rather severe restriction described above concerning the allowable form of the optimal input for parameter estimation experiments. First, in cases where a human pilot implements the designed inputs, the square wave input was considered to have the highest repeatability and lowest potential for implementation distortion. This point is of course rendered moot in the event that the designed inputs are implemented by an automatic control system. Still, the simplicity of the square wave input form makes it easier to account for control system dynamics such as lag and hysteresis, using the solution method described in the next chapter. Such control system characteristics are present regardless of whether a machine or a human is at the controls.

Careful reading of the references suggests the use of a simple square wave input for aircraft parameter estimation experiments. Chen [9] and Reid [3] showed that the minimum flight test time for a simplified problem using a matrix norm of the information matrix as the cost function results in a "bang-bang" optimal control. Mulder [2] and Plaetschke and Schulz [7] evaluated several different input designs in flight, and found that a type of square wave input, the so-called "3211" input (see figure 2), was arguably the best performer overall, although this was not claimed by any of the authors. Gupta and Hall [4] used techniques developed by Mehra [6] to design an optimal input based on a scalar norm of the information matrix. As part of that study, the designed input was approximated by a square wave in order to make the input easier to implement. The authors compared the performance of the optimal input to its square wave approximation through simulation and found that the square wave approximation actually produced lower standard errors for some of the model parameters. Consideration of these results weighed heavily in the decision to restrict the input forms to square waves.

High information content in the data from a flight test is achieved by the use of abrupt, sharp-cornered inputs, since the frequency content for this type of input has a broad range, and thus is good for exciting the various modes of the aircraft response. These response modes have differing frequencies, which of course are not precisely known in the case of flight testing for the purpose of parameter estimation. Inputs comprised of frequencies covering a broad range are therefore superior to inputs with a more limited frequency content, such as a sinusoid. The input design, which necessarily is based on *a priori* models and parameter values, may not include exactly the proper frequencies to properly excite the response modes of the real physical system. Use of wide frequency band signals, such as square waves, is a small hedge against this problem. Interesting experimental data related to this issue has been presented by Mulder [2].

Finally, the restriction on the form of the input is advantageous in the solution algorithm used to compute the optimal input in this study. This point will become clear in the next section, which is concerned with the solution method.

Chapter III - Solution Methodology

The optimal input design problem, as formulated in the preceding chapter, was solved using the principles of dynamic programming [10] [11]. A brief general description of dynamic programming, as applied in this work, is included as Appendix B. In the form of dynamic programming used here, the outputs, sensitivities, and optimality criterion associated with each possible control at each time step are computed, followed by an efficient and sequential solution of the resulting high order combinatorial problem. In this way, the optimal input sequence, in terms of the lowest value of a chosen optimality criterion, can be found for any time period.

There are considerations particular to optimal input design for aircraft parameter estimation which make a solution algorithm based on dynamic programming principles advantageous. These considerations will be highlighted in the course of the description of the solution algorithm, which follows.

Equation (2-6) of Chapter II states that selected model output amplitudes are to be constrained within specified limits. For purposes of illustration, assume that only two such outputs, y_1 and y_2, need to be constrained. The allowable output space at any given time then may be represented by a plane region whose borders correspond to the upper and lower amplitude constraints for y_1 and y_2, see figure 3. The plane region is divided into discrete output space boxes. Time is also divided into discrete steps called stages. The time length of one stage is represented by T_{stage}, and is assumed constant. The constrained outputs of the system are examined at every discrete time, separated by the time T_{stage}. Feasible continuous outputs at any time must be contained in one of the discrete output space boxes for that time. For the aircraft parameter estimation experiment, the initial condition of the constrained outputs is zero, since it is assumed that the model was derived relative to some specified condition. The initial output falls within a specific box in the discretized output space at the initial time. The fact that the initial condition for the problem is known means that only one sweep through time will be necessary for the solution. Assume that a scalar input is to be designed, so that the only input possibilities are full positive amplitude, full negative amplitude, and zero, for a square wave input form. Starting at the initial condition box in discretized output space,

all possible controls are applied over the time length T_{stage}, and the consequences of each control possibility are computed. The consequences of each candidate control include the states, outputs, sensitivities, and cost associated with each control, deferring for the moment the question of how the cost is computed. Fourth order Runge-Kutta numerical integration of the equations of motion (2-1) and the state sensitivity equations (2-12) over the time step T_{stage}, along with calculation of the outputs from equation (2-2) and the output sensitivities from equations (2-11), is required to determine the consequences of each control possibility. Over the period of time T_{stage}, the input is constant and equal to one of the possibilities given by equations (2-25) through (2-28) with m=1. This amounts to allowing scalar square wave input sequences only. The resulting output values fall within one of the discrete output space boxes associated with the next stage, T_{stage} later. The collection of all boxes which have been reached at the next time step might be called the reachable output space at that time. Using the state and state sensitivities of the system corresponding to each box in reachable output space at the next time stage as the new initial conditions, the process of computing the states, outputs, sensitivities, and cost associated with all possible controls is repeated to find the reachable output space for the following stage. If any of the possible controls applied over the time T_{stage} takes an output outside the feasible output space for the next stage, that control is excluded from consideration as part of the optimal input sequence. For figure 3, this means any control which produces an output beyond the output space plane region boundaries at any time would be discarded. This implements the output amplitude constraints in a simple and straightforward way. At this point it is easy to see the importance of keeping the number of possible controls to a minimum, since the consequences of each possible control must be computed for each box in reachable output space at each stage.

For multiple input designs, there are simply more control input possibilities in the admissible control set, U, whose consequences must be computed for each box in reachable output space at each discrete time stage. For m inputs, there would be 3^m different control possibilities. The base three results from there being three choices for the value of each input vector component (full positive amplitude, full negative amplitude, and zero), and the exponent m is the number of elements in the control vector.

At each discrete time stage, the reachable output space is computed as the result of all possible controls starting at the reachable output space boxes found for the preceding time stage. After the computations proceed for several stages, some of the boxes in the reachable output space for a particular stage can be reached from more than one reachable output space box for the preceding stage, perhaps using different controls. Essentially, this means that more than one input sequence can be used to reach the same box in output space at a particular time. The discretization of the constrained output space was done to produce this occurrence. There must be some criterion for deciding which of the input sequences should be preferred to arrive at that box in output space at that time. This criterion is the minimization of a chosen function, which will be referred to as the value function, in keeping with standard dynamic programming terminology. Minimization of the value function is the optimality criterion for the optimal input design.

For the minimum time problem, the objective of the input design is to reach specific goals for the Cramer-Rao bounds in the minimum time. Denote the goal for the Cramer-Rao bound of the k^{th} parameter by ζ_k, and the actual value of the Cramer-Rao bound obtained using a candidate input sequence up to the i^{th} time stage, by σ_{k_i} for the k^{th} parameter, k=1, 2, ..., p. Both σ_{k_i} and ζ_k are positive values. Now define the value function as the square of the shortest Euclidean distance between the point in the p-dimensional space whose coordinates are the Cramer-Rao bounds at a given time, σ_{k_i}, and the p-dimensional parallelepiped on and within which all the goals for Cramer-Rao bounds are achieved. The value function at the i^{th} time stage, $\Psi_i(\vartheta)$, for a candidate input sequence, ϑ, is given by

$$\Psi_i(\vartheta) = \sum_{k=1}^{P} \left(\sigma_{k_i} - \zeta_k \right)^2 \quad \forall\, k \text{ such that } \sigma_{k_i} > \zeta_k \tag{3-1}$$

where the σ_{k_i} depend on the *a priori* model and the candidate input sequence ϑ up to the i^{th} time stage, and ζ_k are constant Cramer-Rao bound goals chosen *a priori*.

Figure 4 depicts the value function calculation for the simple case of two model parameters (p=2). Cases A, B, and C in the figure represent three cases where a nonzero value function is possible for this simple situation.

The location of points A, B, and C would be determined by the computed Cramer-Rao bounds associated with, say, three different inputs, or perhaps the same input sequence at three different times.

In order to use the value function given in (3-1), there must be some way to compute the Cramer-Rao bounds, σ_{k_i}, sequentially. This is in contrast to the usual batch calculation of the dispersion matrix implied by equation (2-15). A sequential dispersion matrix, $\mathbf{D}_i$, calculated at the i^{th} time stage, would give σ_{k_i} values as the square root of its diagonal elements (see equation (2-17)). $\mathbf{D}_i$ would include information from a simulated experiment conducted with a candidate input sequence and the *a priori* model, up to the i^{th} time stage.

The method for this sequential calculation is due to Chen [9], who applied the matrix inversion lemma [13] to equation (2-15) to produce a sequential update expression for the dispersion matrix in the form:

$$\mathbf{D}_{i+1} = \mathbf{D}_i - \mathbf{D}_i \left(\frac{\partial \mathbf{y}(i+1)}{\partial \boldsymbol{\theta}} \right)^T \left[\left(\frac{\partial \mathbf{y}(i+1)}{\partial \boldsymbol{\theta}} \right) \mathbf{D}_i \left(\frac{\partial \mathbf{y}(i+1)}{\partial \boldsymbol{\theta}} \right)^T + \mathbf{R} \right]^{-1} \left(\frac{\partial \mathbf{y}(i+1)}{\partial \boldsymbol{\theta}} \right) \mathbf{D}_i \qquad (3\text{-}2)$$

$\mathbf{D}_{i+1}$ is a symmetric matrix, since $\mathbf{D}$ must be symmetric (see equation (2-15)). Elements of the sensitivity matrix in (3-2) are obtained by solving the state sensitivity equations, (2-12), and the dynamic system equations, (2-1), and then using the output sensitivity equations, (2-11).

The dispersion matrix update in (3-2) produces values of $\sigma_{k_{i+1}}$ for k=1,2,...,p, which give the coordinates of a point in p-dimensional space corresponding to a particular control sequence at the $(i+1)^{th}$ time stage. This sequential calculation allows the association of a scalar value function (from (3-1)) with each candidate input sequence in a manner which is stepwise in time.

From numerical experimentation, it was found that the initial dispersion matrix, $\mathbf{D}_1$, could be made equal to a p-dimensional diagonal matrix having large diagonal elements, with no effect on the calculation of $\mathbf{D}_{i+1}$ past the first sequential update. Thus, the algorithm initializes $\mathbf{D}_1$ as

$$\mathbf{D}_1 = 10{,}000.0 \, (\mathbf{I}_p) \qquad (3\text{-}3)$$

where I_p is a pxp identity matrix.

Each box in the reachable output space at each time stage has a value function, $\Psi_i(\vartheta)$, associated with it, calculated from equation (3-1). As mentioned above, there may be more than one input sequence which results in output response values being contained within a single box in discretized output space. The input sequence which results in the lowest value of $\Psi_i(\vartheta)$ is saved and associated with that particular box, along with the value of $\Psi_i(\vartheta)$. Inferior input sequences with higher $\Psi_i(\vartheta)$ values, which reach the same box in output space, are discarded. This sequential selective process is the manifestation of Bellman's principle of optimality [10] [11], and yields the global optimal input for any reachable output space box at any time stage in terms of the lowest value function. If each reachable discrete output space box is denoted by j, for $j=1,2,\ldots,n_y(i)$, where $n_y(i)$ is the total number of reachable discrete output space boxes at time stage i, then the lowest value function to be associated with each reachable discrete output space box, j, at the i^{th} time stage is denoted by $\Psi_i(\vartheta^*_j)$, and given by

$$\Psi_i(\vartheta^*_j) = \min_{\vartheta_j \in U} \left[\Psi_i(\vartheta_j) \right] \quad , \quad j=1,2,\ldots,n_y(i) \tag{3-4}$$

where the ϑ_j input sequence up to the i^{th} stage produces output in the j^{th} reachable output space box, and the notation $\vartheta_j \in U$ implies that the input sequence ϑ_j is comprised of elements of U which have remained constant for a period of at least one stage time of length T_{stage}. The minimization in equation (3-4) is done by comparing all $\Psi_i(\vartheta_j)$ for a given i and j, and selecting the minimum value. This minimization approach is feasible because the number of $\Psi_i(\vartheta_j)$ for any given i and j is small, due to the discretization of the continuous physical problem.

The fact that this solution process gives the input sequence with the global minimum value function for each reachable output space box at each time can be understood by realizing that this optimality is imposed sequentially from the initial time, and covers all possible (reachable) output space, subject to the chosen output space discretization. This latter condition means that all continuous outputs inside a discrete output space box are

considered the same point in output space. In this way, all of reachable output space at each time is associated with an input sequence ϑ^*_j which reaches that output space at that time with a minimum value function, with the understanding that all continuous output space inside a discrete output space box is treated as the same output.

For the minimum time problem, a zero value of $\Psi_i(\vartheta^*_j)$ corresponds to the achievement of all Cramer-Rao bound goals, since the k^{th} term in the value function summation in equation (3-1) is included only when $\sigma_{k_i} > \zeta_k$. This avoids imposing a penalty for $\sigma_{k_i} \leq \zeta_k$. Thus, to find the minimum time to attain specified Cramer-Rao bound goals, the calculations are stopped at the first time stage where any box, j, in reachable output space is associated with a zero value function, $\Psi_i(\vartheta^*_j)$. The first time stage with zero $\Psi_i(\vartheta^*_j)$ gives the value of the minimum time. The input sequence required to reach that box in reachable output space is the optimal control. Thus, for the minimum time problem, the cost, J, is

$$J = T = (T_{stage})\, i \quad \text{when } \sigma_{k_i} \leq \zeta_k \quad \forall\, k=1,2,\ldots,p \qquad (3\text{-}5)$$

where T_{stage} is the constant stage time. The minimum value of i which satisfies equation (3-5) is called n_{max}, and this integer corresponds to the minimum test time required to achieve all Cramer-Rao bound goals. It follows from equations (3-1) and (3-5) that the integer n_{max} is the index of the first stage which has $\Psi_i(\vartheta^*_j) = 0$ for some $j \in \{1,2,\ldots,n_y(i)\}$. Since $\Psi_i(\vartheta^*_j)$ should be a positive monotonically decreasing function as time goes on (and more information is added), the search for a zero value of $\Psi_i(\vartheta^*_j)$ can be made by finding the smallest value of $\Psi_i(\vartheta^*_j)$ searching over all values of j at a given time stage i. This search will give the optimal value function attainable at any location in feasible output space at the i^{th} time stage. The optimal value function at stage i, Ψ_i^*, is given by

$$\Psi_i^* = \min_{j \in \{1,2,\ldots,n_y(i)\}} \left[\Psi_i(\vartheta^*_j) \right] \qquad (3\text{-}6)$$

So that

$$n_{max} = i \quad \text{when} \quad \Psi_i^* = 0 \tag{3-7}$$

The optimal input sequence up to the i^{th} stage is given by $\vartheta^*_{j^*(i)}$, where $j^*(i)$ is the index j of the optimal value function found from equation (3-6). Then

$$\Psi_i^* = \Psi_i(\vartheta^*_{j^*(i)}) \tag{3-8}$$

and for $i=n_{max}$,

$$\Psi_{n_{max}}{}^* = \Psi_{n_{max}}(\vartheta^*_{j^*(n_{max})}) \tag{3-9}$$

with n_{max} from equation (3-7) in conjunction with equation (3-6).

For the fixed time problem, the solution method is the same, except that the target values for all the Cramer-Rao bounds are set to zero, i.e.,

$$\zeta_k = 0 \quad , \quad k = 1,2,...,p \tag{3-10}$$

and the cost is simply equal to the value function from equation (3-1), with all $\zeta_k = 0$, i.e.,

$$J = \Psi_i(\vartheta) = \sum_{k=1}^{P} \left(\sigma_{k_i}\right)^2 \tag{3-11}$$

The optimal value function, Ψ_i^*, for each time stage, i, is determined in the same way as for the minimum time problem, that is, by equations (3-4) and (3-6). For the fixed time problem, the optimization is stopped after a fixed number of time stages, given by n_{max}, where

$$n_{max} = \frac{T}{T_{stage}} \tag{3-12}$$

Here, T is the fixed test time chosen *a priori*, and T_{stage} is the constant value

of the stage time. The optimization is finished when the number of stages, i, reaches n_{max} , computed from equation (3-12),

$$i = n_{max} = \frac{T}{T_{stage}} \tag{3-13}$$

Equations (3-8) and (3-9) for the optimal input sequence hold exactly as before, with n_{max} now given by equation (3-12).

Equations (3-10) and (3-11) implement an implicit weighting on the parameter accuracies, in that the model parameters with larger absolute values tend to have larger Cramer-Rao bounds σ_{k_i} associated with them, which means that their contribution to the cost in equation (3-11) is larger. In fact, <u>any</u> fixed test time formulation must address the problem of how to weight the relative importance of each parameter accuracy. The scheme used here was found to be most effective in the sense of achieving the lowest Cramer-Rao bounds, because although the optimizer pays more attention to reducing the larger Cramer-Rao bounds, these particular Cramer-Rao bounds also have the most potential for reduction, because the parameters associated with them are large. Large parameters in the model significantly affect the model output, which is equivalent to saying the sensitivity matrix elements associated with these parameters are large. The result is that the complete absence of weighting factors implied by equations (3-10) and (3-11) was found to be the most effective parameter weighting scheme for the fixed time problem.

A fact glossed over until now is that in order to compute the chosen value function in (3-1) or (3-11) recursively, the state sensitivity equations (2-12) must be integrated numerically in time. These equations and the output sensitivity equations (2-11) require that the dynamic system equations (2-1) also be solved, since the state variables appear in the sensitivity equations. At each discrete time stage, a different input sequence, ϑ_j^*, will be associated with the j^{th} reachable output space box. Thus each reachable box in output space has a different state and state sensitivity time history associated with it. In addition, the $p(p+1)/2$ unique elements of a sequentially updated symmetric dispersion matrix, D_i , will also be associated with each reachable box in output space, since the dispersion matrix is a function of the input

sequence through the sensitivities and the system dynamic equations. These considerations point toward a large memory requirement for the solution of the problem.

However, there are aspects of the problem formulation which rescue what would otherwise be a bleak situation in terms of memory requirements. Since the dynamic system model is assumed to be derived relative to some specified condition, the initial conditions on the state and output variables are assumed known and constant for the experiment. The problem of designing inputs for a parameter estimation experiment differs from a general optimal control problem in that a "one time" input sequence (as opposed to a feedback control) is desired for only one initial condition. Thus, only one optimal input sequence beginning at the initial time must be saved for each reachable box in output space at each stage, and the propagation of the dynamic system equations, state sensitivity equations, and the unique elements of the dispersion matrix for each reachable box in output space can be done from stage to stage. Stated another way, the optimal input sequence for all time since the initial time must be saved for any particular reachable box in output space at any stage, but the time histories of the states, state sensitivities, and unique dispersion matrix elements can be discarded for all stages except the immediately preceding stage, since only these immediately preceding values are necessary to propagate the solution. The outputs and output sensitivities can be computed from the states and state sensitivities, and known quantities (see equations (2-2) and (2-11), respectively). Therefore, the variables that must be saved for each reachable box in output space for the current (i^{th}) stage only are given in the top part of Table 1. Since only a few input choices are allowed, each input choice can be associated with an integer index, so that the optimal input sequence, ϑ_j^*, saved for each reachable box in output space at any time stage is a string of integers, one integer for each stage from the initial time to the current time. This is shown at the bottom of Table 1, where array IOPTU holds the integer strings representing ϑ_j^* for each reachable output space box at each time stage. After the input design is completed, and the optimal input sequence determined, the optimal input sequence can be replayed using a numerical integration of the dynamic system equations along with the control system dynamics and the output equations, in order to reconstruct the state and output time histories

associated with the optimal input. This scheme keeps the memory requirement small.

Several special features were incorporated into the basic algorithm described above in order to improve the computed solution. These features are outlined below.

Selection of the output space discretization The chosen size of the output space boxes is important to the optimal input solution. The trade-off is one of increased memory and computation time requirements for more output space boxes versus a compromise of the optimal solution for too few boxes. The number of boxes to be used may be determined by solving the problem repeatedly with an increasingly finer grid for the constrained output variables. When the optimal input design is unchanged in going to a finer grid, the process may be stopped, and the last output space discretization used. The algorithm described in the present work has been designed to facilitate this type of calculation by allowing the number of divisions covering the amplitude range for each constrained output to be specified as input to the program. Combining this information with the output amplitude constraint values (η_k in equation (2-6)), which must also be input to the program, completely specifies the discretization of the output space. If the number of discrete output space boxes for constrained output $y_k(t)$ is denoted by n_{y_k}, the length of the side of the discrete output space box associated with constrained output $y_k(t)$ is given by ε_k ,

$$\varepsilon_k = \frac{2\,\eta_k}{n_{y_k}} \tag{3-14}$$

Then, the dynamic programming grid for constrained outputs $y_k(t)$, $k \in \{1,2,...,q\}$, is set up by computing the boundary values for the discrete output space grid. These boundary values are stored in array YLIM, which is computed by

$$YLIM(k,j) = y_k(0) - \eta_k + (j-1)\,\varepsilon_k \ , \ j=1,2,...,(n_{y_k}+1) \ , \ k \in \{1,2,...,q\} \tag{3-15}$$

where $y_k(0)$ is the known initial value of the k^{th} constrained output, and only the indices corresponding to constrained outputs are used for k. Equations (3-14) and (3-15) specify the dynamic programming grid boundaries for discrete constrained output space.

Selection of the stage time and input frequency spectrum Since control can change only at the discrete time points separated by T_{stage}, and only full positive, full negative, or zero input amplitudes are allowed on each control vector component, it follows that the available input frequency spectrum is influenced by the choice of T_{stage} . In particular, if the high frequency components associated with the sharp corners of a square wave are disregarded, the larger the value of T_{stage} , the more limited the input frequency spectrum palette. Very small values for T_{stage} give the freedom to change the control at more closely spaced times, due to the tight spacing of the stages. In this case, a wider, more nearly continuous frequency spectrum is available to the input design algorithm. A large T_{stage} constrains control changes to be more widely separated in time, corresponding to lower, more widely spaced frequencies in the input. The trade-off is that smaller values of T_{stage} mean more stages for a given time, which means a larger memory requirement, versus the better input frequency resolution available with smaller values of T_{stage}.

The algorithm automatically computes the stage time. Several issues must be weighed to choose the stage time appropriately. On one hand, a small stage time is desirable in order to admit a larger, more nearly continuous field of candidate input frequencies. However, limiting the stage time value on the low end is the memory capacity, particularly for large test times. Even more limiting on the low end for the value of the stage time is what might be called discretization error. If the stage time is very small for a fixed control amplitude, it may happen that application of all control possibilities over one stage time produces output which remains inside the originating box in output space, regardless of the control applied. This happens most apparently at the outset of a single input design, when full positive and full negative controls produce equal value functions. In effect, the algorithm would discard the second of the applied controls (full positive or full negative) as inferior, and in so doing would discard half the subsequent decision tree, and thus seriously compromise the optimal

solution. It is therefore essential that at least one nonzero control application at the outset produce output which travels outside the originating box in output space, and this criterion is used by the algorithm to determine the stage time. For the chosen output space discretization, the equations of motion are integrated from the initial conditions until at least one output crosses a box boundary in discretized output space. The time for this occurrence is designated as the stage time, and calculations proceed as usual. Assume that the initial value of the k^{th} constrained output is between $YLIM(k,j_L)$ and $YLIM(k,j_H)$, that is,

$$YLIM(k,j_L) \le y_k(0) \le YLIM(k,j_H) \quad , \quad k \in \{1,2,...,q\} \qquad (3\text{-}16)$$

Now, the dynamic system equations (2-1) are integrated forward in time using the first nonzero input from equation (2-27), and the resulting outputs are computed from (2-2) until

$$y_k(t) < YLIM(k,j_L) \quad OR \quad y_k(t) > YLIM(k,j_H) \quad , \quad k \in \{1,2,...,q\} \qquad (3\text{-}17)$$

The minimum time for the condition in equation (3-17) to be satisfied for any constrained output, k, is designated the stage time, T_{stage}. So that

$$T_{stage} = \text{minimum t satisfying (3-17)} \qquad (3\text{-}18)$$

With this feature, the minimum stage time possible (equivalently, the widest and most nearly continuous input frequency spectrum) is used for a given selected output space discretization.

Practical upper limit on input frequency If the optimal input design is to be implemented by a pilot, an upper limit exists for the input frequencies which can be implemented, due to human physiology. The algorithm allows specification of this upper limit on frequency in the time domain by providing the means to specify the minimum time for the spacing between control changes. This time is an input to the program, and is denoted t_{mp}.

The program converts this time into an equivalent number of stages, n_{mp}, by the relation

$$n_{mp} = \frac{t_{mp}}{T_{stage}} + 1 \qquad (3\text{-}19)$$

where n_{mp} is an integer, and one count is added to offset the truncation which occurs when assigning a real quotient to an integer variable. The top of Table 1 shows that array IREPU keeps track of important control parameters, including the number of times the last control was applied consecutively for each reachable output space box at the current time stage. To implement the high frequency limit in the time domain, the program simply limits the admissible control set for n_{mp} stages after a control switch to only the last control, i.e.,

$$U_{L(j)} = \{ w_{L(j)} \} \quad , \quad L(j) \in \{1,2,...,3^m\} \qquad (3\text{-}20)$$

where L(j) is the integer index for the last control used to reach the discrete output space box, j, at the current time stage, which is the initial condition for the trial of control possibilities. If $n_{L(j)}$ represents the number of stages control $w_{L(j)}$ has been applied consecutively up to the current stage for the j^{th} discrete output space box, the admissible control set is given by (3-20) as long as

$$n_{L(j)} < n_{mp} \quad , \quad j \in \{1,2,...,n_y(i)\} \qquad (3\text{-}21)$$

where i is the stage index, and $n_y(i)$ is the number of reachable output space boxes for the i^{th} stage. When equation (3-21) no longer holds, the admissible control set reverts to the usual set given in equation (2-27). In this way, an optimal input can be designed including the practical constraint imposed by the speed of reliable human pilot inputs. A similar limitation may be desired when using automatic implementation of the optimal input design for a variety of other reasons, such as instrumentation dynamic response, known control system dynamics, modelling errors related to frequency, or avoiding resonance with aircraft structural modes.

Control system dynamics A basic objection to a true square wave input design is that although the simplicity of its implementation is often touted, in practice, the implementation of a true square wave is impossible, due to the requirement for an infinite control surface displacement rate, see figures 1 and 2. In order to design a truly practical optimal input, the capacity to include control system dynamics was built into the algorithm. The examples in chapter V employ a simple first order lag on the control surface deflections, though other more complicated dynamics could be incorporated. Referring again to the top of Table 1, the input amplitudes resulting from the application of the input sequence ϑ_j^* , including control system dynamics, are saved for each reachable output space box of the current stage. These amplitudes represent the initial control amplitudes for the computations over the next time period of length T_{stage}. The control amplitudes represented by the components of each member of U in equation (2-27) can be thought of as commanded values for the control amplitudes. A scalar function of time, called AMPLAG(t), represents the control system dynamics. Assuming $\mathbf{w_1}$ is the control possibility being examined, and denoting the saved input amplitude vector for the current stage from array UASTR (see Table 1) by $\mathbf{u_{old}}$, the input vector, $\mathbf{u}(t)$, is given by

$$\mathbf{u}(t) = (\mathbf{w_1} - \mathbf{u_{old}}) \cdot \mathrm{AMPLAG}(t - (i-1)T_{stage}) + \mathbf{u_{old}} \qquad (3\text{-}22)$$

For a first order lag with time constant τ, the AMPLAG(t) function is

$$\mathrm{AMPLAG}(t) = 1 - e^{-t/\tau} \qquad (3\text{-}23)$$

The control surface dynamics are included directly in the calculation of the value function associated with each control applied over any stage, and are **not** applied after the fact to make the implementation of the input design practical. This procedure preserves the optimality of the designed input; the input simply has added practical constraints imposed by the dynamics of the control system.

Specification of initial and final input amplitudes As mentioned previously, the input design for aircraft parameter estimation experiments is essentially an input time history superimposed on trim or nominal input amplitudes.

Thus, a desirable feature of an input time history designed for aircraft parameter estimation is that the initial and final input amplitude values be zero. This enhances the safety of the flight test by helping the pilot recover the aircraft from the maneuver. It makes sense to include the requirement that the parameter estimation input begin and end with zero amplitude as an integral part of the optimal input design problem formulation. The algorithm in the present work is capable of implementing this requirement. The forward time evolution is continued until there is a box in output space which satisfies the conditions of optimality given previously, but also has been reached by application of the zero control vector. The time that the final control should be zero is an input to the program, called t_{fc}. This time is converted to a number of stages, n_{fc} , by

$$n_{fc} = \frac{t_{fc}}{T_{stage}} + 1 \qquad (3\text{-}24)$$

where the same comments apply here as to equation (3-19) above. Now in addition to the stopping criterion for the minimum time problem (equation (3-7)) and the fixed time problem (equation (3-13)), another criterion is added for an optimal input ending with zero control deflections. Denote the index for the zero control vector in U by l_0 , $l_0 \in \{1,2,...,3^m\}$, and the control index of the last control for the j^{th} discrete output space box at the current stage by L(j). The number of times this last control was applied is $n_{L(j)}$. The quantities L(j) and $n_{L(j)}$ are saved for the current stage (see top of Table 1). Then the additional stopping criterion is

$$L(j) = l_0 \quad \text{AND} \quad n_{L(j)} \geq n_{fc} \quad , \quad j \in \{1,2,...,n_y(i)\} \qquad (3\text{-}25)$$

where i is the stage index, and $n_y(i)$ is the number of reachable output space boxes for the i^{th} stage. The first stage where this modified stopping criterion is satisfied is the end of the optimization, and all else remains the same. Due to the included control system dynamics, several time stages with a zero control may be required for the input amplitudes to actually return to zero. All the examples presented in the sequel include this requirement as part of the optimal input design.

Automatic adjustment of input amplitude Appropriate values for output amplitude constraints are easily specified *a priori* from physical considerations related to the safety of the aircraft and pilot, and the validity of the model. Input amplitude constraint values are not as easily chosen, since they may be strongly related to the imposed output amplitude constraints. For the aircraft parameter estimation problem, the starting point for input amplitude constraint values are the physical limits on control deflection, as implemented by mechanical stops, flight control software limiters, or linear control effectiveness. In general, higher input amplitudes give more system excitation per unit time, so that the accuracy requirements for the parameter estimates are achieved in a shorter time or more parameter accuracy is available for a fixed time. Thus, if no output amplitude constraints were imposed, the maximum input amplitude possible would be preferred. When output constraints are imposed, as is commonly the case, it may occur that the input amplitude is so large that feasible outputs are produced only when the controls are applied at the initial time. For example, assume that all controls applied at the second stage, starting from an output space box different from the initial box, produce output which travels outside feasible output space. In this case, all controls are disallowed, there are no reachable output space boxes for the next stage, and no optimal control exists. This problem is exacerbated by the maximum input frequency limit feature described above, since that feature specifies a minimum pulse width for each control. The algorithm has the capability to recognize this problem. This is done by setting a flag when the only feasible outputs computed for any stage beyond the second stage originate from the initial output condition. Corrective action consists of decreasing the input amplitude constraint by an amount which can be specified, and restarting the algorithm. Denote the input amplitude decrements by $\delta\mu_j$ for j=1,2,...,m. These input amplitude decrements are positive-valued inputs to the program. Then the input amplitude constraints are modified by

$$\mu_j = \mu_j - \delta\mu_j \quad , \quad j=1,2,...,m \tag{3-26}$$

At this point, the algorithm is restarted. This iterative procedure ensures that the maximum possible input amplitude is used for the input design, consistent with the imposed output amplitude constraints. The input amplitudes are determined directly and iteratively as a function of imposed constraints on the output amplitudes and the practical limits for the maximum input amplitudes, all of these being easily specified in practice. Another occurrence which requires equation (3-26) can be called a monotonic optimal value function violation. This situation arises when the optimal value function for the i^{th} stage, Ψ_i^* from equation (3-6), is substantially larger than Ψ_{i-1}^*, the optimal value function from the preceding stage. In this case, the imposed output amplitude constraints are severely compromising the optimal solution. The problem is also addressed by reducing the input amplitude constraint using equation (3-26), and restarting the algorithm.

Multiple input switching Multiple input design for aircraft parameter estimation experiments presents another practical difficulty, namely the coordination of the controls by a human pilot. In particular, a pilot may be unable to implement an input design where more than one input is changing at the same time in a relatively complicated fashion. To combat this problem, the optimal input design algorithm provides the capability to specify time periods where only one control will be allowed to vary from zero. This amounts to additional restrictions on the allowable controls at any given time stage and is an additional constraint on the form of the input. Assume that the control vector, **u**, has only two components (m=2). The time length during which only a single control vector component is allowed to move is an input to the program, called t_{sw}. This time is converted to an equivalent number of stages in the manner described previously,

$$n_{sw} = \frac{t_{sw}}{T_{stage}} + 1 \qquad (3\text{-}27)$$

Now denote the subset of the admissible control set U which moves only one control vector component, including the zero control vector, by U_1. Then,

$$U \supset U_1 \qquad (3\text{-}28)$$

where in the case under consideration (m=2), U has 3^2 elements, and

$$U_1 = \left\{ \begin{bmatrix} +\mu_1 \\ 0 \end{bmatrix}, \begin{bmatrix} 0 \\ 0 \end{bmatrix}, \begin{bmatrix} -\mu_1 \\ 0 \end{bmatrix} \right\} \tag{3-29}$$

U_1 represents the admissible control set for square wave inputs moving only the first component of the control vector. As long as

$$i \leq n_{sw} \tag{3-30}$$

where i is the stage counter, then the admissible control set is given by U_1. When $i > n_{sw}$, the admissible control set changes to U_2, where

$$U_2 = \left\{ \begin{bmatrix} 0 \\ +\mu_2 \end{bmatrix}, \begin{bmatrix} 0 \\ 0 \end{bmatrix}, \begin{bmatrix} 0 \\ -\mu_2 \end{bmatrix} \right\} \tag{3-31}$$

The extension to more than two components in the control vector is straightforward. The control switching time length, t_{sw}, is constant for all control vector components, and the control sequencing is fixed, in the interest of simplicity. Modifications could easily be made in the direction of more sophistication. This additional constraint on the form of the optimal input (or any additional input form constraint, for that matter) actually decreases the computation time for the optimal input design, since fewer control choices must be considered for any reachable output space box at any time stage.

Chapter IV - Summary of Algorithm Characteristics

The following list with brief descriptions summarizes the features of the algorithm developed in this work for designing optimal inputs for aircraft parameter estimation.

Global optimum solution - Expensive flight test time is minimized by formulating the problem as a minimum time problem. The global minimum time solution is the input sequence for the shortest flight test required to reach target values for the Cramer-Rao bounds. The global optimum fixed time input design is achieved by setting target values for the Cramer-Rao bounds to zero, and choosing the input sequence associated with the lowest Cramer-Rao bounds at the final time. Both solutions are globally optimal by virtue of Bellman's principle of optimality [10] [11], which is the *modus operandi* of the algorithm. As with any other optimal solution, the optimality is meaningful only in the context of the problem formulation, which was given in Chapter II.

Multiple input design capability - Multiple input problems increase the number of input choices whose consequences must be evaluated for each reachable output space box at each time stage. The result is an increase in the computation time required to solve the optimal input problem. This is to be expected, since the multiple input problem is inherently more complicated. The solution algorithm has been formulated so that the additional memory required to solve a multiple input problem is small.

Closed loop model capability - The program was designed in a modular fashion, so that various linear system dynamic and output models could be used. The algorithm can accommodate a model structure for linear closed loop models, thus allowing the design of optimal inputs for open loop airframe parameters when only closed loop data are available.

Practically achievable input design - Constraints on the input form were incorporated to alleviate repeatability and coordination problems which might be encountered when a human pilot is used to implement flight test inputs, particularly for a multiple input design. In addition, the algorithm

includes control system dynamics directly in the calculation of the optimal input design. This addresses the problem of implementation distortion, which would otherwise degrade the efficacy of the designed input.

Direct implementation of output amplitude constraints - Inclusion of the output amplitude constraints in the problem formulation results in an input design which excites the system response modes to the fullest extent possible, but no further. This characteristic is important for a optimal input design in the practical sense.

Input frequency chosen in the time domain - Control changes may occur only at discrete time points which are separated by one stage time. For square wave input forms, this means that the input frequency spectrum will be chosen by the determination of the optimal time for the input to switch. These switching times for the input will be optimal to within plus or minus one stage time. The algorithm automatically determines the minimum usable stage time, based on the output space discretization. This ensures that the widest and most nearly continuous input frequency spectrum is considered in the design of the optimal input. Practical constraints on the input frequency spectrum resulting from inherent characteristics of the pilot, flight test operational procedure, and the control system dynamics are implemented in the time domain.

Single pass solution - The solution algorithm described here requires no iterative calculations or special start-up procedures. The optimal input solution is obtained in a single pass, which marches stepwise forward in time. When the problem solution is not possible with the specified input and output constraints, the algorithm decreases the input amplitude and restarts the solution. However, this iteration is on the proper conditions for the problem solution, and not on the solution *per se*.

Well-suited to design studies - The algorithm presented here can be used for a meaningful trade-off design study of optimal input design for aircraft parameter estimation. For example, the analyst can easily examine the effect of changes in measurement noise characteristics, Cramer-Rao bound goals, input amplitude constraints, output amplitude constraints, or control system

dynamics in terms of their effect on the required flight test time or achievable parameter accuracies.

To complete the picture, drawbacks of the algorithm are listed and described below.

Memory requirement - A requirement for a large amount of memory is inherent in dynamic programming solutions to optimal control problems. The originator of the dynamic programming approach, Richard Bellman, has referred to this problem as " the curse of dimensionality " [10] [11]. In the present work, the memory requirements were kept to reasonable levels by taking advantage of characteristics peculiar to the problem of optimal input design for aircraft parameter estimation. These characteristics are the "one time" nature of the input design, the fact that the dynamic model was formulated relative to a specified initial condition, and the limitations which could be legitimately imposed on the form of the input. For this work, memory requirements were impacted most significantly by the number of constrained output variables required, the output space discretization, and the maximum number of time stages. To a much lesser extent, the model order and the number of parameters in the model increased memory requirements as well. While more complex problems will naturally increase memory requirements, this is not seen as a serious problem for several reasons. First, the algorithm has been designed with an eye toward minimizing the memory requirements, in a time when the run-time memory of new computers is increasing at a rapid pace. In addition, the current version of the program can handle a sixth order dynamic system model, with twelve model parameters, two inputs, two constrained outputs, and a maximum of one hundred fifty time stages, with still some room for expansion. The current capability will be sufficient for many practical problems of interest.

Run time requirement - The required run time depends mainly on the model order, the number of model parameters, the output space discretization, and the number of control choices available for each output space box at each time stage. To give some idea of the execution time required, using a Digital Vaxstation II, the open loop single input example presented in this work took about 3 minutes for a 3.2 second input design.

Chapter V - Examples

Example 1

The first example was investigated previously by Mehra [5] and subsequently by Chen [9]. The problem is to design a single input for the purpose of estimating the parameters contained in an approximate model of the short period dynamics for an airplane. The model is given by

$$\begin{bmatrix} \dot{\alpha} \\ \dot{q} \end{bmatrix} = \begin{bmatrix} Z_\alpha & 1 \\ M_\alpha & M_q \end{bmatrix} \begin{bmatrix} \alpha \\ q \end{bmatrix} + \begin{bmatrix} Z_{\delta_e} \\ M_{\delta_e} \end{bmatrix} \delta_e \tag{5-1}$$

where α is the angle of attack, q is the pitch rate, and δ_e is the elevator deflection. The output model is

$$\begin{bmatrix} y_1(t) \\ y_2(t) \end{bmatrix} = \begin{bmatrix} 1 & 0 \\ 0 & 1 \end{bmatrix} \begin{bmatrix} \alpha(t) \\ q(t) \end{bmatrix} \tag{5-2}$$

The measurement equations are

$$\begin{bmatrix} y_{m_1}(i) \\ y_{m_2}(i) \end{bmatrix} = \begin{bmatrix} 1 & 0 \\ 0 & 1 \end{bmatrix} \begin{bmatrix} y_1(i) \\ y_2(i) \end{bmatrix} + \begin{bmatrix} \upsilon_1(i) \\ \upsilon_2(i) \end{bmatrix} \qquad i = 1, 2, \ldots, N \tag{5-3}$$

$$\upsilon(i) = \begin{bmatrix} \upsilon_1(i) \\ \upsilon_2(i) \end{bmatrix} \tag{5-4}$$

where $\upsilon(i)$ is the i^{th} realization of a zero-mean Gaussian white noise vector random process with the following measurement noise covariance matrix:

$$\mathbf{R} = \begin{bmatrix} 2.0 & 0.0 \\ 0.0 & 1.0 \end{bmatrix} \tag{5-5}$$

The *a priori* values of the model parameters are the true values for the parameters, given in Table 2. The physical system is the system given above using the true parameter values from Table 2, which means that there is no modelling error in the *a priori* model. For this problem, Mehra [5] used a fixed time for the flight test data run, and maximized the trace of the information matrix (see equation (2-9)), subject to an energy constraint on the input of the form given in equation (2-21), i.e.:

$$\int_0^T \left[u(t)\right]^2 dt = E \tag{5-6}$$

where T=4.0 seconds and E=311. Figure 5 shows the Mehra input design, and the associated time histories for α and q. The third column of Table 2 gives the performance of this input design in terms of the Cramer-Rao bounds.

In reference [9], Chen solved the identical problem using the same energy constraint on the input. Instead of minimizing some scalar norm of the information matrix, the minimum time required to achieve the parameter accuracy represented by the Cramer-Rao bounds from the Mehra input was sought. The procedure used was iterative, and assumed the input form to be a member of an orthogonal set of Walsh functions, which are "bang-bang" input forms. The solution obtained was suboptimal, and is shown in figure 6, with resulting Cramer-Rao bounds given in the fourth column of Table 2.

The new technique for optimal input design was used to find the minimum time solution for square wave input forms for the same problem. Since no energy constraint of the form (5-6) was imposed, the problem was solved for two cases - once using the maximum input amplitude of the Chen solution as an input amplitude constraint, and a second time using the maximum input amplitude of the Mehra solution. The results for the former case are shown in figure 7, while the results for the latter case are given in figure 8. Values for the Cramer-Rao bounds for these inputs appear in columns 5 and 6 of Table 2.

The problem was solved a third time using the technique developed in the present work. Input amplitude was again constrained to be the same as the Mehra solution, but this time a first order control system lag was

included, with time constant equal to 0.1 second. The input design and output variable time histories are given in figure 9. The resulting Cramer-Rao bounds for the parameters are given in column 7 of Table 2.

The Cramer-Rao bounds in Table 2 for the input designs of Mehra and Chen were obtained with the same computing means used to obtain the Cramer-Rao bounds for the optimal input designs generated by the technique described in this dissertation. That is, only the form of the input was borrowed from the works by Mehra and Chen ; the resulting Cramer-Rao bounds were computed with the same computer and algorithm (equation (2-11) and numerical solution of (2-1) and (2-12)). This was done in the interest of a fair comparison among the input designs.

The input designs associated with the present work included the stipulations that the input begin and end with zero amplitude, and the minimum pulse width was set at 0.6 second. In addition, the α and q output variables were constrained to $\pm$ 10 degrees and $\pm$ 12 degrees per second respectively, so as to limit output variable excursions to values similar to those obtained from the Mehra and Chen input designs. The sampling interval, Δt, was set at 0.02 second. The goals for the Cramer-Rao bounds were taken to be the values associated with the Mehra input, from column 3 of Table 2. Thus, the objective for the optimal input designs was to attain these goals in minimum time.

Column 5 of Table 2 shows the results of the present work using the same input amplitude as for the Chen design. A lower value of total time is attained by giving up some accuracy on the Z force parameters, while picking up some additional accuracy on the moment equation parameters. All Cramer-Rao bounds are lower than the Mehra input values, as required. This trade-off among the parameter accuracies beneath the goal values in order to achieve a smaller test time was done implicitly and automatically by the algorithm, thus obviating the need for parameter weighting and all the *ad hoc* procedures that usually accompany it. Maximum output amplitudes were virtually the same as for the Chen input design, and lower than those for the Mehra input design, as required by the output constraints built into the solution algorithm (see figures 5,6, and 7).

The results in column 6 of Table 2 demonstrate that if the higher maximum input amplitude of the Mehra design is used as an input amplitude constraint, the goals for the Cramer-Rao bounds can be achieved in

an even smaller total time. All Cramer-Rao bounds were below their respective goal values from the Mehra input in column 3 of Table 2. Output variable amplitudes were again within their constrained ranges, see figure 8. This case demonstrates some of the points made in chapter II regarding input characteristics and the appropriate types of constraints for aircraft parameter estimation experiments.

The effect of including a control system lag on the input design solution is given in the last column of Table 2. Cramer-Rao bounds were again less than the goal values from the Mehra input for every parameter, as required. These accuracies were virtually the same as in column 6, but required a test time increase of 0.16 second. This slightly longer test time was expected, since the higher frequencies associated with the sharp corners of a square wave input were filtered out by the control system lag. Output variable amplitudes were again within their constrained ranges, see figure 9.

Table 3 shows the results of maximum likelihood estimation of the model parameters, based on simulated flight test runs using each of the input designs discussed above and listed in Table 2. Excellent agreement was obtained between the parameter standard errors in Table 3, and the Cramer-Rao lower bounds for these standard errors, given in Table 2. This exceptional agreement was due mainly to the fact that no modelling error existed for the simulated flight tests and the measurement noise was precisely known. Real flight test situations do not enjoy such luxuries. As a result, the performance of the input designs would be degraded in a real flight test situation. However, Mulder [2] has presented experimental evidence that the relative merits of various input designs based on the Cramer-Rao bounds remain intact when applied in a real flight test environment. This was demonstrated likewise for the simulated flight test results in Table 3.

The results in Tables 2 and 3 and figures 5 through 9 demonstrate the quality of the input designs which result from the problem formulation and solution algorithm described in this dissertation.

Example 2

This example exhibits the expanded capability of the input design algorithm by computing the optimal input for a fourth-order model with twelve model parameters and two inputs, subject to restrictive output amplitude constraints.

The lateral dynamics of an advanced fighter aircraft in level flight at 10,000 m altitude and an airspeed of 179.7 mps may be represented by the following dynamic system and measurement model :

$$\begin{bmatrix} \dot{\beta} \\ \dot{p} \\ \dot{r} \\ \dot{\phi} \end{bmatrix} = \begin{bmatrix} Y_\beta & 0 & -1 & g/V \\ L_\beta & L_p & L_r & 0 \\ N_\beta & N_p & N_r & 0 \\ 0 & 1 & 0 & 0 \end{bmatrix} \begin{bmatrix} \beta \\ p \\ r \\ \phi \end{bmatrix} + \begin{bmatrix} 0 & Y_{\delta_r} \\ L_{\delta_a} & L_{\delta_r} \\ N_{\delta_a} & N_{\delta_r} \\ 0 & 0 \end{bmatrix} \begin{bmatrix} \delta_a \\ \delta_r \end{bmatrix} \tag{5-7}$$

where β is the sideslip angle, p is the roll rate, r is the yaw rate, ϕ is the roll angle, δ_a is the aileron deflection, and δ_r is the rudder deflection. The output is given by

$$\begin{bmatrix} y_1(t) \\ y_2(t) \\ y_3(t) \\ y_4(t) \end{bmatrix} = \begin{bmatrix} 1 & 0 & 0 & 0 \\ 0 & 1 & 0 & 0 \\ 0 & 0 & 1 & 0 \\ 0 & 0 & 0 & 1 \end{bmatrix} \begin{bmatrix} \beta(t) \\ p(t) \\ r(t) \\ \phi(t) \end{bmatrix} \tag{5-8}$$

The constraints are

$$| \delta_a | \leq 0.07 \text{ radians} \quad \forall t \tag{5-9}$$

$$| \delta_r | \leq 0.07 \text{ radians} \quad \forall t \tag{5-10}$$

$$| y_1(t) | \leq 0.15 \text{ radians} \quad \forall t \tag{5-11}$$

$$| y_4(t) | \leq 1.0 \text{ radians} \quad \forall t \tag{5-12}$$

The measurement equations are

$$\begin{bmatrix} y_{m_1}(i) \\ y_{m_2}(i) \\ y_{m_3}(i) \\ y_{m_4}(i) \end{bmatrix} = \begin{bmatrix} 1 & 0 & 0 & 0 \\ 0 & 1 & 0 & 0 \\ 0 & 0 & 1 & 0 \\ 0 & 0 & 0 & 1 \end{bmatrix} \begin{bmatrix} y_1(t) \\ y_2(t) \\ y_3(t) \\ y_4(t) \end{bmatrix} + \begin{bmatrix} \upsilon_1(i) \\ \upsilon_2(i) \\ \upsilon_3(i) \\ \upsilon_4(i) \end{bmatrix} \quad i = 1, 2, \ldots, N \tag{5-13}$$

$$\boldsymbol{\upsilon}(i) = \begin{bmatrix} \upsilon_1(i) \\ \upsilon_2(i) \\ \upsilon_3(i) \\ \upsilon_4(i) \end{bmatrix} \tag{5-14}$$

where $\boldsymbol{\upsilon}(i)$ is the i^{th} realization of a zero-mean Gaussian white noise vector random process with the following measurement noise covariance matrix:

$$\mathbf{R} = \begin{bmatrix} 0.000361 & 0.0 & 0.0 & 0.0 \\ 0.0 & 0.04 & 0.0 & 0.0 \\ 0.0 & 0.0 & 0.0064 & 0.0 \\ 0.0 & 0.0 & 0.0 & 0.0059 \end{bmatrix} \tag{5-15}$$

The values for the diagonal elements of **R** in equation (5-15) are derived from information in reference [14] concerning appropriate data system characteristics for aircraft parameter estimation experiments. These values represent random fluctuations due to the instrumentation system only, and thus do not include such real effects as modelling error and gusts, which typically manifest themselves in the measurement noise.

As in the last example, the physical system is represented by the model structure given above using the true values of the parameters, which are also assumed to be the *a priori* parameter values. The true values of the model parameters are given in Table 4. The above model does not correspond to any existing fighter aircraft or instrumentation system. The nominal values used are for demonstration purposes only, although the model structure is quite generally applicable.

The output amplitude constraints imposed on the sideslip angle and the roll angle are such that a straightforward input design using past experience and heuristic arguments is difficult. A common practical input design procedure employs doublets in the rudder and aileron with frequencies close to the damped natural frequency of the aircraft Dutch roll mode. This type of input is shown in figure 10. A first order lag with time constant 0.1 second was implemented to model pilot and control system actuation delay. By trial and error, an input amplitude of 0.07 radian was found to satisfy the output amplitude constraints using the doublet inputs. Cramer-Rao bounds associated with this 10 second input design appear in column 3 of Table 4.

For the optimal input designs, input amplitude constraints were applied instead of input energy constraints, as discussed previously. The same input amplitude constraints were used for both control surfaces (see equations (5-9) and (5-10)), and the controls were sequenced, with the control switching time, t_{sw} , set to 5 seconds, and the rudder control sequenced first. Maximum input frequency depends on the minimum pulse width. For this problem, the assumption was that 0.6 seconds was the minimum time necessary to acquire a control amplitude and return the control to zero (i.e., nominal or trim) deflection.

In order to allow comparison with the doublet inputs, the optimal input design technique was used to produce a fixed time design by setting the goals for all Cramer-Rao bounds to zero, and limiting the run of the input design program to a maximum of 10 seconds. The resulting input design and output responses appear in figure 11. The Cramer-Rao bounds were lowered for all parameters (compare columns 3 and 4 of Table 4), with all output amplitude constraints satisfied.

In figure 12, the optimal input design was performed for the same problem using a larger (0.1 radian) input amplitude constraint on both inputs. Allowing a larger input amplitude constraint means that there is potential for more system excitation over a fixed time, compared to a case with a lower input amplitude constraint. Thus, one would expect a shorter test time to be required to reach the same Cramer-Rao bound goals, provided that the output amplitude constraints can be enforced with the larger input amplitude. For the case shown here, a minimum time solution was computed. The goals for the Cramer-Rao bounds were the accuracies associated with the doublet

inputs in column 3 of Table 4. The same accuracy or better for each parameter relative to the doublet inputs case was obtained in a shorter total test time of 8.7 seconds, as shown in column 5 of Table 4.

For all input designs presented thus far, the control inputs were sequenced; that is, only one control was moved at a time. This feature is helpful when human pilots must implement the input design. For cases when a computer can realize the inputs, the requirement for sequenced control inputs can be relaxed. This case is shown in figure 13, using the same input amplitude as in figure 12. Again, a fixed time solution was computed by setting all goals for the Cramer-Rao bounds to zero with a 10 second maximum test time. Columns 5 and 6 of Table 4 show that a gain of at least 25% in accuracy for all parameters except those associated with the Y force was achieved for a 10 second total test time by relaxing the control sequencing requirement. The improvement in the Cramer-Rao bounds for column 6 of Table 4 relative to the Cramer-Rao bounds for the doublet inputs ranges from 19.0% for Y_β to 72.4% for N_β, based on the Cramer-Rao bounds for the doublet inputs. All optimal input designs excited the aircraft response as much as possible to obtain small Cramer-Rao bounds, but still kept the output response within the imposed amplitude constraints.

This example demonstrates the computation of practical, optimal, multiple input designs. In addition, the effects of increased input amplitude constraint values and relaxing the input sequencing were easily quantified in terms of lower Cramer-Rao bounds for a fixed time design, or reduced flight test time required to achieve fixed target values for the Cramer-Rao bounds for a minimum time design. The effects were precisely quantifiable because of the global optimality of the solutions.

Example 3

In this final example, the optimal input design technique is used under conditions which mimic a real flight test situation. The test aircraft is a six degree of freedom nonlinear simulation of the F-18 fighter aircraft [15]. Only the longitudinal dynamics of the aircraft are considered.

The F-18 aircraft is designed with inherent longitudinal static instability, in order to enhance maneuverability and performance. As a result of this, the aircraft must operate under closed loop automatic control at all times during the flight test for safety considerations.

The flight condition is 20,630 ft. altitude and 8 degrees angle of attack at trim. Geometry and mass characteristics are given in Table 5. The open loop dynamic model is:

$$\begin{bmatrix} \dot{V} \\ \dot{\alpha} \\ \dot{q} \end{bmatrix} = \begin{bmatrix} X_V & X_\alpha & 0 \\ 0 & Z_\alpha & Z_q \\ 0 & M_\alpha & M_q \end{bmatrix} \begin{bmatrix} V \\ \alpha \\ q \end{bmatrix} + \begin{bmatrix} X_{\delta_h} \\ Z_{\delta_h} \\ M_{\delta_h} \end{bmatrix} \begin{bmatrix} \delta_h \end{bmatrix} \tag{5-16}$$

where V is the airspeed, α is the angle of attack, q is the pitch rate, and δ_h is the symmetric stabilator deflection. The output is

$$\begin{bmatrix} y_1(t) \\ y_2(t) \\ y_3(t) \end{bmatrix} = \begin{bmatrix} 1 & 0 & 0 \\ 0 & 1 & 0 \\ 0 & 0 & 1 \end{bmatrix} \begin{bmatrix} V(t) \\ \alpha(t) \\ q(t) \end{bmatrix} \tag{5-17}$$

subject to the constraints

$$| y_1(t) | \leq 2.5 \text{ ft/sec} \quad \forall t \tag{5-18}$$

$$| y_2(t) | \leq 0.035 \text{ radians} \quad \forall t \tag{5-19}$$

The measurement equations are

$$\begin{bmatrix} y_{m_1}(i) \\ y_{m_2}(i) \\ y_{m_3}(i) \end{bmatrix} = \begin{bmatrix} 1 & 0 & 0 \\ 0 & 1 & 0 \\ 0 & 0 & 1 \end{bmatrix} \begin{bmatrix} y_1(i) \\ y_2(i) \\ y_3(i) \end{bmatrix} + \begin{bmatrix} \upsilon_1(i) \\ \upsilon_2(i) \\ \upsilon_3(i) \end{bmatrix} \quad i = 1, 2, ..., N \tag{5-20}$$

$$\boldsymbol{\upsilon}(i) = \begin{bmatrix} \upsilon_1(i) \\ \upsilon_2(i) \\ \upsilon_3(i) \end{bmatrix} \tag{5-21}$$

where $\boldsymbol{\upsilon}(i)$ is the i^{th} realization of a zero-mean Gaussian white noise vector random process with the following measurement noise covariance matrix:

$$\mathbf{R} = \begin{bmatrix} 0.25 & 0.0 & 0.0 \\ 0.0 & 2.22\text{x}10^{-7} & 0.0 \\ 0.0 & 0.0 & 1.10\text{x}10^{-5} \end{bmatrix} \tag{5-22}$$

A problem in designing an optimal input for this open loop model is that δ_h , the stabilator deflection, is not under direct control of the designer. The deflection of this control surface is a function of flight condition and motion variables, as well as the pilot stick input, due to the action of the control system. It is therefore necessary to model the control system, so that the input design algorithm can deflect the stabilator indirectly in a manner which will be most advantageous for accurate estimation of the open loop parameters in equation (5-16). An adequate model structure for the control system was found to be:

$$\dot{\delta}_h = \left[\mu_{\delta_h}\right]\delta_h + \begin{bmatrix} \mu_{\eta_c} & \mu_V & \mu_\alpha & \mu_q \end{bmatrix} \begin{bmatrix} \eta_c \\ V \\ \alpha \\ q \end{bmatrix} \tag{5-23}$$

where η_e is the longitudinal stick deflection at the pilot station. The output is

$$y_4(t) = \delta_h(t) \tag{5-24}$$

The measurement equation is

$$y_{m_4}(i) = y_4(i) + \upsilon_4(i) \quad i = 1, 2, ..., N \tag{5-25}$$

where

$$r_{44} = E\left\{ \upsilon_4(i)^2 \right\} = 4.17 \times 10^{-9} \tag{5-26}$$

For the control system model, longitudinal stick deflection, η_e , as well as the aircraft motion variables V, α, and q, are treated as known inputs. This simple first order model for the control system is adequate for the small perturbations in η_e from trim which are typical of inputs designed for parameter estimation experiments.

In general, the F-18 control system schedules leading edge and trailing edge flap deflections with angle of attack. This means that there should be two more rows in the control system model of equation (5-23) and two more controls in the open loop model of equation (5-16), corresponding to leading edge and trailing edge flap deflections. Including these controls, however, produces a collinearity in the data, since the flap deflections depend linearly on angle of attack at this flight condition. This causes parameter identifiability problems which are difficult to surmount. If one does not account for the fact that the flap settings change with angle of attack, a parameter estimation algorithm such as maximum likelihood assigns the effect of the flaps to the angle of attack parameters, thus rendering these parameter values inaccurate. For these reasons, the flap scheduling was turned off by setting the computed flap deflections from the flight control system subroutine inside the F-18 simulation to zero. With this done, the control system deflected only the symmetric stabilator, δ_h , in response to longitudinal stick deflections.

Combining the open loop dynamic model in equation (5-16) with the control system model in equation (5-23), and assuming that the measurement

noise in (5-20) is uncorrelated with the measurement noise in (5-25), gives the model for the closed loop longitudinal dynamics. The stabilator deflection is treated as an element of an augmented state vector, and can be viewed as an additional state, since its dynamics depend on state variables and the input, which is longitudinal stick deflection, η_c. In the notation already introduced, the closed loop model takes the form:

$$\begin{bmatrix} \dot{V} \\ \dot{\alpha} \\ \dot{q} \\ \dot{\delta}_h \end{bmatrix} = \begin{bmatrix} X_V & X_\alpha & 0 & X_{\delta_h} \\ 0 & Z_\alpha & Z_q & Z_{\delta_h} \\ 0 & M_\alpha & M_q & M_{\delta_h} \\ \mu_V & \mu_\alpha & \mu_q & \mu_{\delta_h} \end{bmatrix} \begin{bmatrix} V \\ \alpha \\ q \\ \delta_h \end{bmatrix} + \begin{bmatrix} 0 \\ 0 \\ 0 \\ \mu_{\eta_c} \end{bmatrix} [\eta_c] \tag{5-27}$$

$$\begin{bmatrix} y_1(t) \\ y_2(t) \\ y_3(t) \\ y_4(t) \end{bmatrix} = \begin{bmatrix} 1 & 0 & 0 & 0 \\ 0 & 1 & 0 & 0 \\ 0 & 0 & 1 & 0 \\ 0 & 0 & 0 & 1 \end{bmatrix} \begin{bmatrix} V(t) \\ \alpha(t) \\ q(t) \\ \delta_h(t) \end{bmatrix} \tag{5-28}$$

subject to the constraints

$$| y_1(t) | \leq 2.5 \text{ ft/sec} \quad \forall t \tag{5-29}$$

$$| y_2(t) | \leq 0.035 \text{ radians} \quad \forall t \tag{5-30}$$

The measurement equations are

$$\begin{bmatrix} y_{m_1}(i) \\ y_{m_2}(i) \\ y_{m_3}(i) \\ y_{m_4}(i) \end{bmatrix} = \begin{bmatrix} 1 & 0 & 0 & 0 \\ 0 & 1 & 0 & 0 \\ 0 & 0 & 1 & 0 \\ 0 & 0 & 0 & 1 \end{bmatrix} \begin{bmatrix} y_1(i) \\ y_2(i) \\ y_3(i) \\ y_4(i) \end{bmatrix} + \begin{bmatrix} \upsilon_1(i) \\ \upsilon_2(i) \\ \upsilon_3(i) \\ \upsilon_4(i) \end{bmatrix} \quad i = 1, 2, \ldots, N \tag{5-31}$$

where

$$\mathbf{R} = \begin{bmatrix} 0.25 & 0 & 0 & 0 \\ 0 & 2.22\times10^{-7} & 0 & 0 \\ 0 & 0 & 1.10\times10^{-5} & 0 \\ 0 & 0 & 0 & 4.17\times10^{-9} \end{bmatrix} \tag{5-32}$$

The open loop dynamic model (5-16) and the control system model (5-23) must be considered separately to estimate their respective parameters using maximum likelihood estimation. This is because the maximum likelihood parameter estimation algorithm integrates the dynamic and sensitivity equations using candidate model parameters as part of the process of finding parameter estimates. When attempting to estimate all the parameters in the closed loop model (5-27) using the data from a simulated experiment, the maximum likelihood algorithm diverges for nearly any initial values of the parameters, unless these initial values are very close to the "true" parameter values. This happens because the open loop system is inherently unstable. Estimating parameters in the open loop model (5-16) treating the closed loop stabilator from the experiment as a known input, and then separately estimating the parameters in the control system model (5-23), treating η_c, V, α, and q from the experiment as known inputs, eliminates the problem of a divergent parameter estimation algorithm. This separated estimation procedure was used to obtain all parameter estimates from simulated experimental data in this example.

In accord with what might be true for a real flight test input design problem, it was assumed that the only available data from which to assemble an *a priori* model for the input design were from a simple doublet input sequence for the longitudinal stick deflection, η_c. This doublet was in fact taken from an actual pilot input during the flight test of the real F-18 aircraft, see Klein et al [16]. The simple doublet input and the output time histories which result from applying this input form to the F-18 simulation test aircraft appear as figure 14. A first order lag with time constant 0.05 second was used in producing this input form. The same control input dynamics were used for all input forms in this example.

Based on the information from the simple doublet input, parameter estimates for the closed loop model were determined using maximum likelihood estimation and the separated model procedure described above. The dotted lines in figures 14(b) through 14(e) indicate model fits for each variable, as computed using the separated model procedure. The parameter estimates from the doublet input are given in Table 6. These parameter estimates and the model structure in equation (5-27) comprised the *a priori* model for the optimal input design. Figures 14(f) through 14(i) show the model responses using the closed loop model (5-27) and the parameter values from Table 6, as compared to the open loop model responses, which are the same as the dotted lines in figures 14(b) through 14(e).

The parameters of principal interest in the open loop dynamic model of (5-16) are contained in the bottom two rows, and are generally associated with the two state approximation of the short period dynamics. For the doublet input, the drag equation (top row) of (5-16) is included in the open loop model for two reasons. First, it was discovered that the control system model fit and predictive capability were considerably improved by including the velocity term in the control system model (5-23). This control system model fit is shown in figure 14(b). Second, the two state short period approximation is valid only for small changes in the velocity from trim. Thus, the input for parameter estimation must be designed so that the velocity excursions from trim are small in order to ensure validity of a two state short period model structure. The velocity is considered an output variable with the amplitude constraint (5-18). The model for the velocity (top row of (5-16)) must be included in the closed loop model (5-27) used for the optimal input design, so that maximum velocity changes from the trim value can be limited. Then the two state short period model can be used without significant degradation in parameter accuracy due to an invalid model structure. In general, using the open loop model (5-16) for inputs which do not excite the velocity very much (such as the simple doublet input) produces poor estimates of the parameters in the top row of equation (5-16). However, the model structure in (5-16) is required to build the *a priori* closed loop model (5-27) needed for the optimal input design.

With the velocity perturbations limited (equation (5-18)), all subsequent parameter estimation can be based on the two state short period model:

$$\begin{bmatrix} \dot{\alpha} \\ \dot{q} \end{bmatrix} = \begin{bmatrix} Z_\alpha & Z_q \\ M_\alpha & M_q \end{bmatrix} \begin{bmatrix} \alpha \\ q \end{bmatrix} + \begin{bmatrix} Z_{\delta_h} \\ M_{\delta_h} \end{bmatrix} \begin{bmatrix} \delta_h \end{bmatrix} \tag{5-33}$$

$$\begin{bmatrix} y_1(t) \\ y_2(t) \end{bmatrix} = \begin{bmatrix} 1 & 0 \\ 0 & 1 \end{bmatrix} \begin{bmatrix} \alpha(t) \\ q(t) \end{bmatrix} \tag{5-34}$$

$$\begin{bmatrix} y_{m_1}(i) \\ y_{m_2}(i) \end{bmatrix} = \begin{bmatrix} 1 & 0 \\ 0 & 1 \end{bmatrix} \begin{bmatrix} y_1(i) \\ y_2(i) \end{bmatrix} + \begin{bmatrix} v_1(i) \\ v_2(i) \end{bmatrix} \quad i = 1, 2, \ldots, N \tag{5-35}$$

$$\mathbf{R} = \begin{bmatrix} 2.22\text{x}10^{-7} & 0.0 \\ 0.0 & 1.10\text{x}10^{-5} \end{bmatrix} \tag{5-36}$$

A longitudinal stick input design proposed by Klein et al [16] was applied to the F-18 simulation test aircraft, with the input amplitude adjusted by trial and error so that the velocity and angle of attack amplitude constraints were satisfied. This input will be referred to as the compound doublet input. The time histories from the experiment using the compound doublet input are shown by the solid lines in figure 15. The dotted lines in figures 15(b) and 15(c) show the model fits for α and q, respectively, from maximum likelihood estimation using the open loop model (5-33). Closed loop stabilator deflection from the F-18 nonlinear simulation is shown in figure 15(d).

The optimal input technique was applied using the closed loop model (5-27) with the model parameters from Table 6 as the *a priori* model. The optimal input design and time histories from the experiment using the F-18 simulation test aircraft are shown in figure 16. A fixed time input design was produced by setting all Cramer-Rao bound goals to zero, and setting the maximum test time to 8.0 seconds. A first order lag with time constant 0.05 second was used for the longitudinal stick control dynamics. The 0.75 inch maximum input amplitude for the optimal input was determined

automatically by the algorithm. Maximum input amplitude was initially set at 1.0 inch, to agree with the maximum input amplitude for the simple doublet. Input amplitude decrements were set at 0.25 inch to design an input with an amplitude which could be easily input by the pilot. The algorithm thus required one iteration on the problem formulation to arrive at the final input amplitude of 0.75 inch. Minimum input pulse width was set at 0.5 second, and the final time required with zero input amplitude was 0.4 second.

Table 7 gives the results of maximum likelihood estimation using the data from each of the input designs. The parameter values listed in the second column were obtained using finite differences with the nonlinear F-18 simulation. The standard errors for each parameter are lowered using the optimal input, except for the small parameter $Z_{\delta h}$, which is difficult to estimate accurately because of its small magnitude. Figure 16(a) shows the optimal input, and figures 16(b) and 16(c) give the F-18 simulation responses and the model fits using the open loop model (5-33) and maximum likelihood parameter estimates. The closed loop stabilator deflection from the F-18 simulation is shown in figure 16(d). Figures 16(e) through 16(h) compare the time histories from the optimal input experiment with the computed time histories from the optimal input design algorithm using the *a priori* closed loop model (5-27) with parameters from Table 6. The time histories from the experiment violate the imposed output amplitude constraints because the closed loop model estimated from the doublet input does not exactly describe the nonlinear response from the F-18 simulation. The *a priori* closed loop model time histories in figures 16(e) through 16(h) satisfy the output amplitude constraints (5-18) and (5-19), as required.

The example presented here demonstrates that the optimal input algorithm can be successfully used for optimal input design problems when the estimation of open loop parameters is required, but only closed loop data are available. For modern fighter aircraft, this situation has become the norm rather than the exception.

Chapter VI - Summary and Conclusions

This dissertation describes a new formulation of the optimal input problem for aircraft parameter estimation experiments, the development of a new solution algorithm for the optimal input design, and the demonstration of the capabilities of the new technique. The examples presented are mainly for demonstration purposes.

The optimal input design for aircraft parameter estimation experiments was done in the time domain using the principles of dynamic programming. The problem was formulated with the objective of achieving specified Cramer-Rao bound goals in a time optimal fashion or minimizing the Cramer-Rao bounds for a fixed test time. Optimization in the time domain using the dynamic programming approach allowed various practical aspects of the input design to be incorporated in a straightforward manner. Bellman's principle of optimality was enforced so that the designed inputs were globally time optimal, subject to the imposed constraints on the input form, the output amplitude constraints, the dynamic and measurement models, and the discretization of both time and the constrained output variables in the formulation of the dynamic programming problem.

The first example presented in this work demonstrated that the present approach to optimal input design for aircraft parameter estimation improves on previous solutions by lowering the Cramer-Rao bounds and/or requiring a shorter total test time.

In the second example, the expanded capability of the optimal input design technique was exhibited by application to a fourth order multiple input system with restrictive output amplitude constraints. The input design solution contained provisions to assist in the practical implementation of the designed inputs.

The third example developed a procedure for the use of the optimal input design technique when open loop model parameters are of interest, but the system must be tested under closed loop control due to safety considerations. Conditions for a real flight test of the F-18 fighter aircraft were simulated, and the utility of the optimal input design technique was demonstrated.

The capabilities of the new algorithm can be summarized as:

1. Global optimum solution for minimum or fixed flight test time
2. Multiple input design capability
3. Closed loop model capability
4. Practically achievable input design
5. Direct implementation of output amplitude constraints
6. Input frequency selection in the time domain
7. Single pass solution
8. Well-suited to design studies

The main contributions of this work are the formulation and practical, optimal solution of the input design problem for aircraft parameter estimation experiments, along with the demonstrations of the improved quality of the optimal inputs and the expanded capabilities of the optimal input design technique.

Based on the findings documented in this work, conclusions and recommendations for further study are listed below.

1. The optimal input design technique should be evaluated with regard to pilot acceptability as compared with conventional input designs. A ground-based simulator could be used for this study.

2. Application to a free flight wind tunnel model test, drop model test, or full scale flight test would verify the predicted capabilities of the optimal input design technique.

3. Other input design problems which could be addressed using the input design procedure outlined here include experiments for data compatibility check of the flight instrumentation system, and input designs to reduce parameter correlation. The latter should be straightforward, since the input design technique currently computes the full dispersion matrix recursively, and parameter correlation can be computed from the off-diagonal terms of this matrix, normalized by the appropriate diagonal elements.

4. A study could be done to determine the effect on the optimal input design of inaccuracy in the *a priori* model, i.e., the robustness of the optimal input design technique.

5. Studies concerning various trade-offs among experiment design parameters could be done. For instance, what are the effects of different measurement noise characteristics or different control system dynamics on the optimal input design and the resulting achievable parameter accuracies ?

6. Although the optimal input technique was developed for aircraft dynamic models, any other physical system which can be described with a linear state space model structure could have been the subject of the input design for a parameter estimation experiment.

References

1. Maine, R. E. and Iliff, K. W. 1986. Application of Parameter Estimation to Aircraft Stability and Control. NASA Reference Publication 1168.

2. Mulder, J. A. 1986. Design and Evaluation of Dynamic Flight Test Manoeuvres. Report LR-497. Delft, The Netherlands : Delft University of Technology, Department of Aerospace Engineering.

3. Reid, D. B. 1972. Optimal Inputs for System Identification. Ph.D. dissertation, SUDAAR No. 440. Stanford, California : Stanford University, Department of Aeronautics and Astronautics.

4. Gupta, N. K. and Hall, E. H. Jr. 1975. Input Design for Identification of Aircraft Stability and Control Derivatives. NASA CR-2493.

5. Mehra, R.K. 1974. *Optimal Inputs for Linear System Identification.* IEEE Transactions on Automatic Control, Vol. AC-10, No. 3, pp. 192-200.

6. Mehra, R. K. and Gupta, N. K. 1975. *Status of Input Design for Aircraft Parameter Identification.* AGARD-CP-172, paper 12.

7. Plaetschke, E. and Schulz, G. 1979. *Practical Input Signal Design.* AGARD-LS-104, paper 3.

8. Stepner, D. E. and Mehra, R. K. 1973. Maximum Likelihood Identification and Optimal Input Design for Identifying Aircraft Stability and Control Derivatives. NASA CR-2200.

9. Chen, R. T. N. 1975. *Input Design for Aircraft Parameter Identification: Using Time-Optimal Control Formulation.* AGARD-CP-172, paper 13.

10. Dreyfus, S. E. 1965. Dynamic Programming and the Calculus of Variations. New York : Academic Press.

11. Kirk, D. E. 1970. Optimal Control Theory: An Introduction. Englewood Cliffs, N.J. : Prentice-Hall Inc.

12. Mehra, R. K. 1981. *Choice of Input Signals.* Trends and Progress in System Identification, Eykhoff, P., Ed. Elmsford, N.Y. : Pergamon Press Inc. pp. 305-366.

13. Brogan, W. L. 1974. Modern Control Theory. New York, N.Y. : Quantum Publishers, Inc.

14. Klein, V. 1989. *Estimation of Aircraft Aerodynamic Parameters from Flight Data.* Prog. in Aerospace Sci., Vol. 26, pp. 1-77.

15. Buttrill, C. S., Arbuckle, P. D., and Leath, W.J. 1990. *F-18 ACSL Simulation* ; undocumented working version. Aircraft Guidance and Control Branch, NASA Langley Research Center, Hampton, VA.

16. Klein, V., Breneman, K. P., and Ratvasky, T. P. July 1989. Aerodynamic Parameters of an Advanced Fighter Aircraft Estimated from Flight Data - Preliminary Results. NASA TM 101631.

17. Maine, R. E. and Iliff, K. W. 1985. Identification of Dynamic Systems: Theory and Formulation. NASA Reference Publication 1138.

Appendix A - The Information Matrix and the Cramer-Rao Lower Bound

In this appendix, the form of the information matrix used to design optimal inputs for parameter estimation is derived. Following this, it is shown that the inverse of the information matrix is the theoretical lower bound on the parameter covariances. This lower bound is called the Cramer-Rao lower bound for the parameter covariances.

Consider the following state, output, and measurement equations :

$$\dot{x}(t) = f(x(t), u(t), \theta) \quad , \qquad x(0) = 0 \tag{A-1}$$

$$y(t) = h(x(t), u(t), \theta) \tag{A-2}$$

$$y_m(i) = y(i) + v(i) \tag{A-3}$$

$$E\{v(i)\} = 0 \quad , \qquad E\{v(i)\, v^T(j)\} = R \cdot \delta_{ij} \tag{A-4}$$

The sequence of measured output vectors is $y_m(i)$, i=1,2,3,...,N, where N is the total number of sample times. For a given parameter vector θ in the state and output equations (A-1) and (A-2), respectively, assuming each $y_m(i)$ is a realization of a Gaussian vector random process, the joint conditional probability of realizing the observed sequence of measured output vectors is [17]:

$$p(y_m(1), y_m(2), \ldots, y_m(N) \mid \theta) = \left[(2\pi)^{-\frac{q}{2}} |R|^{-\frac{1}{2}} \right]^N \exp \left\{ \sum_{i=1}^{N} -\frac{1}{2} \left[y_m(i) - y(i) \right]^T R^{-1} \left[y_m(i) - y(i) \right] \right\} \tag{A-5}$$

The object of parameter estimation is to choose a parameter vector $\hat{\theta}$ for θ in expressions (A-1) and (A-2) such that the conditional probability in (A-5) is maximized. Usually the natural logarithm of equation (A-5) is used for computational simplicity. Since probabilities are always positive, and the natural logarithm function is a monotonically increasing function for

positive arguments, the same $\hat{\theta}$ vector maximizes both the probability in (A-5) and its logarithm. The logarithm of the probability in equation (A-5) will be denoted by $L(\theta)$ and is generally referred to as the log likelihood function:

$$L(\theta) = \ln\left[p(y_m(1),y_m(2),...,y_m(N) \mid \theta)\right] \tag{A-6}$$

$$L(\theta) = -\frac{N}{2}\left[q\ln(2\pi) + \ln|R|\right] + \sum_{i=1}^{N} -\frac{1}{2}\left[y_m(i)-y(i)\right]^T R^{-1}\left[y_m(i)-y(i)\right] \tag{A-7}$$

The information matrix is defined in terms of the log likelihood function [17]:

$$M = E\left\{\frac{\partial L(\theta)}{\partial \theta} \cdot \frac{\partial L(\theta)}{\partial \theta^T}\right\} \tag{A-8}$$

where $E\{\cdot\}$ denotes the conditional expectation taken over all possible realizations of the measurement vector sequence, $y_m(i)$, i=1,2,3,...,N and conditioned on the parameter vector, θ. Using (A-6), equation (A-8) may also be written as:

$$M = E\left\{\frac{\partial \ln[p(Y \mid \theta)]}{\partial \theta} \cdot \frac{\partial \ln[p(Y \mid \theta)]}{\partial \theta^T}\right\} \tag{A-9}$$

where **Y** represents the sequence of measurement vectors, $y_m(i)$, i=1,2,3,...,N.

At this point, a small side excursion is made to find an alternate expression for the information matrix, **M**. Let **Y** denote a particular realization of the measurement vector sequence, $y_m(i)$, i=1,2,3,...,N. Then, by the definition of conditional probability density functions,

$$\int_{-\infty}^{\infty} p(Y \mid \theta)\, dY = 1 \tag{A-10}$$

The notation here implies that the integral is taken over all possible realizations of the measurement vector sequence, $\mathbf{y_m}(i)$, i=1,2,3,...,N. By differentiation,

$$\frac{\partial p(\mathbf{Y} \mid \boldsymbol{\theta})}{\partial \boldsymbol{\theta}} = p(\mathbf{Y} \mid \boldsymbol{\theta}) \frac{\partial(\ln[p(\mathbf{Y} \mid \boldsymbol{\theta})])}{\partial \boldsymbol{\theta}} \tag{A-11}$$

Differentiating (A-10) twice with respect to $\boldsymbol{\theta}$, and using (A-11) each time,

$$\int_{-\infty}^{\infty} \left[\frac{\partial^2 \ln[p(\mathbf{Y} \mid \boldsymbol{\theta})]}{\partial \boldsymbol{\theta}\, \partial \boldsymbol{\theta}^T} + \left(\frac{\partial \ln[p(\mathbf{Y} \mid \boldsymbol{\theta})]}{\partial \boldsymbol{\theta}} \cdot \frac{\partial \ln[p(\mathbf{Y} \mid \boldsymbol{\theta})]}{\partial \boldsymbol{\theta}^T} \right) \right] p(\mathbf{Y} \mid \boldsymbol{\theta})\, d\mathbf{Y} = \mathbf{0} \tag{A-12}$$

Or, using the expectation operator notation, and recalling (A-6),

$$E\left\{ \frac{\partial L(\boldsymbol{\theta})}{\partial \boldsymbol{\theta}} \cdot \frac{\partial L(\boldsymbol{\theta})}{\partial \boldsymbol{\theta}^T} \right\} = - E\left\{ \frac{\partial^2 L(\boldsymbol{\theta})}{\partial \boldsymbol{\theta}\, \partial \boldsymbol{\theta}^T} \right\} \tag{A-13}$$

Invoking (A-8),

$$\mathbf{M} = E\left\{ \frac{\partial L(\boldsymbol{\theta})}{\partial \boldsymbol{\theta}} \cdot \frac{\partial L(\boldsymbol{\theta})}{\partial \boldsymbol{\theta}^T} \right\} = - E\left\{ \frac{\partial^2 L(\boldsymbol{\theta})}{\partial \boldsymbol{\theta}\, \partial \boldsymbol{\theta}^T} \right\} \tag{A-14}$$

Equation (A-14) contains the alternate expression for the information matrix, **M**. For the system (A-1) – (A-4), the information matrix may be expressed as follows by combining (A-3), (A-4), (A-7), and (A-14), and keeping in mind that the measurement vector $\mathbf{y_m}(i)$ is considered a realization of a random vector sequence, and is therefore not a function of $\boldsymbol{\theta}$:

$$\mathbf{M} = \left[\sum_{i=1}^{N} \left(\frac{\partial \mathbf{y}(i)}{\partial \boldsymbol{\theta}} \right)^T \mathbf{R}^{-1} \left(\frac{\partial \mathbf{y}(i)}{\partial \boldsymbol{\theta}} \right) \right] \tag{A-15}$$

It will now be shown that the inverse of the information matrix is the theoretical minimum value for the covariances of the elements in the estimated parameter vector, $\hat{\boldsymbol{\theta}}$. The dependence of $L(\boldsymbol{\theta})$ on the input is through the state, output, and measurement equations, (A-1) - (A-4); see also (A-7).

Let $\mathbf{Y}$ again denote any realized sequence of measurement vectors, $\mathbf{y_m}(i)$, i=1,2,3,...,N. Then for an unbiased estimator [1],

$$E\left\{\hat{\boldsymbol{\theta}}(Y) - \boldsymbol{\theta}\right\} = \int_{-\infty}^{\infty} \left(\hat{\boldsymbol{\theta}}(Y) - \boldsymbol{\theta}\right) p(Y \mid \boldsymbol{\theta})\, dY = \mathbf{0} \tag{A-16}$$

Differentiating (A-16) with respect to $\boldsymbol{\theta}$ gives

$$-\int_{-\infty}^{\infty} \mathbf{I} \cdot p(Y \mid \boldsymbol{\theta})\, dY + \int_{-\infty}^{\infty} \left(\hat{\boldsymbol{\theta}}(Y) - \boldsymbol{\theta}\right) \frac{\partial p(Y \mid \boldsymbol{\theta})}{\partial \boldsymbol{\theta}^T} dY = \mathbf{0} \tag{A-17}$$

The first integral on the left in (A-17) is the identity matrix by the definition of the conditional probability density function. Substituting into the second integral on the left from equation (A-11),

$$\int_{-\infty}^{\infty} \left(\hat{\boldsymbol{\theta}}(Y) - \boldsymbol{\theta}\right) \frac{\partial(\ln[p(Y \mid \boldsymbol{\theta})])}{\partial \boldsymbol{\theta}^T} p(Y \mid \boldsymbol{\theta})\, dY = \mathbf{I} \tag{A-18}$$

The last equation may also be written as

$$E\left\{ \left(\hat{\boldsymbol{\theta}}(Y) - \boldsymbol{\theta}\right) \frac{\partial(\ln[p(Y \mid \boldsymbol{\theta})])}{\partial \boldsymbol{\theta}^T} \right\} = I \tag{A-19}$$

The following lemma is now required [1]:

Lemma A.1 Let x and y be two random p-dimensional vectors. Then,

$$E\{ x x^T \} \geq E\{ x y^T \} [E\{ y y^T \}]^{-1} E\{ y x^T \} \tag{A-20}$$

Proof:

Let **Q** be an arbitrary non-random p-by-p matrix. Then, since all covariances must be non-negative,

$$E\{ (x - Qy)(x - Qy)^T \} \geq 0 \tag{A-21}$$

Expanding the left side of (A-21),

$$E\{ x x^T \} - QE\{ y x^T \} - E\{ x y^T \} Q^T + QE\{ y y^T \} Q^T \geq 0 \tag{A-22}$$

$$E\{ x x^T \} \geq QE\{ y x^T \} + E\{ x y^T \} Q^T - QE\{ y y^T \} Q^T \tag{A-23}$$

Now choose

$$Q = E\{ x y^T \} [E\{ y y^T \}]^{-1} \tag{A-24}$$

so that the two terms on the far right of (A-23) cancel. Substituting (A-24) into (A-23) and simplifying,

$$E\{ x x^T \} \geq E\{ x y^T \} [E\{ y y^T \}]^{-1} E\{ y x^T \} \tag{A-25}$$

This ends the proof of the lemma.

Returning to (A-19), and invoking lemma A.1 (Equation (A-25)) with

$$\hat{\theta}(Y) - \theta = x \quad ; \quad \frac{\partial (\ln[p(Y \mid \theta)])}{\partial \theta} = y \tag{A-26}$$

gives

$$E\left\{\left(\hat{\theta}(Y) - \theta\right)\left(\hat{\theta}(Y) - \theta\right)^T\right\} \geq I \cdot \left[E\left\{\left(\frac{\partial \ln[p(Y \mid \theta)]}{\partial \theta}\right)\left(\frac{\partial \ln[p(Y \mid \theta)]}{\partial \theta^T}\right)\right\}\right]^{-1} \cdot I \qquad \text{(A-27)}$$

Or, using (A-9),

$$E\left\{\left(\hat{\theta}(Y) - \theta\right)\left(\hat{\theta}(Y) - \theta\right)^T\right\} \geq M^{-1} \qquad \text{(A-28)}$$

Equation (A-28) is called the Cramer-Rao inequality and states that the minimum expected values of the parameter covariances for an unbiased estimator are given by the inverse of the information matrix. This latter matrix is also referred to as the Cramer-Rao lower bound for the parameter covariances, or the dispersion matrix, D:

$$D = M^{-1} \qquad \text{(A-29)}$$

When designing the optimal input for the purpose of parameter estimation, only the dispersion matrix is considered, since this separates the merits of an input with regard to the parameter estimation accuracy from the merits of whatever unbiased estimator may be chosen for the parameter estimation. In effect, an input form is evaluated "upstream" of the actual parameter estimation calculations by looking only at the theoretical minimum parameter covariances possible with that input form, as embodied in the elements of the dispersion matrix. The dispersion matrix depends only on the sensitivities of the output quantities to changes in the parameters. In general, the higher these sensitivities, the more accurately the parameters can be estimated, since small changes in parameter values will be manifested in large changes in the model output for the system. With large values for the sensitivities, the parameter values may be determined very accurately by matching measured output with output from the proposed model. The diagonal elements of the dispersion matrix are of principal interest, since they are the theoretical minimum values of the parameter variances. The square root of these diagonal elements are the theoretical lower bounds on the parameter standard errors.

For the system (A-1) - (A-4), the dispersion matrix may be expressed as follows by combining (A-15) and (A-29):

$$\mathbf{D} = \left[\sum_{i=1}^{N} \left(\frac{\partial \mathbf{y}(i)}{\partial \boldsymbol{\theta}} \right)^{T} \mathbf{R}^{-1} \left(\frac{\partial \mathbf{y}(i)}{\partial \boldsymbol{\theta}} \right) \right]^{-1} \tag{A-30}$$

No assumptions of linearity in the system equations (A-1) - (A-4) were necessary in this development.

Appendix B - Dynamic Programming

The algorithm for input optimization described and demonstrated in this dissertation employed the principles of dynamic programming. The purpose of this appendix is to provide an understanding of the fundamental concepts of dynamic programming in the form required for the present work. These fundamental concepts are completely contained and described in references [10] and [11], along with more specialized information concerning dynamic programming and the connection between dynamic programming and the calculus of variations.

Dynamic programming is an efficient means of solving sequential multi-stage optimization problems. In figure B-1, the dots represent various states of some abstract system. Time is represented by horizontal distance left to right, with time zero at the leftmost edge. Time is discretized into stages, so that the system states exist only at times which are an integer multiple of one stage time. The lines between the dots represent a specific control choice, which results in the state trajectory starting from the dot representing the initial system state and ending at the dot representing the final system state at the next time stage. Each possible control is applied as a constant over one stage time, so that each possible state transition (connecting line) corresponds to a possible control choice at the initial state. State transitions must always move left to right, corresponding to increasing time. All state transitions shown in figure B-1 are associated with a cost, which is shown as a number along the state transition line. The objective is to reach one of the target states, represented by the column of dots aligned above the final time stage, by starting at the initial state and optimizing the sequence of state transitions such that the total cost of the travel from the initial state to one of the possible final states is a minimum. Since each state transition corresponds to a control choice at the current state, the objective may also be considered to be the optimization of a sequence of control choices. The optimal sequence of control choices is called the optimal policy. The problem described here is often referred to as a discrete multi-stage optimization.

An exhaustive search for the optimal policy would require the investigation of 2^{n-1} different paths, where n is the number of discrete time stages from the initial condition to one of the target states at the final time stage, inclusive. The base 2 in the above expression results from the fact that

only two choices are possible at any state for any stage. As the number of stages (or the number of control choices) increases, the exhaustive search quickly becomes prohibitive in terms of computation time. There is an alternative method for the computation of the optimal policy, which is known as "the principle of optimality", due to Richard Bellman. In the form required here, this principle states :

> An optimal sequence of decisions in a multistage decision process problem has the property that whatever the final decision and state preceding the terminal one, the prior decisions must constitute an optimal sequence of decisions leading from the initial state to that state preceding the terminal one.[1]

In figure B-2, the optimal policy was computed by moving left to right and using the above principle of optimality. The arrows along the state trajectory lines indicate the control and state trajectory which represents the best path (lowest total cost) to reach the given state from the immediately preceding stage. The italic number at each state indicates the value of the cost required to reach that state at that time stage, using the optimal policy indicated by the arrows. Figure B-2 represents the results of applying the principle of optimality to each state of each stage in a sequential manner, moving left to right. The bold line in figure B-2 indicates the overall optimal policy and thus the optimal state trajectory, since this path gives the lowest cost from the initial state at the initial stage to any of the states at the final stage, using an optimal policy.

The principle of optimality not only gives a systematic method for choosing an optimal policy from a large number of possibilities, but also does so in a way which realizes a significant savings in computation over an exhaustive search. It is this latter quality which makes dynamic programming a practical tool for optimization.

---

[1] Dreyfus, S. E. 1965. Dynamic Programming and the Calculus of Variations. New York : Academic Press. p. 8.

In Table B-1, the computations required to solve this multi-stage optimization problem are compared for the dynamic programming solution method versus an exhaustive enumeration, using an increasing number of stages. The general expressions for the number of additions and comparisons using dynamic programming and exhaustive enumeration are shown at the top of Table B-1 as a function of the number of stages, n. The total number of additions and comparisons required for a dynamic programming solution with the grid geometry of figure B-1 is on the order of n^2 and 3n, respectively; whereas exhaustive enumeration calculations are on the order of $n2^{n-1}$ and n, respectively. Dynamic programming enjoys a considerable computational advantage over exhaustive enumeration, even for a relatively small number of total stages, as shown in Table B-1. This computational advantage becomes even more dramatic when there are more than two control choices at any state.

The grid geometry in figure B-1 and B-2 might be considered a discrete multi-stage optimization with no state constraints, since for all states at all stages except the last, the full range of controls and accompanying state transitions are available. That is, a state transition "up" or "down" diagonally was possible from any state at any stage except the last. State constraints can be introduced by arranging the grid geometry as shown in figure B-3. Here, states on the border of some interior stages have only one control choice or state transition possibility to the next stage. This can be interpreted as a constraint on deviation of the state from the initial state in the abstract sense corresponding to vertical displacement within the grid.

Although the entire discussion here considered the **state** of some abstract system, the **output** of the same abstract system could just have well been used with absolutely no change in any of the development. In fact, the present work considers the dots within each grid as representative of some abstract system output at the given stage. The reason for this is so that the constraints will be on the output variable excursions from their initial values.

Real dynamical systems are generally modelled as continuous systems whose states, outputs, and controls exist at any time. In order to use the dynamic programming optimization technique as presented here, it is necessary to discretize the continuous problem corresponding to physical reality. This is done by dividing an allowable range of output variable excursions into small subdivisions. For the case of two constrained output

variables, the allowable output space at any stage can be represented by a plane region divided into discrete output space boxes, as in figure B-4. Outputs are computed from the continuous dynamic and output equations. Those outputs which fall inside or on part of the border of a given box in output space are considered the same output "state", corresponding directly with the dots in figures B-1 and B-2. In this way the continuous problem is converted into a discrete problem. All controls are constrained to remain constant over the time period corresponding to one stage time, so that time can be discretized into stages. The cost computed for each control possibility in the optimal input design algorithm is directly analogous to the costs associated with each state transition in figures B-1 and B-2, the latter being represented by the numbers next to each state transition line. This completes the conversion of the continuous problem into a discrete multi-stage optimization, which can be handled using the principle of optimality in the manner described above.

Appendix C - Algorithm Flow Chart

The following pages contain a functional flow chart for the algorithm used to design optimal inputs for aircraft parameter estimation experiments. The numbers in parentheses refer to equation numbers in the text.

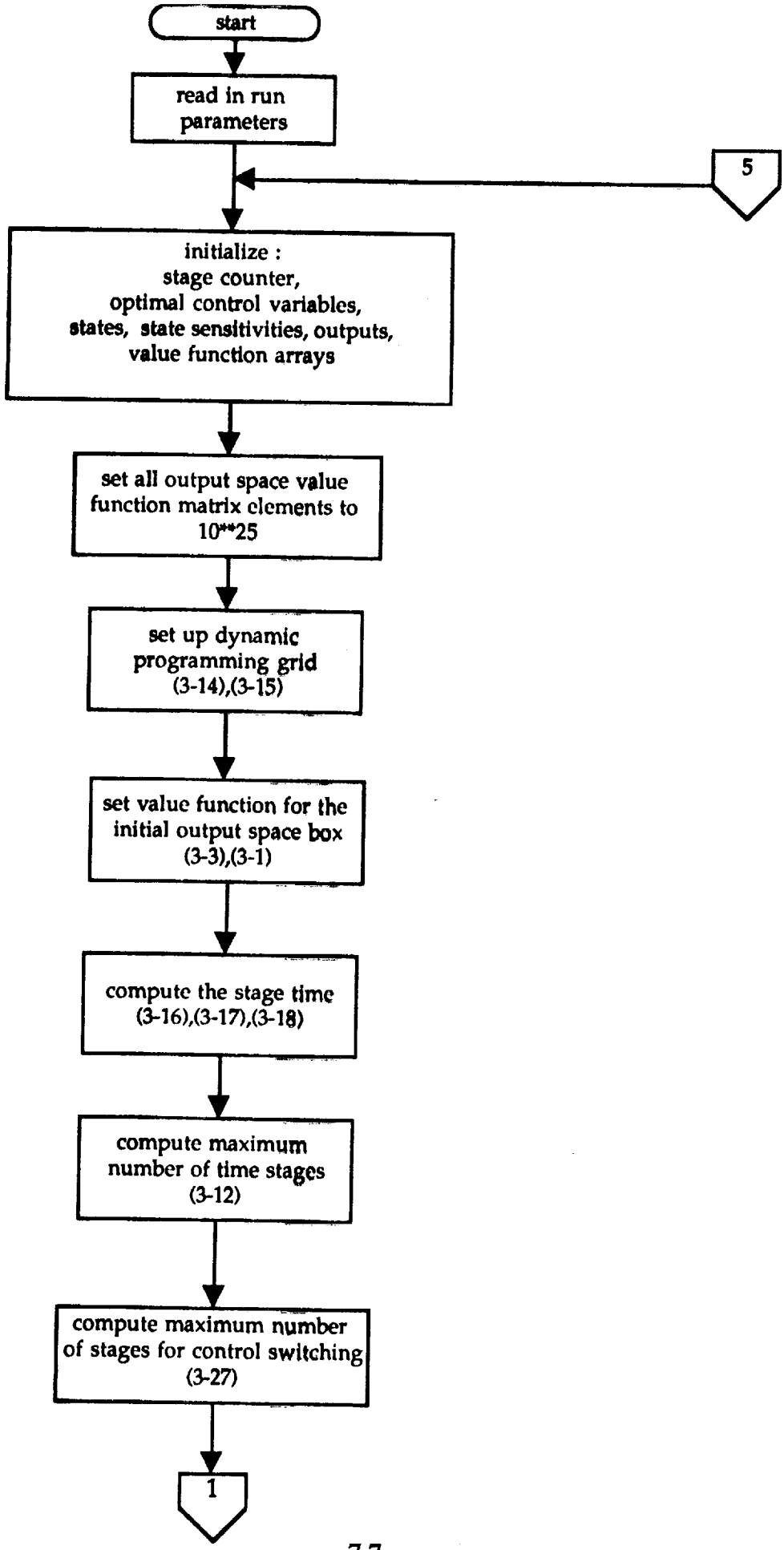
start
read in run parameters
5
initialize : stage counter, optimal control variables, states, state sensitivities, outputs, value function arrays
set all output space value function matrix elements to 10**25
set up dynamic programming grid (3-14),(3-15)
set value function for the initial output space box (3-3),(3-1)
compute the stage time (3-16),(3-17),(3-18)
compute maximum number of time stages (3-12)
compute maximum number of stages for control switching (3-27)
1

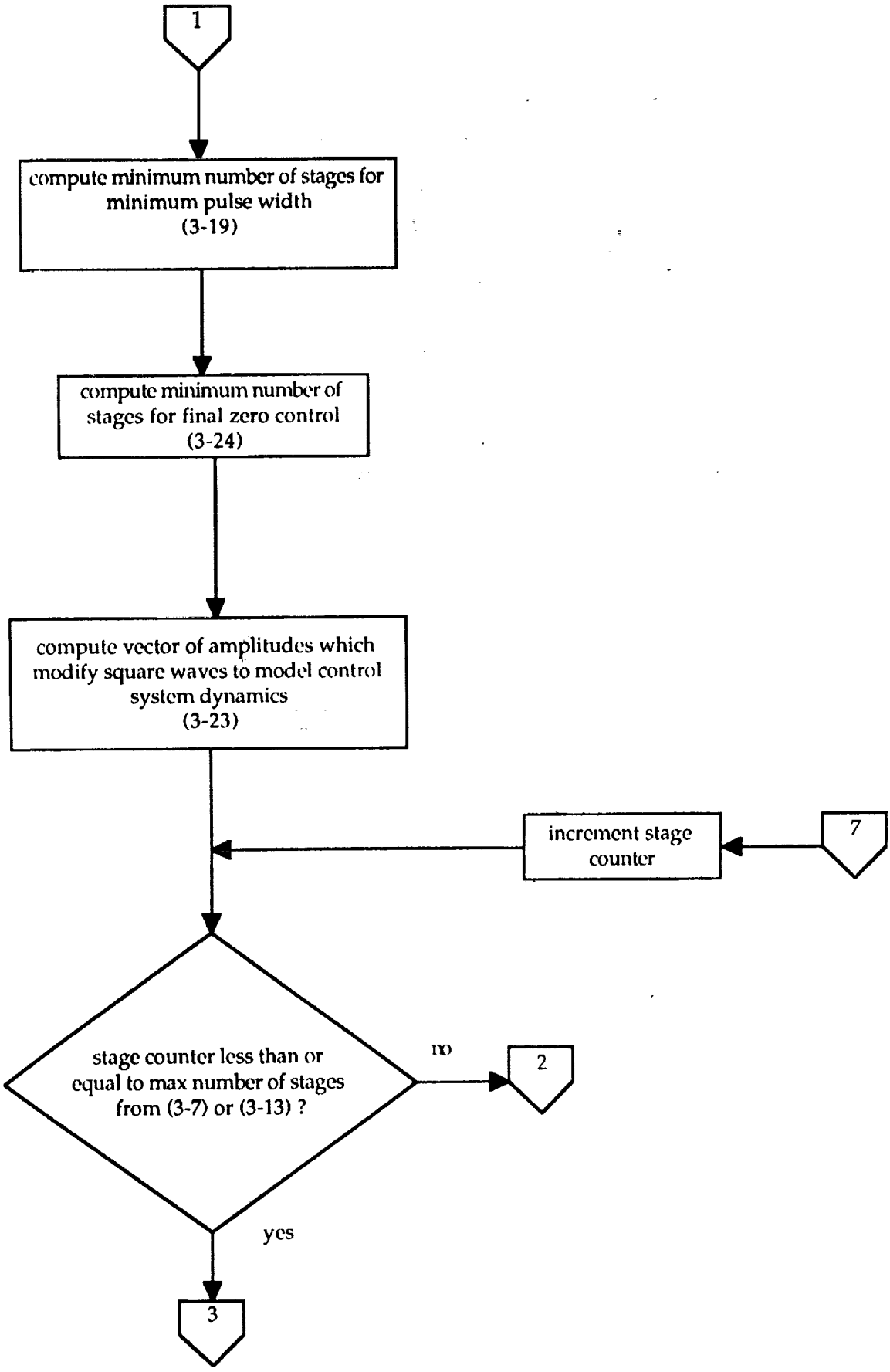
1
compute minimum number of stages for minimum pulse width (3-19)
compute minimum number of stages for final zero control (3-24)
compute vector of amplitudes which modify square waves to model control system dynamics (3-23)
increment stage counter
7
stage counter less than or equal to max number of stages from (3-7) or (3-13) ?
no
2
yes
3

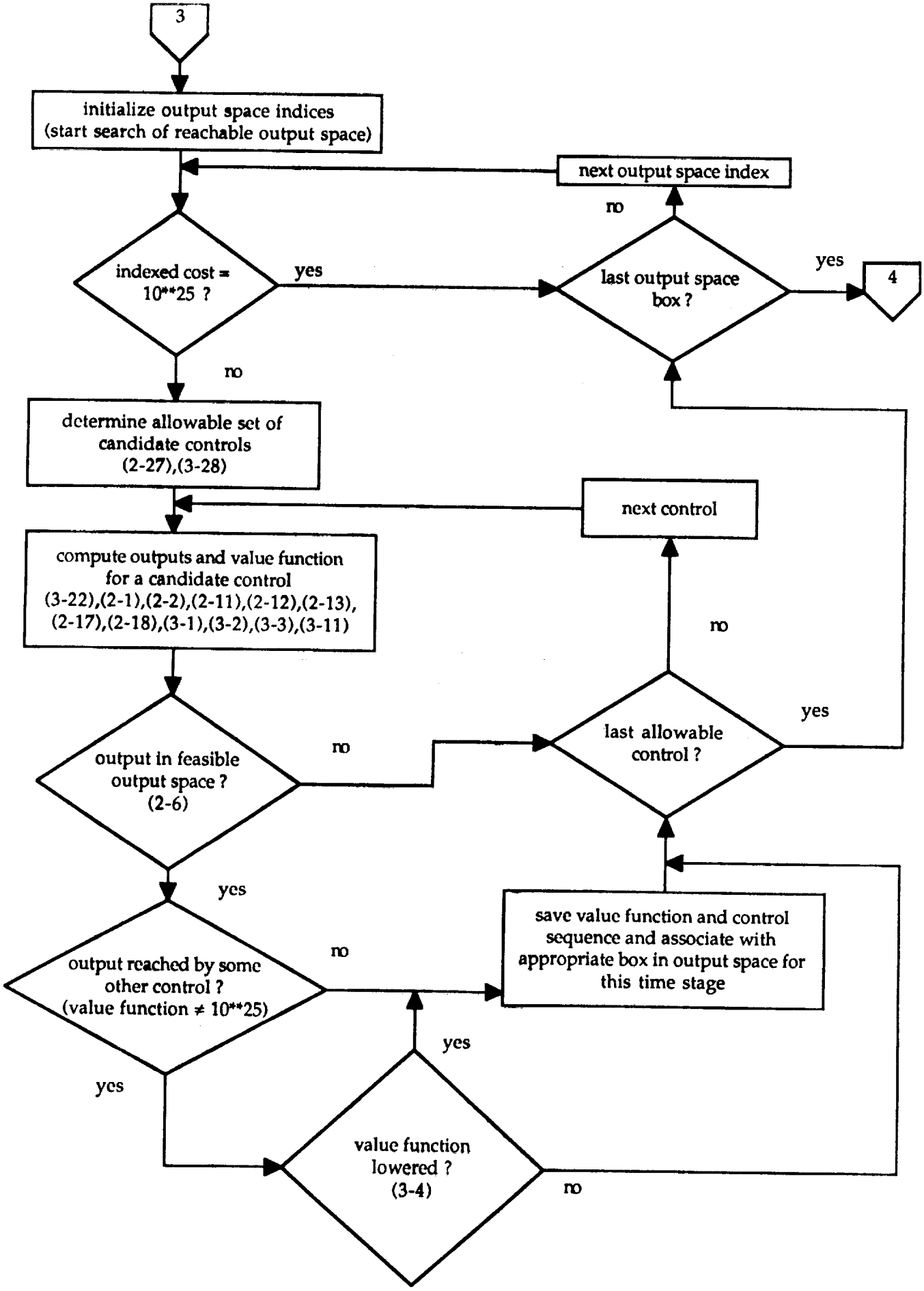
3
initialize output space indices
(start search of reachable output space)
next output space index
no
indexed cost = 10**25 ?
yes
last output space box ?
yes
4
no
determine allowable set of candidate controls
(2-27),(3-28)
next control
compute outputs and value function for a candidate control
(3-22),(2-1),(2-2),(2-11),(2-12),(2-13),
(2-17),(2-18),(3-1),(3-2),(3-3),(3-11)
no
output in feasible output space ?
(2-6)
no
last allowable control ?
yes
yes
save value function and control sequence and associate with appropriate box in output space for this time stage
output reached by some other control ?
(value function ≠ 10**25)
no
yes
yes
value function lowered ?
(3-4)
no

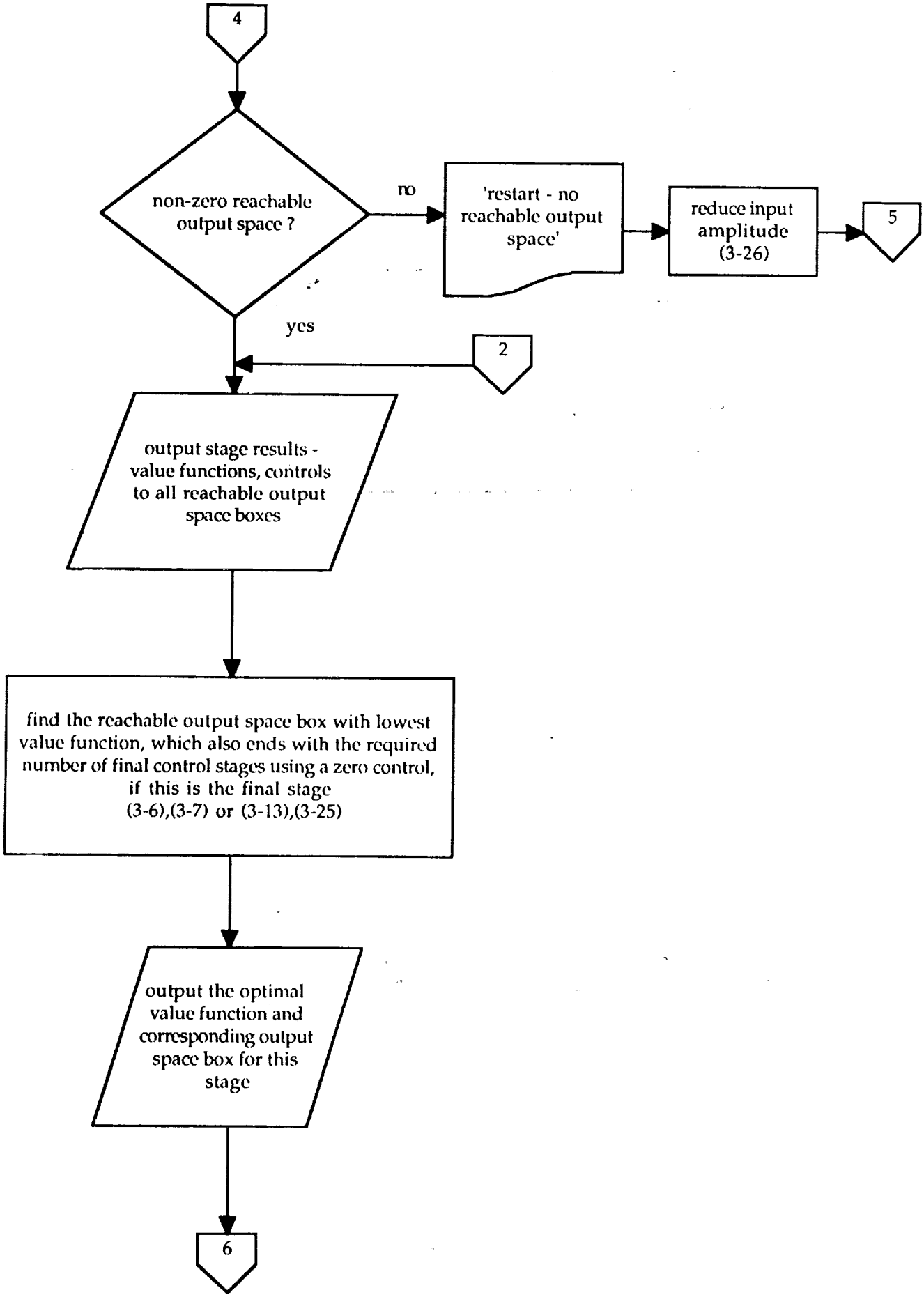
4
non-zero reachable output space ?
no
'restart - no reachable output space'
reduce input amplitude (3-26)
5
yes
2
output stage results - value functions, controls to all reachable output space boxes
find the reachable output space box with lowest value function, which also ends with the required number of final control stages using a zero control, if this is the final stage (3-6),(3-7) or (3-13),(3-25)
output the optimal value function and corresponding output space box for this stage
6

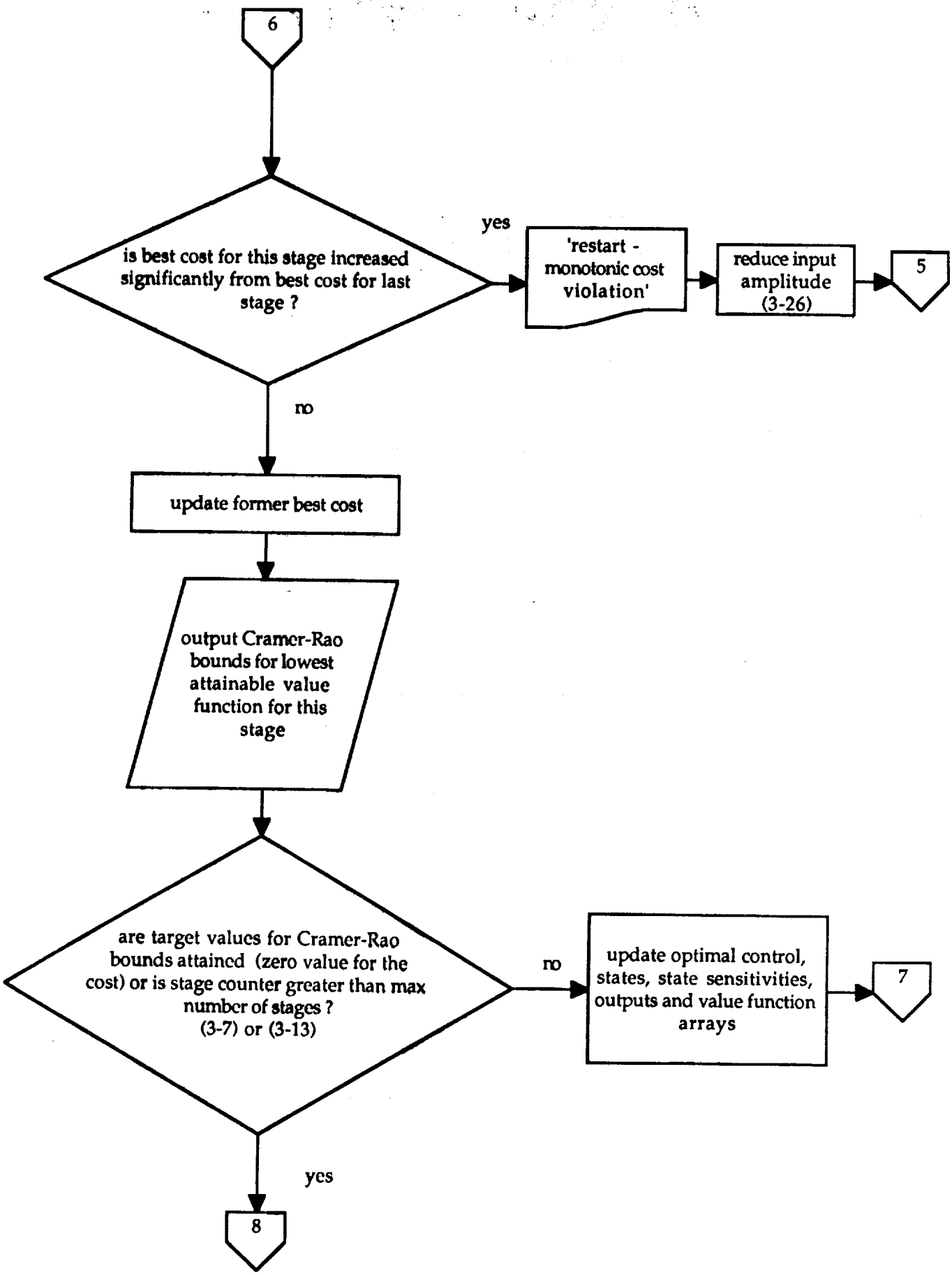
6
is best cost for this stage increased significantly from best cost for last stage ?
yes
'restart - monotonic cost violation'
reduce input amplitude (3-26)
5
no
update former best cost
output Cramer-Rao bounds for lowest attainable value function for this stage
are target values for Cramer-Rao bounds attained (zero value for the cost) or is stage counter greater than max number of stages ? (3-7) or (3-13)
no
update optimal control, states, state sensitivities, outputs and value function arrays
7
yes
8

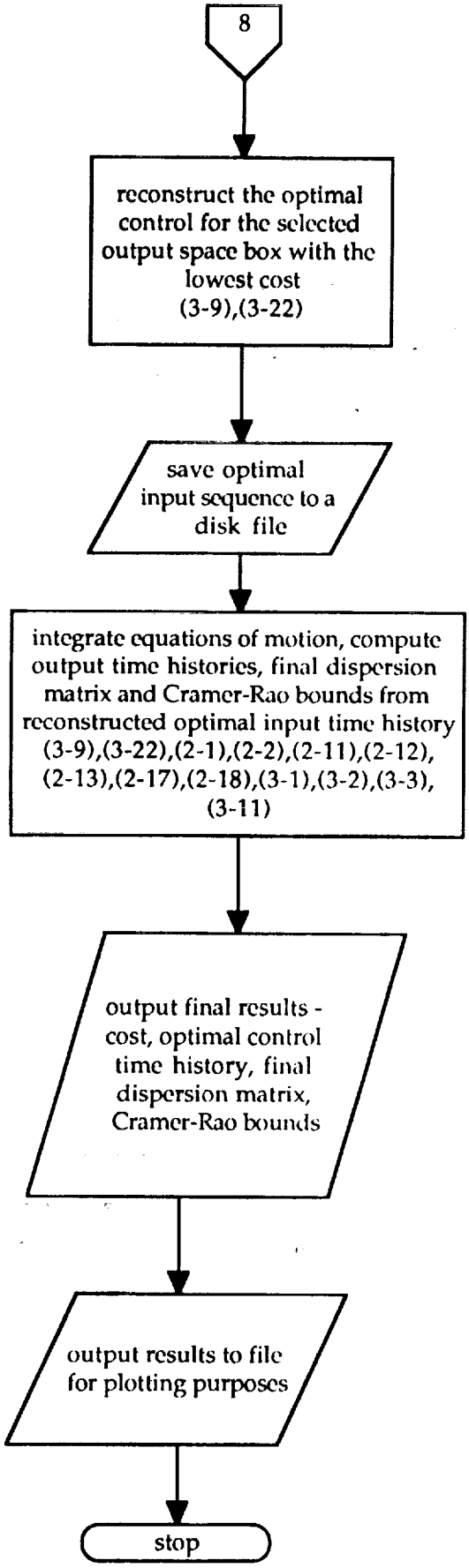
8
reconstruct the optimal control for the selected output space box with the lowest cost (3-9),(3-22)
save optimal input sequence to a disk file
integrate equations of motion, compute output time histories, final dispersion matrix and Cramer-Rao bounds from reconstructed optimal input time history (3-9),(3-22),(2-1),(2-2),(2-11),(2-12),(2-13),(2-17),(2-18),(3-1),(3-2),(3-3),(3-11)
output final results - cost, optimal control time history, final dispersion matrix, Cramer-Rao bounds
output results to file for plotting purposes
stop

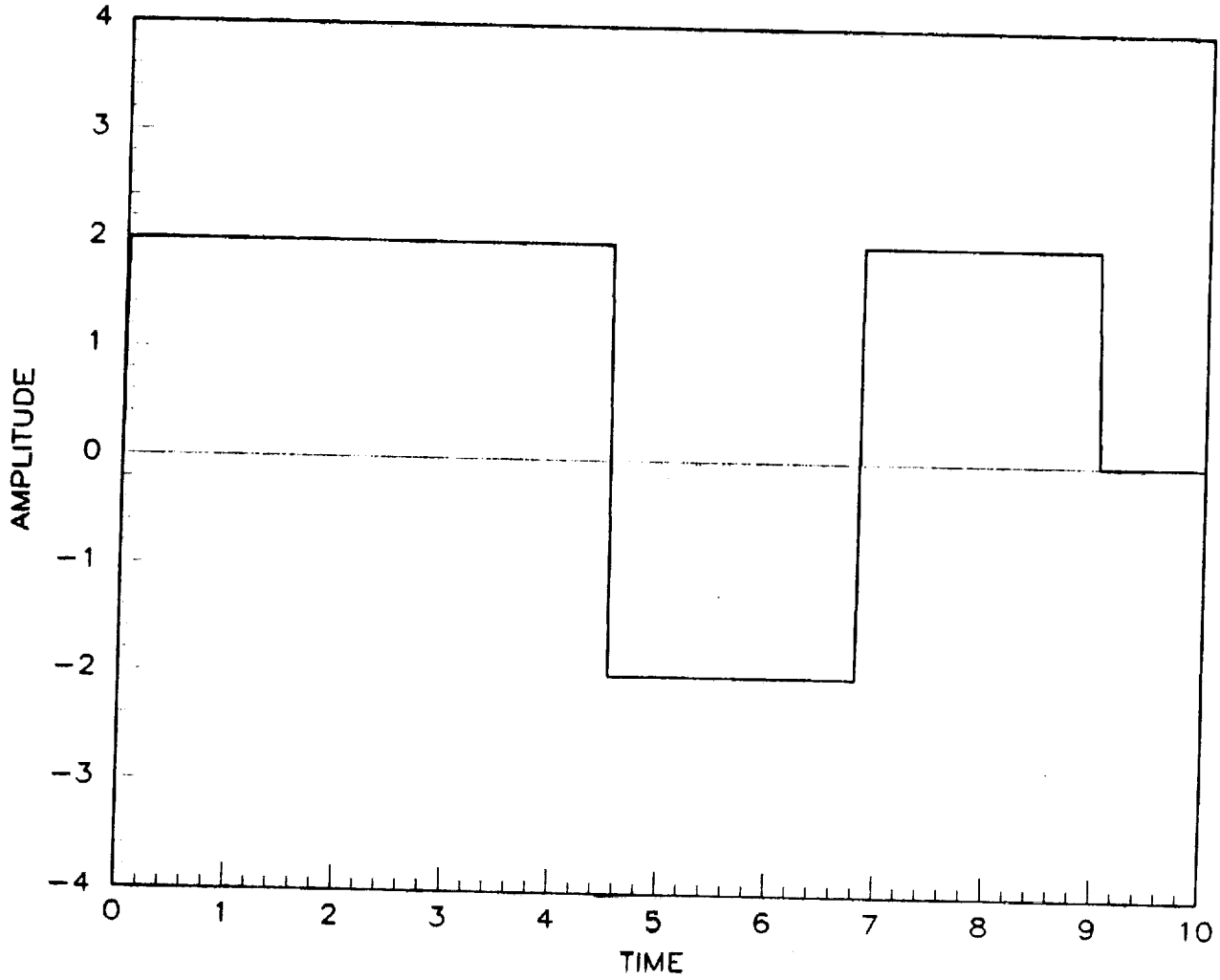

Figure 1(a) – Square Wave, Energy = 36

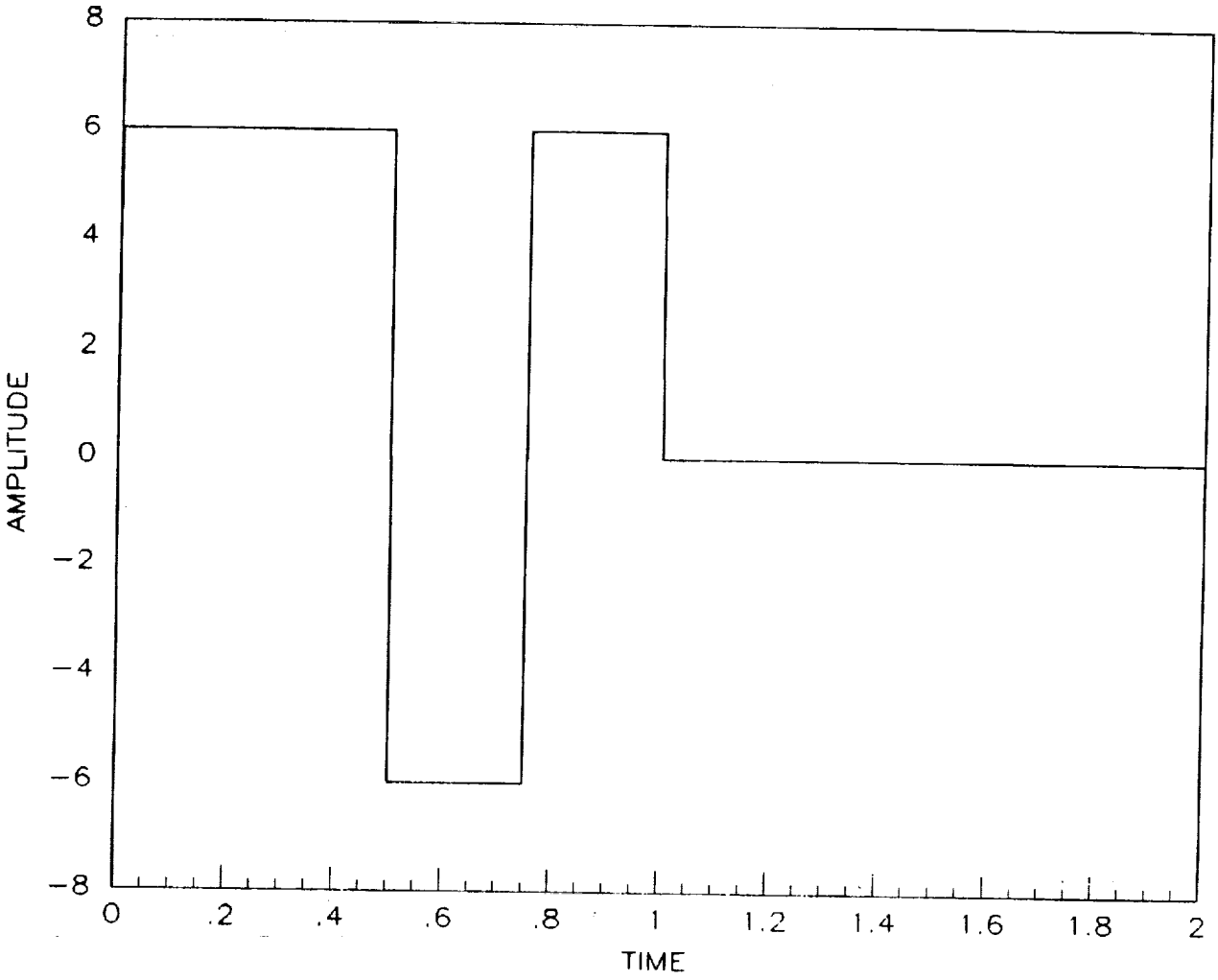

Figure 1(b) – Square Wave, Energy = 36

C-2

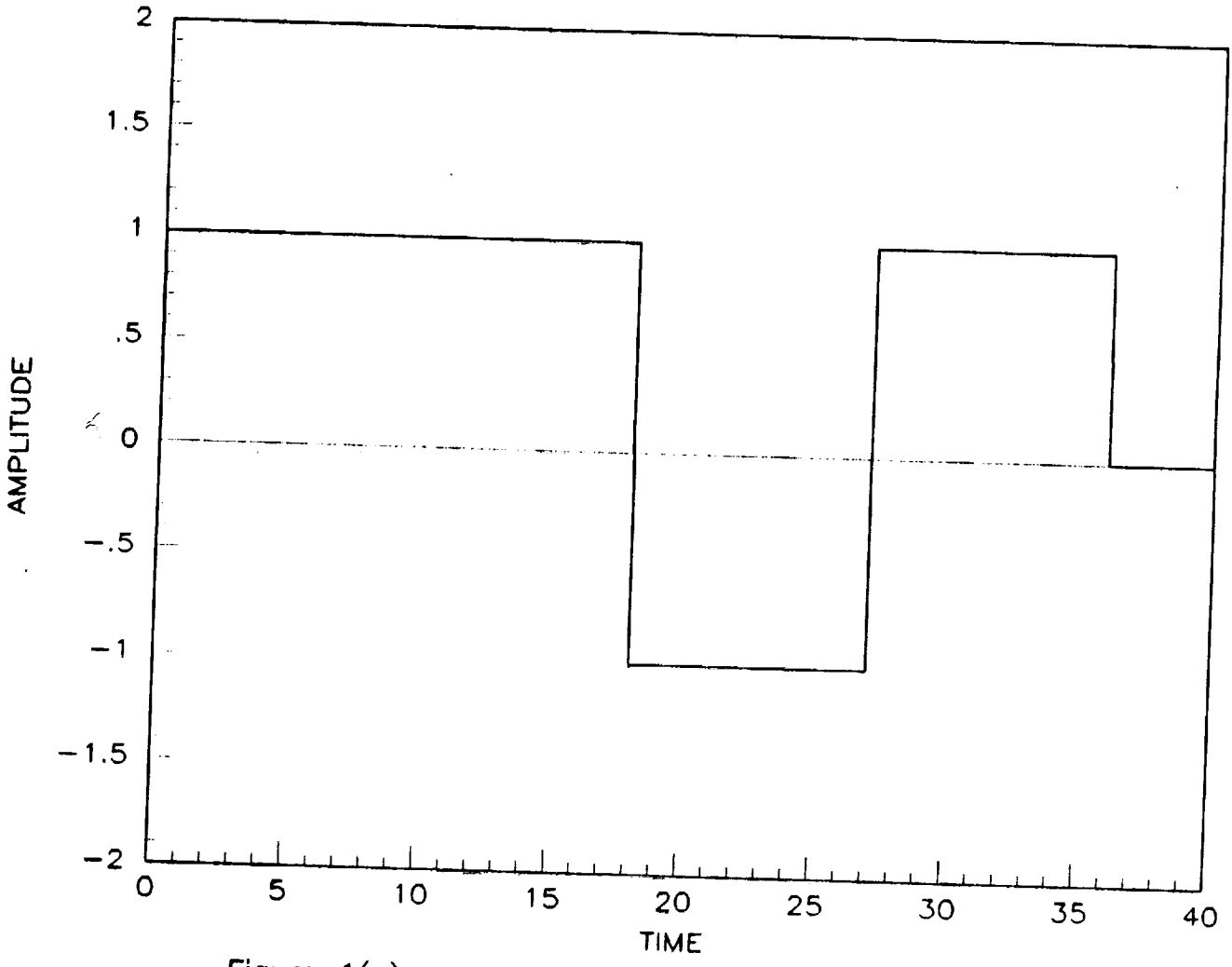

Figure 1(c) – Square Wave, Energy = 36

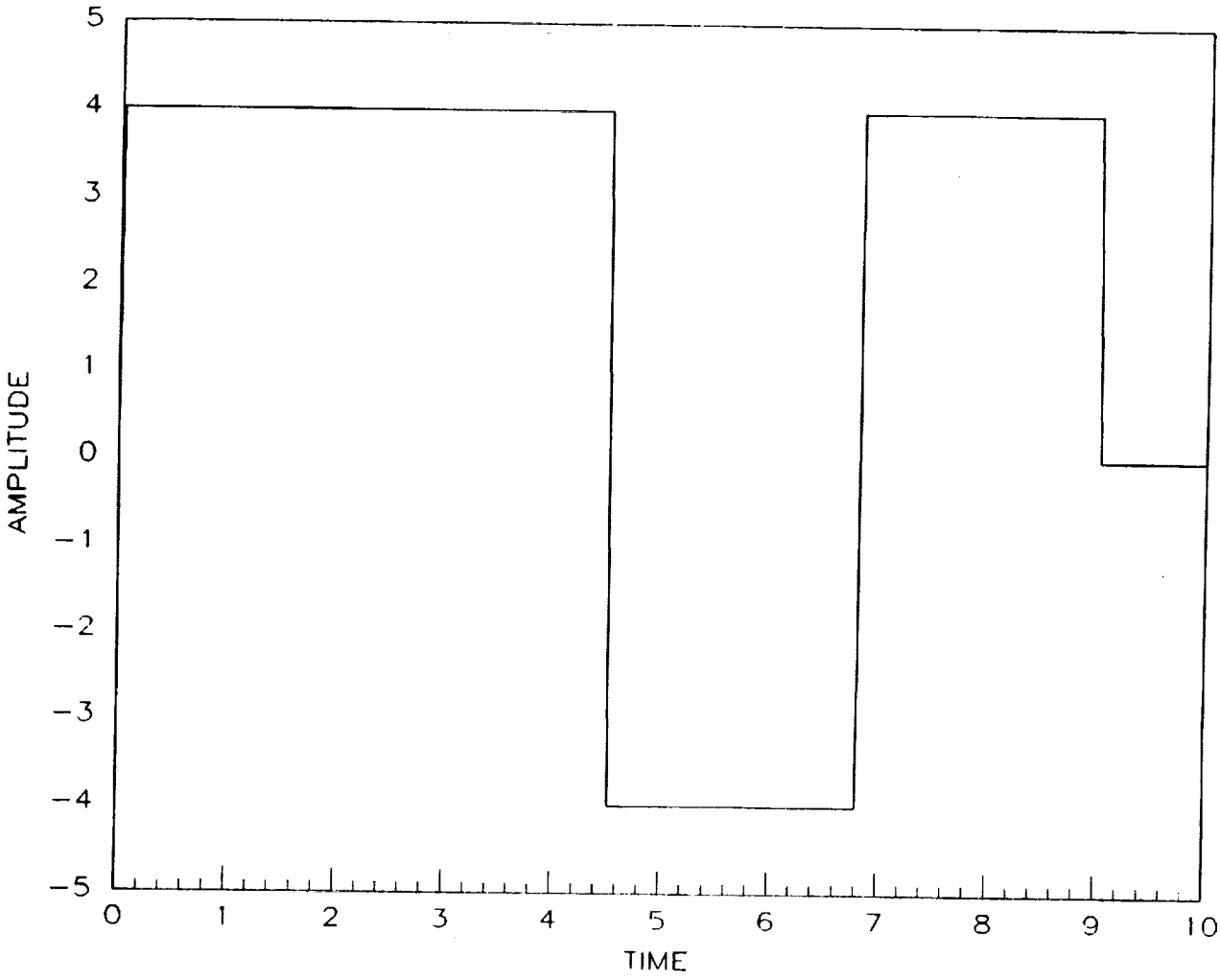

Figure 1(d) – Square Wave, Energy = 144

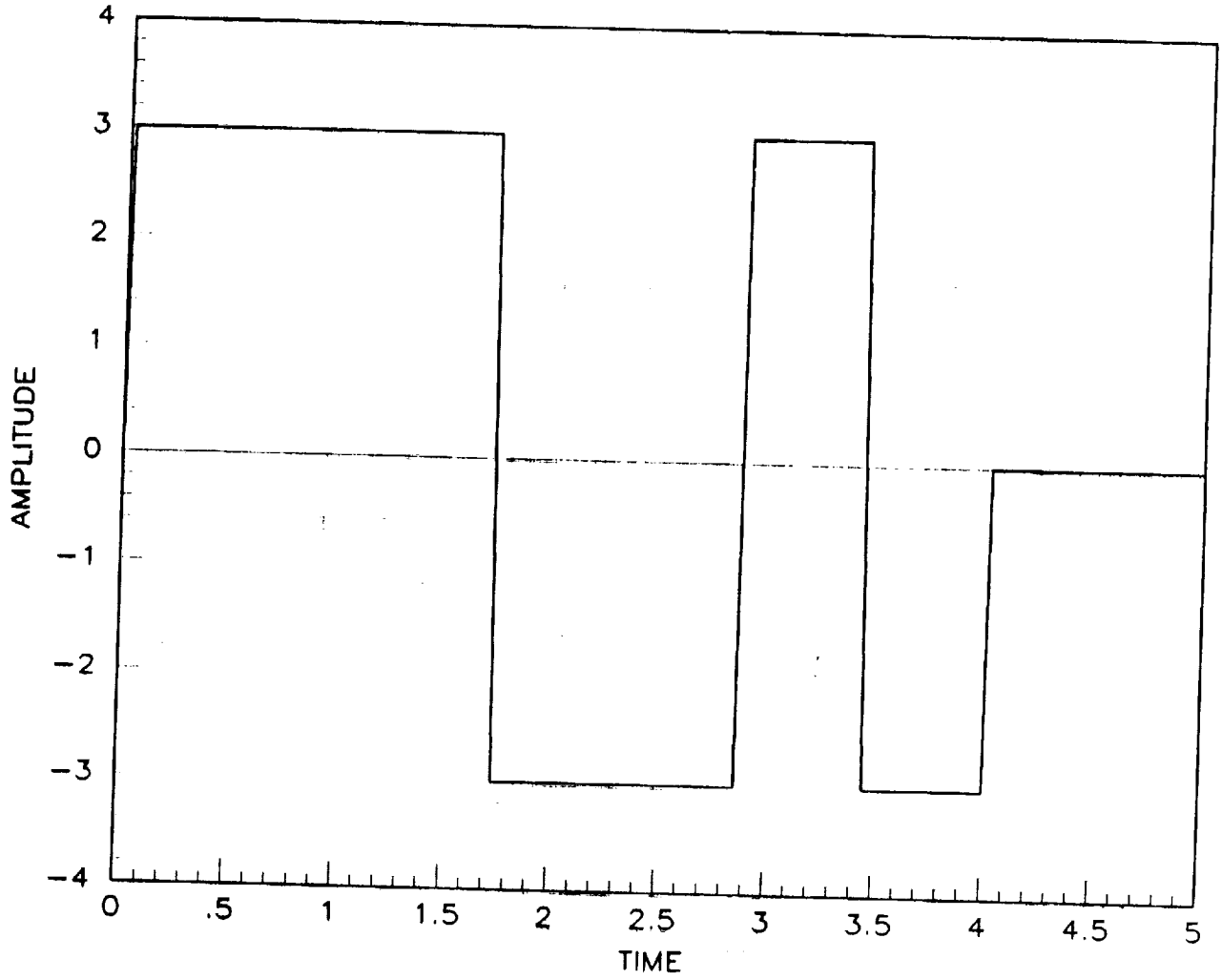

Figure 2 – 3211 Input

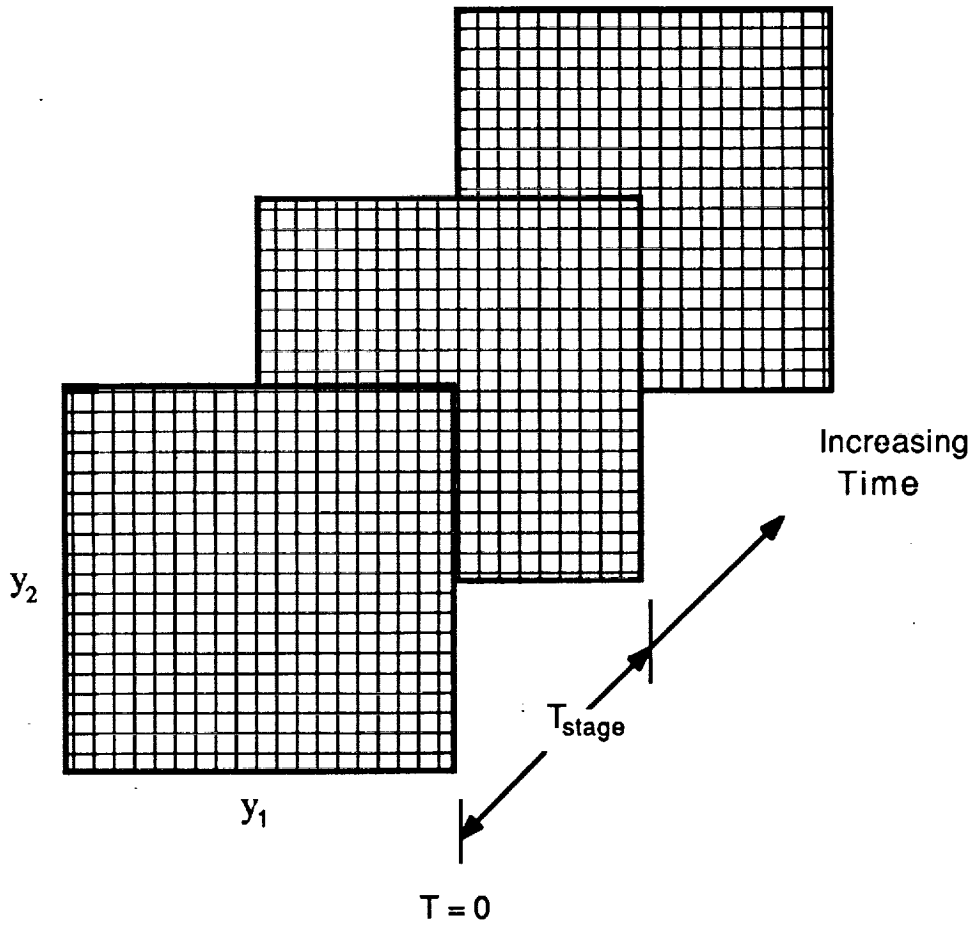

Figure 3 - Dynamic Programming Grids

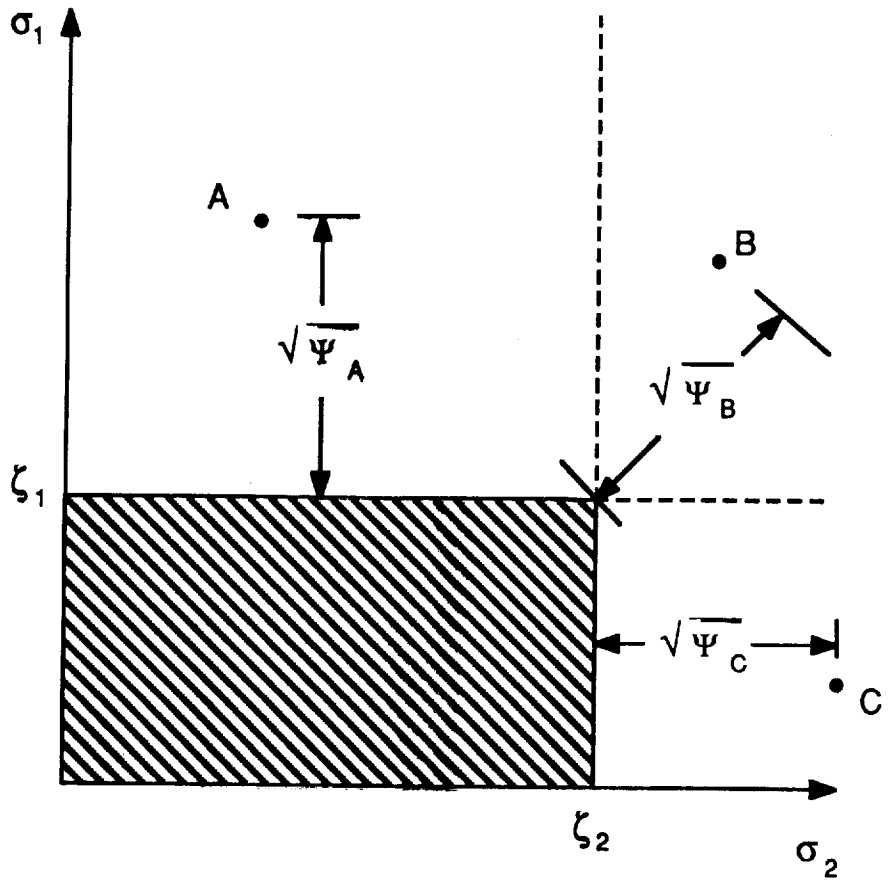

Figure 4 - Value Function Calculation

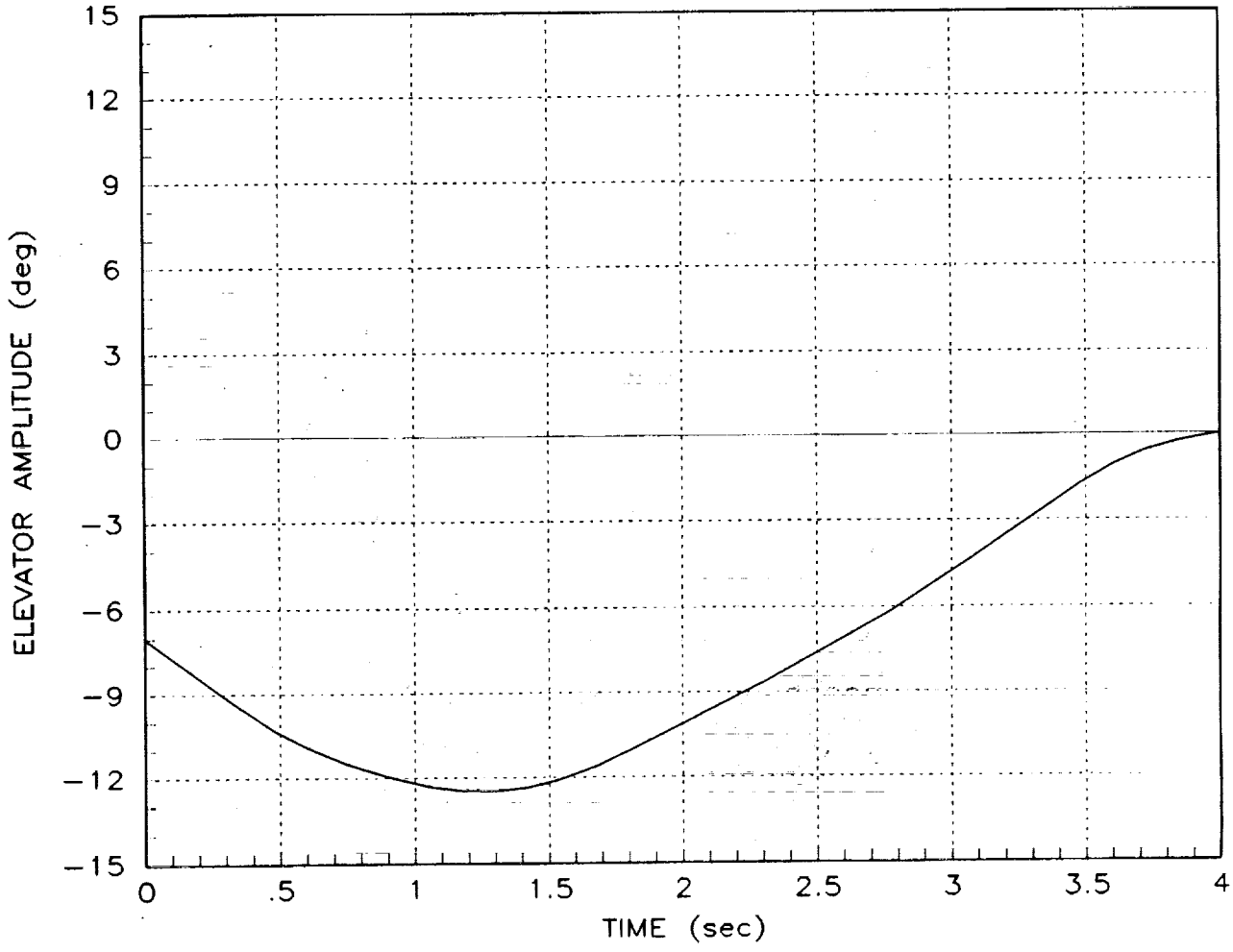

Figure 5 (a) – Mehra Input

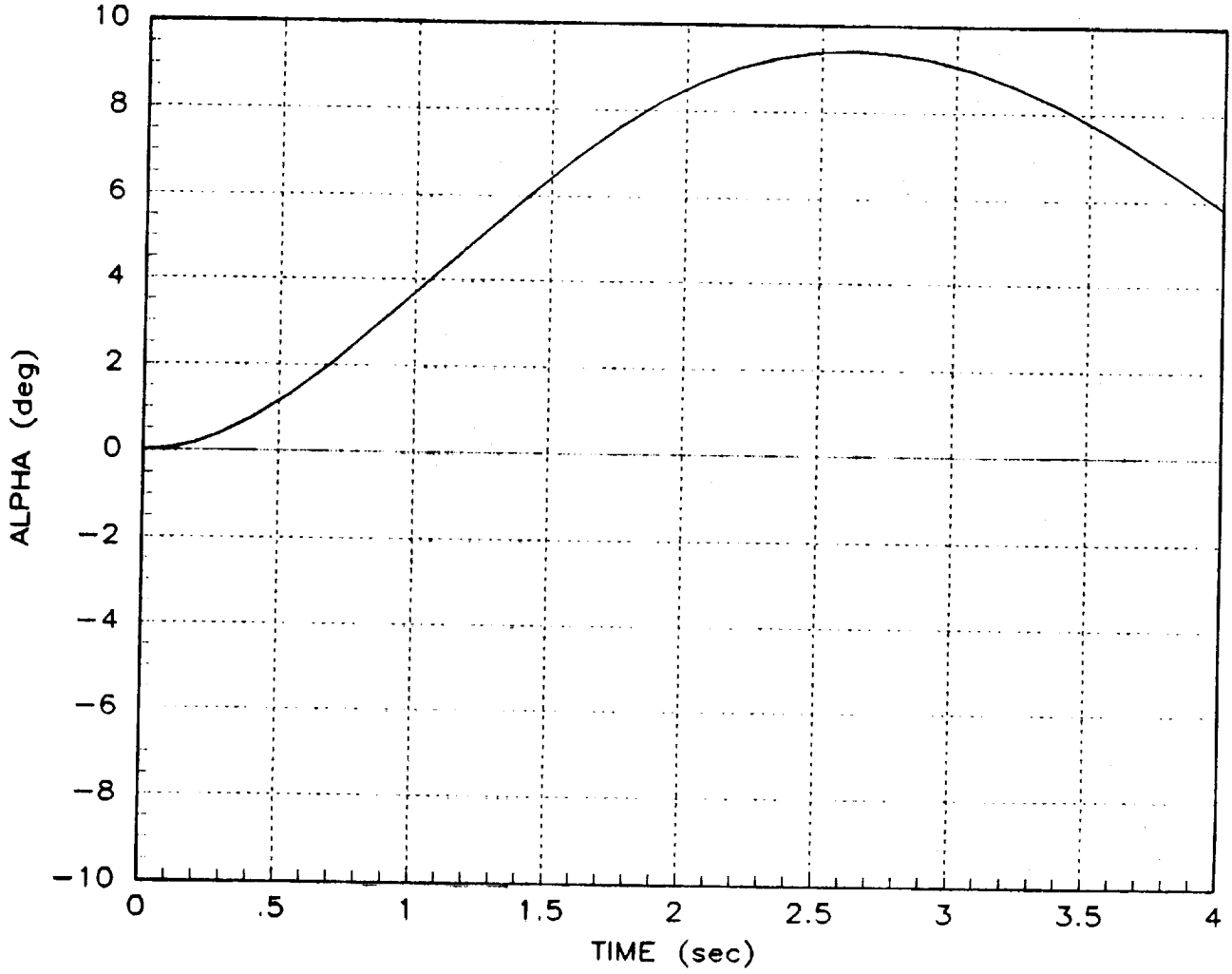

Figure 5 (b) – Mehra Input

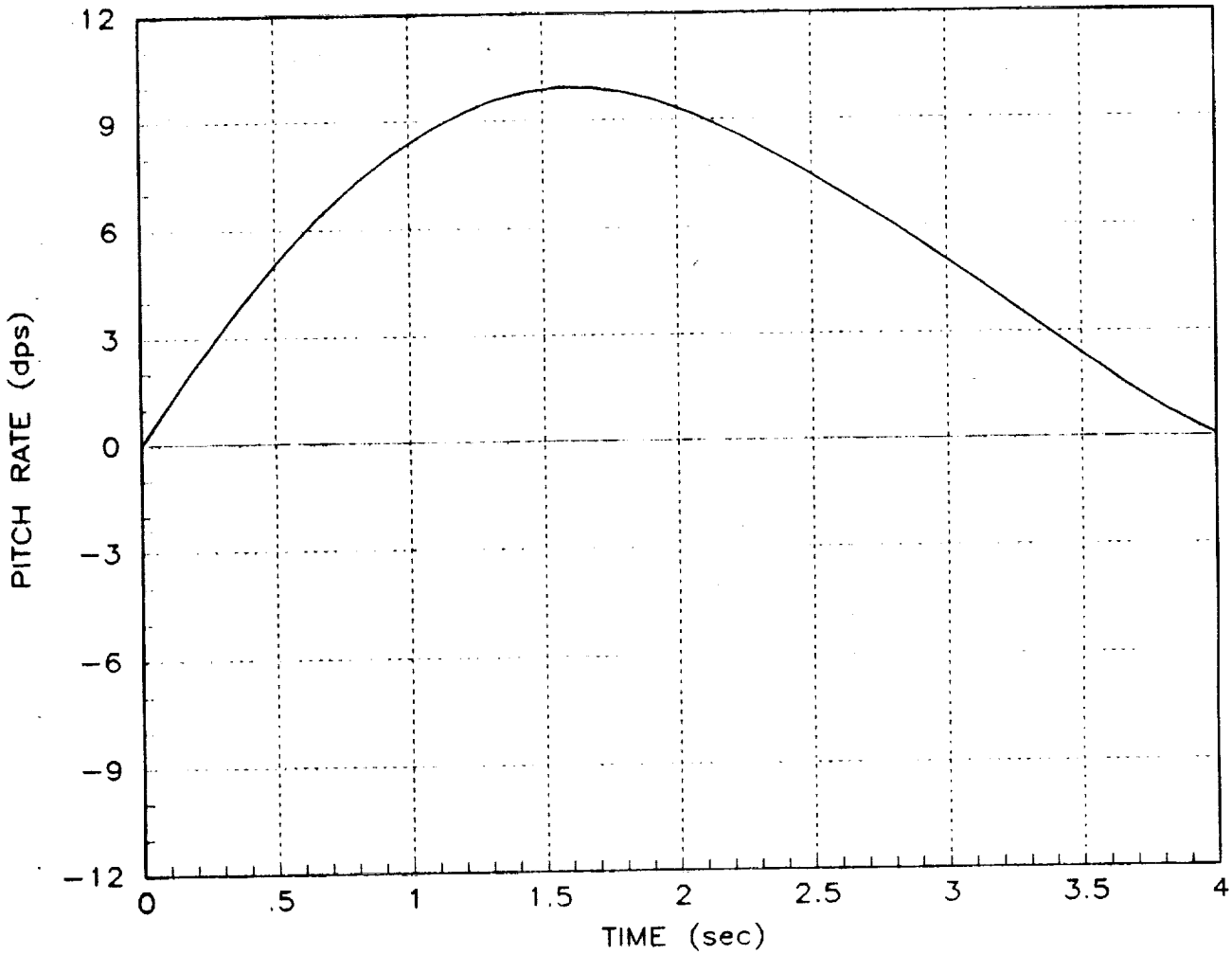

Figure 5 (c) — Mehra Input

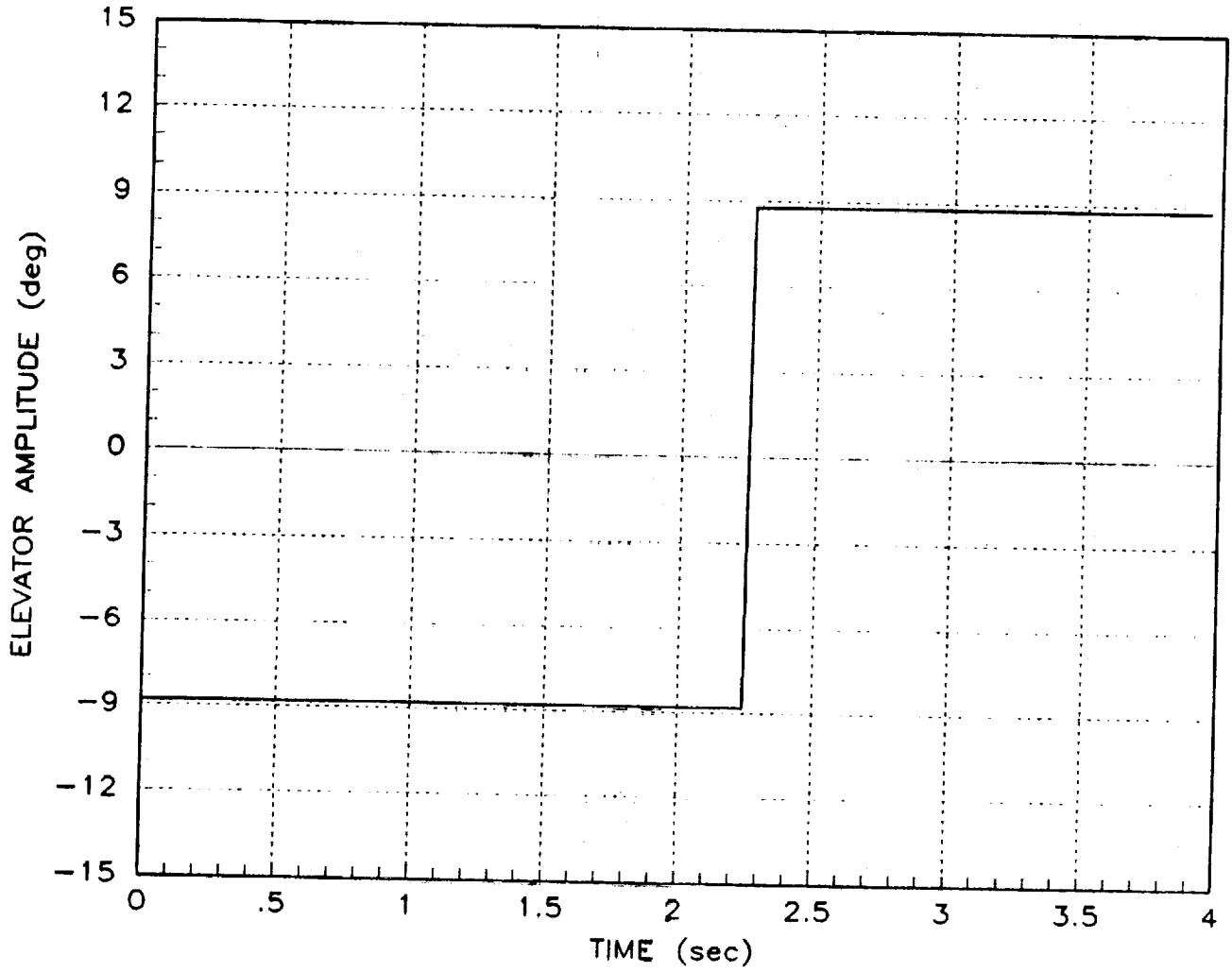

Figure 6 (a) – Chen Input

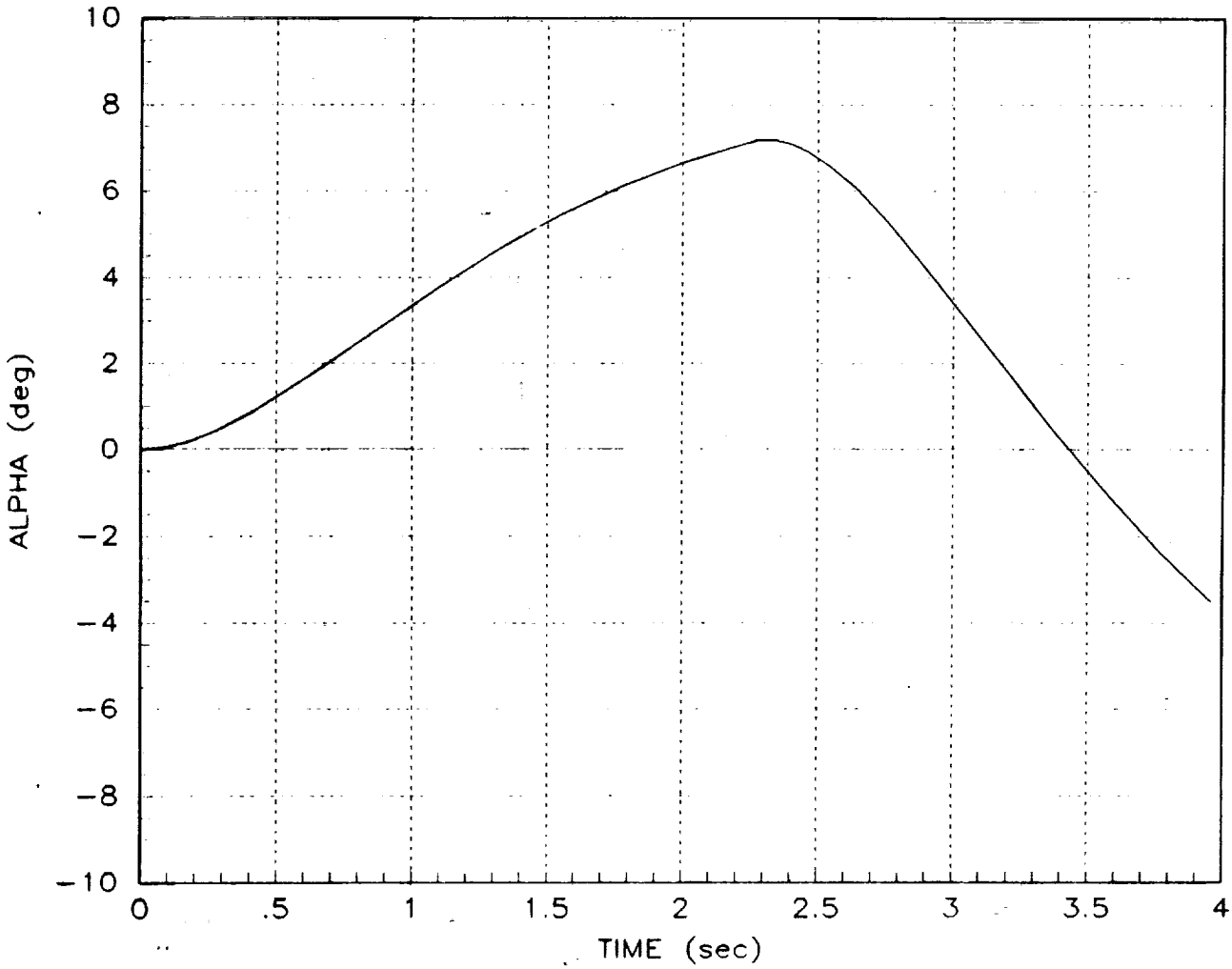

Figure 6 (b) — Chen Input

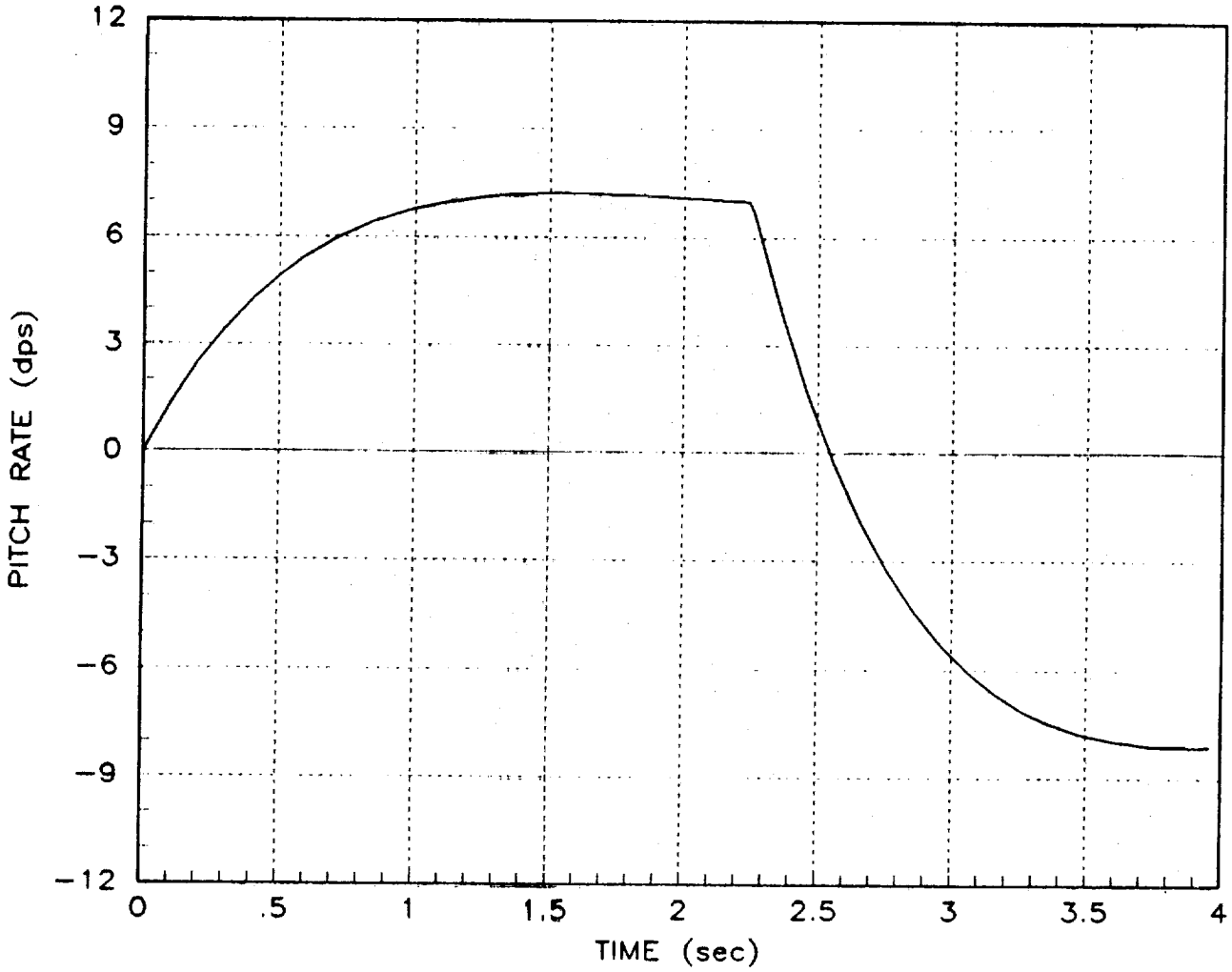

Figure 6 (c) – Chen Input

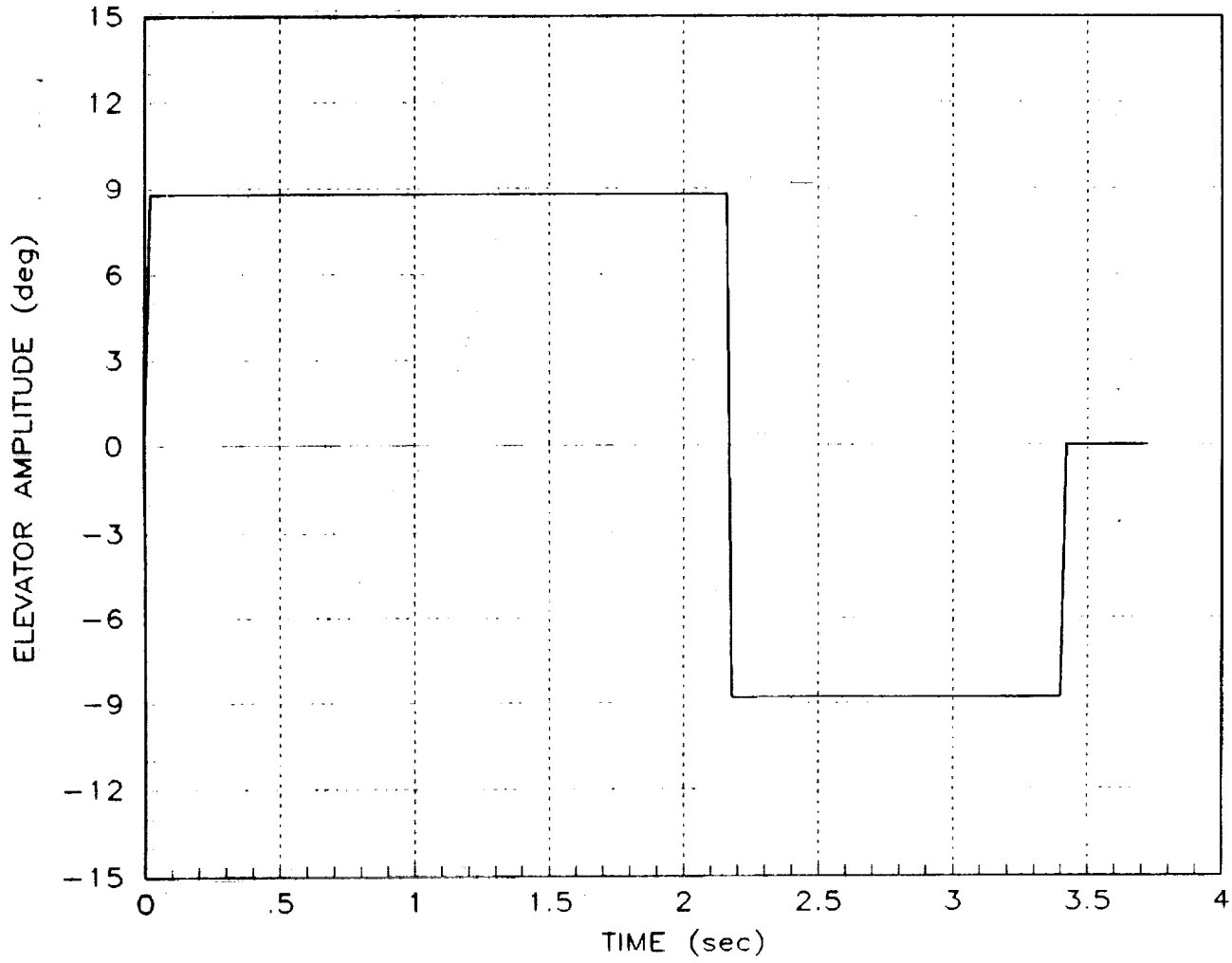

Figure 7 (a) — Optimal Input, Chen Amplitude

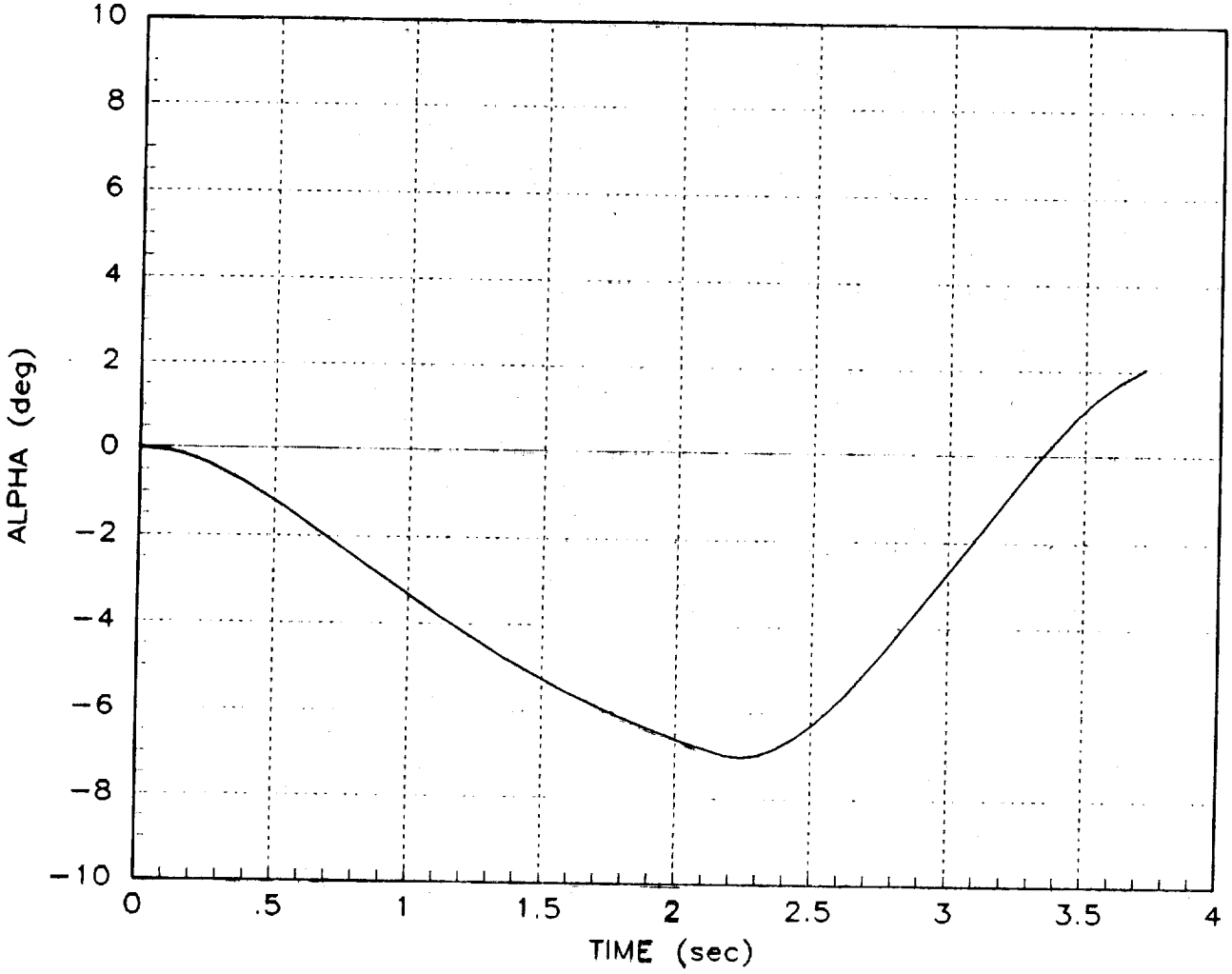

Figure 7 (b) – Optimal Input, Chen Amplitude

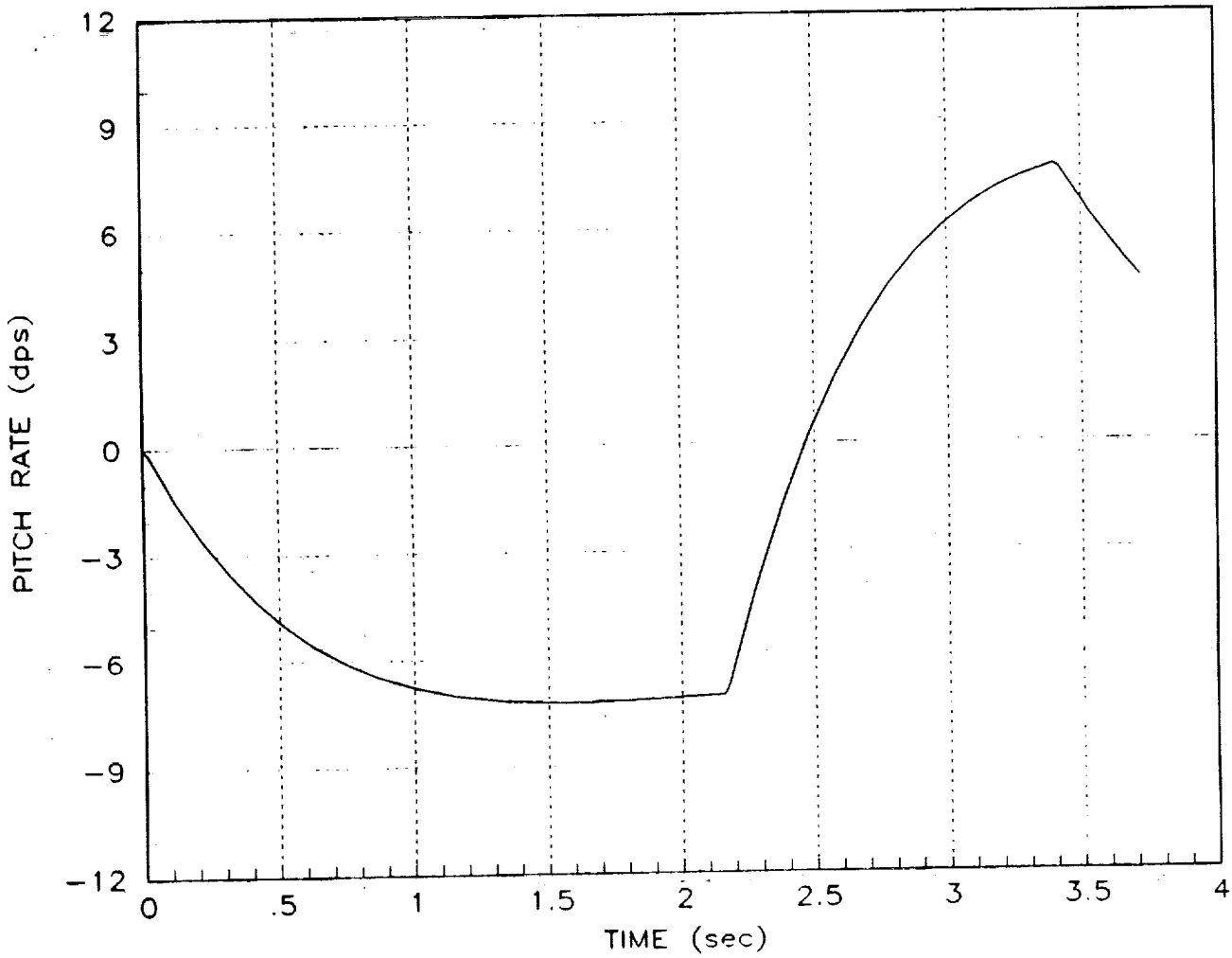

Figure 7 (c) – Optimal Input, Chen Amplitude

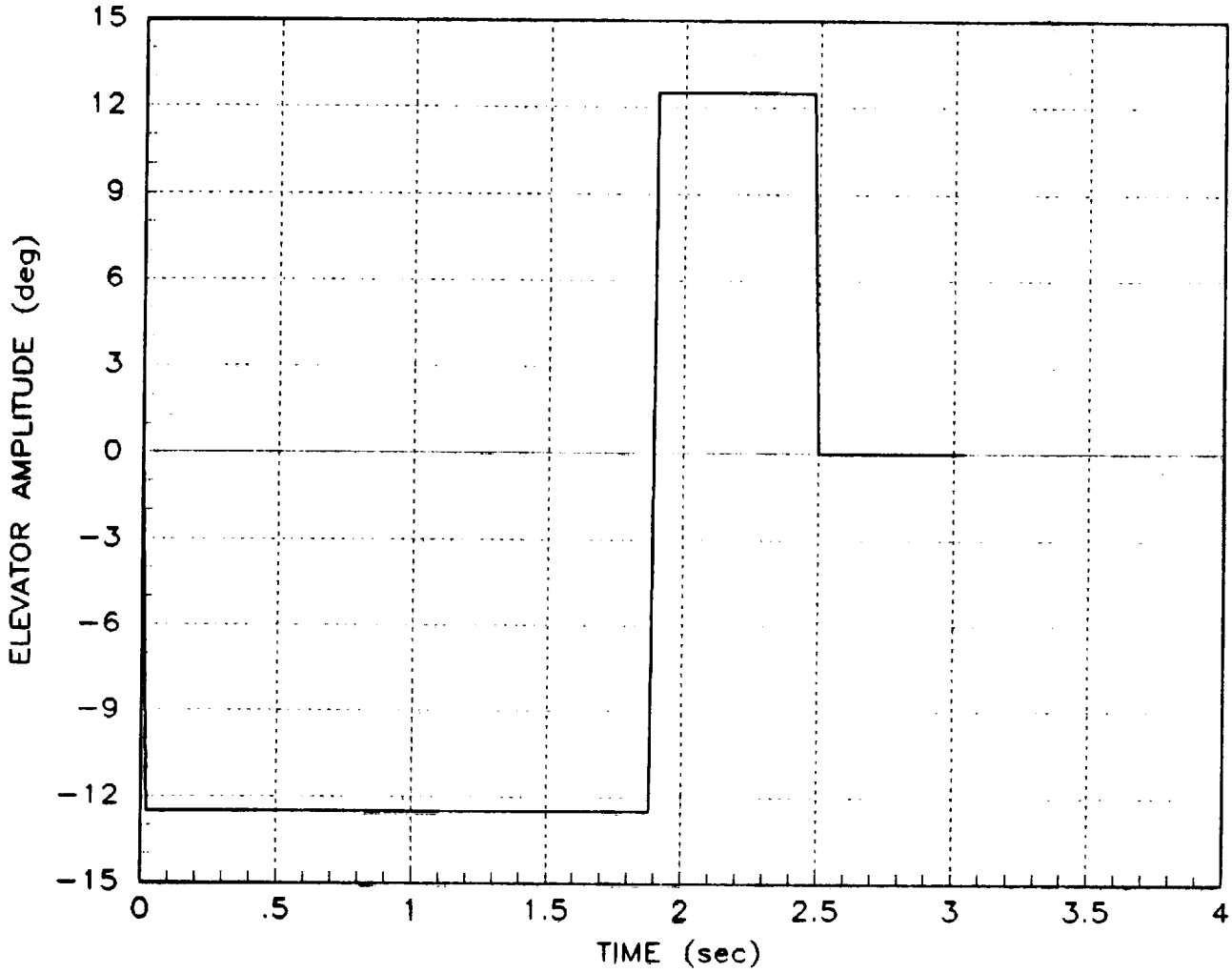

Figure 8 (a) – Optimal Input, Mehra Amplitude

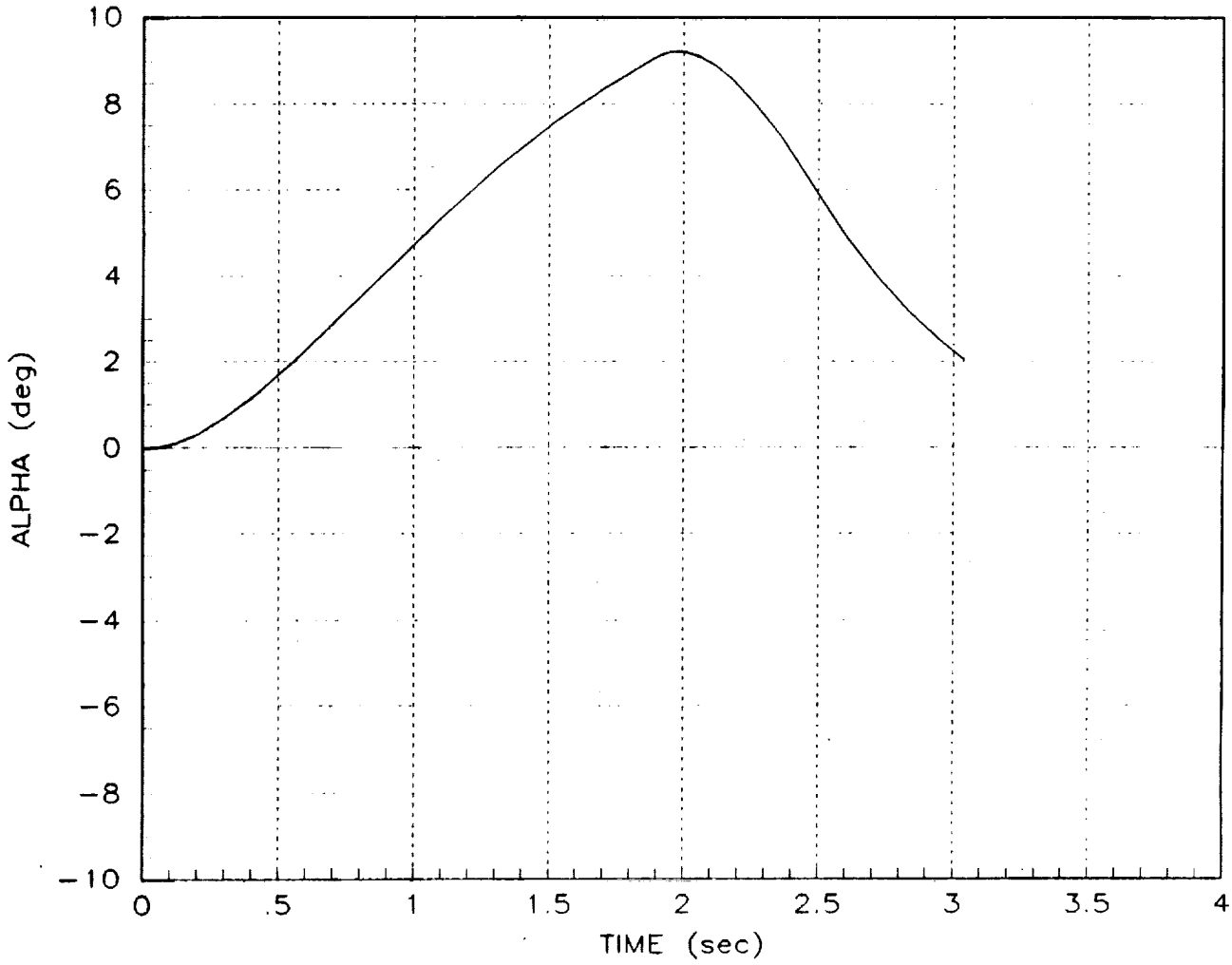

Figure 8 (b) – Optimal Input, Mehra Amplitude

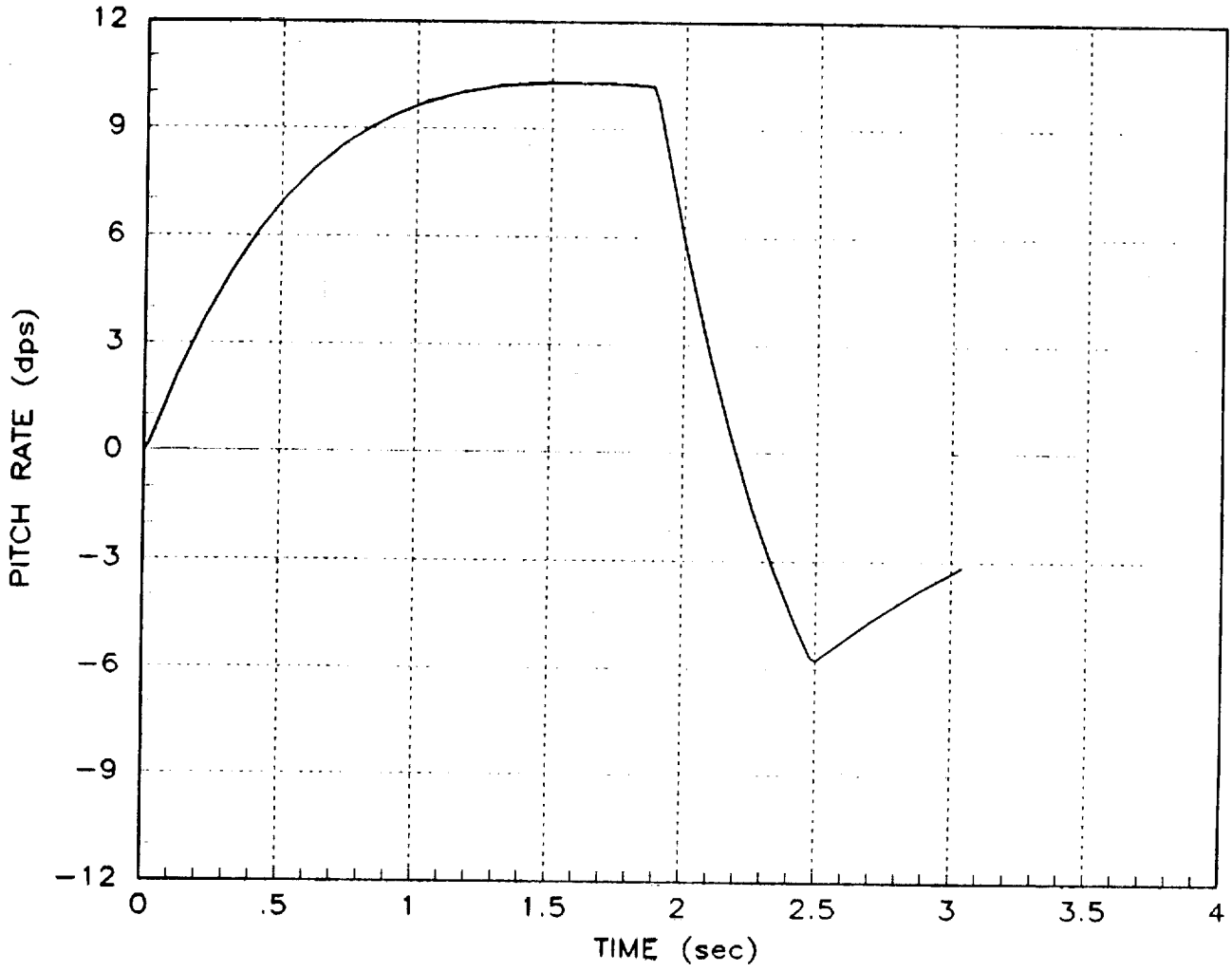

Figure 8 (c) — Optimal Input, Mehra Amplitude

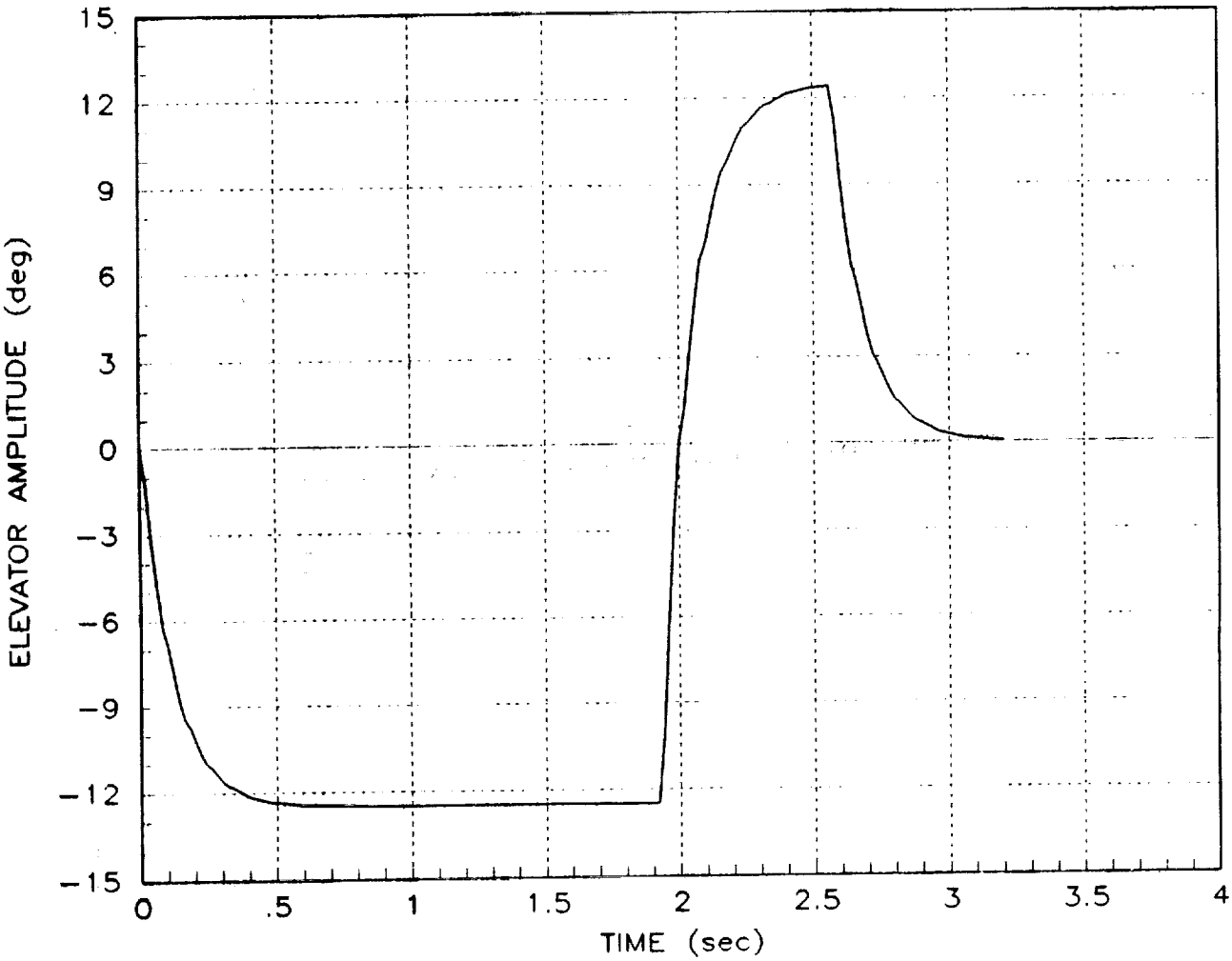

Figure 9 (a) – Optimal Input, Mehra Amplitude with lag

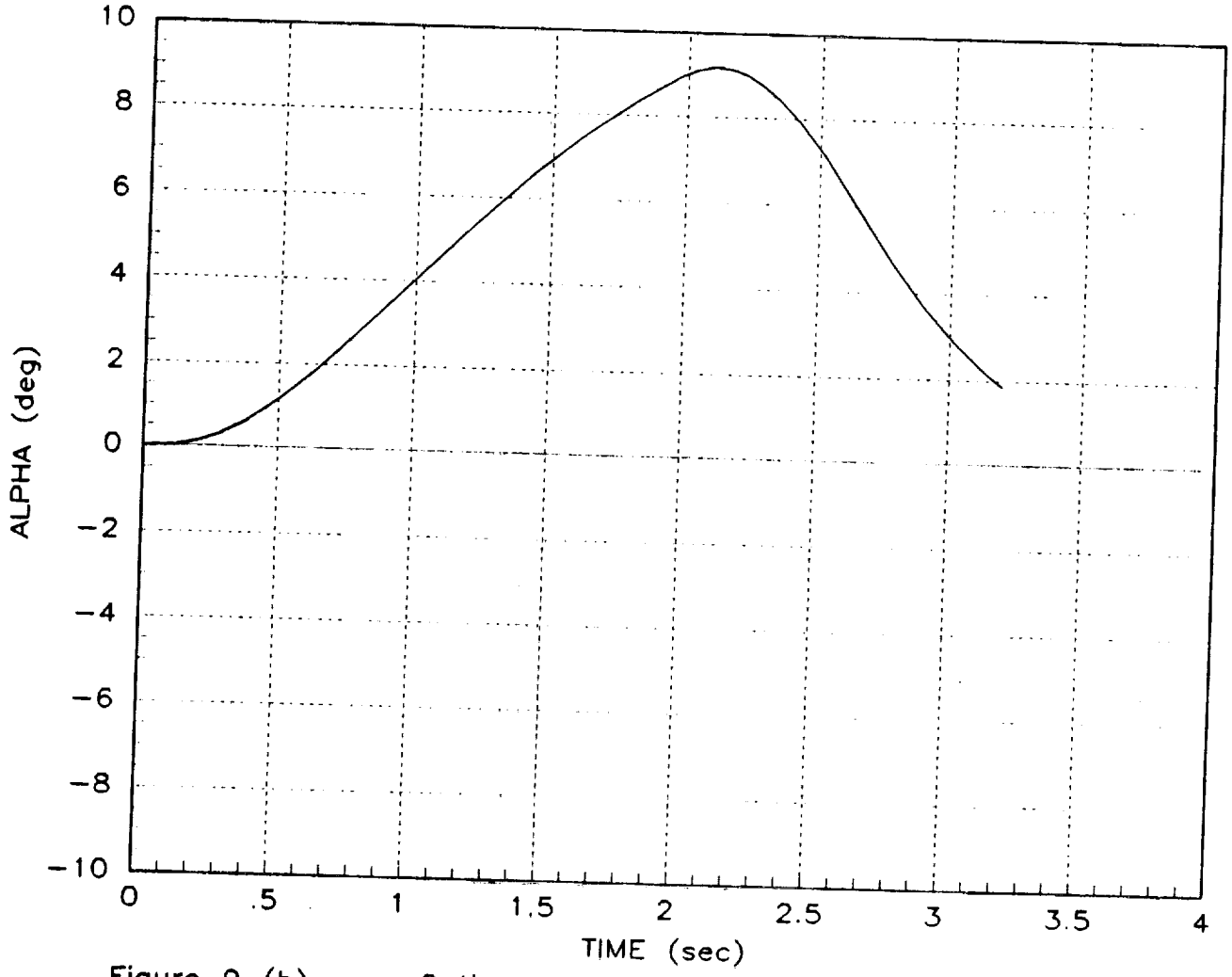

Figure 9 (b) – Optimal Input, Mehra Amplitude with lag

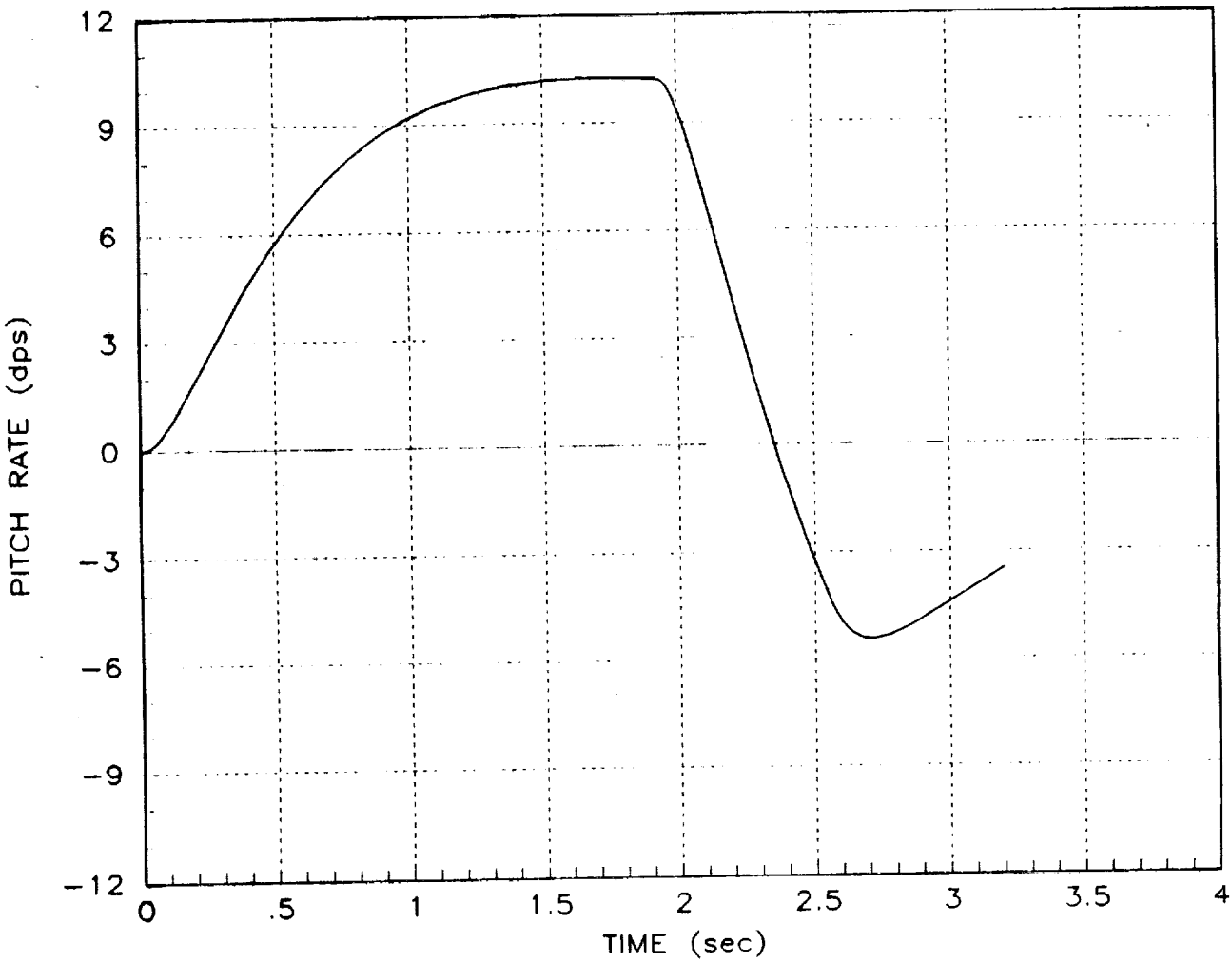

Figure 9 (c) – Optimal Input, Mehra Amplitude with lag

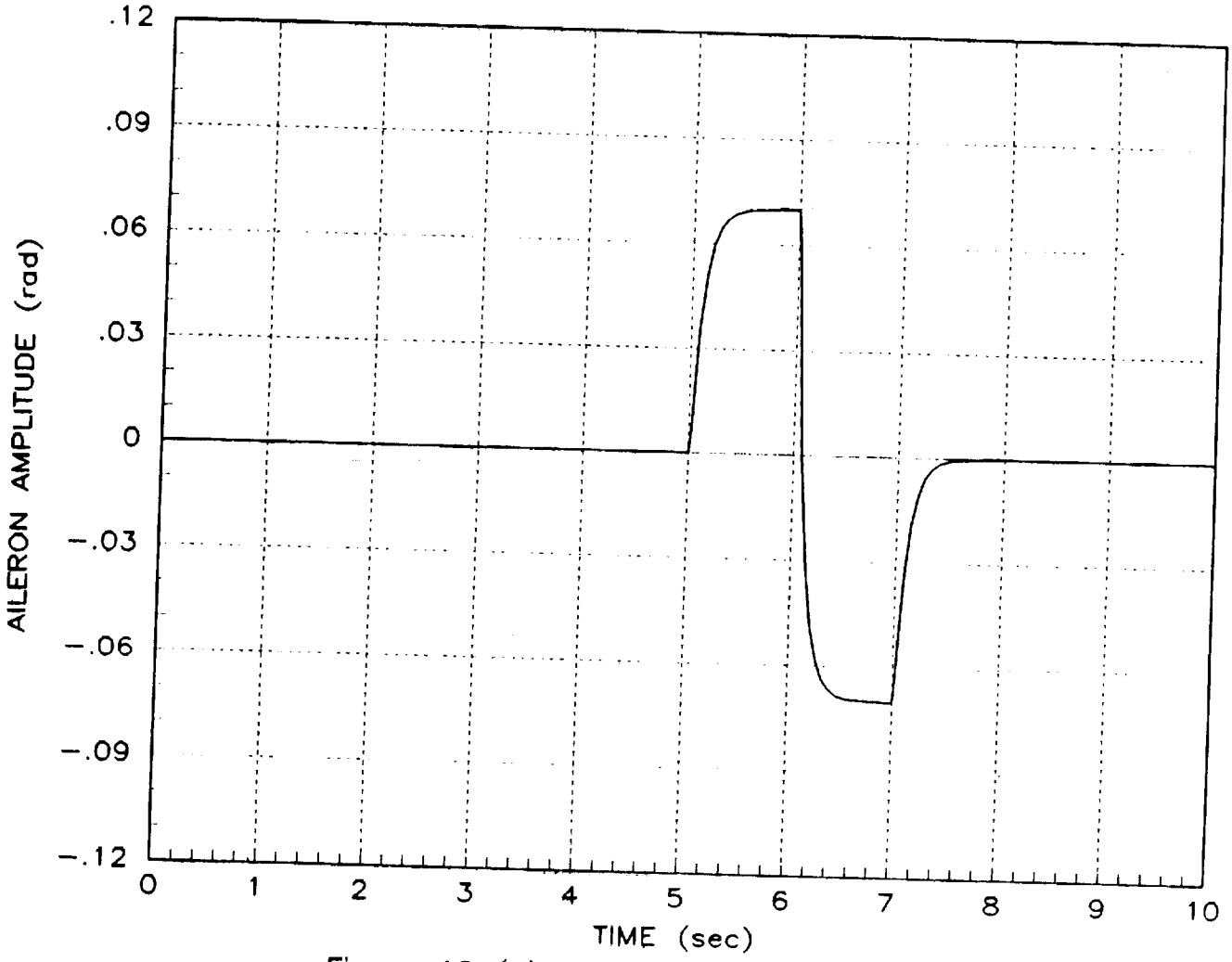

Figure 10 (a) – Doublet Inputs

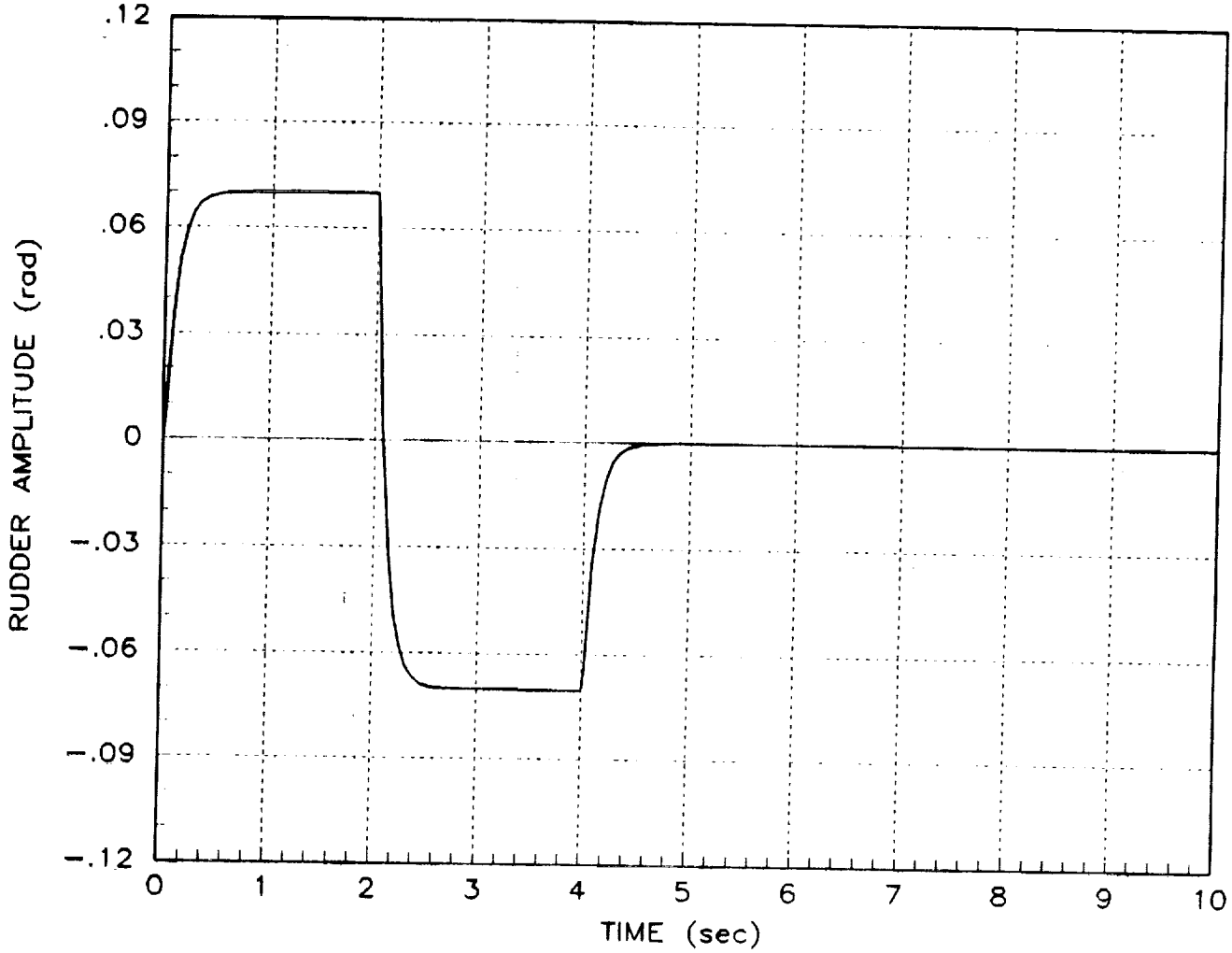

Figure 10 (b) – Doublet Inputs

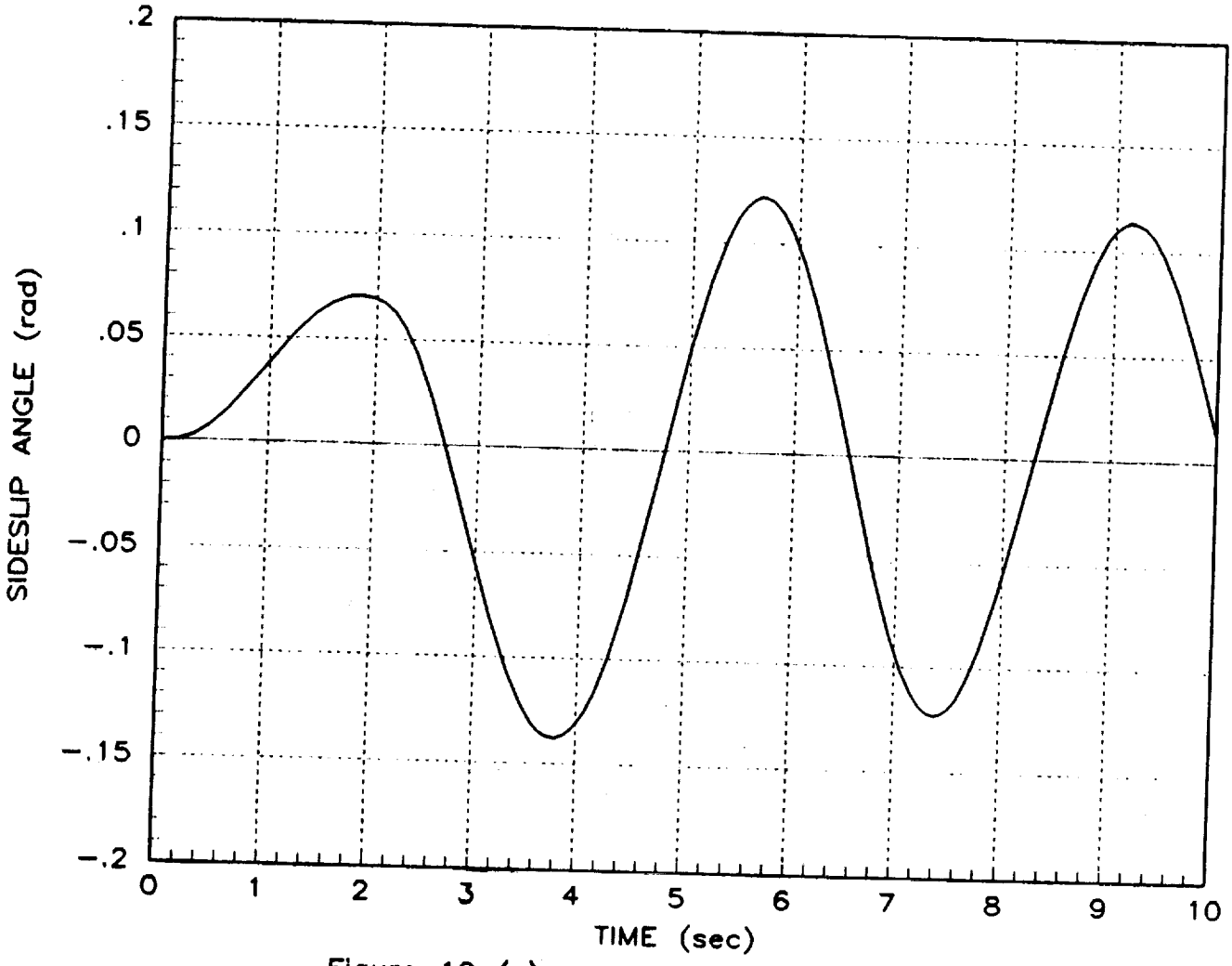

Figure 10 (c) – Doublet Inputs

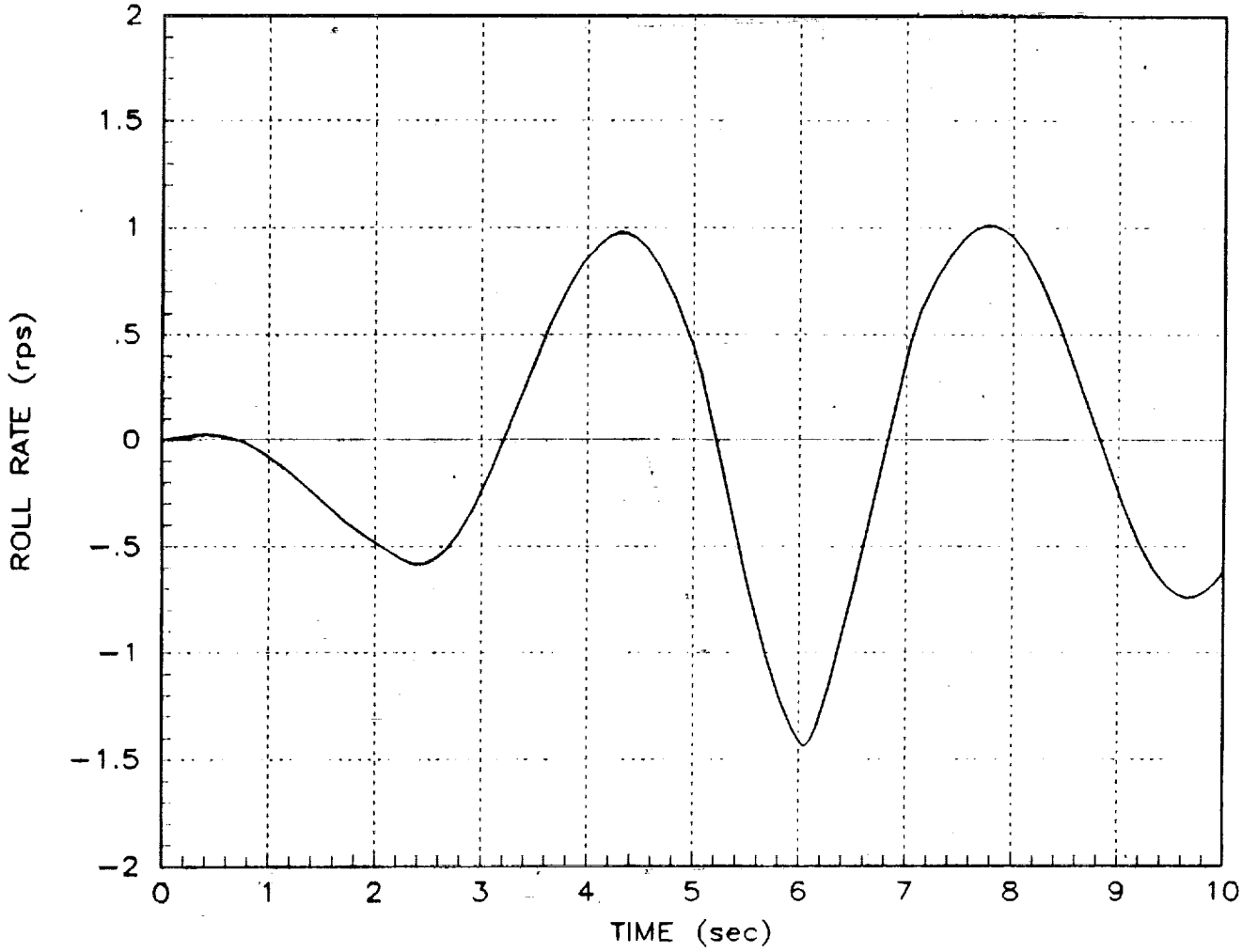

Figure 10 (d) — Doublet Inputs

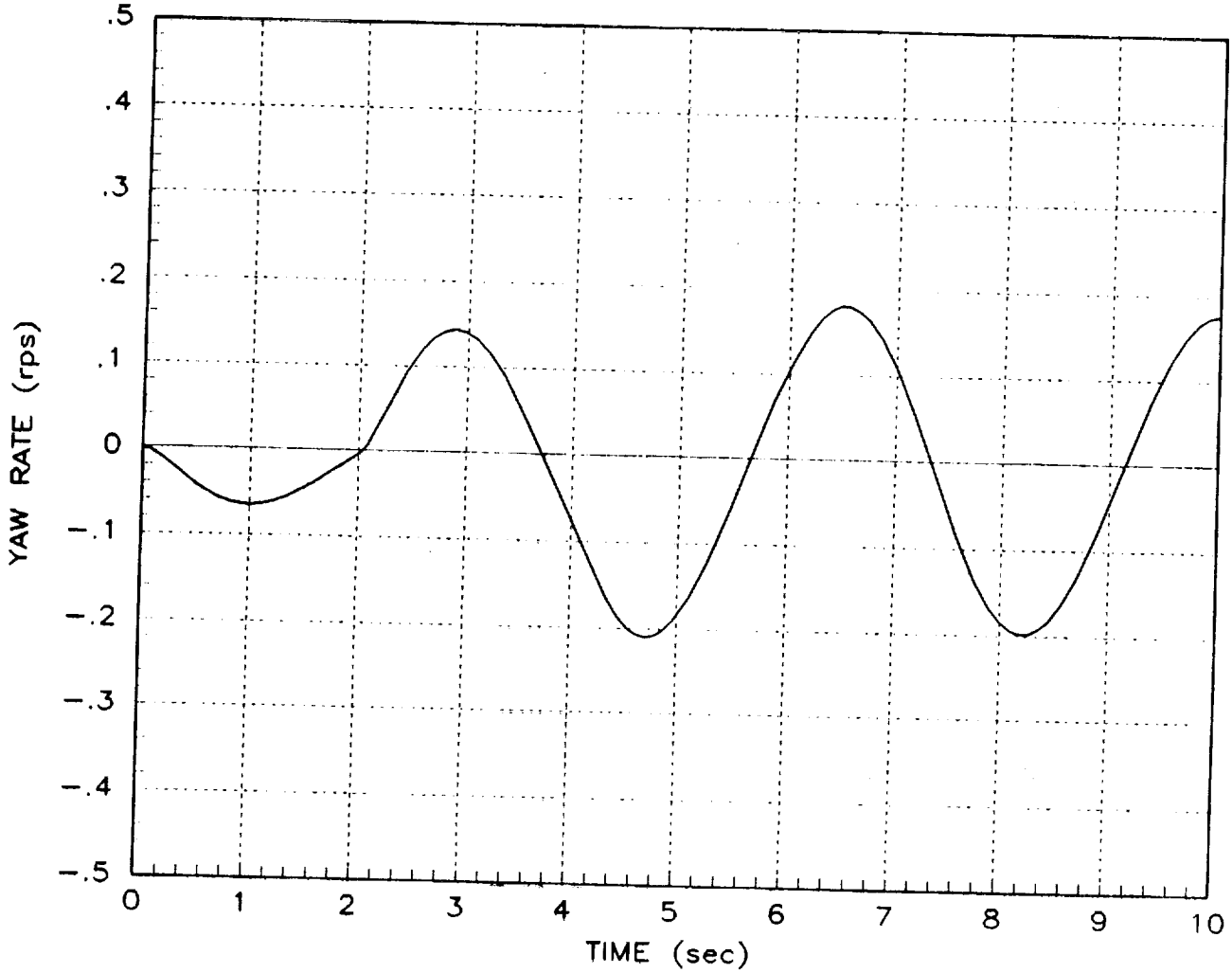

Figure 10 (e) – Doublet Inputs

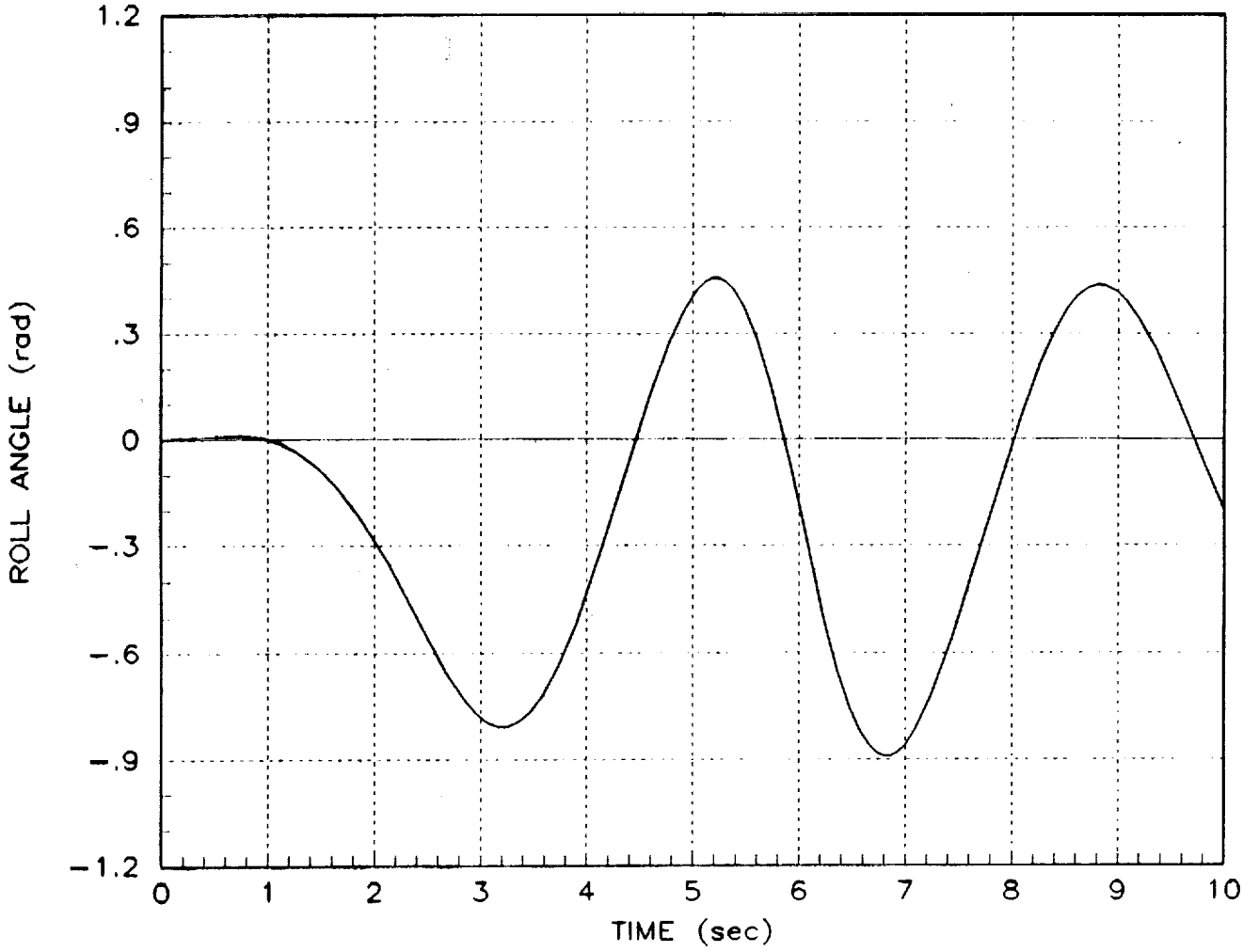

Figure 10 (f) – Doublet Inputs

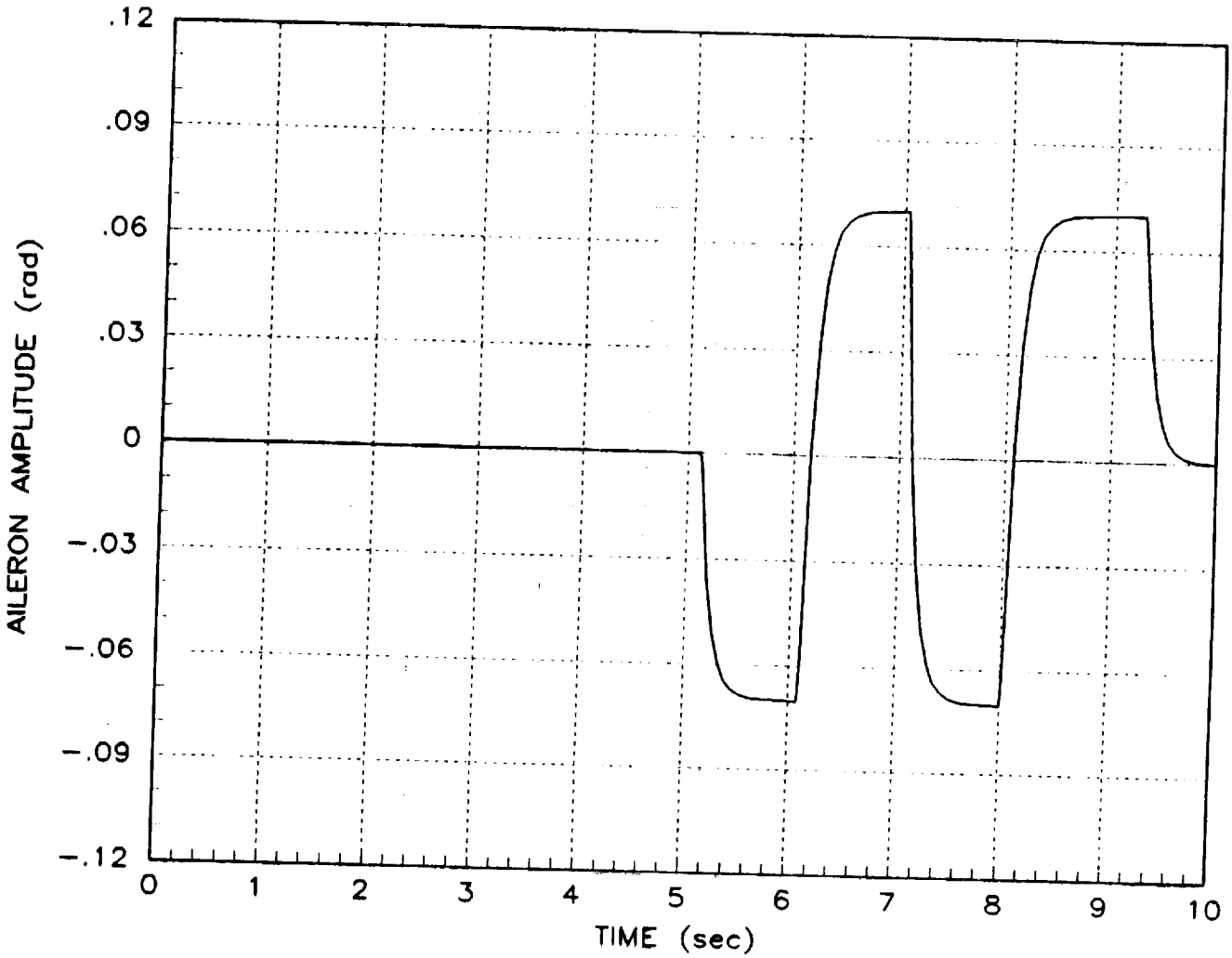

Figure 11 (a) – Optimal Inputs

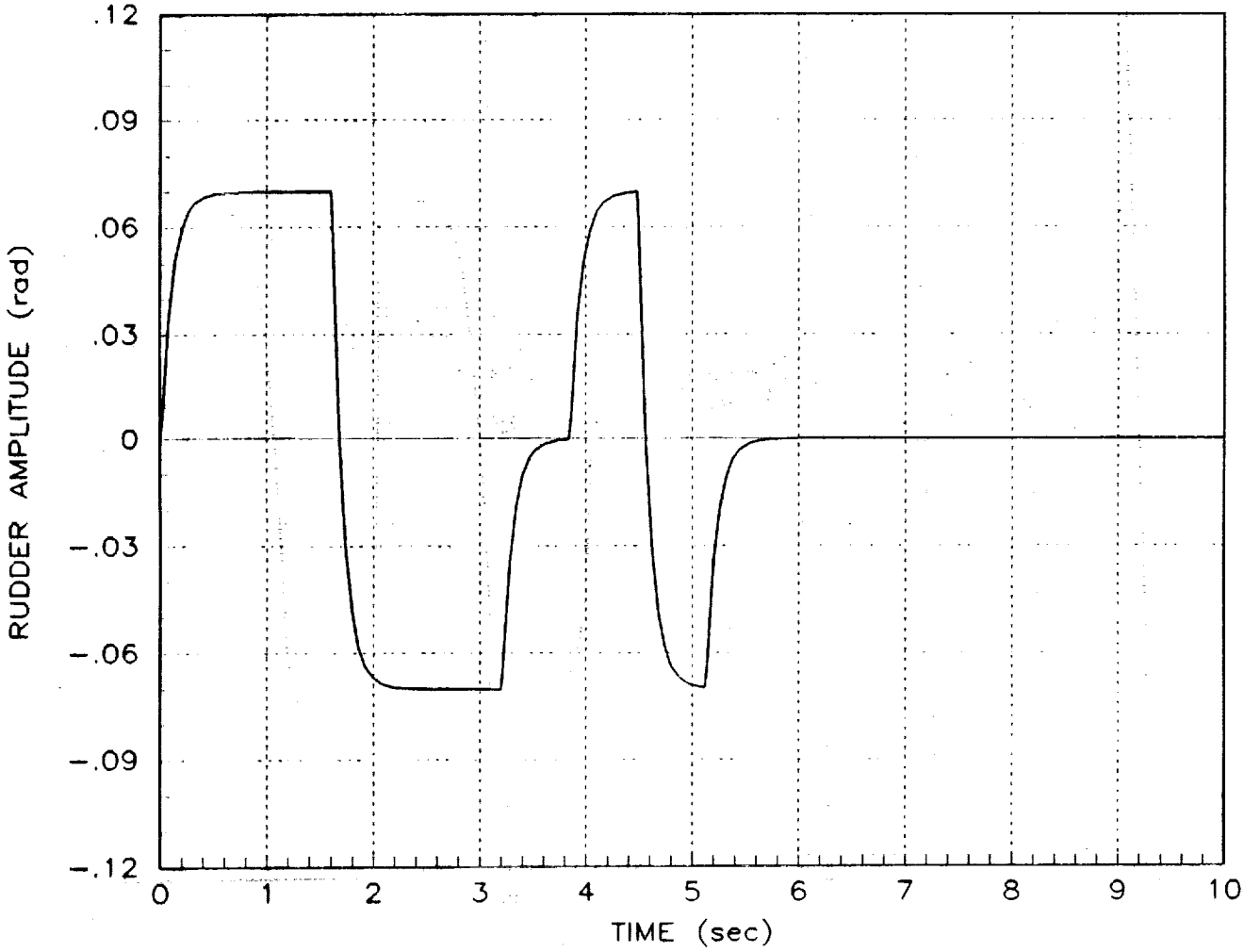

Figure 11 (b) – Optimal Inputs

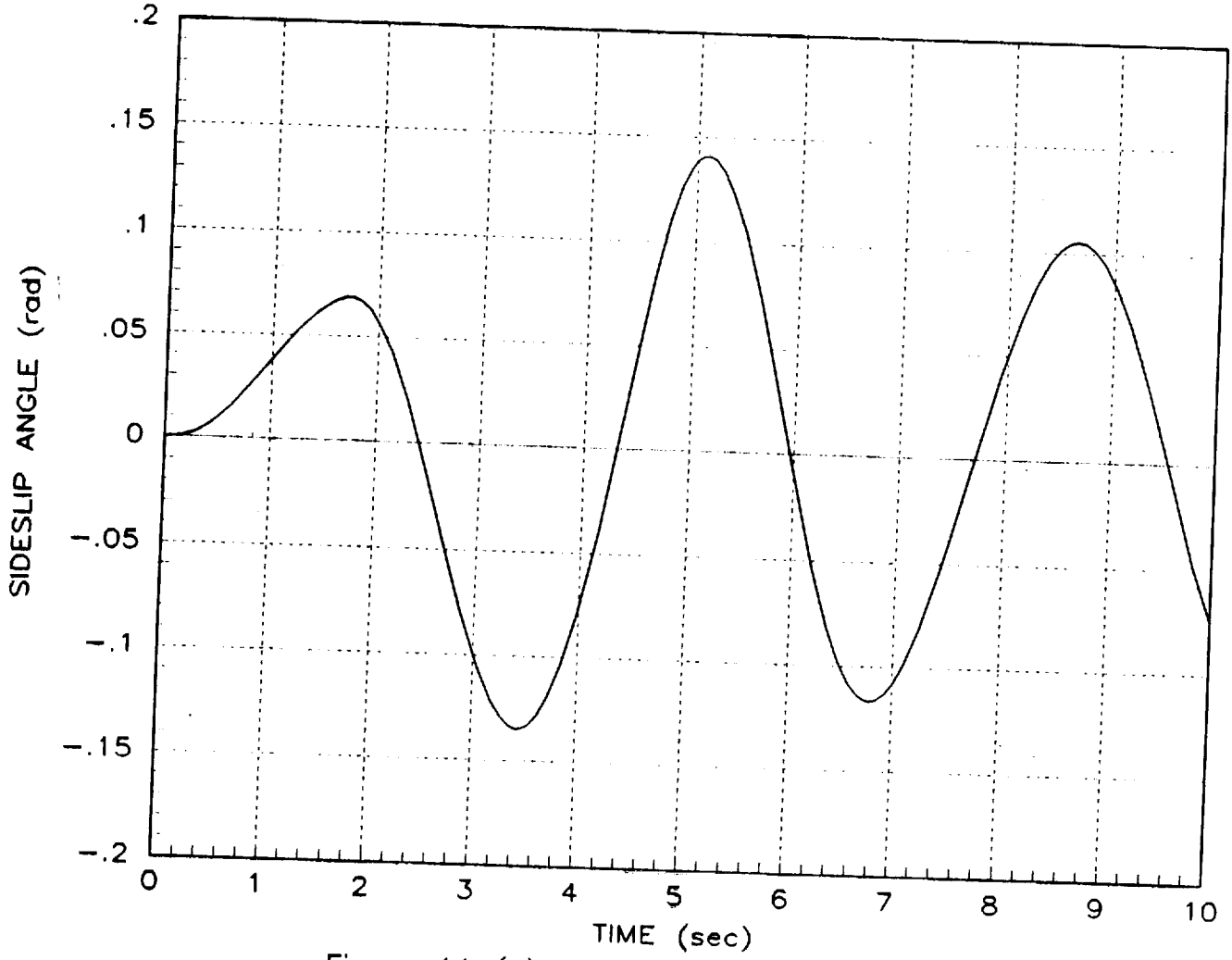

Figure 11 (c) – Optimal Inputs

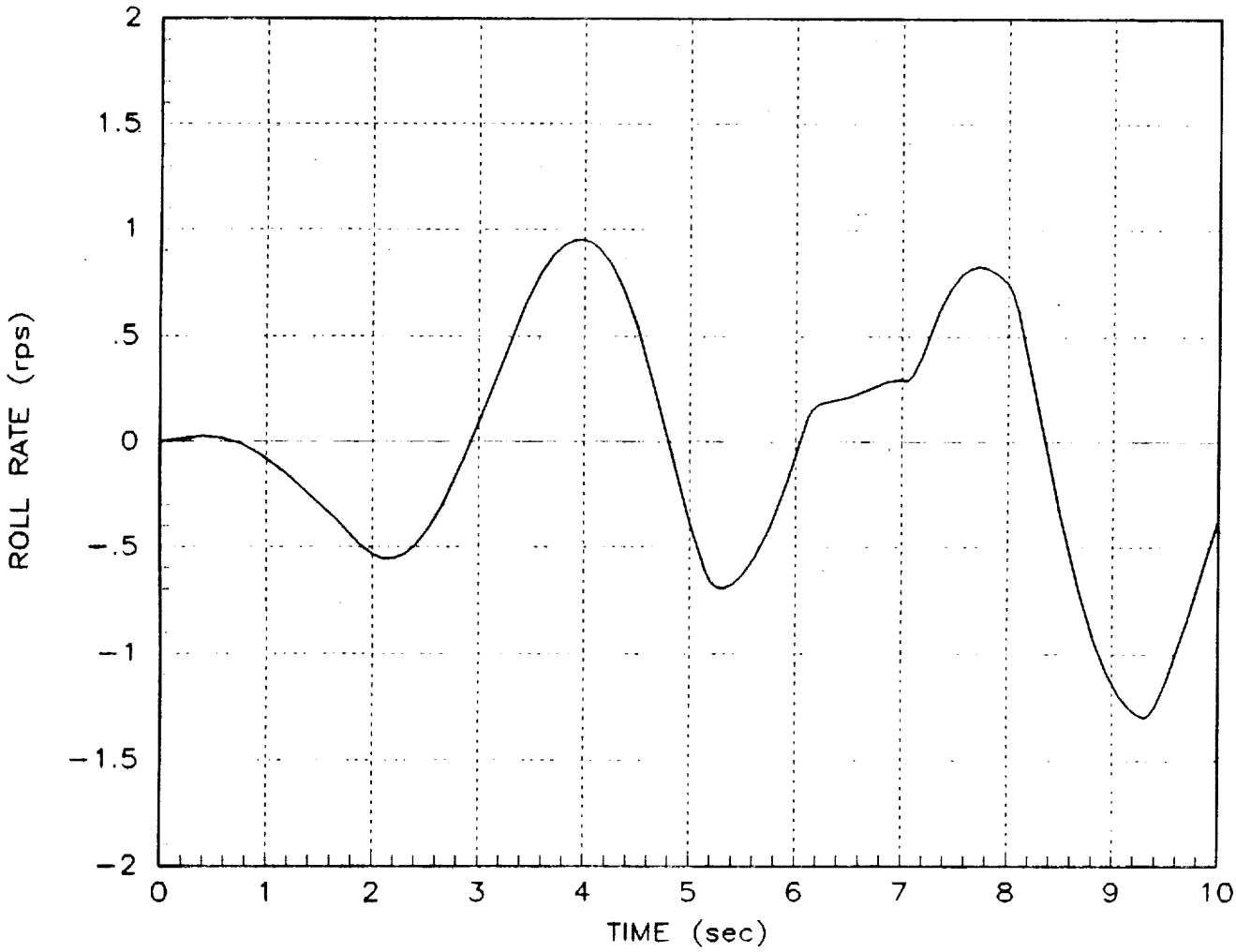

Figure 11 (d) – Optimal Inputs

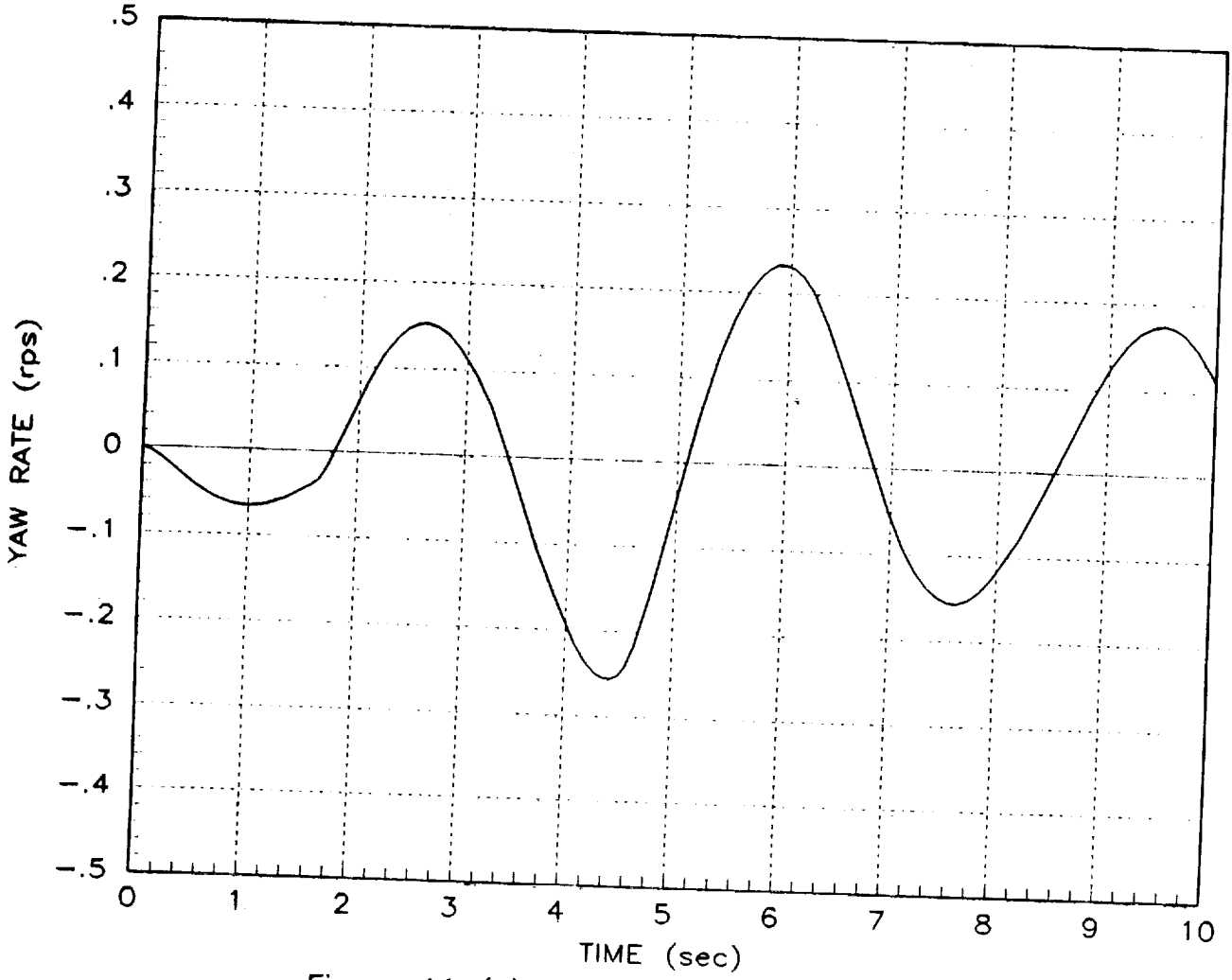

Figure 11 (e) – Optimal Inputs

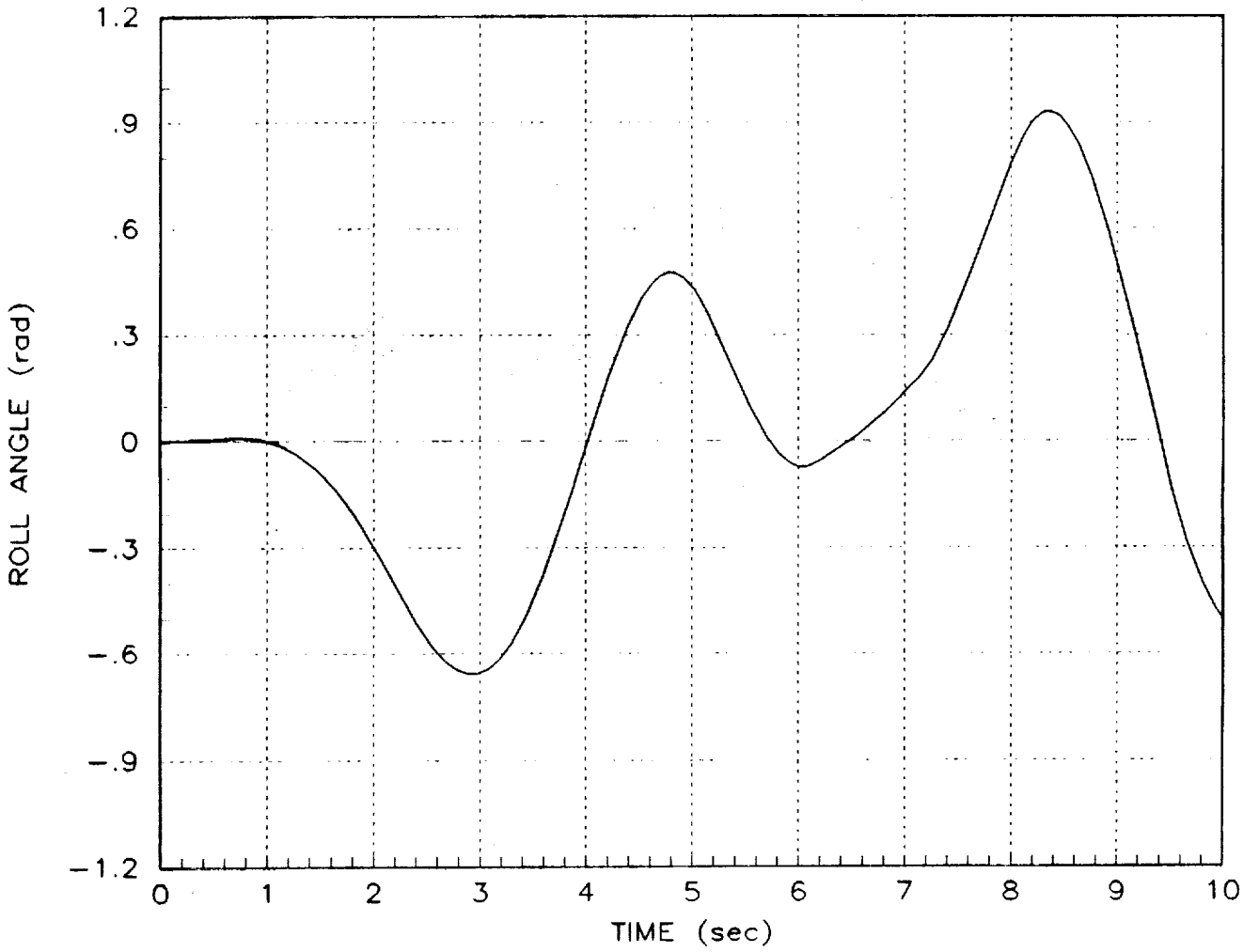

Figure 11 (f) — Optimal Inputs

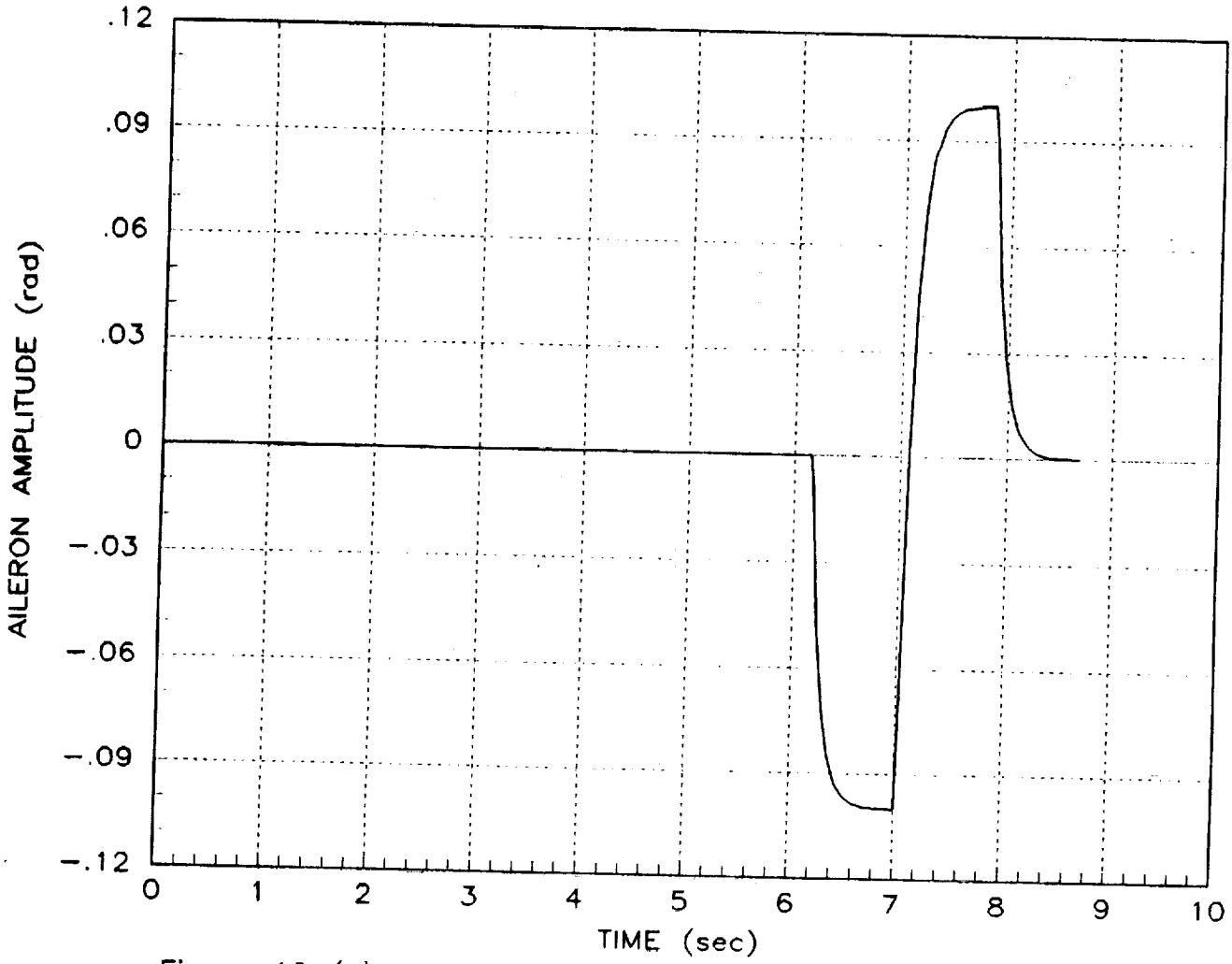

Figure 12 (a) – Optimal Inputs, Increased Amplitude

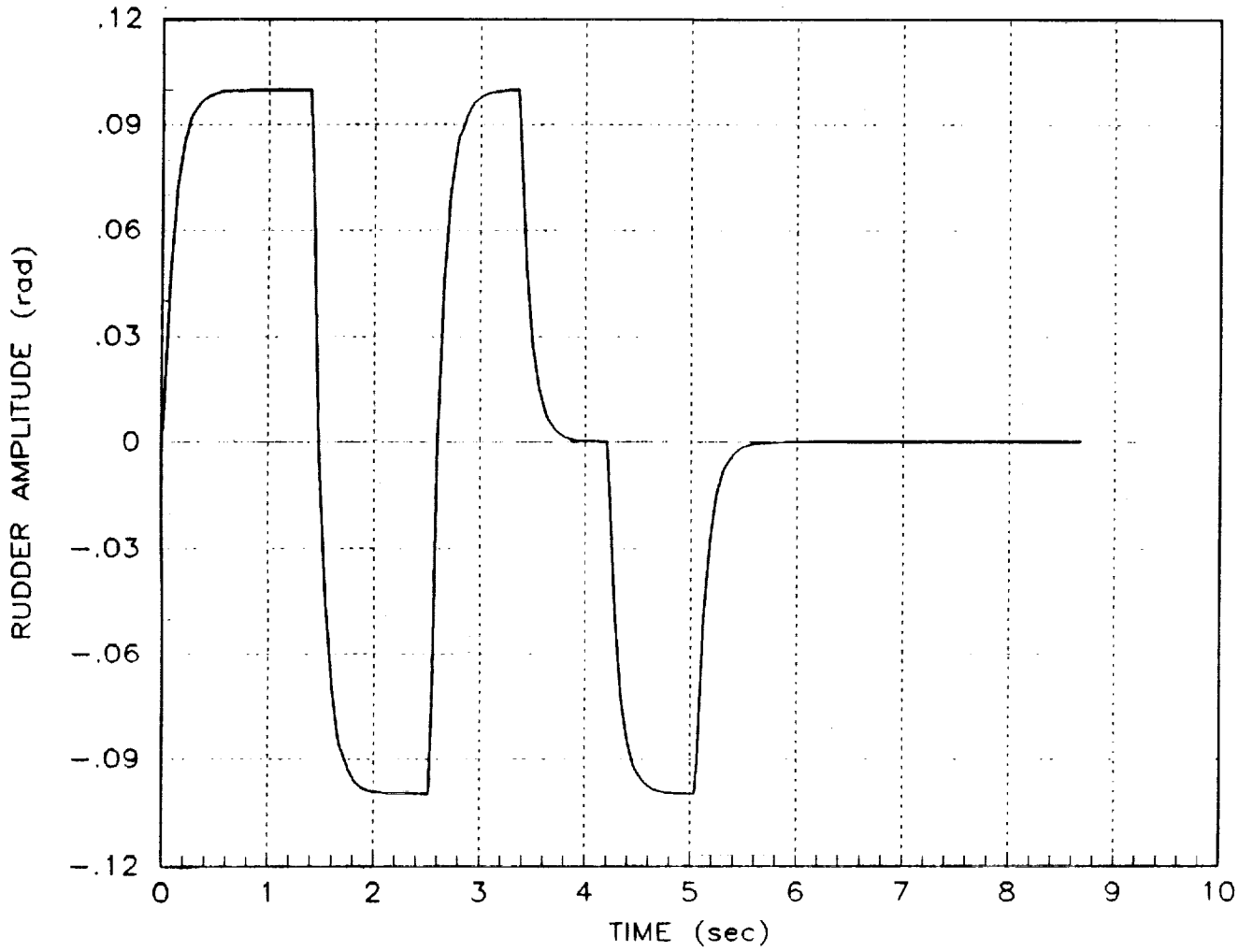

Figure 12 (b) – Optimal Inputs, Increased Amplitude

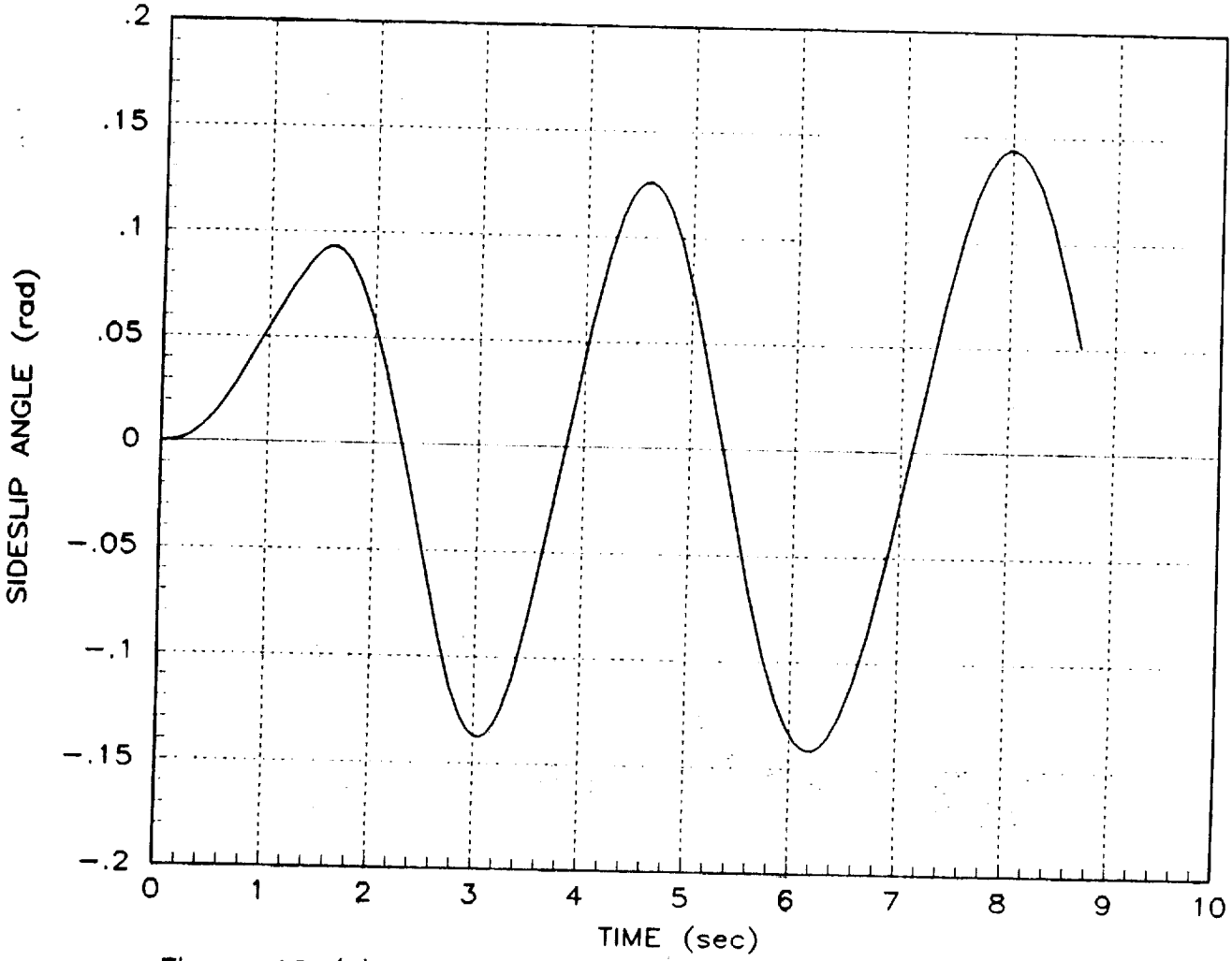

Figure 12 (c) – Optimal Inputs, Increased Amplitude

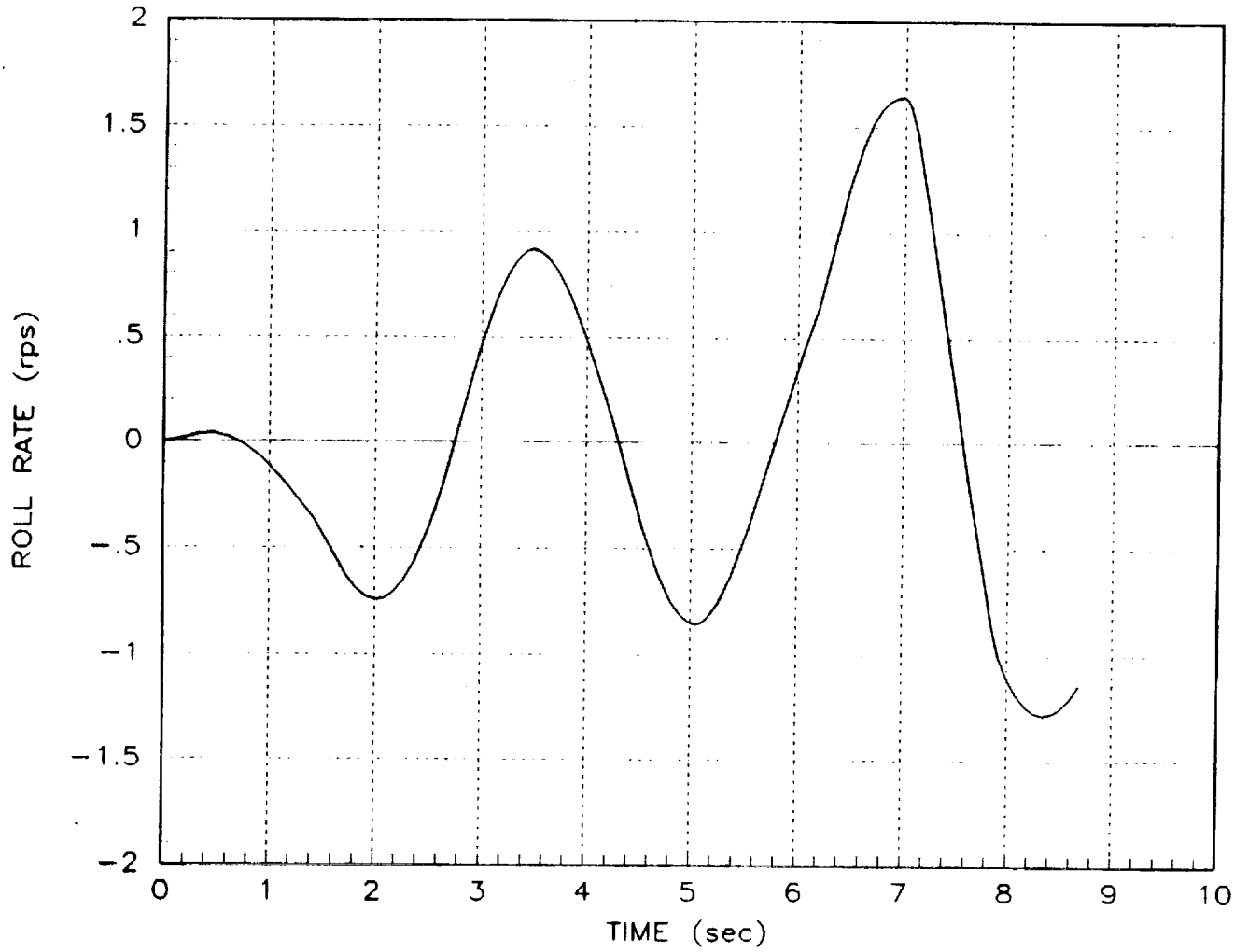

Figure 12 (d) – Optimal Inputs, Increased Amplitude

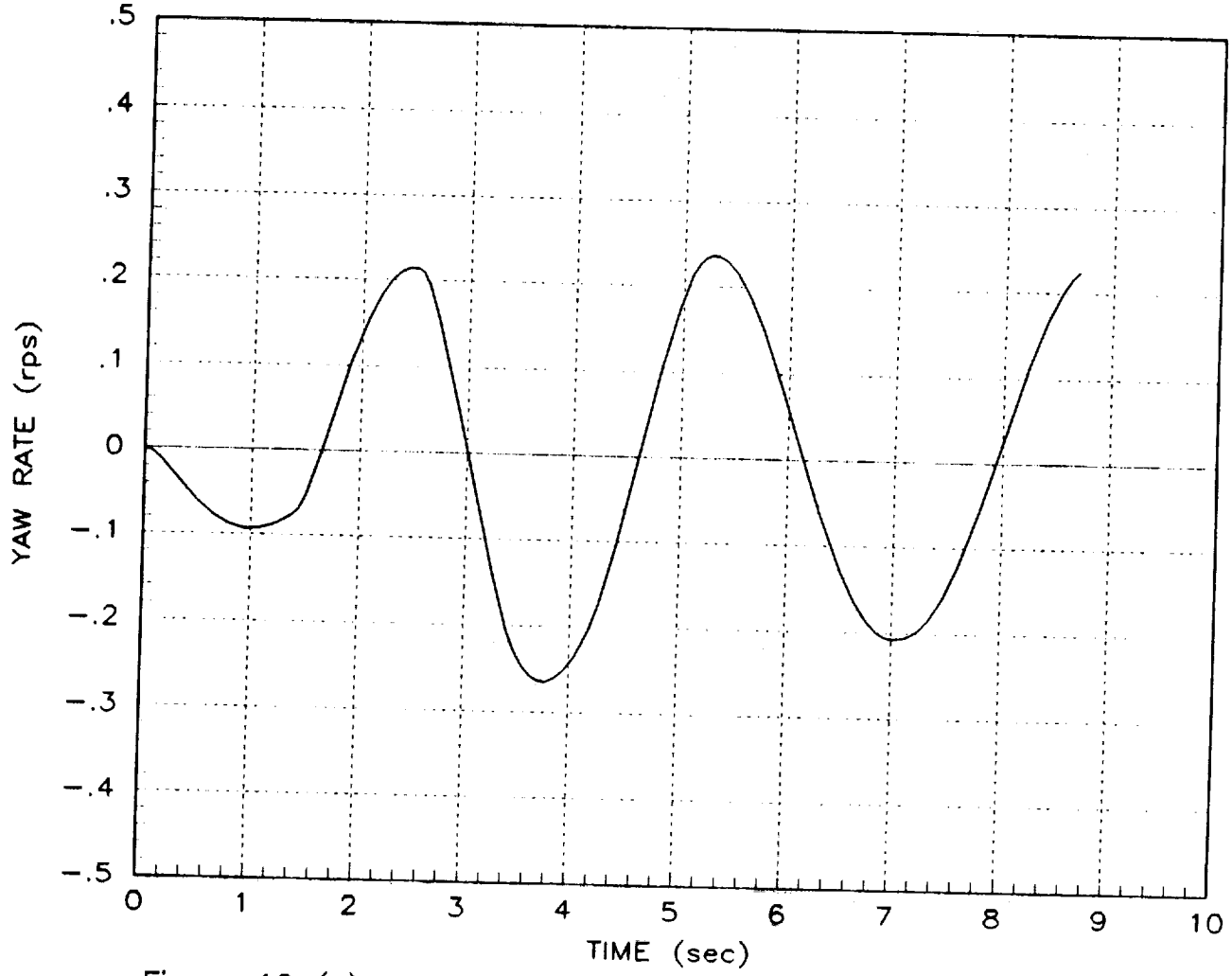

Figure 12 (e) – Optimal Inputs, Increased Amplitude

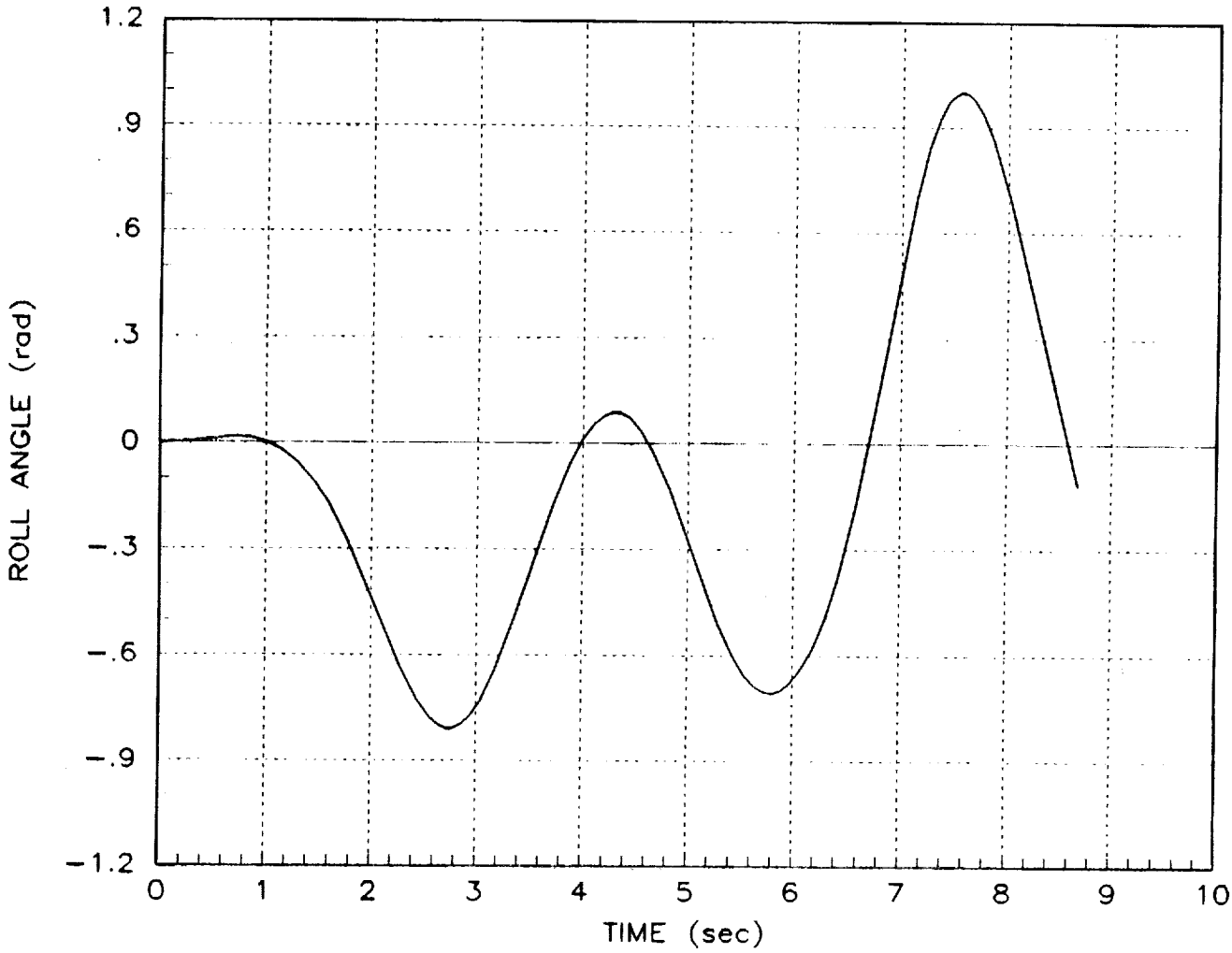

Figure 12 (f) – Optimal Inputs, Increased Amplitude

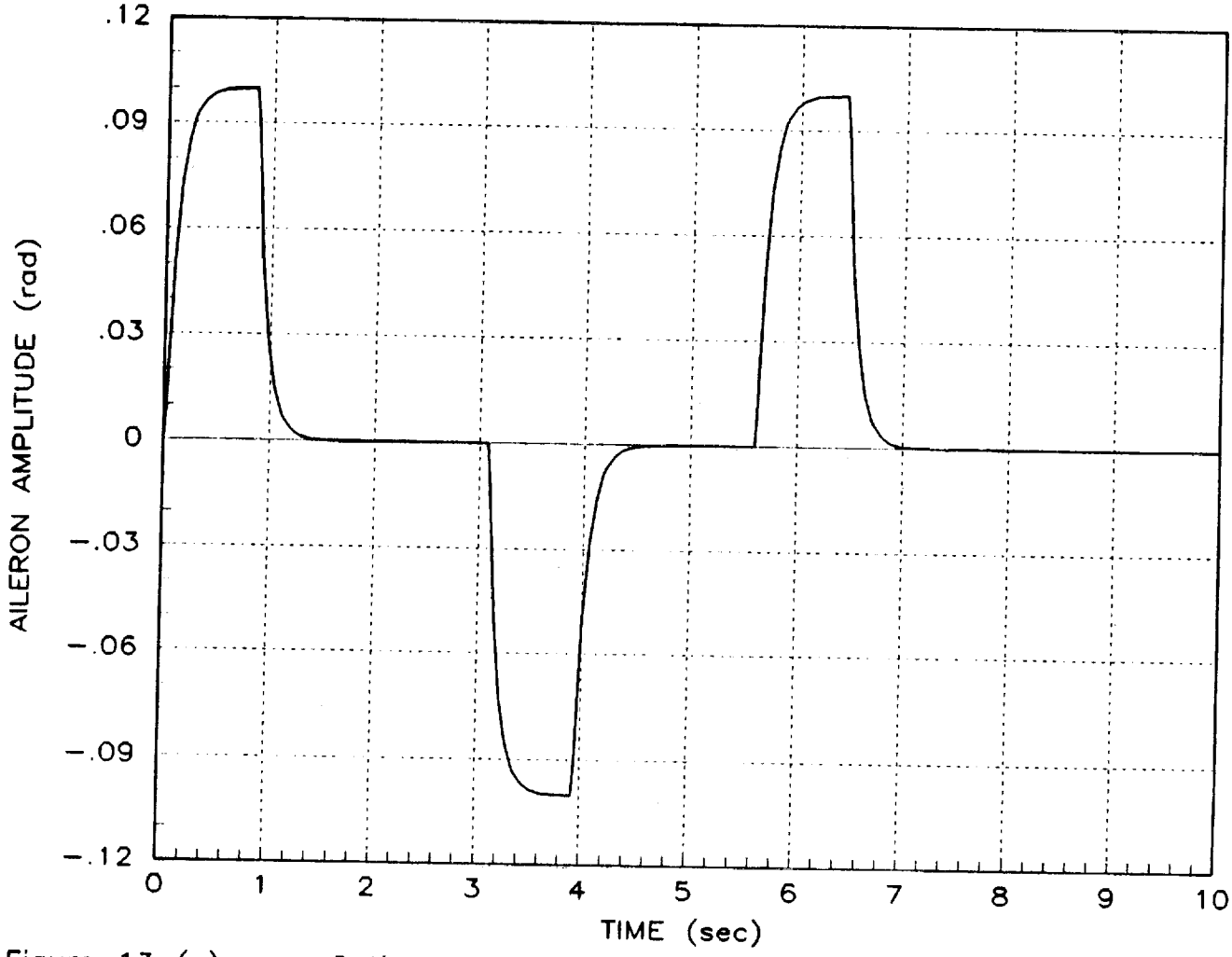

Figure 13 (a) — Optimal Inputs, Increased Amp., No Control Sequencing

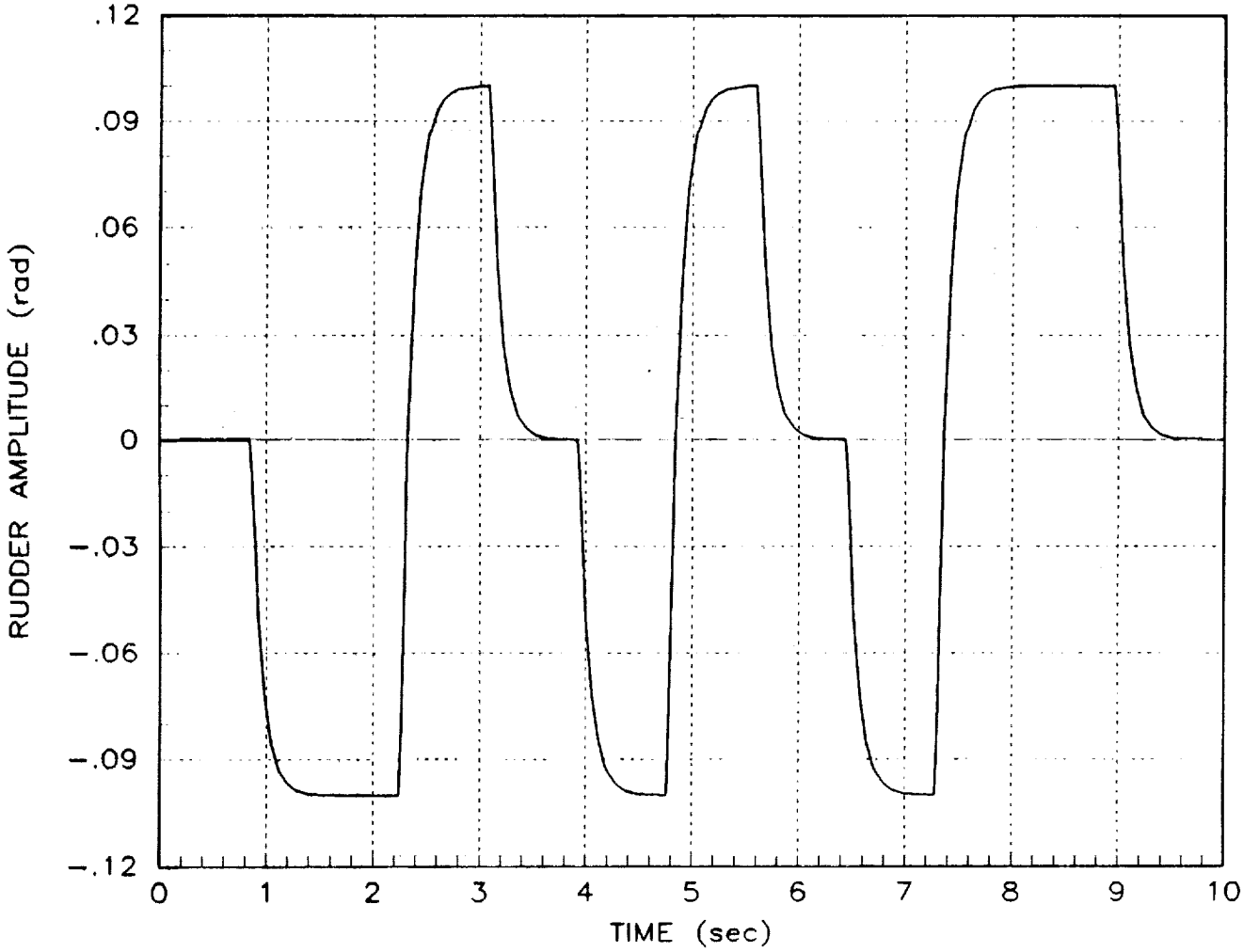

Figure 13 (b) — Optimal Inputs, Increased Amp., No Control Sequencing

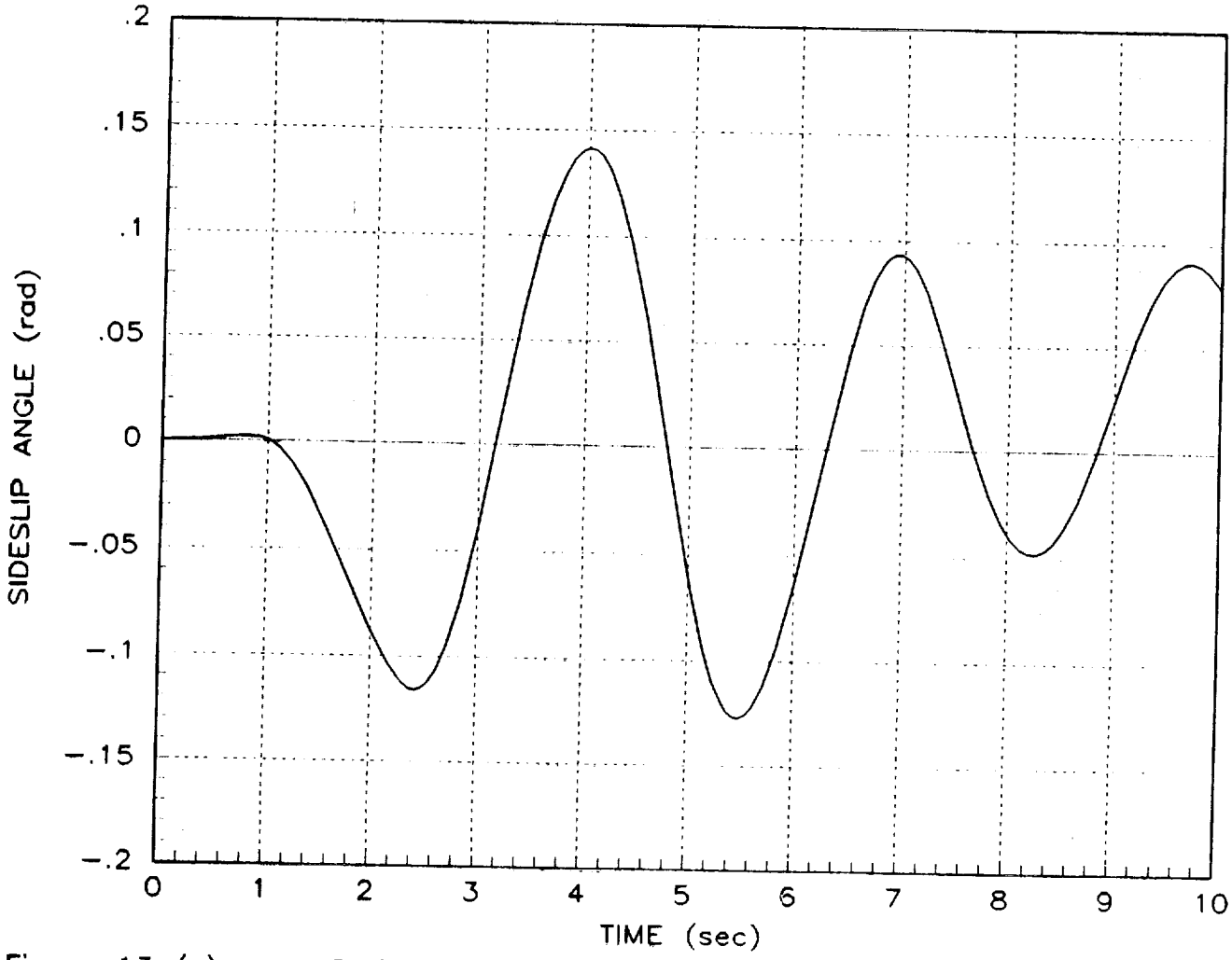

Figure 13 (c) – Optimal Inputs, Increased Amp., No Control Sequencing

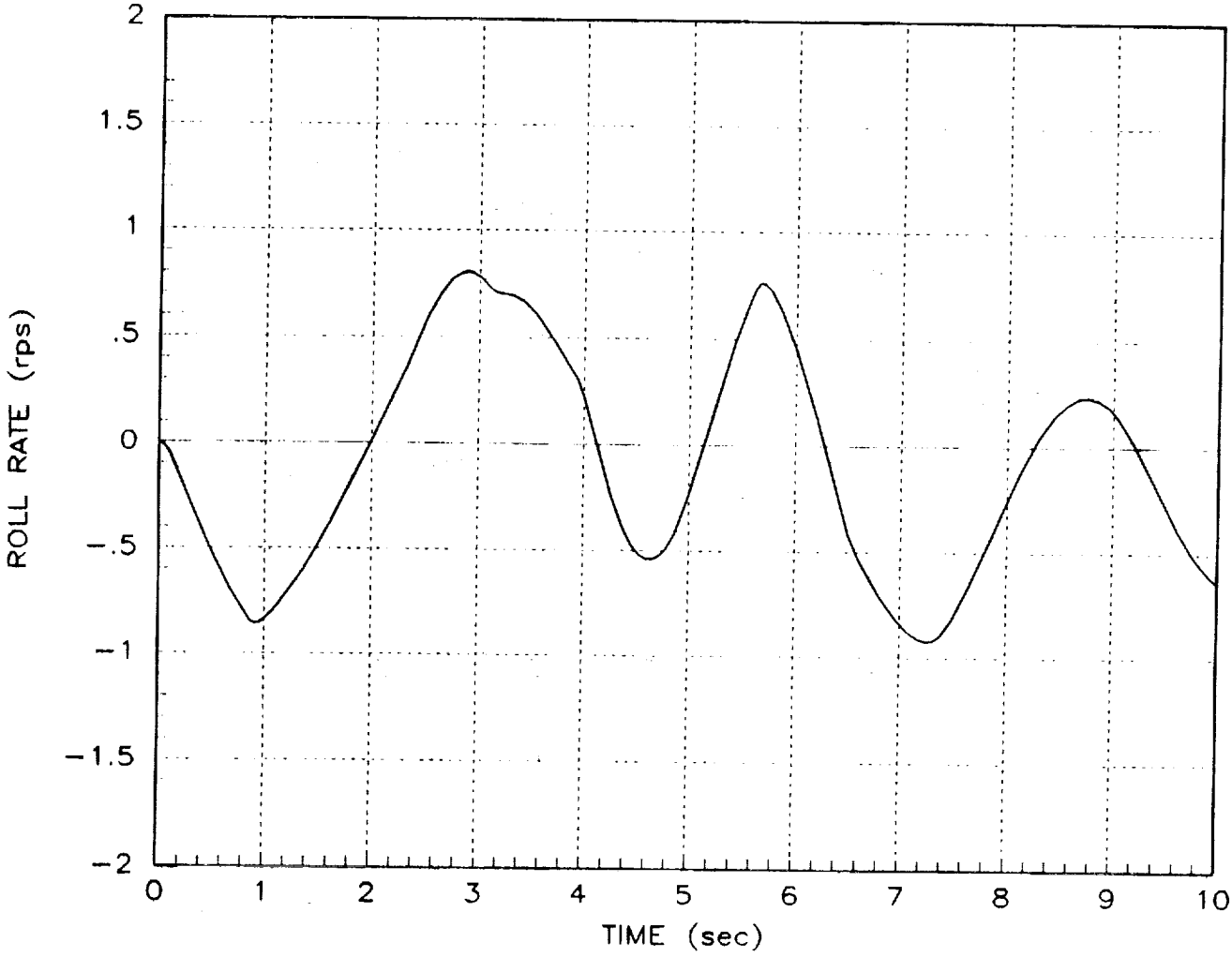

Figure 13 (d) – Optimal Inputs, Increased Amp., No Control Sequencing

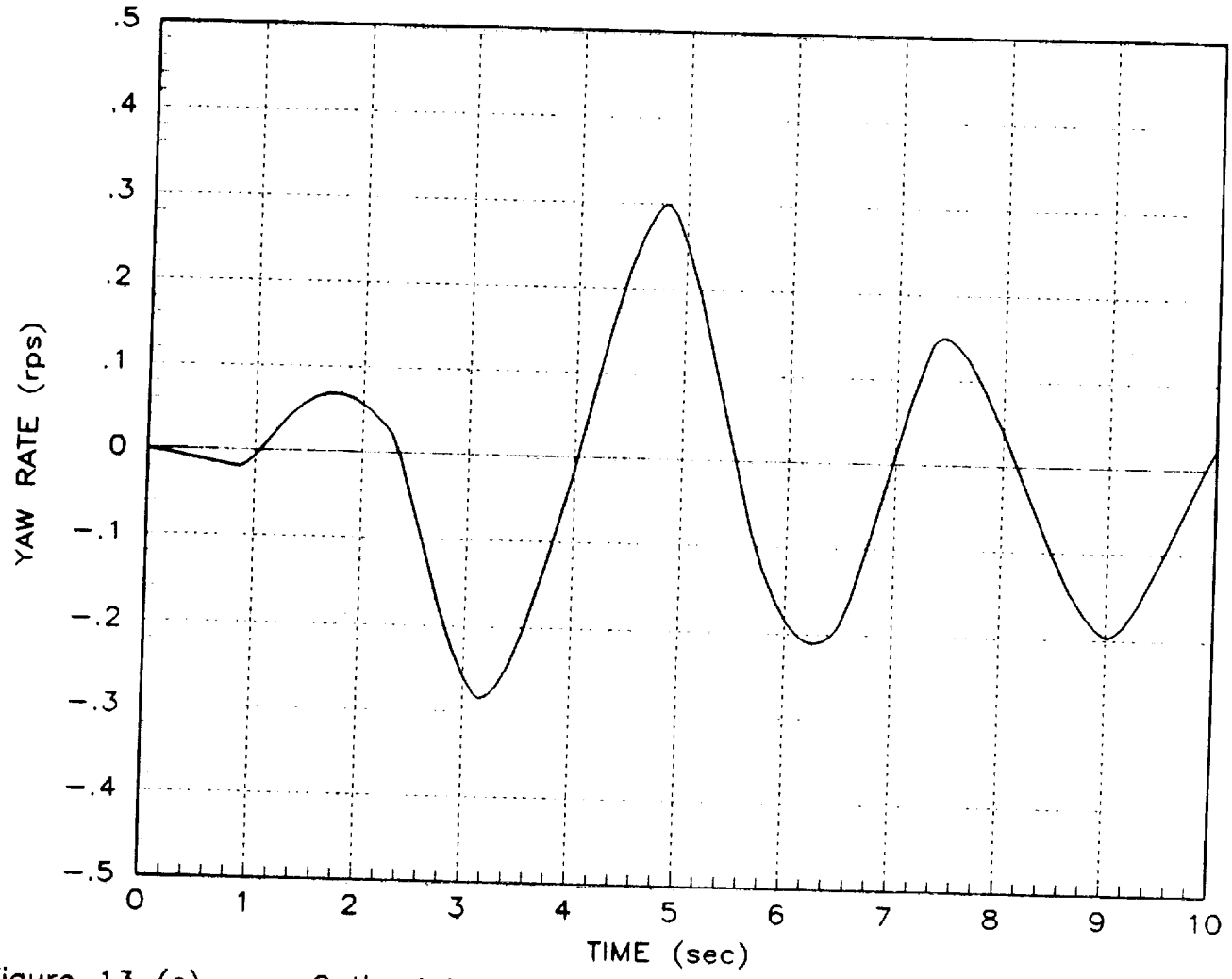

Figure 13 (e) – Optimal Inputs, Increased Amp., No Control Sequencing

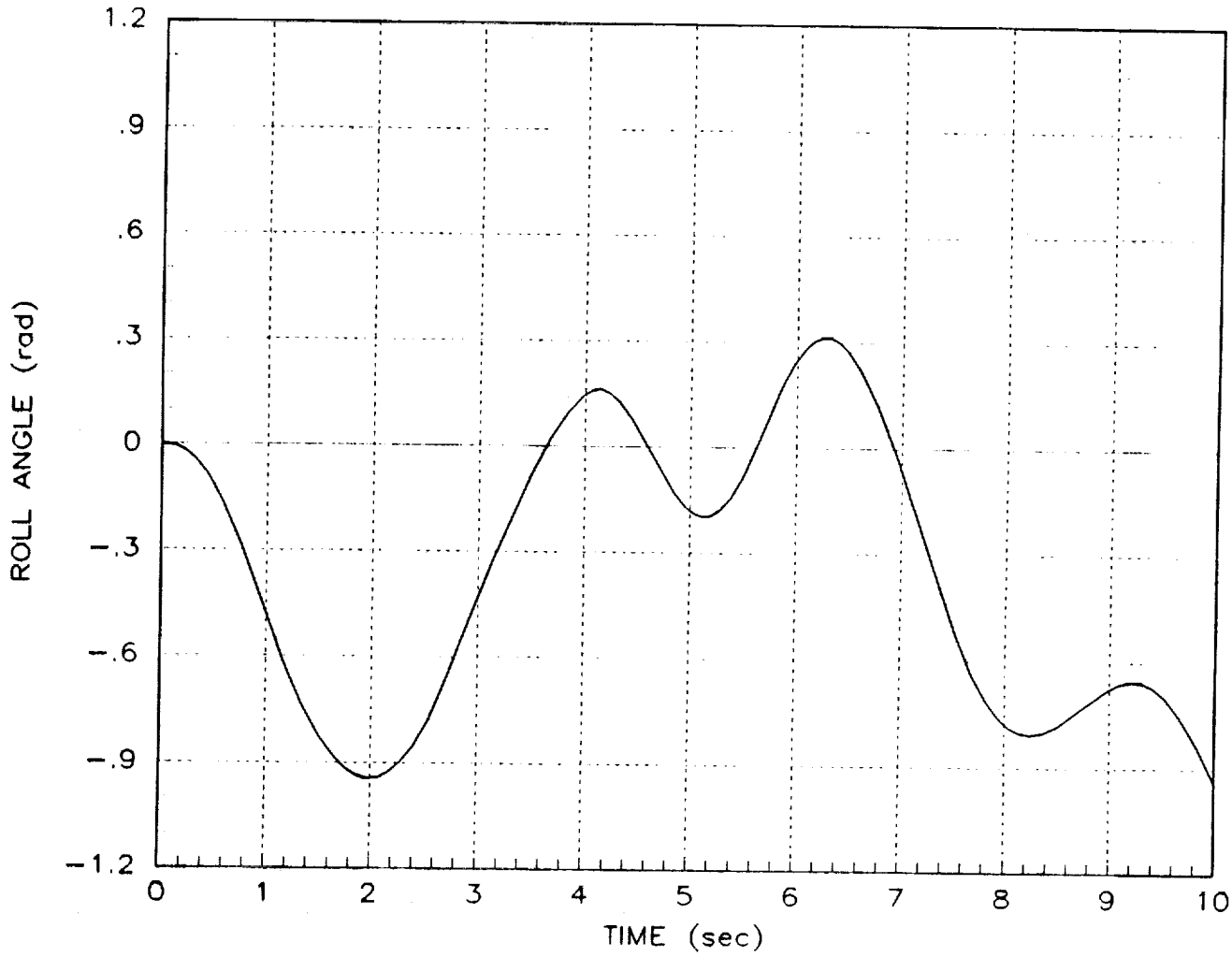

Figure 13 (f) – Optimal Inputs, Increased Amp., No Control Sequencing

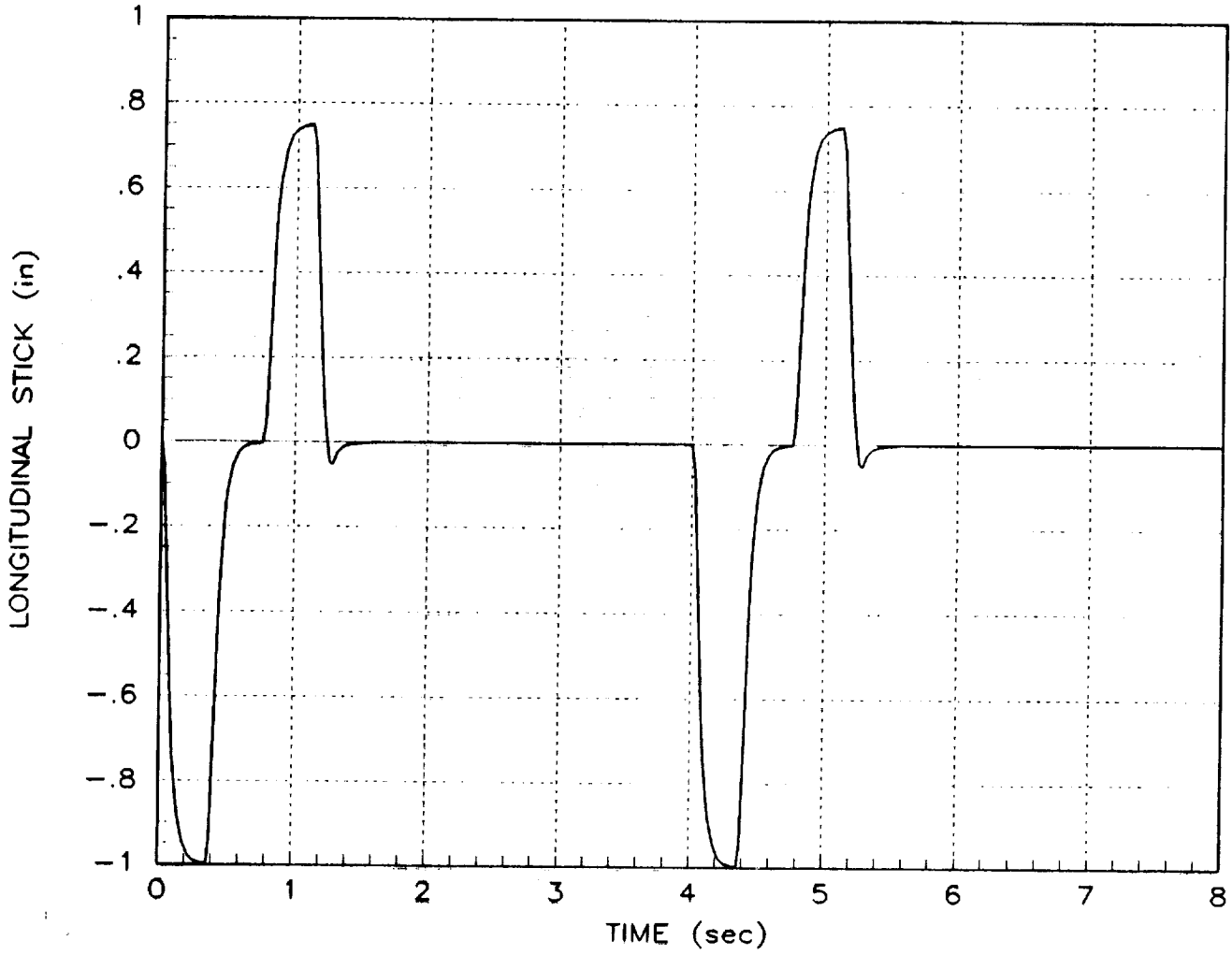

Figure 14 (a) Doublet Input

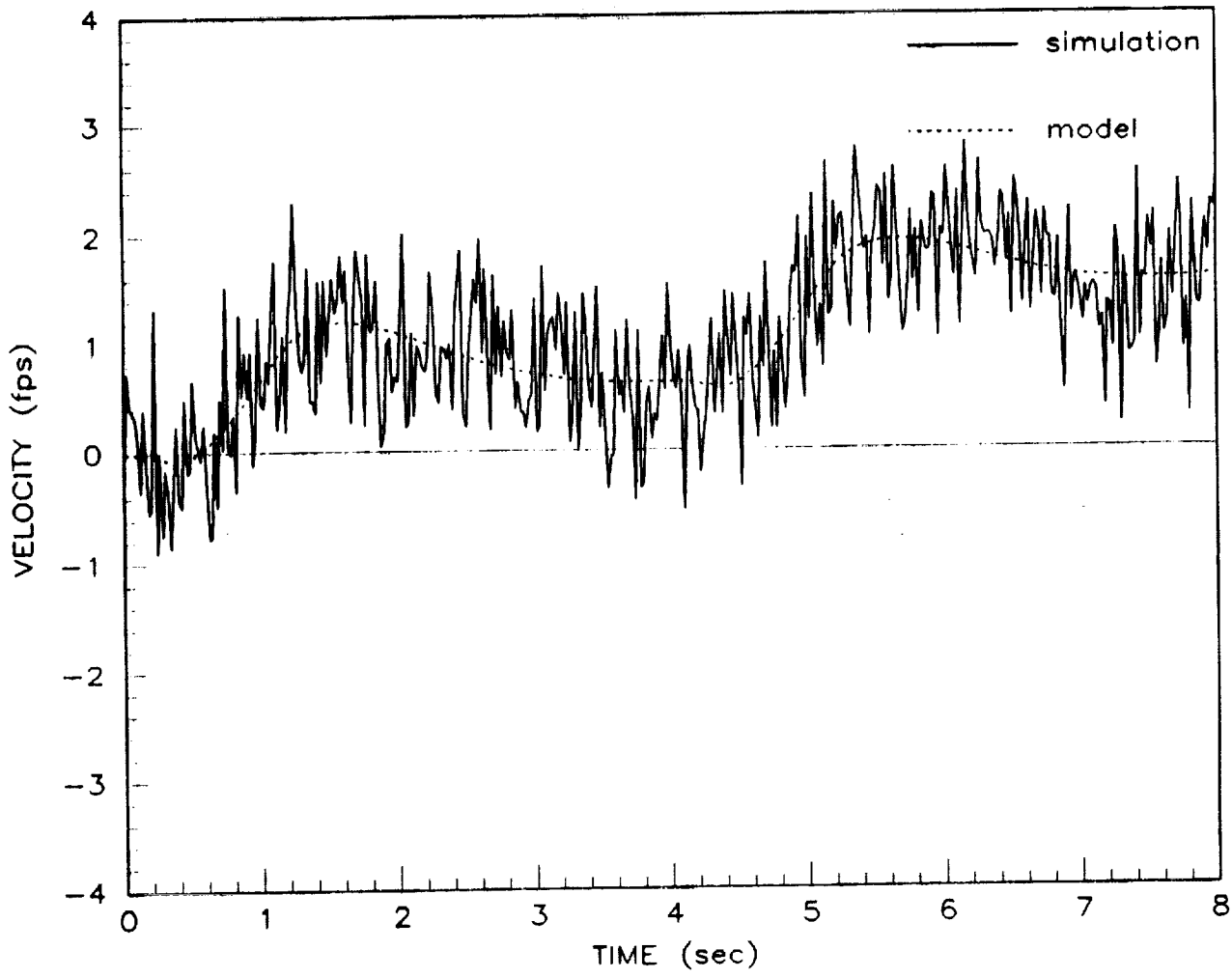

Figure 14 (b) Doublet Input

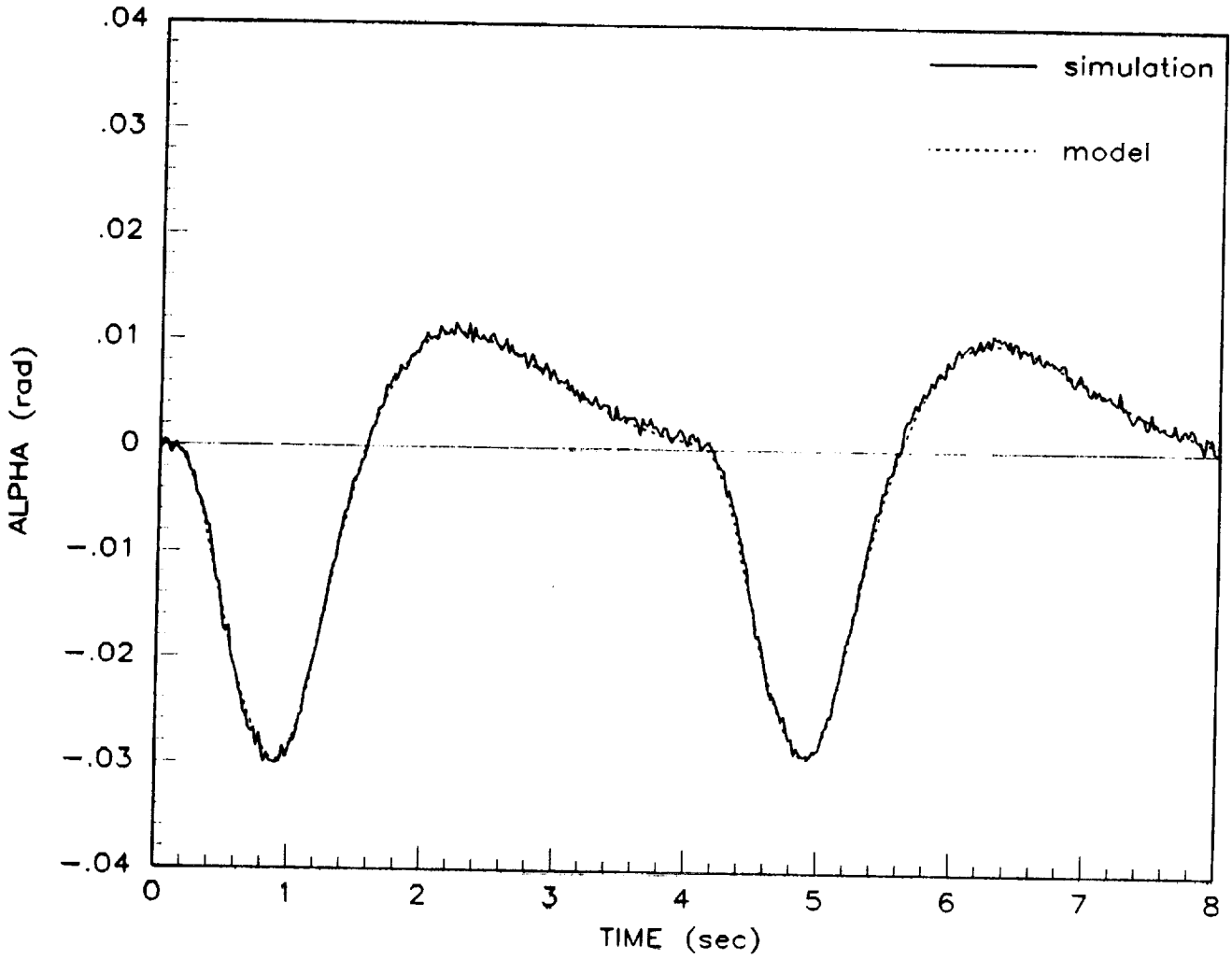

Figure 14 (c) Doublet Input

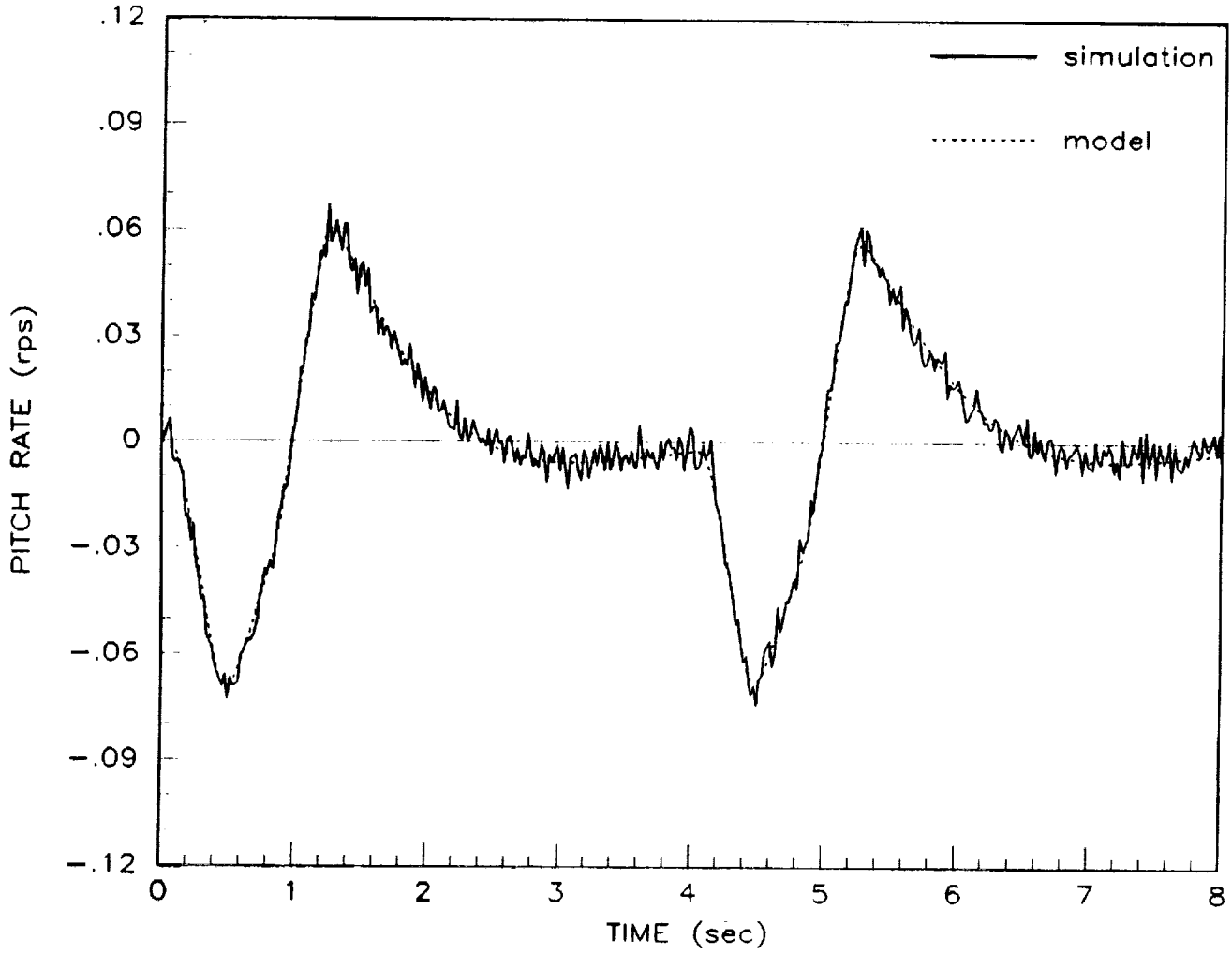

Figure 14 (d) Doublet Input

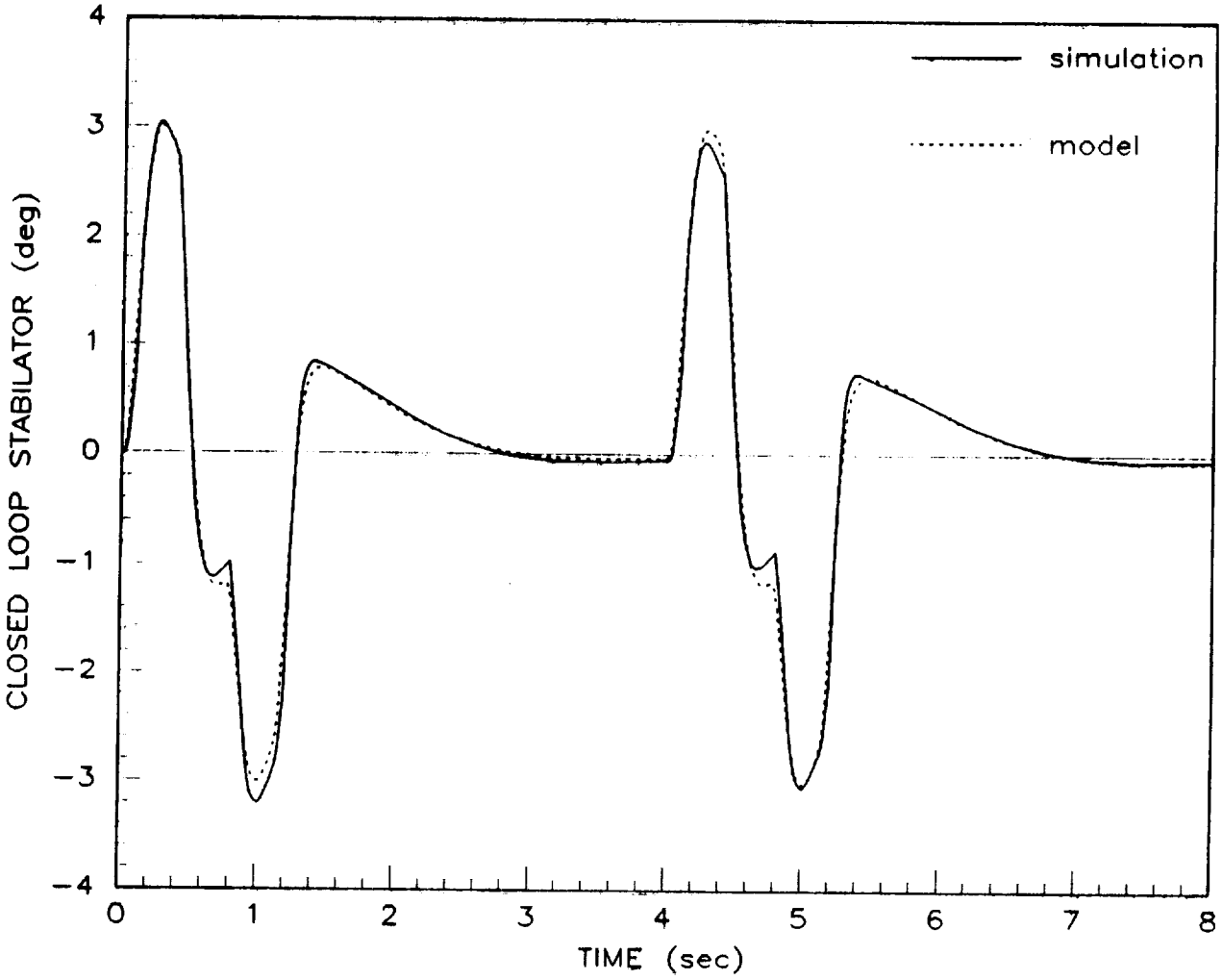

Figure 14 (e) Doublet Input

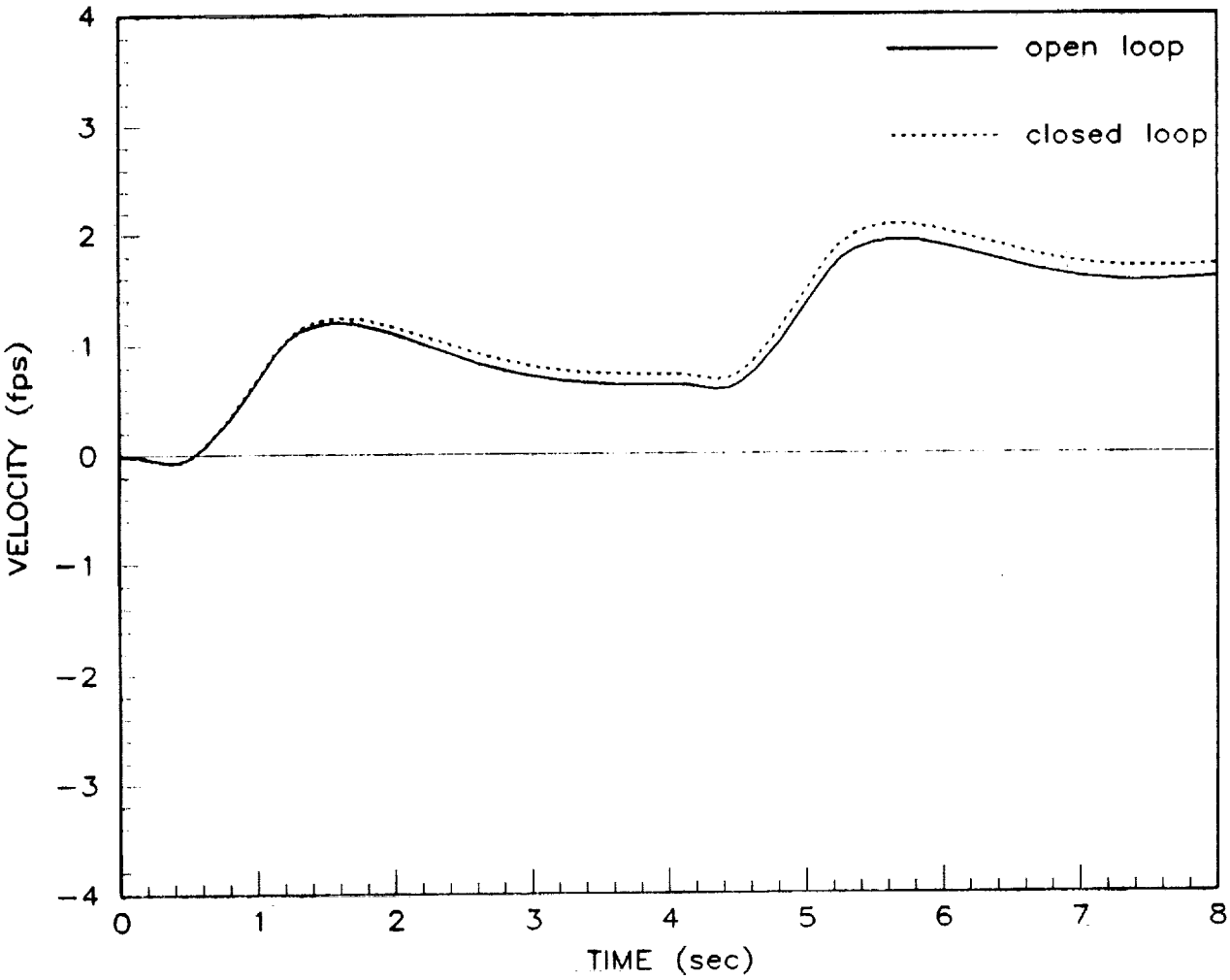

Figure 14 (f) Doublet Input

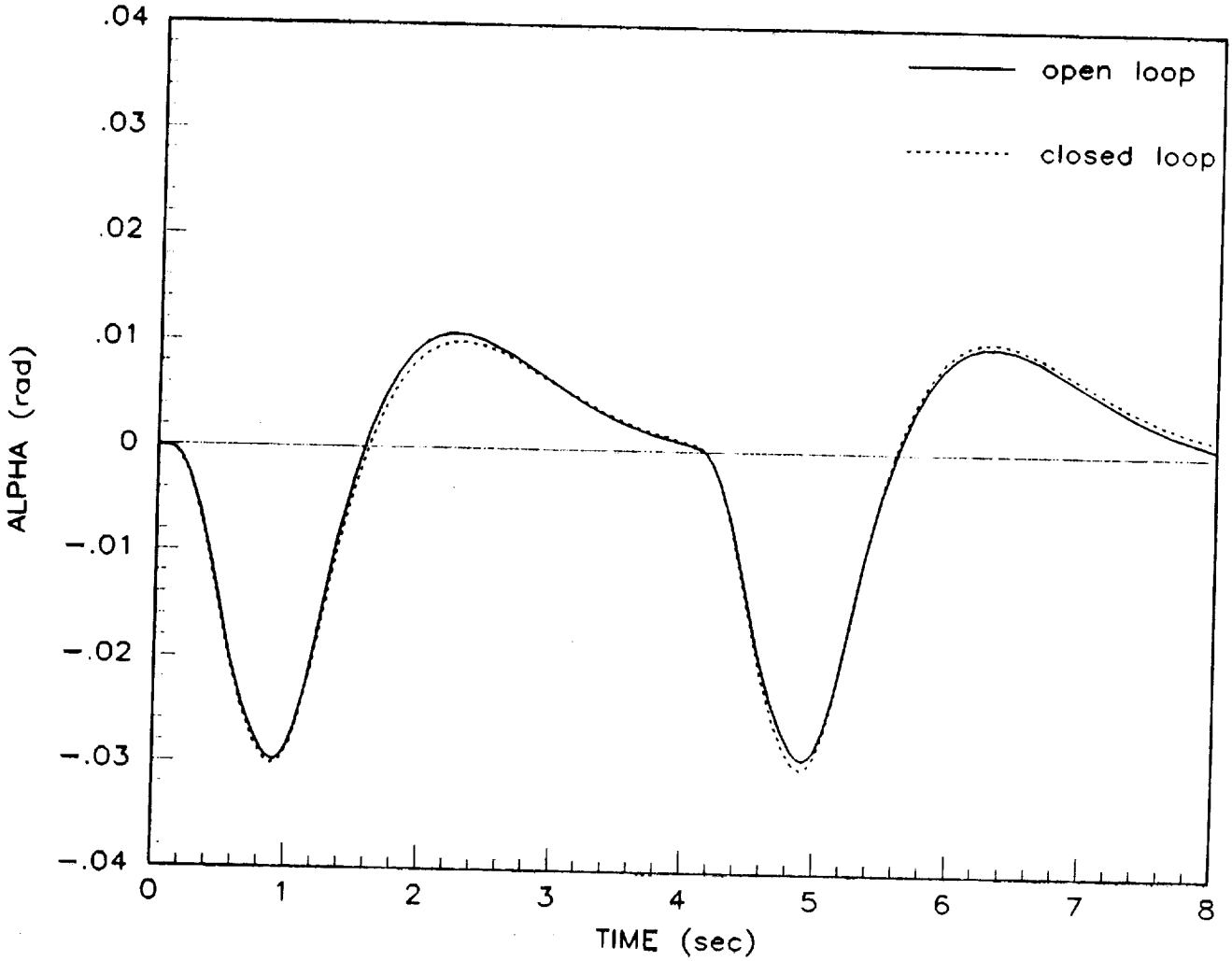

Figure 14 (g) Doublet Input

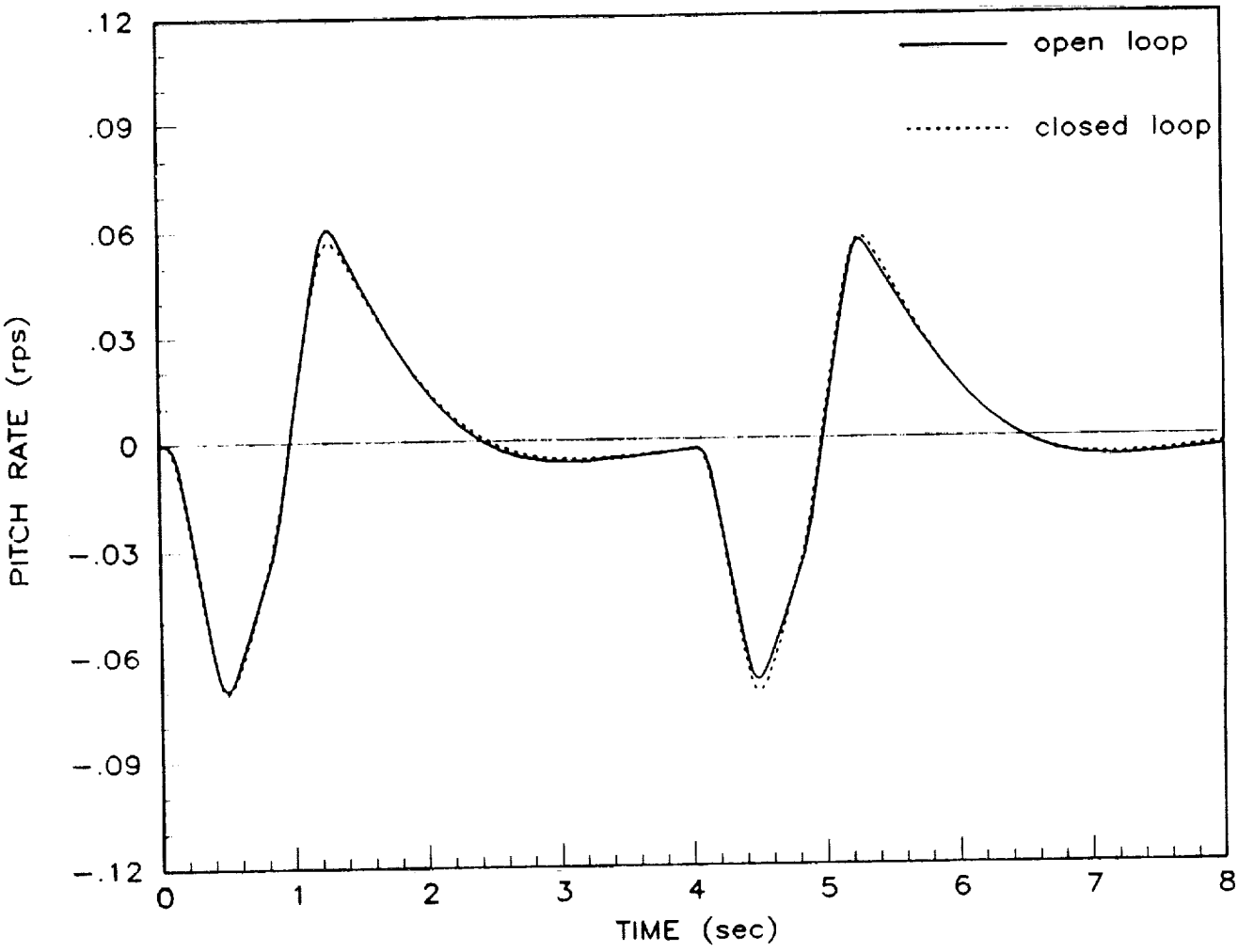

Figure 14 (h) Doublet Input

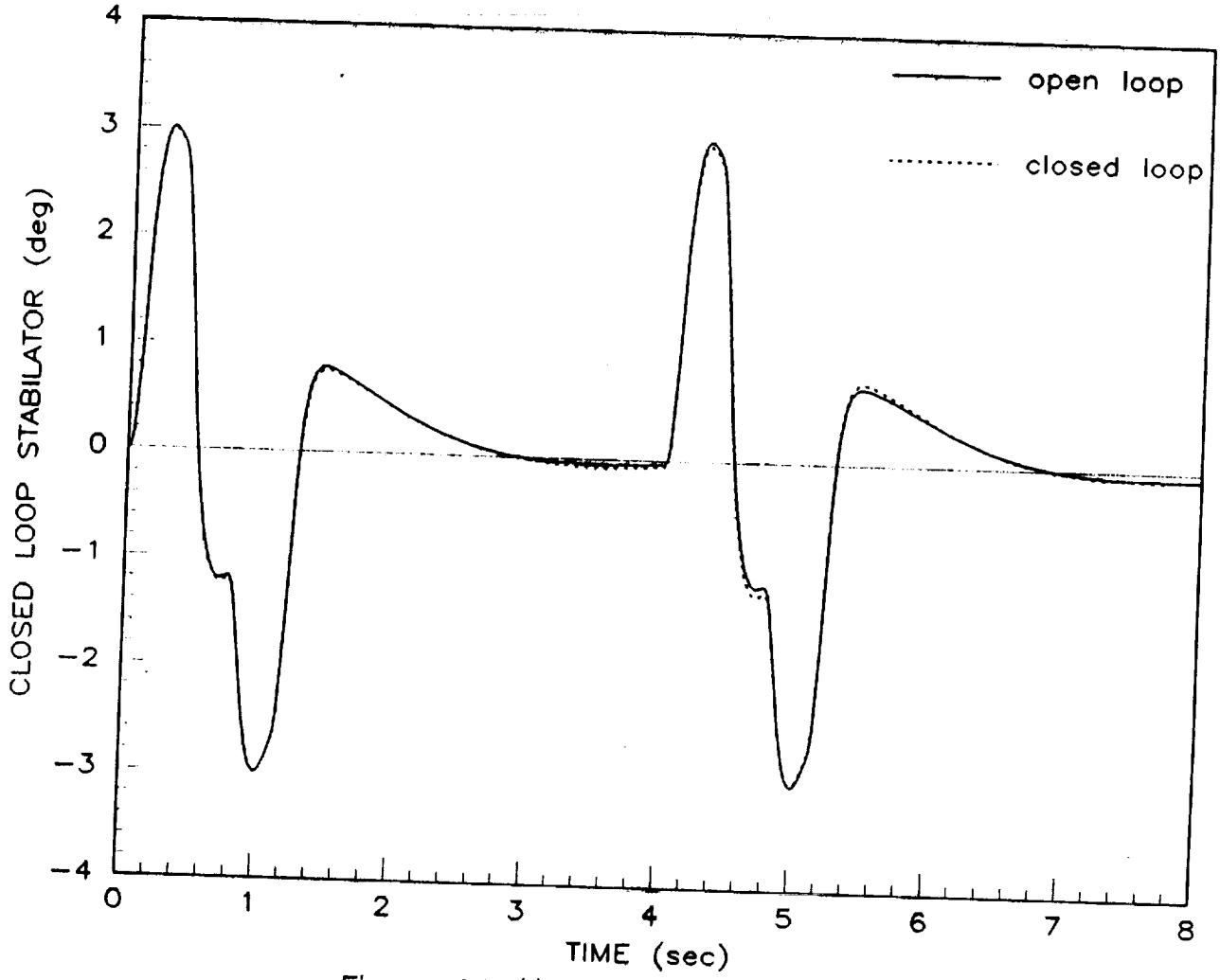

Figure 14 (i) Doublet Input

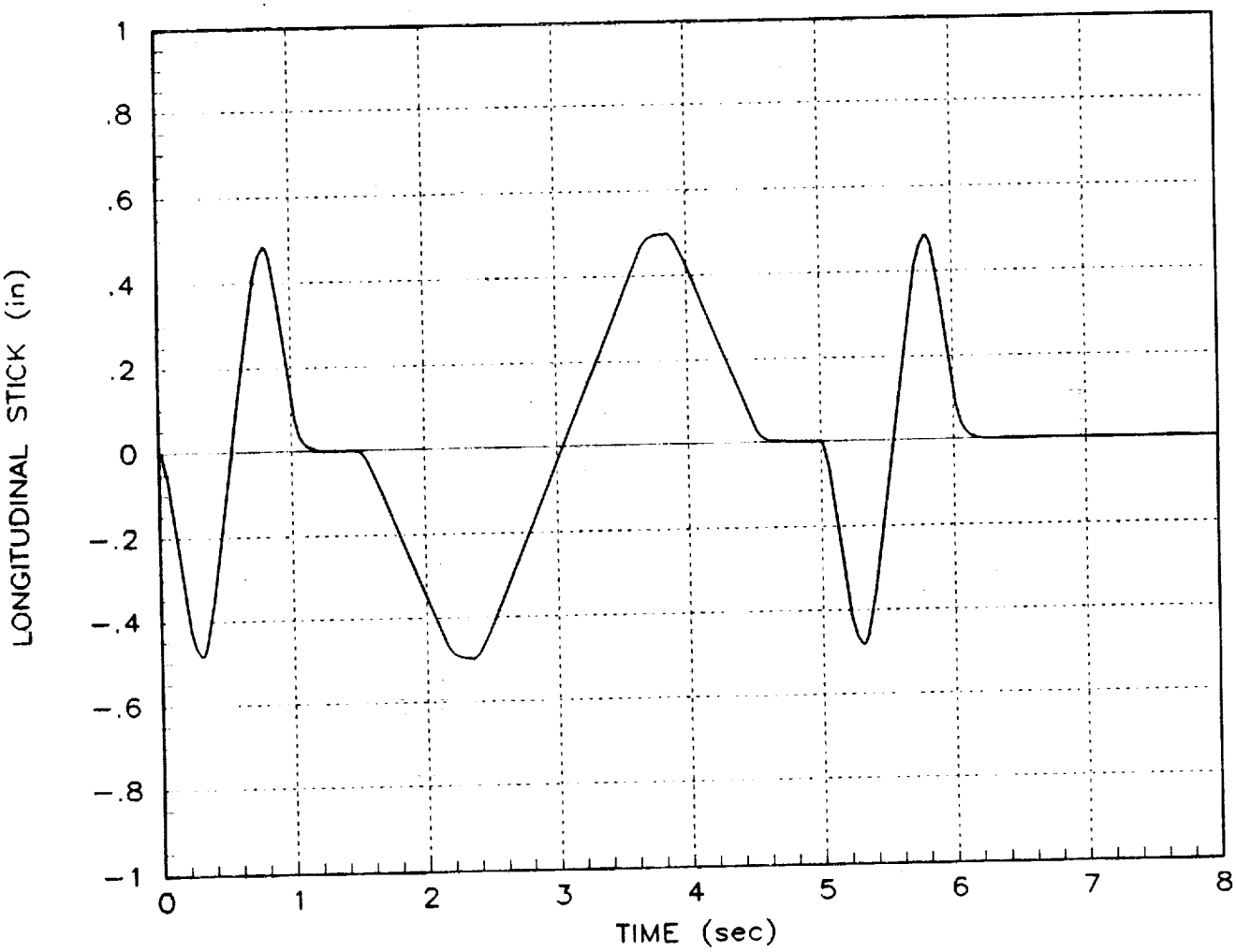

Figure 15 (a) Compound Doublet Input

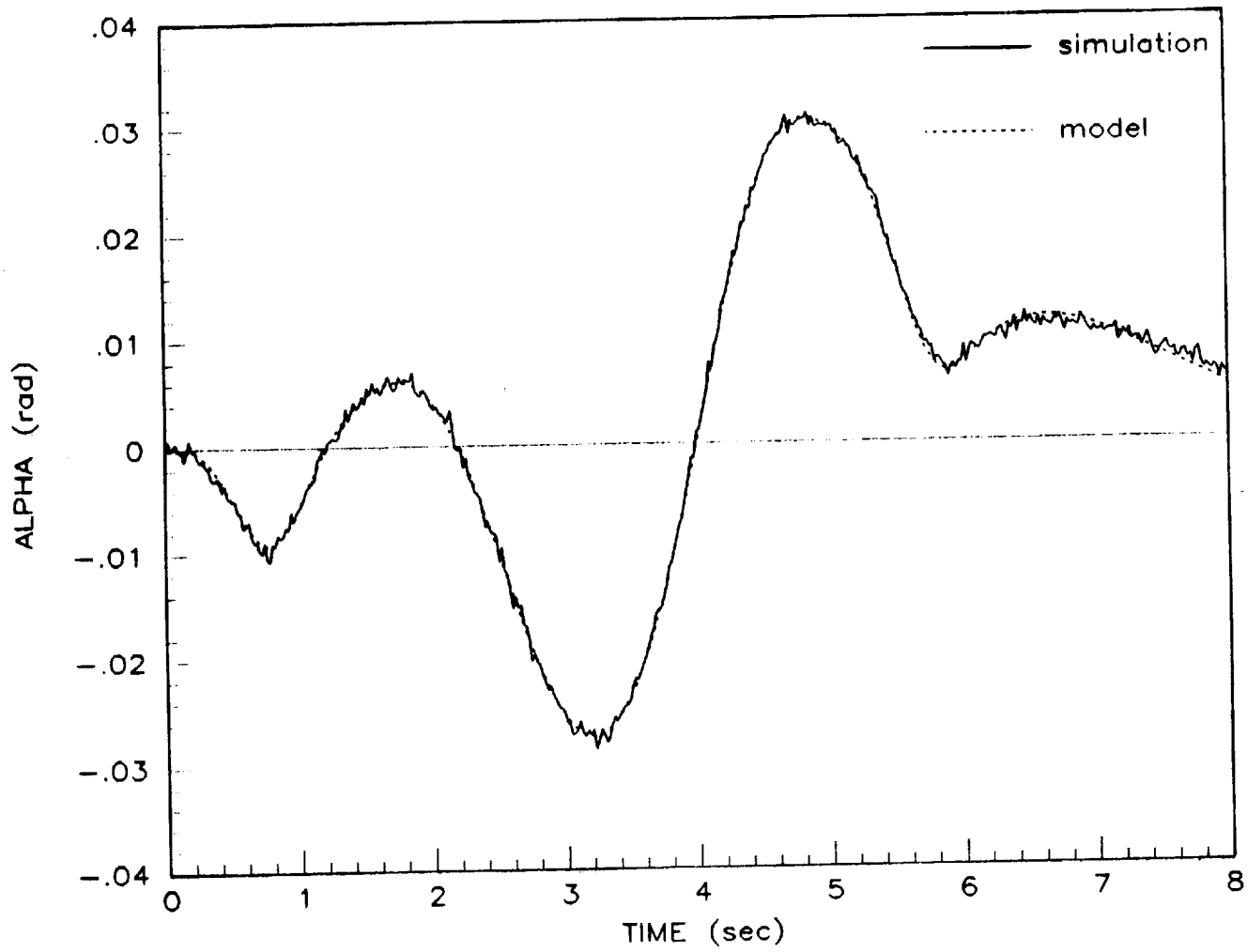

Figure 15 (b) Compound Doublet Input

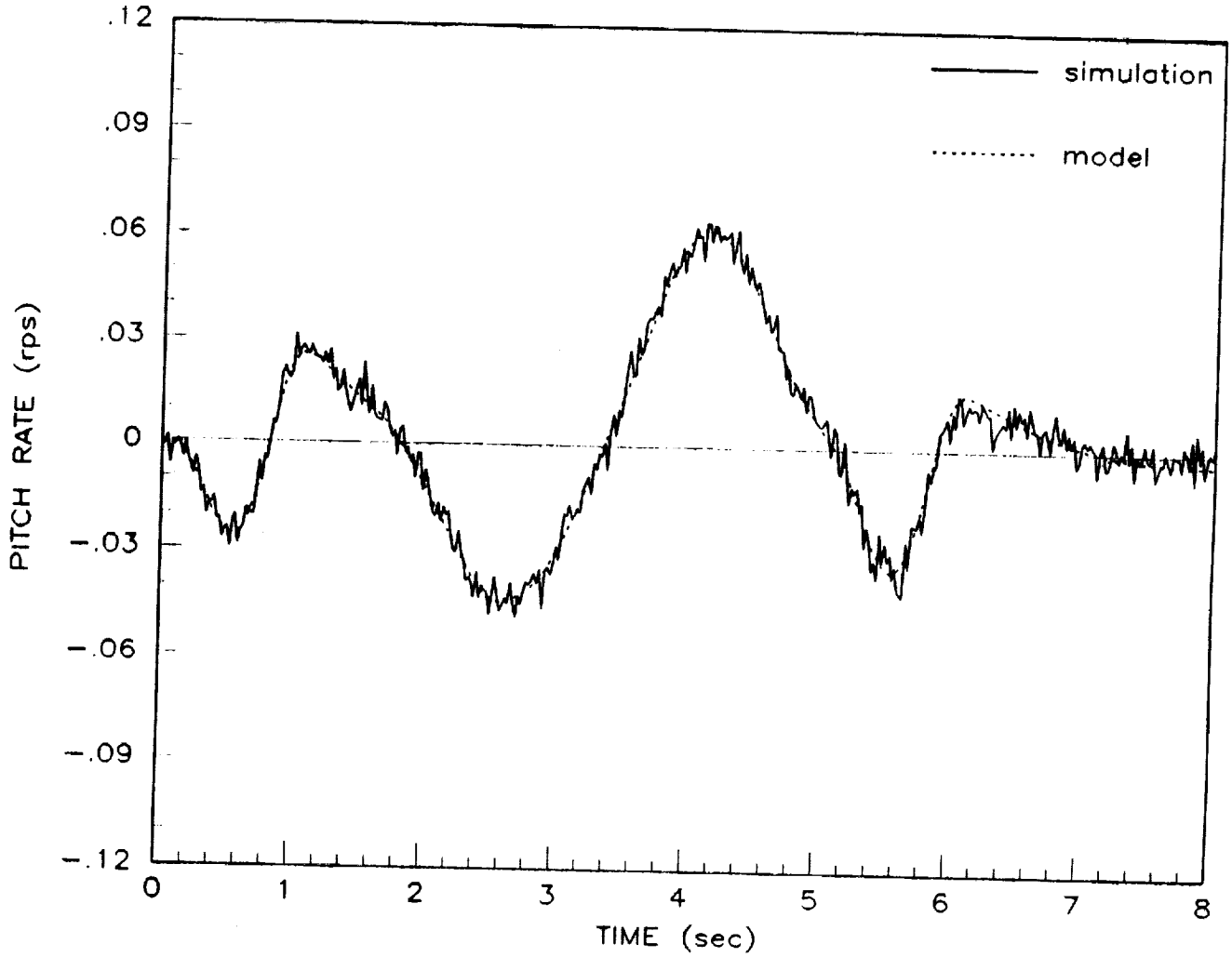

Figure 15 (c) Compound Doublet Input

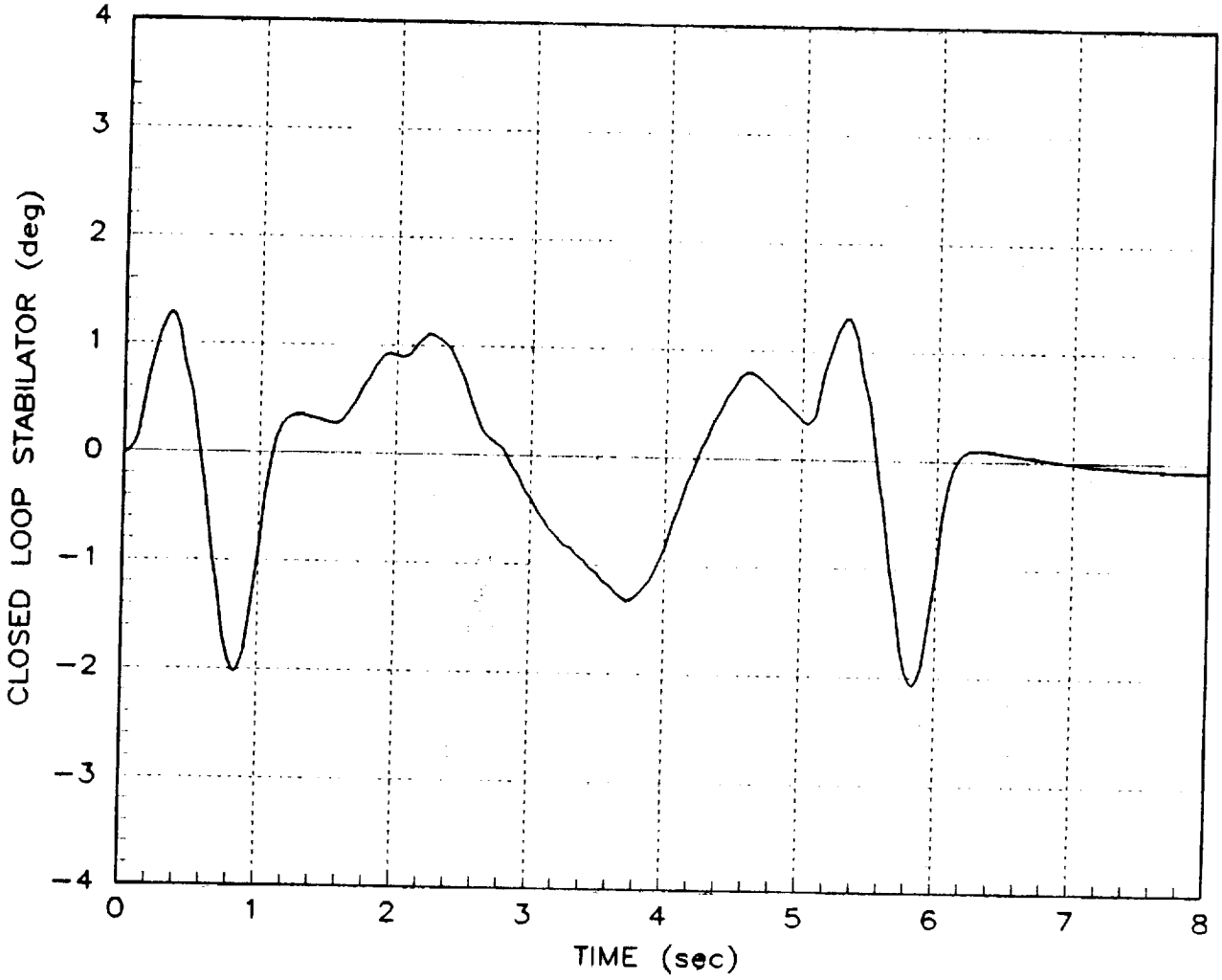

Figure 15 (d) Compound Doublet Input

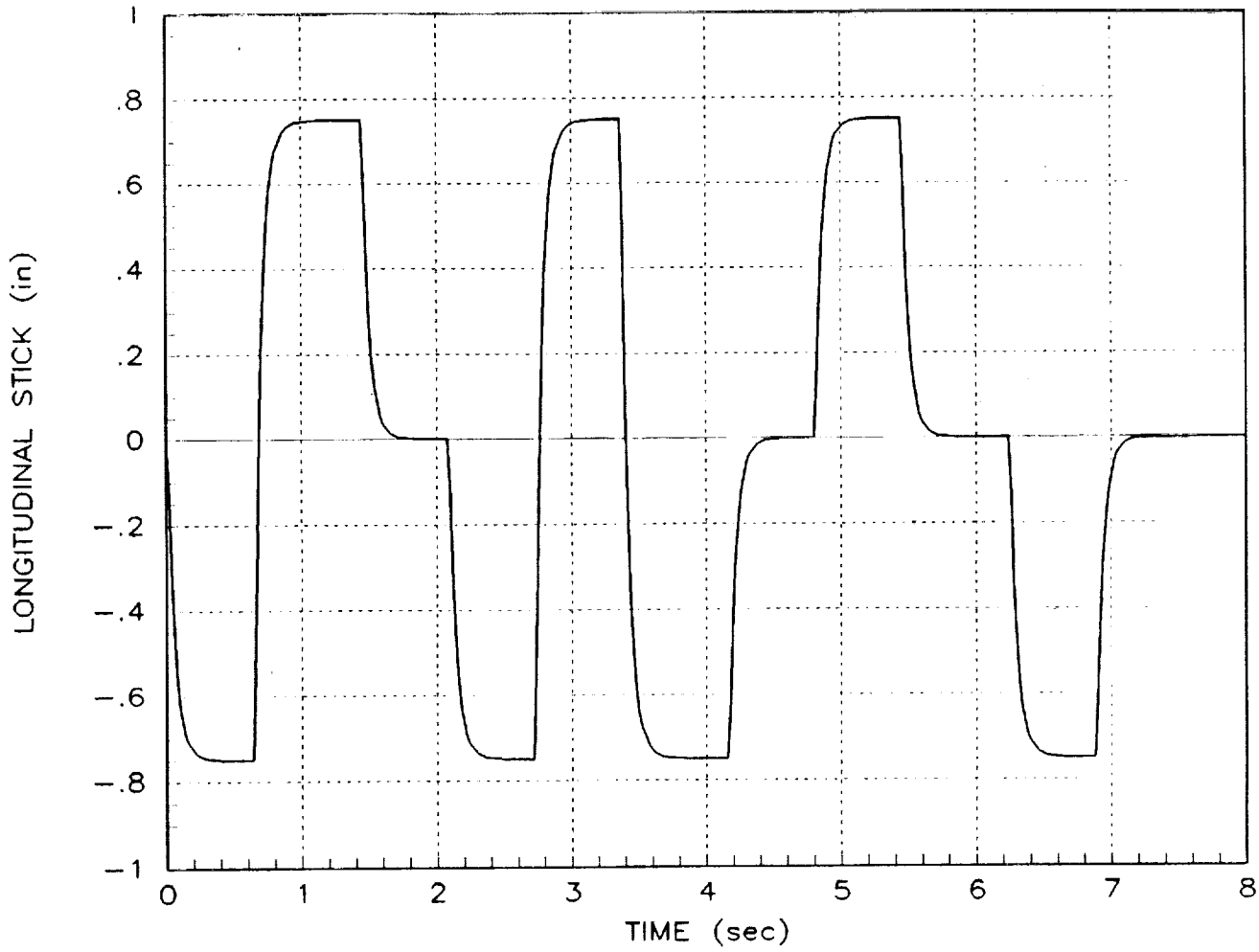

Figure 16 (a) Optimal Input

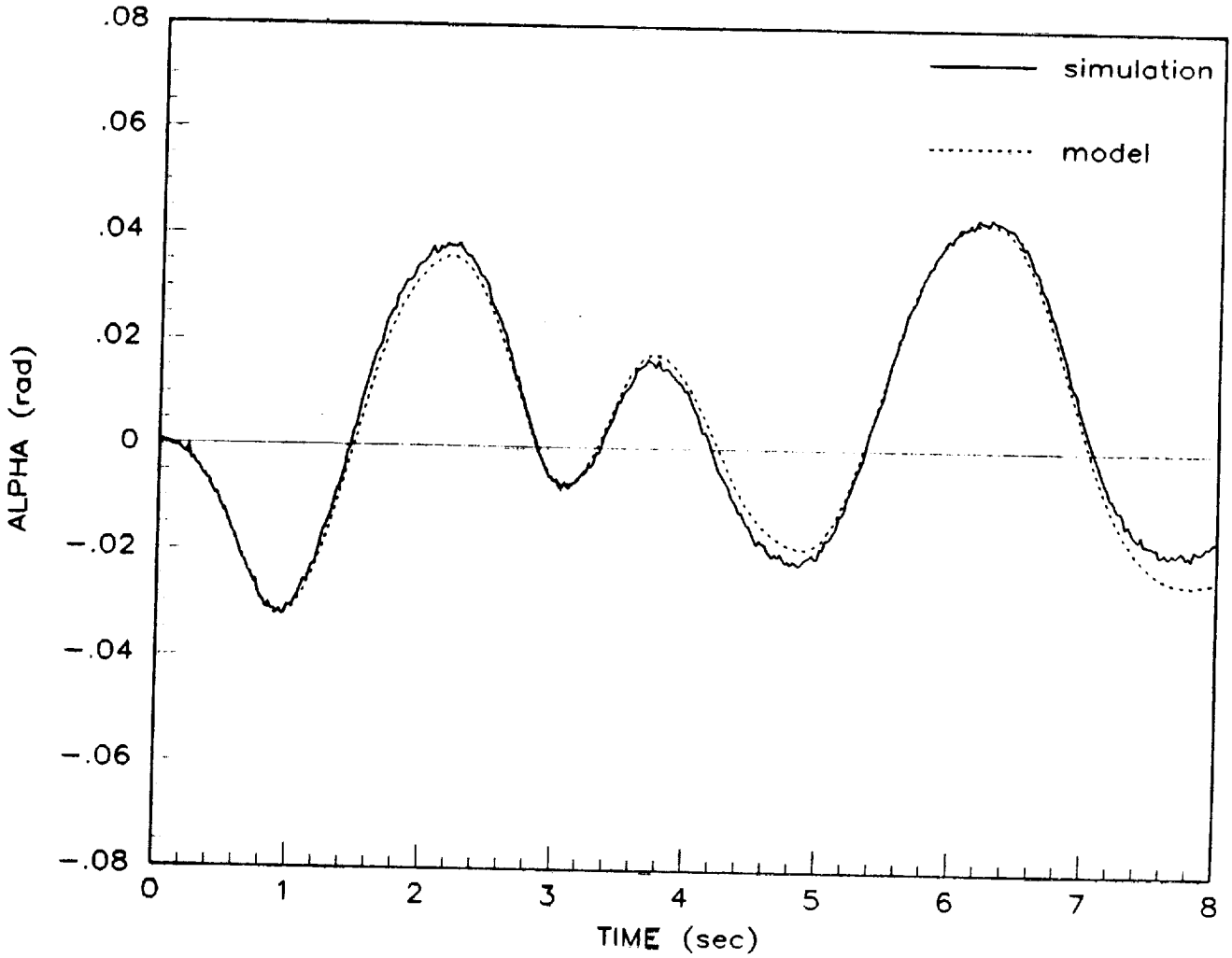

Figure 16 (b) Optimal Input

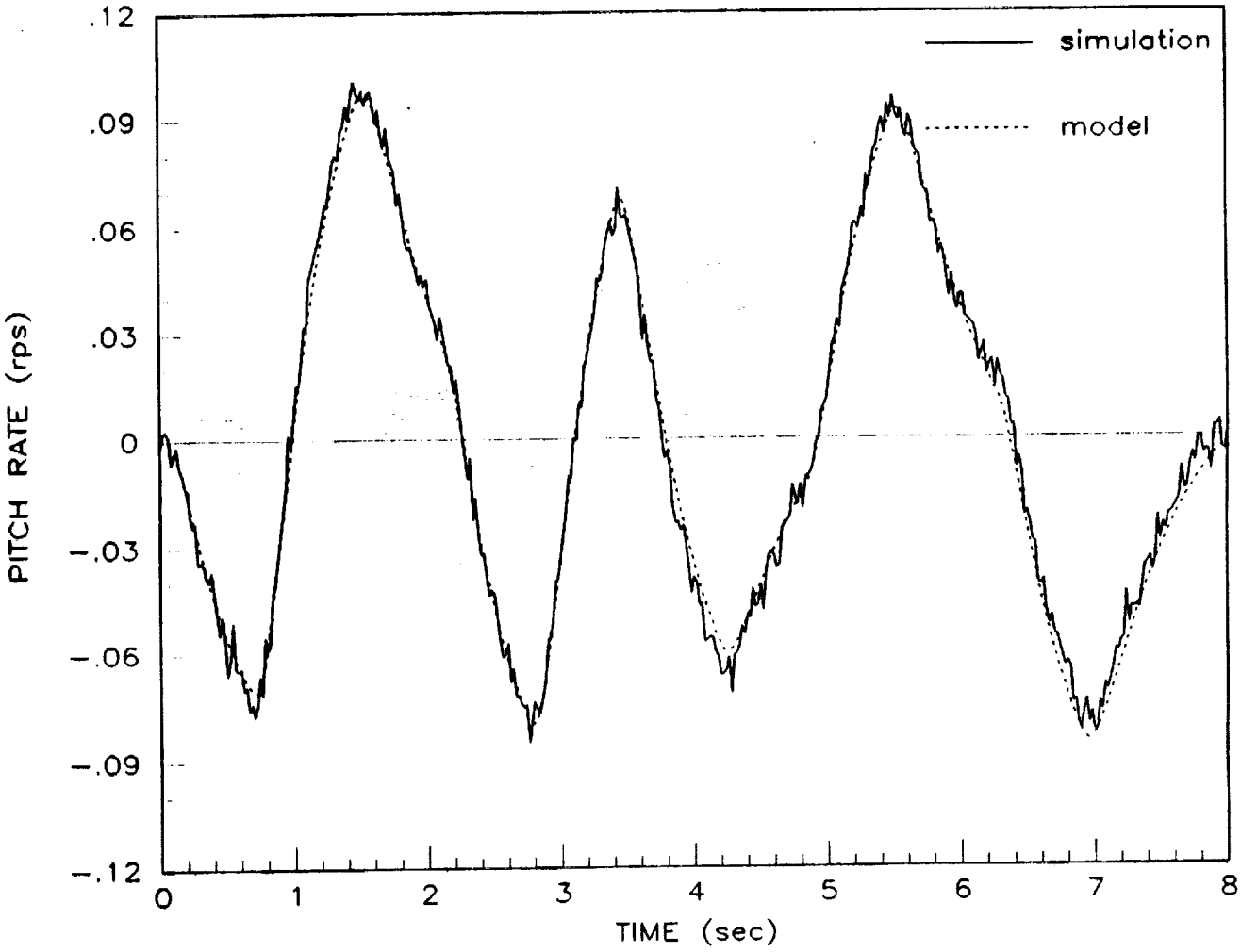

Figure 16 (c) Optimal Input

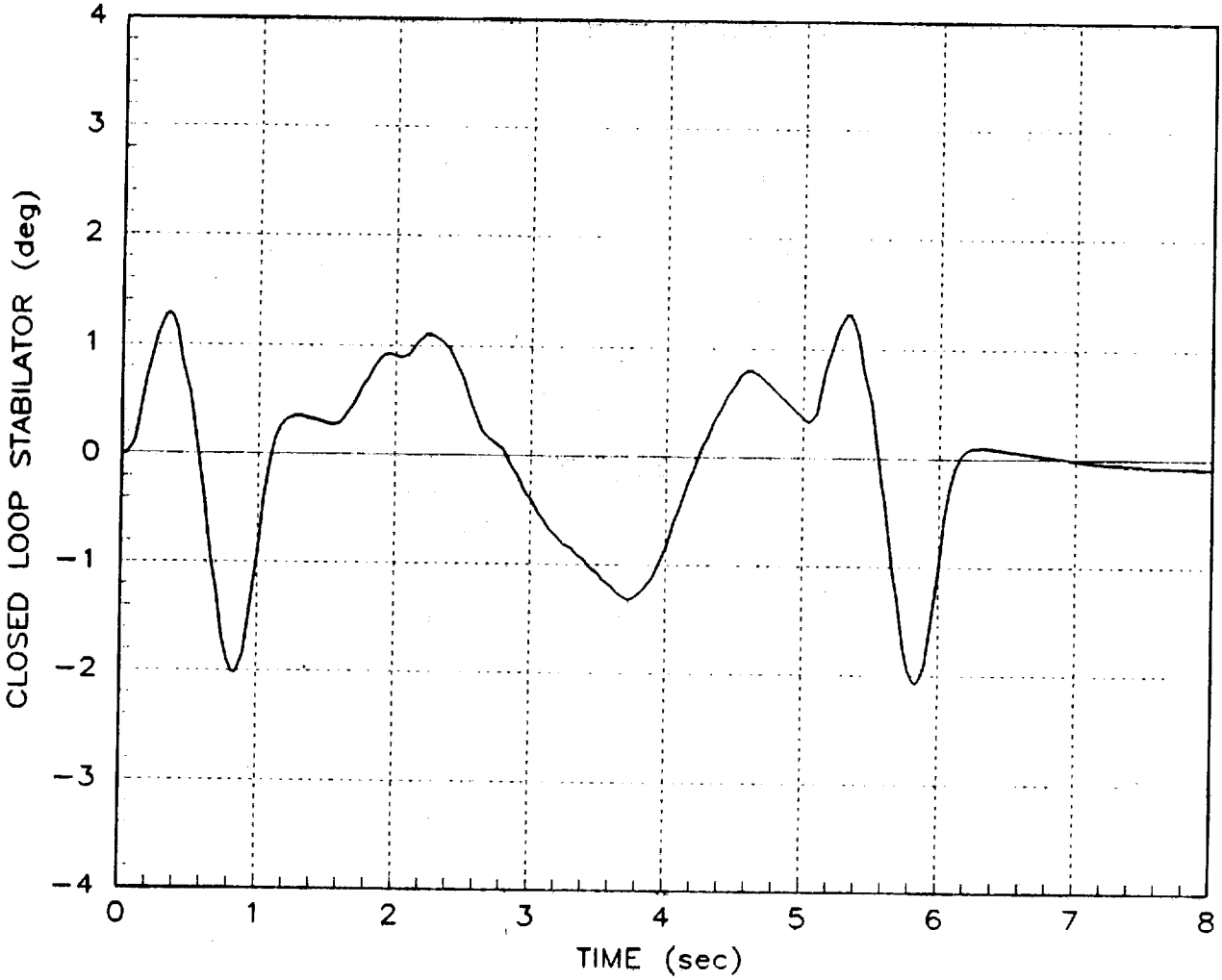

Figure 16 (d) Optimal Input

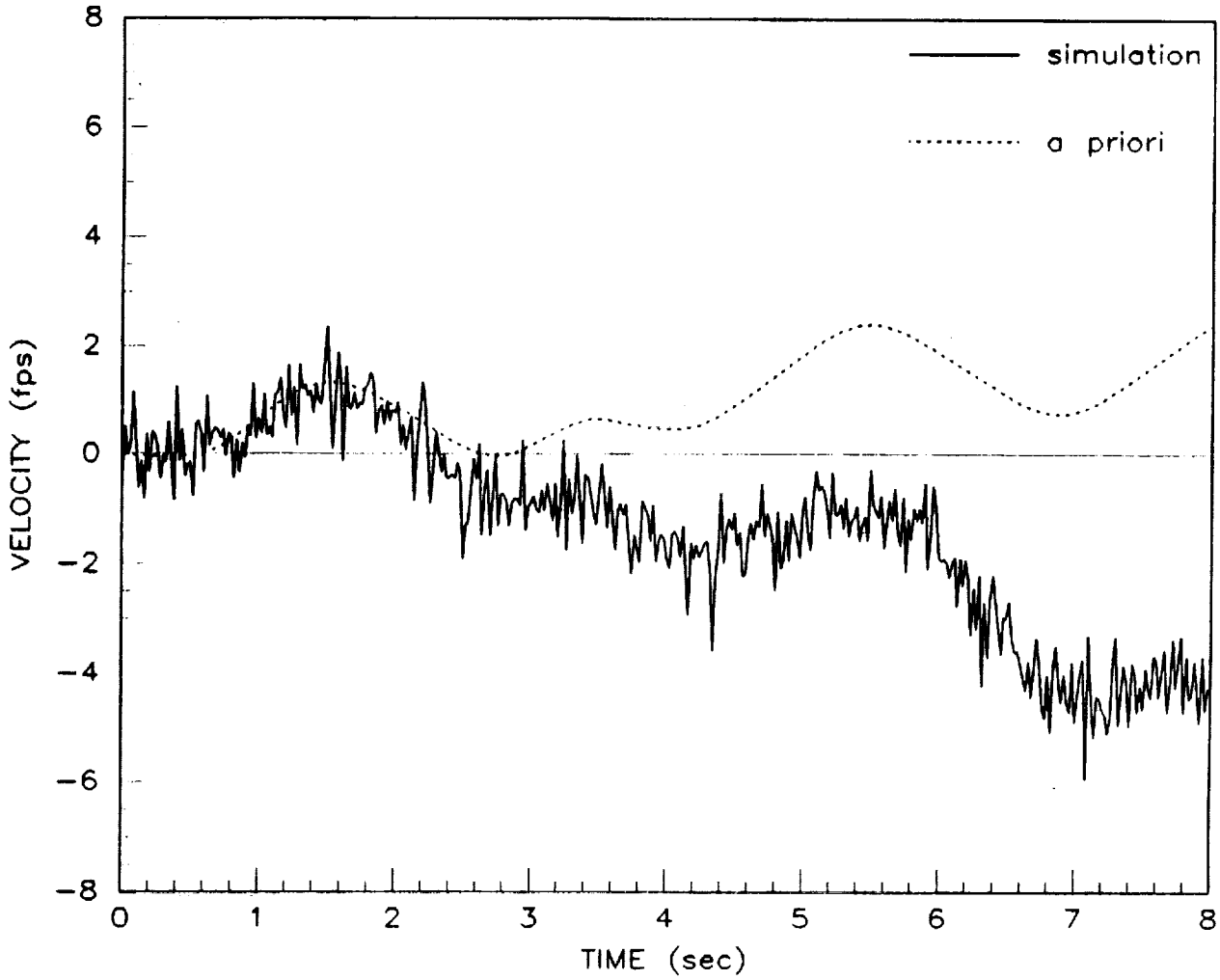

Figure 16 (e) Optimal Input

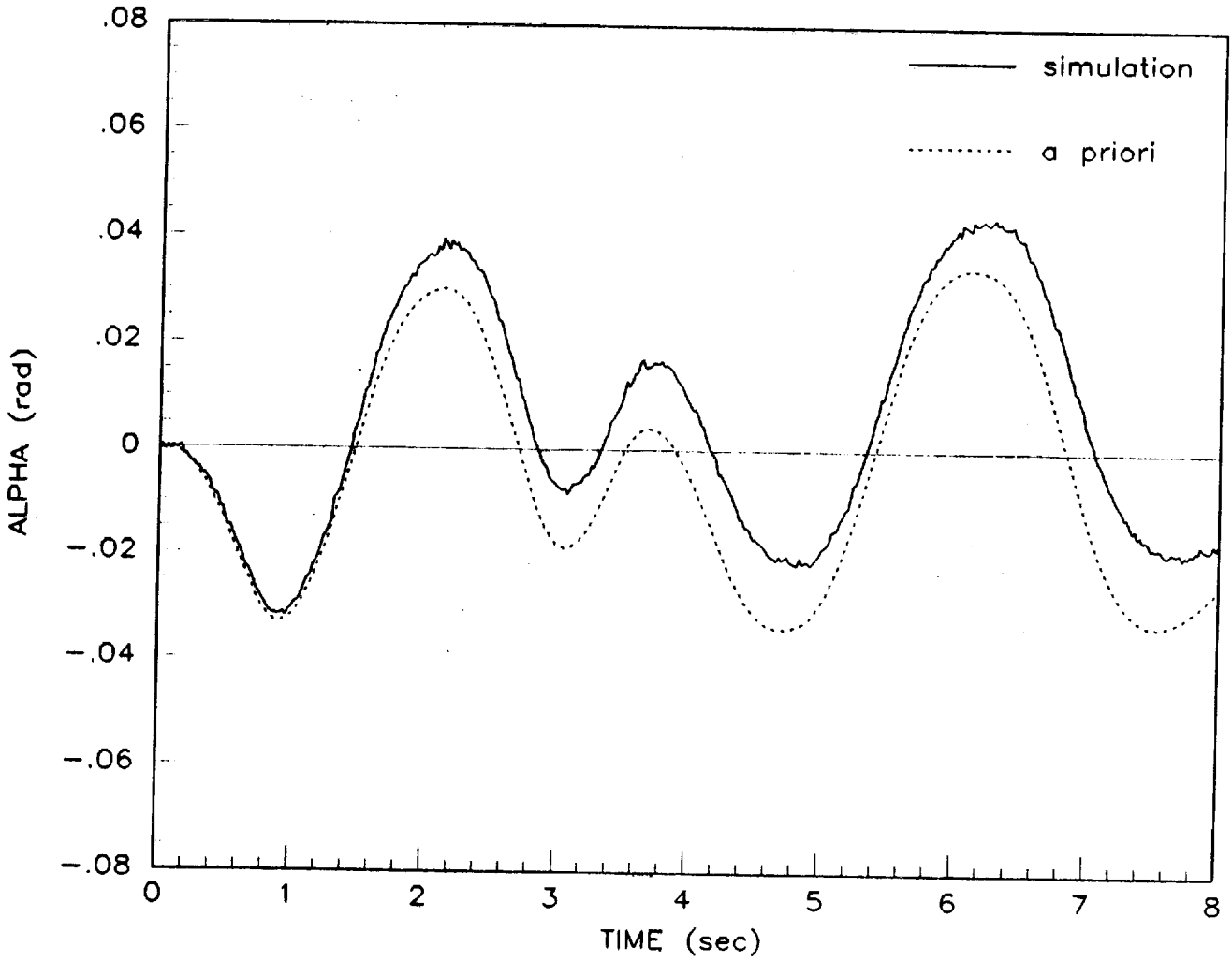

Figure 16 (f) Optimal Input

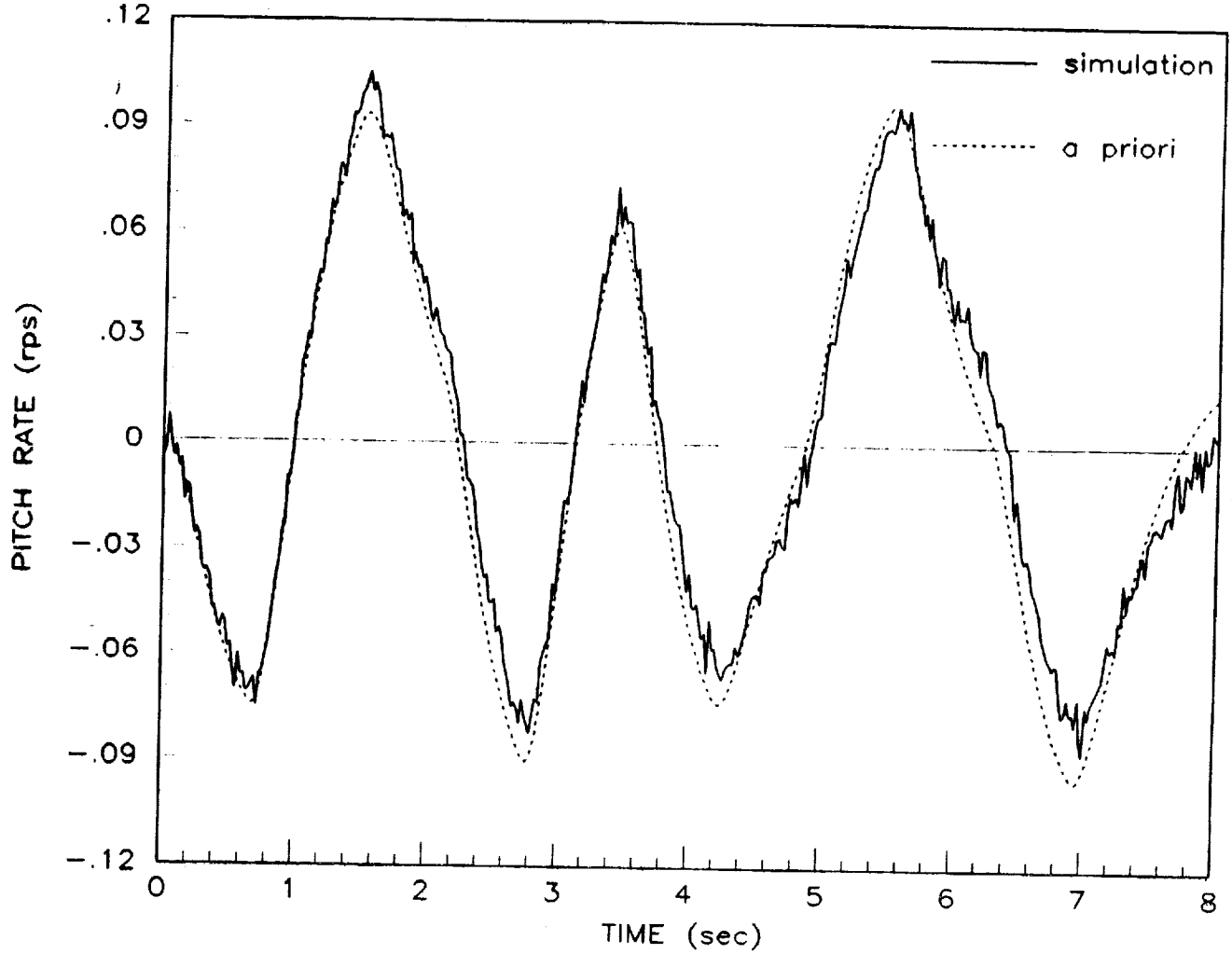

Figure 16 (g) Optimal Input

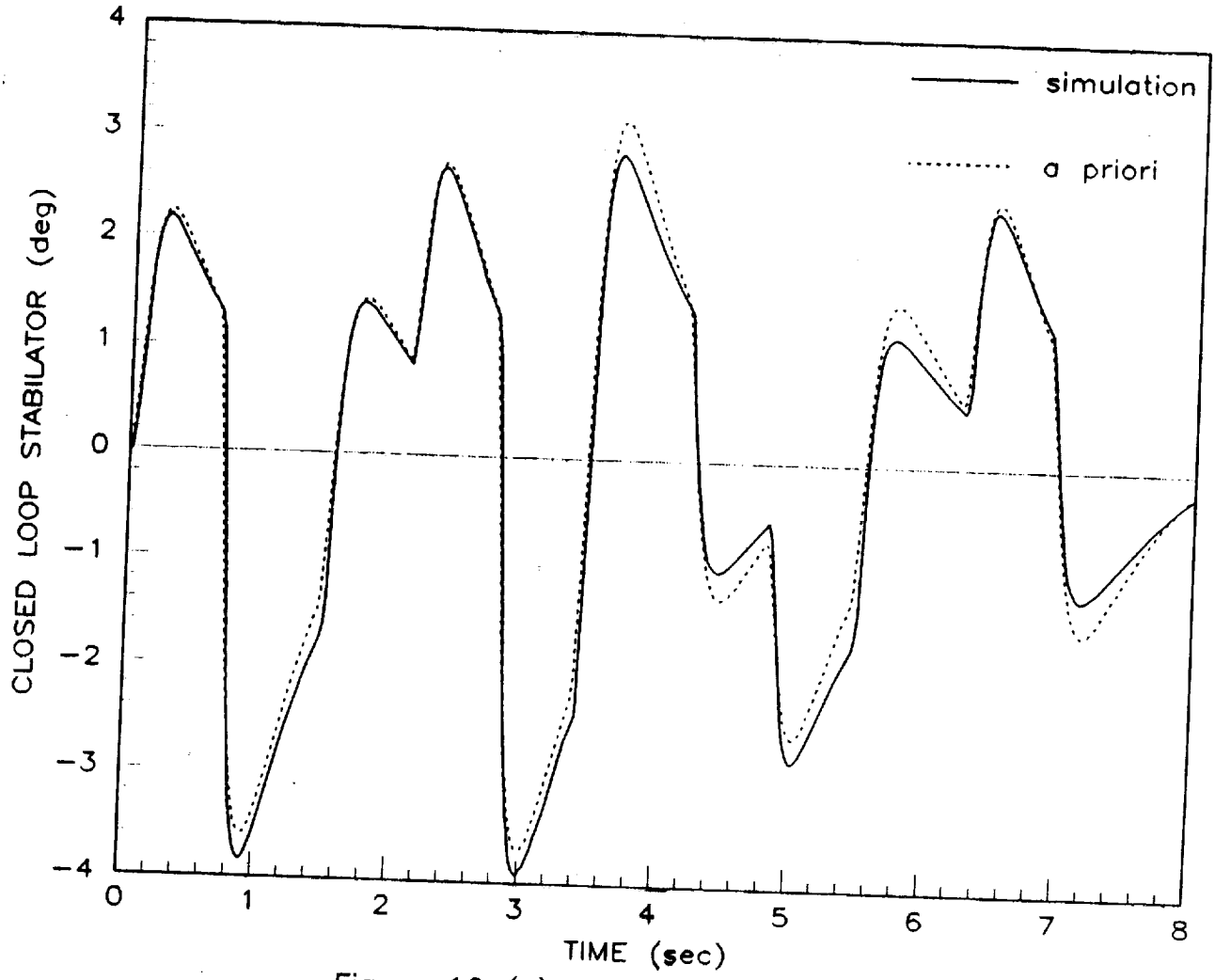

Figure 16 (h) Optimal Input

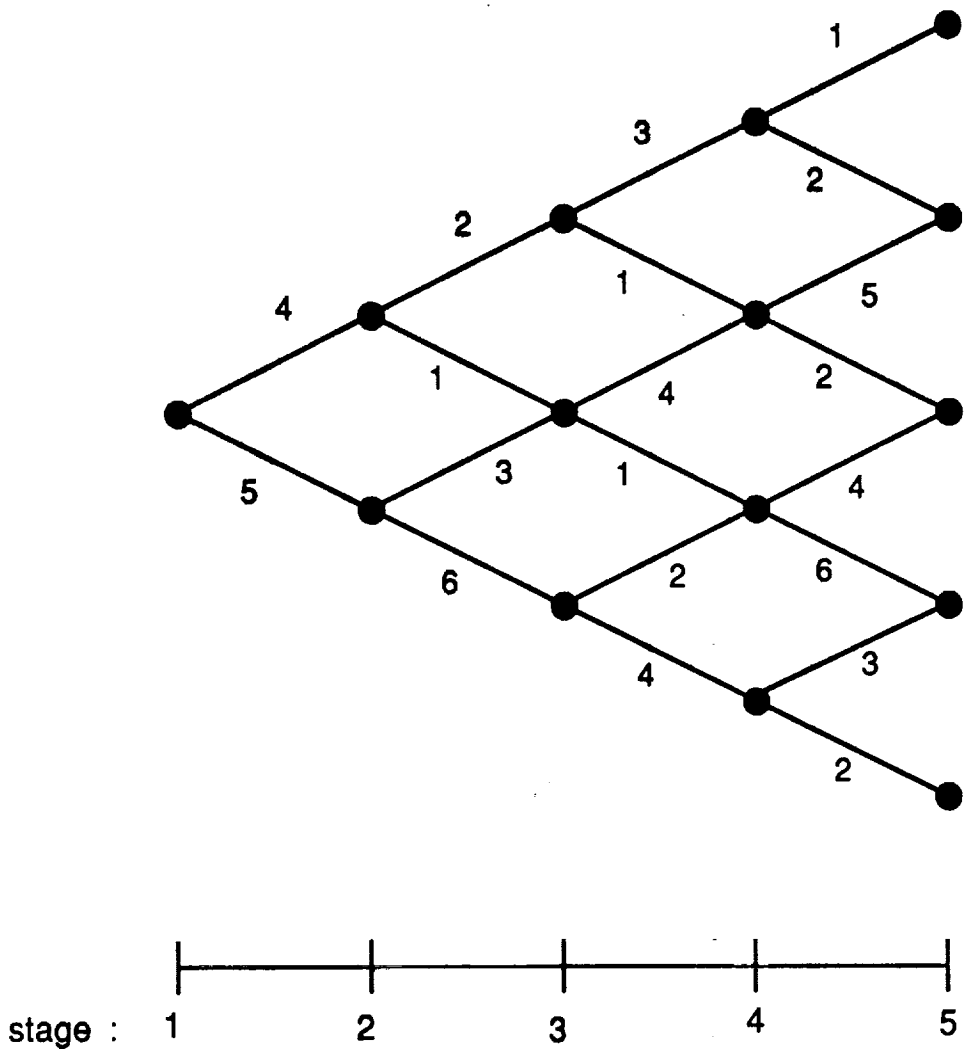

Figure B-1 - Discrete Dynamic Programming Grid

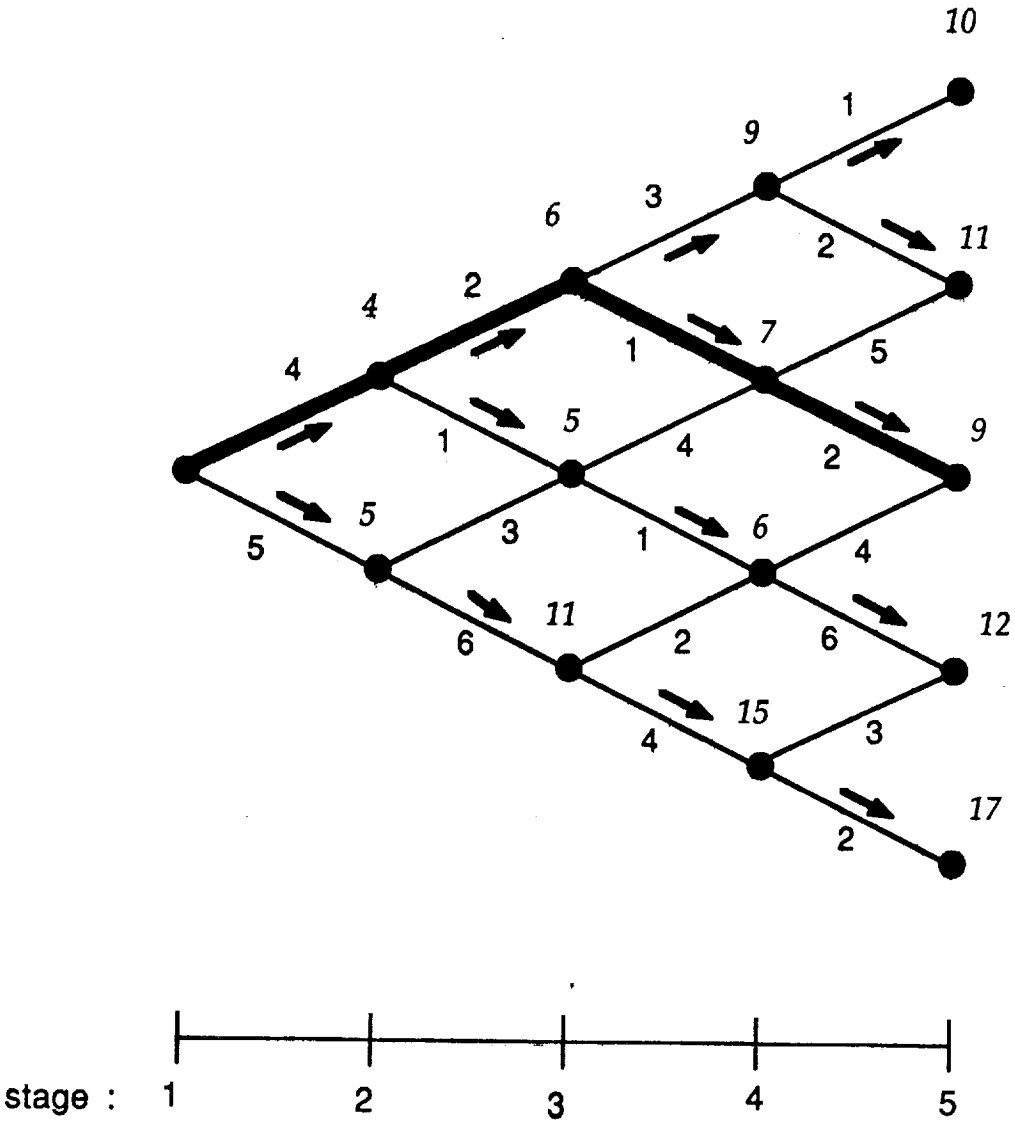

Figure B-2 - Discrete Dynamic Programming Solution

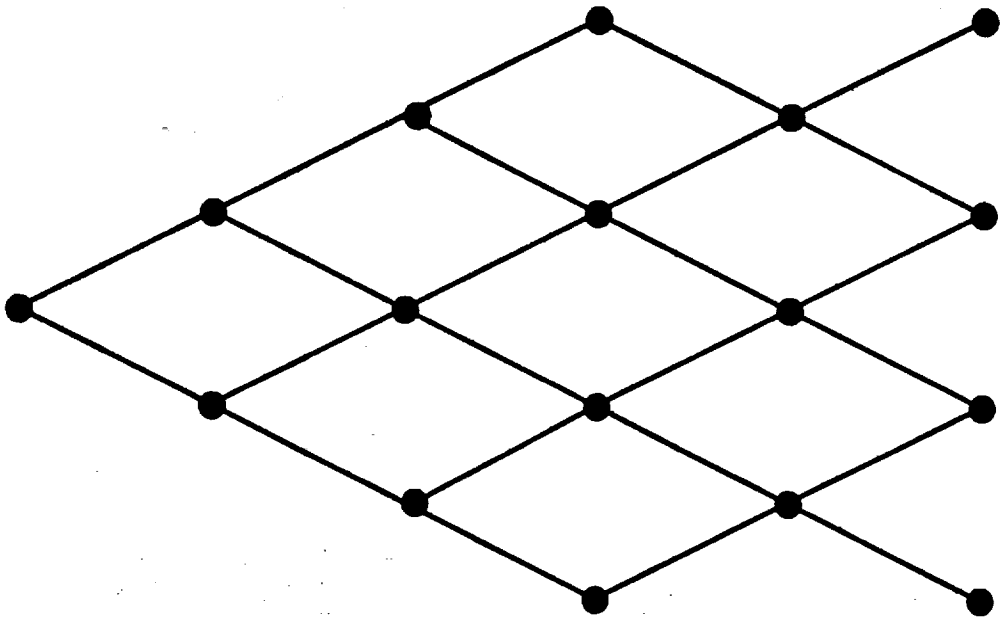

Figure B-3 - Constrained Dynamic Programming Grid

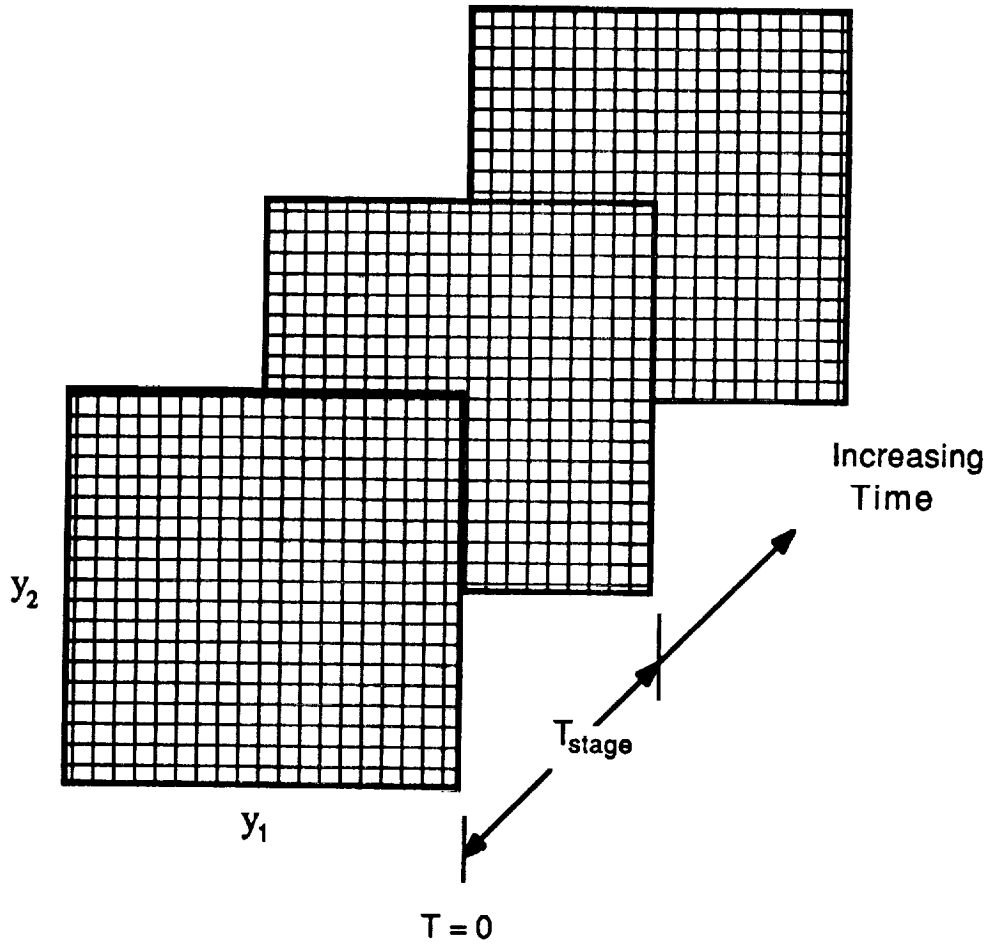

Figure B-4 - Continuous to Discrete Grid Conversion

(Figure 3, repeated)

Table 1 - Saved Variable List

Saved Variables, Current Time Stage Only, All Reachable Output Space Boxes

1.) state vector, **x** (n x 1 real vector)

2.) state sensitivities, $\partial x/\partial \theta$ (n x p real matrix)

3.) input amplitudes, **UASTR** (m x 1 real array)

4.) input information, **IREPU** (3 x 1 integer array)
contains:
a.) index of last control (integer)
b.) number of stages a.) was applied (integer)
c.) index of last control different from a.) (integer)

5.) $[d_{jk}] \ \forall \ j \geq k,$ ($p(p+1))/2$ real elements)

where $D_i = [d_{jk}]_i$,
j=1,2,...,p
k=1,2,...,p
i=time stage index

Saved Variables, Initial to Current Time Stage, All Reachable Output Space Boxes

1.) input sequence
control indices , **IOPTU** (i x 1 integer vector)

Table 2 - Single Input Design Results

Parameter	Parameter Values	Cramer-Rao bounds				
		Figure 5 Mehra (Ref. 5)	Figure 6 Chen (Ref. 9)	Figure 7 Optimal Input, Chen Amp.	Figure 8 Optimal Input, Mehra Amp.	Figure 9 Optimal Input, Mehra Amp. with lag
Z_α	-0.737	0.0364	0.0332	0.0358	0.0351	0.0343
Z_{δ_e}	0.005	0.0256	0.0212	0.0231	0.0214	0.0213
M_α	-0.562	0.0660	0.0663	0.0658	0.0641	0.0647
M_q	-1.588	0.1731	0.1247	0.1167	0.1005	0.1053
M_{δ_e}	-1.660	0.0988	0.0740	0.0682	0.0528	0.0559
Max.Amp. (rad.)		12.5	8.792	8.792	12.5	12.5
Total Time (sec.)		4.0	3.96	3.68	3.04	3.20

Table 3 - Single Input Maximum Likelihood Results

	True Value	Mehra (Ref. 5)	Chen (Ref.9)	Optimal Input, Chen Amp.	Optimal Input, Mehra Amp.	Optimal Input, Mehra Amp. with lag
Z_α	-0.7370	-0.7531	-0.7104	-0.7518	-0.7360	-0.7331
σ_{Z_α}		0.0369	0.0329	0.0366	0.0362	0.0344
Z_{δ_e}	0.005	0.0045	0.0227	0.0232	0.0223	0.0238
$\sigma_{Z_{\delta_e}}$		0.0261	0.0209	0.0232	0.0213	0.0212
M_α	-0.5620	-0.5481	-0.5629	-0.5780	-0.6598	-0.5819
σ_{M_α}		0.0690	0.0651	0.0675	0.0639	0.0642
M_q	-1.5880	-1.7050	-1.5921	-1.5979	-1.4670	-1.6232
σ_{M_q}		0.1829	0.1232	0.1158	0.0978	0.1035
M_{δ_e}	-1.660	-1.7552	-1.6516	-1.6900	-1.5857	-1.7097
$\sigma_{M_{\delta_e}}$		0.1064	0.0736	0.0688	0.0507	0.0566

Table 4 - Multiple Input Design Results

Parameter	Parameter Values	Cramer-Rao bounds			
		Figure 10	Figure 11	Figure 12	Figure 13
Y_β	-0.10950	0.0493	0.0447	0.0422	0.0383
Y_{δ_r}	0.0219	0.0231	0.0201	0.0216	0.0187
L_β	-14.4240	0.4954	0.3220	0.4202	0.2761
L_p	-1.2039	0.0903	0.0626	0.0702	0.0490
L_r	0.9029	0.3990	0.2249	0.3000	0.1442
L_{δ_a}	-16.8280	0.7133	0.4606	0.6317	0.4029
L_{δ_r}	2.4040	0.2883	0.2358	0.2299	0.1726
N_β	2.8640	0.1031	0.0491	0.0617	0.0284
N_p	-0.0090	0.0171	0.0107	0.0124	0.0059
N_r	-0.2241	0.0786	0.0493	0.0543	0.0363
N_{δ_a}	-0.3580	0.1320	0.0826	0.0946	0.0539
N_{δ_r}	-1.7900	0.0516	0.0298	0.0378	0.0271
Max.Amp. (rad.)		0.07	0.07	0.10	0.10
Total Time (sec.)		10.0	10.0	8.7	10.0

Table 5 - F-18 Geometry and Mass Characteristics

Total length, m	17.07
Wing:	
Area, m^2	37.16
Span, m	11.41
Mean geometric chord, m	3.51
Aspect Ratio	3.5
Quarter-chord sweep angle, deg	20.0
Horizontal Tail:	
Area (wetted), m^2	16.35
Span, m	6.58
Mean geometric chord, m	1.91
Aspect ratio	2.4
Quarter-chord sweep angle, deg	42.8
Moment arm (c.g. at 0.25 m.a.c.), m	5.12
Weight, lbs	31,748.9
Inertia:	
I_{xx}, slug-ft^2	22,294.7
I_{yy}, slug-ft^2	123,095.3
I_{zz}, slug-ft^2	138,116.7
I_{xz}, slug-ft^2	-1797.4
c.g. location:	
fuselage station, in	456.0
buttock line, in	0.0
water line, in	103.4

Table 6 - F-18 Closed Loop Model Parameter Estimates
(from simple doublet input)

Parameter	Parameter Value
X_V	0.0977
X_α	-47.4030
X_{δ_h}	-0.1560
Z_α	-0.4169
Z_q	0.9555
Z_{δ_h}	-0.0024
M_α	-0.9422
M_q	-0.2867
M_{δ_h}	-0.0791
μ_V	-0.3488
μ_α	188.2560
μ_q	268.4946
μ_{δ_h}	-14.7542
μ_{η_e}	-55.2387

Table 7 - F-18 Maximum Likelihood Results

Parameter	Parameter Values	Figure 14	Figure 15	Figure 16
Z_α	-0.4906	-0.4169	-0.3506	-0.3553
σ_{Z_α}		0.0135	0.0112	0.0080
Z_q	0.9902	0.9555	0.9487	0.9665
σ_{Z_q}		0.0060	0.0068	0.0035
Z_{δ_h}	-0.0017	-0.0024	-0.0059	-0.0023
$\sigma_{Z_{\delta_h}}$		0.0001	0.0001	0.0001
M_α	-1.0570	-0.9422	-0.9588	-0.7368
σ_{M_α}		0.0076	0.0068	0.0036
M_q	-0.3289	-0.2867	-0.2397	-0.3024
σ_{M_q}		0.0131	0.0112	0.0075
M_{δ_h}	-0.0755	-0.0791	-0.0733	-0.0766
$\sigma_{M_{\delta_h}}$		0.0005	0.0005	0.0003
Max.Amp. (in.)		1.0	0.5	0.75
Total Time (sec.)		8.0	8.0	8.0

Table B-1 - Computational Load Contrast

	Dynamic Programming		Exhaustive Enumeration	
n	Additions $\sum_{i=2}^{n-1} 2i = n^2-n-2$	Comparisons $2(n-2)+(n-1) = 3n-5$	Additions $2^{n-1} * (n-2)$	Comparisons $n-1$
5	18	10	48	4
10	70	25	4096	9
20	340	55	9,437,184	18

1694 F

REPORT DOCUMENTATION PAGE

Form Approved
OMB No. 0704-0188

1. AGENCY USE ONLY (*Leave blank*)	2. REPORT DATE	3. REPORT TYPE AND DATES COVERED
	May 1993	Contractor Report

4. TITLE AND SUBTITLE
Practical Input Optimization for Aircraft Parameter Estimation Experiments

5. FUNDING NUMBERS
505-64-52-01

NCC1-29

6. AUTHOR(S)
Eugene A. Morelli

7. PERFORMING ORGANIZATION NAME(S) AND ADDRESS(ES)
George Washington University
Joint Institute for Advancement of Flight Sciences
NASA Langley Research Center
Hampton, VA 23681 - 0001

8. PERFORMING ORGANIZATION REPORT NUMBER

9. SPONSORING / MONITORING AGENCY NAME(S) AND ADDRESS(ES)
National Aeronautics and Space Administration
Langley Research Center
Hampton, VA 23681-0001

10. SPONSORING / MONITORING AGENCY REPORT NUMBER
NASA CR-191462

11. SUPPLEMENTARY NOTES
Dissertation submitted in partial fulfillment of the requirements for the degree of Doctor of Science in Aerospace Engineering at The George Washington University, Joint Institute for Advancement of Flight Sciences, Langley Research Center, Hampton, Virginia, July 1990. Langley Technical Monitor: Frederick R. Morrell. Author now at Lockheed Engineering & Sciences Co., Langley Research Center, MS 489, Hampton, VA ((804) 864-4078).

12a. DISTRIBUTION / AVAILABILITY STATEMENT
Unclassified - Unlimited

Subject Category-08

12b. DISTRIBUTION CODE

13. ABSTRACT (*Maximum 200 words*)

The object of this research was to develop an algorithm for the design of practical, optimal flight test inputs for aircraft parameter estimation experiments. A general, single pass technique was developed which allows global optimization of the flight test input design for parameter estimation using the principles of dynamic programming with the input forms limited to square waves only. Provision was made for practical constraints on the input, including amplitude constraints, control system dynamics, and selected input frequency range exclusions. In addition, the input design was accomplished while imposing output amplitude constraints required by model validity and considerations of safety during the flight test. The algorithm has multiple input design capability, with optional inclusion of a constraint that only one control move at a time, so that a human pilot can implement the inputs. It is shown that the technique can be used to design experiments for estimation of open loop model parameters from closed loop flight test data.

The report includes a new formulation of the optimal input design problem, a description of a new approach to the solution, and a summary of the characteristics of the algorithm, followed by three example applications of the new technique which demonstrate the quality and expanded capabilities of the input designs produced by the new technique. In all cases, the new input design approach showed significant improvement over previous input design methods in terms of achievable parameter accuracies.

14. SUBJECT TERMS	15. NUMBER OF PAGES
Experiment design, Input optimization, Parameter estimation	174
	16. PRICE CODE: A08

17. SECURITY CLASSIFICATION OF REPORT	18. SECURITY CLASSIFICATION OF THIS PAGE	19. SECURITY CLASSIFICATION OF ABSTRACT	20. LIMITATION OF ABSTRACT
Unclassified	Unclassified	Unclassified	